Politecnico di Milano

SCHOOL OF ARCHITECTURE, URBAN PLANNING AND CONSTRUCTION ENGINEERING

Master's Degree – Building and Architectural Engineering

A tool for assessing thermal resilience in existing Italian school buildings

parametric evaluation and mitigation strategies for overheating

Supervisor

Prof. Andrea Giovanni MAININI

Co-Supervisor

Eng. Giacomo CACCIA

Candidate

Bianca Adele CAVIGIOLI – 252041

Academic Year 2024 – 2025

Abstract of the Thesis

In Italy, only 10% of schools have a cooling system, and high occupancy rates, coupled with low envelope performance, lead to overheating in most classrooms in the summer and intermediate seasons, with an increase over the years according to future climate projections. This is mainly why Italian schools are usually closed during the summer months, creating a social problem for families and parents. The present thesis, following the results of the RERoadS project for the renovation of the Italian school building stock, aims thus at assessing the magnitude of this phenomenon, and at providing possible strategies to reduce the overheating risk in the classrooms during the occupied periods, evaluating moreover the possibility of their use also in the summer season, for didactic or other purposes. In the study, the overheating magnitude of several classroom configurations is assessed using a parametric simulation tool that, leveraging the IESVE energy simulation software, returns the risk of overheating for each case. Additional configurations that exploit passive strategies for the reduction of internal operative temperatures are then compared, to determine their overheating reduction potential and possible limitations, guiding towards the improvement of the existing building stock and suggesting the possible steps to allow the use of school spaces in the hotter months, especially considering natural ventilation, night ventilation, the use of fans to increase the air speed and the use of external shading devices.

Global warming and local climate effects are also considered in the simulations, comparing different climatic scenarios, from the future weather projections to the Urban Heat Island effect, to provide results that can help decision makers to identify the best strategies for the whole life cycle of the building.

In the end, thanks to the simulations performed on a set of cases and to all the implemented analyses, a user-friendly tool has been created to provide school owners with a simplified methodology for the assessment of the overheating risk of schools and classrooms, and to evaluate possible passive retrofit scenarios and their effectiveness.

Table of Contents

Abstract of the Thesis ..... **I**

Table of Contents ..... **II**

List of Figures ..... **IV**

List of Tables ..... **VIII**

List of Acronyms ..... **IX**

Chapter 1 – Introduction **1**

Chapter 2 – Context **3**
2.1 Energy efficiency 3
2.2 Energy efficiency in schools 4
2.3 REROADS project 6
2.4 Energy efficiency strategies 7
2.5 Summer season energy efficiency 8

Chapter 3 – State of the Art **10**
3.1 Overheating assessment 10
3.1.1 Adaptive comfort thresholds 11
3.1.2 CIBSE's overheating assessment 11
3.1.3 Heat waves and day-night temperature differences 13
3.2 Overheating reduction passive retrofit strategies 13
3.2.1 Solar heat gain coefficient 14
3.2.2 Shading devices 14
3.2.3 Natural ventilation 14
3.3 Overheating reduction active strategies 15
3.3.1 Fan use and air movement 15
3.3.2 Building systems for the reduction of overheating 16

Chapter 4 – Methodology **32**
4.1 Model description 32
4.1.1 Loads 33
4.1.2 Constructions 34
4.2 Parametric tool script 40
4.2.1 Model variations 40
4.2.2 Model simulation 44
4.2.3 Results extraction 44

4.2.4 Results elaboration 45
4.3 Additional passive strategies analysis 48
4.3.1 Shadings 49
4.3.2 Night-time natural ventilation 49
4.4 Overheating drivers analysis 50
4.4.1 Future climate scenarios 51
4.4.2 Urban Heat Island effect 51
4.5 Overheating evaluation 54
4.5.1 Classroom overheating evaluation 55
4.5.2 School overheating evaluation tool 57
4.6 Simulations tool validation 59
4.6.1 Test simulations 59
4.6.2 Different software results comparison 60
4.7 Sensitivity analysis 73

Chapter 5 – Results 77
5.1 Simulation results 77
5.1.1 Example results 77
5.1.2 Configurations comparison 87
5.1.3 Additional passive strategies simulation results 95
5.1.4 Overheating drivers' simulation results 101
5.2 Tool usage examples 109
5.1.2 School overheating evaluation 109
5.2.2 Classroom overheating evaluation 109
5.3 Tool application 110

Chapter 6 – Limitations & future works 115

Chapter 7 – Conclusions 119

Bibliography 121

Acknowledgements 129

Appendix A – test simulations 131

Appendix B – day of the week variation study 144

Appendix C – tool reports 147

List of Figures

Figure 1 – Requirements for buildings scheme according to the EPBD [6] 4
Figure 2 – School buildings with Energy Certificate according to Legambiente Report 2023 [14] .. 5
Figure 3 – RERoadS logo 6
Figure 4 – Fan use advantages according to [48] 15
Figure 5 – Energy savings and comfort improvement with fan use according to [36] 16
Figure 6 – Data for heating and conditioning systems for Italian schools according to SNAES [10] 17
Figure 7 – Venn chart for the SNAES [10] data 17
Figure 8 – Share of heating systems in the different parts of Italy 18
Figure 9 – Share of fuel oil and diesel heating systems per region 18
Figure 10 – Share of methane, GPL, electric, DH, ventilation and solar thermal systems per region 19
Figure 11 – Average plant power per plant type (Lombardy) 21
Figure 12 – Plant power distribution for school heating plants in Lombardy and Liguria 22
Figure 13 – Heating power per floor surface in Lombardy (left) and Liguria (right) 22
Figure 14 – Energetic class distribution of school buildings in Lombardy (left) and Liguria (right) 23
Figure 15 – Climatic zone distribution of school buildings in Lombardy (left) and Liguria (right) 23
Figure 16 – Year of construction distribution of school buildings in Lombardy (top) and Liguria (bottom) 25
Figure 17 – Heating plant power per climatic zone in Lombardy and Liguria 26
Figure 18 – Heating plant power per period of construction in Lombardy and Liguria 27
Figure 19 – Cooling plant power distribution for Lombardy 27
Figure 20 – Cooling power per floor surface in Lombardy 28
Figure 21 – Cooling plant power per climatic zone in Lombardy 28
Figure 22 – IES-VE model 33
Figure 23 – Conduction values table 34
Figure 24 – SOL04 stratigraphy 35
Figure 25 – MCV01 stratigraphy 36
Figure 26 – COP01 stratigraphy 37
Figure 27 – Base-case single glass characteristics 39
Figure 28 – Improved case double-glazing system characteristics 40
Figure 29 – Italian climatic zones based on the Degree-Days 41
Figure 30 – Air and operative temperature for an example case located in climatic zone A, with base-case ventilation and with the addition of night-time ventilation 50
Figure 31 – UHI to base-case EPW file temperature difference in the three cases of source to target LCZs 53
Figure 32 – Simulation parameters combination diagram 55
Figure 33 – Classroom and whole school overheating evaluation for the intermediate and summer season diagram 59

Figure 34 – Indoor operative temperature over the year simulated in the three software and compared to running mean temperature (Trm), maximum temperature with zero air speed (Tmax), and higher air speed (TmaxVent) 65
Figure 35 – Indoor operative temperature frequency charts and cumulative frequency plots for the 8 considered cases simulated with the three software 66
Figure 36 – Comparison plot between the EnergyPlus and IESVE operative temperatures for the 8 cases 68
Figure 37 – Operative temperature difference between the IESVE and EnergyPlus simulations distribution plot for the 8 cases 69
Figure 38 – Indoor operative temperature simulated in the 3 software over the day with the highest temperature for the 8 cases 70
Figure 39 – Indoor operative temperature simulated in the 3 software over the day with the lowest temperature for the 8 cases 71
Figure 40 – Comfort hours for the 8 cases simulated with the 3 software in the case of no air speed 72
Figure 41 – Comfort hours for the 8 cases simulated with the 3 software in the case of air speed equal to 1.2 m/s 72
Figure 42 – Temperature thresholds correction according to the air speed from EN 16798 [45] 74
Figure 43 – Tornado chart for the share of hours above the threshold and above 2°C over the threshold 75
Figure 44 – Tornado chart for the share of hours that do not meet each of the TM52 criteria 75
Figure 45 – Tornado chart for the number of heat stress days 76
Figure 46 – Comfort bands per period in the case of Milan, with the base-case configuration and room in the middle floor and middle position, with all the combinations of SHGC, exposition and WFR 78
Figure 47 – Cumulative frequency of temperature exceedance for Milan with the base-case configuration and room on the middle floor and middle position (blue for zero and red for higher air speed) 80
Figure 48 – TM52 compliance for all the combinations in the case of Milan with the base-case configuration and room on the middle floor and middle position 81
Figure 49 – TM52 compliance for each criterion for all the combinations in the case of Milan, with the base-case configuration and room in the middle floor and middle position 82
Figure 50 – Parallel plot for the TM52 criteria in the case of Milan with the base-case configuration and room on the middle floor and middle position 83
Figure 51 – Parallel plot for the TM52 criteria in the case of Milan with the base-case configuration and room in the middle floor and middle position, with highlighting of the cases with criterion 2 equal or close to zero 84
Figure 52 – Parallel plot for the TM52 criteria in the case of Milan with the base-case configuration and room in the middle floor and middle position, with highlighting of the cases with the worst values for criterion 1 85
Figure 53 – Share of heat wave days for Milan with base-case configuration and room on the middle floor, middle position 86
Figure 54 - Share of heat wave days in the five periods for the Milan base-case configuration and room in the middle floor, middle position 87
Figure 55 – Example distribution of heat wave days for the case Top Centre Base 12% WFR, south, 0.3 SHGC 87
Figure 56 – Average of the share of hours outside the comfort bands heatmap 90

Figure 57 – Average of the share of hours with temperature higher than 2°C above the maximum temperature heatmap....91
Figure 58 – Share of cases that are not compliant with the TM52 heatmap....92
Figure 59 – Average number of heat stress days heatmap....93
Figure 60 – Average number of heat stress days heatmap for increased air speed cases....94
Figure 61 – Different shading configuration comparison for high and low SHGC for the 8 l/s/person ventilation scenario....96
Figure 62 – Different shading configuration comparison for high and low SHGC for the 1.2 ACH ventilation scenario....97
Figure 63 – Night ventilation with respect to normal ventilation configurations comparison for high and low SHGC for the 8 l/s/person ventilation scenario....99
Figure 64 – Night ventilation with respect to normal ventilation configurations comparison for high and low SHGC for the 1.2 ACH ventilation scenario....100
Figure 65 – Future weather results comparison for high and low SHGC for the 8 l/s/person ventilation scenario....102
Figure 66 – Future weather results comparison for high and low SHGC for the 1.2 ACH ventilation scenario....103
Figure 67 – UHI weather results comparison for high and low SHGC for the 8 l/s/pers ventilation scenario....105
Figure 68 – UHI weather results comparison for high and low SHGC for the 1.2 ACH ventilation scenario....106
Figure 69 – UHI weather results comparison for high and low SHGC for the 8 l/s/person ventilation plus night ventilation scenario....107
Figure 70 – UHI weather results comparison for high and low SHGC for the 1.2 ACH ventilation plus night ventilation scenario....108
Figure 71 – Floor plans scheme for the example school....112
Figure 72 – Share of hours in each comfort band in the different periods for the different classrooms of the example school....113
Figure 73 – Comfort bands comparison for the east-exposed middle floor middle position classroom of the example school....114
Figure 74 – Temperature and solar radiation plots for Milan....131
Figure 75 – Temperature frequency chart for Milan cases. Here and in the following charts, all the subplots on the left represent the cases with SHGC equal to 0.3, while the right-side ones represent the 0.9 SHGC cases; the 4 charts on top represent the lower WFR and the lower ones the higher WFR; and among those, the first line corresponds to the window facing south, while the second line corresponds to the window facing north....132
Figure 76 – Cumulative frequency of temperature exceedance for Milan (blue for zero and red for higher air speed)....133
Figure 77 – Cumulative frequency comparison charts for specific cases for Milan....133
Figure 78 – Comfort bands for the cases of Milan....134
Figure 79 – Comfort bands per period in the case of Milan, with all the cases....135
Figure 80 – Temperature and solar radiation plots for Palermo....137
Figure 81 – Temperature frequency chart for Palermo cases....138
Figure 82 – Cumulative frequency of temperature exceedance for Palermo (blue for zero and red for higher air speed)....139
Figure 83 – Cumulative frequency comparison charts for specific cases for Palermo....139
Figure 84 – Comfort bands for the cases of Palermo....140
Figure 85 – Comfort bands per period in the case of Palermo, with all the cases....141

Figure 86 – Milan and Palermo outdoor dry-bulb temperature comparison.....143
Figure 87 – Comfort hours distribution for the variation of weekdays in the 8 test cases.....145
Figure 88 – Variation of discomfort hours for the 8 test cases, with the variation of the day of the week.....145
Figure 89 – Indoor operative temperature on the highest temperature day for the seven weekday cases in the 8 test cases.....146

List of Tables

Table 1 – Comfort categories....11
Table 2 – Heat wave definitions in the literature....13
Table 3 – Internal partitions stratigraphy....35
Table 4 – Base-case stratigraphies....38
Table 5 – U-values [W/m^{2}K] requirements for building envelope components according to DM 28-10-2025 [64] 38
Table 6 – Improved stratigraphies 39
Table 7 – Climatic zones and locations 41
Table 8 – Orientation values....43
Table 9 – Glazing stratigraphies 43
Table 10 – Comfort categories equations 45
Table 11 – End and start of the heating season for each climatic zone 46
Table 12 – Transmission factor values for 0° and 45° inclinations 49
Table 13 – Local Climate Zones for the source and target EPWs for each city 52
Table 14 – Validation model scenarios parameter values....59
Table 15 – Minimum, average and maximum temperature for all the simulations 67
Table 16 – Parameter values for the base-case configuration and the ±30% variations....73
Table 17 – Glazing properties for the sensitivity analysis....73
Table 18 – Average monthly maximum, mean, and minimum temperatures for Milan (°C)....131
Table 19 – Milan TM52 results for the validation case studies....136
Table 20 – Milan TM52 results for the validation case studies with a higher air speed....136
Table 21 – Average monthly maximum, mean, and minimum temperatures for Palermo (°C)....137
Table 22 – Palermo TM52 results for the validation case studies 142
Table 23 – Palermo TM52 results for the validation case studies with a higher air speed....142

List of Acronyms

ACH	Air Change Rate
AIVC	Air Ventilation and Infiltration Centre
APE	Attestato di Prestazione Energetica (Energy Performance Certificate)
API	Application Programming Interface
ASHRAE	American Society of Heating, Refrigerating and Air-Conditioning Engineers
BEMS	Building Energy Management System
BRP	Building Renovation Passport
CCHP	Combined Cooling Heat and Power
CENED	Certificazione ENergetica EDifici (Buildings Energetic Certification)
CHP	Combined Heat and Power
CIBSE	Chartered Institution of Building Services Engineers
CMIP	Couples Model Intercomparison Project
DBL	Digital Building Logbook
DHW	Domestic Hot Water
EEA	European Environment Agency
ENEA	Agenzia Nazionale per le nuove tecnologie, l'Energia e lo sviluppo economico sostenibile (National Agency for new technologies, Energy and sustainable economic growth)
EPBD	Energy Performance of Buildings Directive
EPW	Energy Plus Weather File
ERA	Elementary Renovation Actions
GCM	Global Climate Models
HVAC	Heating, Ventilation and Air Conditioning
IDF	Input Data File (for EnergyPlus)
IEA	International Energy Agency
IEQ	Indoor Environmental Quality

IES	Integrated Environmental Solutions
IESVE	Integrated Environmental Solutions Virtual Environment
IPCC	Intergovernmental Panel for Climate Change
LBNL	Lawrence Berkeley National Laboratory
LCZ	Local Climatic Zones
LED	Light-Emitting Diode
MIUR	Ministero dell'Istruzione, dell'Università e della Ricerca
MUR	Ministero dell'Università e della Ricerca
PRIN	Progetti di Ricerca di Interesse Nazionale
PV	Photovoltaic Panel
REB	Reference Educational Buildings
RR	Renovation Roadmap
SHGC	Solar Heat Gain Coefficient
SNAES	Sistema Nazionale dell'Anagrafe dell'Edilizia Scolastica
SSP	Shared Socioeconomic Pathways
Tmax	Maximum allowed temperature for the considered comfort band
TmaxVent	Maximum allowed temperature for the considered comfort band with increased air speed
TM	Technical Memoranda
TMY	Test Meteorological Year
Trm	Running Mean Temperature
UHI	Urban Heat Island
UNDRR	United Nations Office for Disaster Risk Reduction
WFR	Widow to Floor Ratio
WMO	World Meteorological Organisation
WP	Work Package
WWR	Window to Wall Ratio
ZEB	Zero Energy Building

Chapter 1 – Introduction

Buildings' operation accounts for 30% of the global energy consumption and 26% of the global energy-related emissions, both directly and indirectly [1]. It is thus necessary to reduce this impact, and therefore to cut down the consumption and emissions of buildings through careful evaluation of the occupants' needs. Buildings are indeed the place where most of our lives are spent, and are meant to provide comfort to the users and facilitate their activities. This topic is even more relevant when talking about school buildings, as those are the places where children and young people spend most of their first years and get an education. It is thus fundamental for those buildings to provide the best environment for the development of the students and to give a tangible example of energy efficiency to future generations [2], [3].

In the next chapter, the context in which the project is developed is described, including a summary of the current regulations connected to energy efficiency of buildings, both at the national and European levels. The following chapters and the core of the thesis focus on the summer comfort performance of Italian schools, in particular replying to two main research questions:

- Can the school building be used during the intermediate and summer seasons for didactic and other activities, providing a comfortable environment? And for how long, considering climate change and global warming?
- What passive strategies can be used to improve comfort in the hotter months? And when must the school building be equipped with a summer climatisation plant to guarantee comfort during the whole year?

The topic is first described with a state of the art, then the methodology and findings of the research are presented in the following chapters. The analysis is developed through the use of a parametric simulation tool, and the results are presented in Chapter 5.

In the introduction of this thesis, it is fundamental to define clearly the assumptions and the final goal of the study, which is based on the analysis of a simulation tool's results. The main purpose of the research is to assess the magnitude of the overheating phenomenon in Italian school buildings and classrooms, and estimate their resilience to future weather and extreme weather events, while comparing possible mitigation strategies and the magnitude of their effect. To achieve the proposed goal, an energy simulation tool, IESVE, is leveraged to determine the internal operative temperature of different classroom configurations, thus basing the results on a variety of assumptions. The assumptions, which concern mainly the model characteristics in terms of geometry, envelope and loads, and the values assumed by

the parameters in the different configurations, are described in Chapter 4 and discussed in Chapter 6. Taking these assumptions into consideration, it is thus necessary to state that the present research is founded on a comparative process and can only be used to identify the relationship between different solutions and configurations within the same study.

Chapter 2 – Context

In this chapter, the context of development of the thesis is described, starting from the framework in which the European Union's countries are working, through the scope and motivations of the project and in the end, to the possible strategies that are being implemented. The research project described in the thesis was realized in collaboration with SEEDLAB@DABC and lays its foundations in the framework of the RERoadS project, that aims at studying possible renovation strategies for school buildings and is presented in the chapter and aims at continuing the work. In particular, at the end of the chapter, a focus is made on the buildings' summer performance, and on the need to assess and improve it.

2.1 Energy efficiency

Energy efficiency is the strategy that allows for reducing the energy consumption in a process to get the same output, or to increase the production with the same energy input, and with the reduction and minimisation of energy waste. It is fundamental in the transition to a carbon-neutral environment, as it reduces the total consumed energy and thus the amount of energy that has to be provided with renewable sources ([4], [5]). In recent years, and especially after the oil crisis and major studies about climate change, countries are committing to reducing emissions and energy consumption, and at the COP28 of 2023, the 200 involved countries agreed to double the annual rate of energy efficiency improvements by 2030 [5].

The building sector accounts for more than a third of the total global energy consumption and emissions [1]. This represents the largest energy consumption share in Europe, with more than 80% of the energy consumed in residential buildings used for heating, cooling and domestic hot water. Most buildings in the EU have a poor energy performance, as around 85% of them were built before the 2000s. It is thus fundamental to reduce the built environment's footprint, and the European Union aims at decarbonising the building stock by 2050 and has provided the Energy Performance of Buildings Directive (EPBD) to reach this goal [6]. The revised document was made effective in 2024 and is meant to help improve the quality of the building stock, leaving the possibility to each member state to identify the best strategies to fit with the existing building stock and the specific country's climate.

In the EPBD, goals are set for both new and existing buildings, with the requirement for constructions to be Zero Energy Buildings (ZEB) by 2028 for public buildings and by 2030 for private ones. As regards existing non-residential buildings, two energy consumption thresholds must be set at the beginning of the process: a 16% one and a 26% one, meaning

that 16% or 26% of the national non-residential building stock is above this threshold in terms of energy consumption. The requirement is that all the non-residential existing buildings are below the 16% energy consumption threshold by 2030 and below the 26% energy consumption threshold by 2033. In the end, for residential existing buildings, the energy consumption must be decreased of 16% by 2030 and by 20-22% by 2035, compared to the values of 2020. Moreover, by 2040 and every 5 years thereafter, the energy consumption of existing residential buildings must be equivalent to or lower than a value determined progressively to reach the zero-emission building stock by 2050. In particular, it is also stated that the reduction that must be accomplished by 2035 must be accomplished for at least the 55% with the renovation of the 43% worst-performing residential buildings. The scheme in Figure 1 resumes all the requirements that were presented in this paragraph.

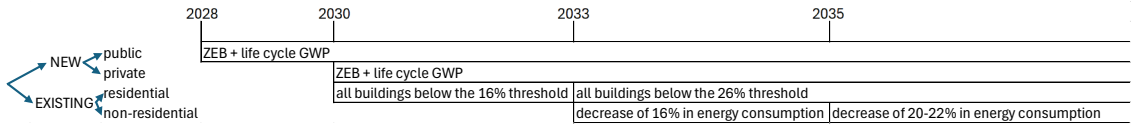

Figure 1 – Requirements for buildings scheme according to the EPBD [6]

Within the scope of the EPBD, all the member states have to determine some guidelines to reach the expected goals, and in particular, create renovation passports including the roadmap and its steps for the complete renovation of the building. The passport should also include the optimal sequence of renovation steps, as well as the estimated energy savings in primary and final energy consumption, in kWh and percentage with respect to the previous step, the estimated reduction of the operational greenhouse gas emissions, the estimated economic savings and the estimated energy class. Moreover, there should be information about the possible connection to a district heating and cooling network, the share of renewable energy generation and self-consumption and the options for improving the life-cycle footprint.

As far as Italy is concerned, the energy performance requirements for buildings are set by the D.M. 26-06-15 [7]. Some specific guidelines have to be set following the EPBD, in order to reach the energy efficiency goals. For this reason, it is necessary at present to generate renovation passports for the different types of buildings, and the project to which this thesis is associated aims at this goal. Moreover, the Criteri Ambientali Minimi (CAM – Environmental Minimum Criteria) are set by the D.M. 24-11-25 [8] to guide the public administration choices towards innovative and sustainable projects.

2.2 Energy efficiency in schools

In Italy, the school building stock plays a fundamental role in this context for many reasons, starting with its extension, its poor energetic performance and its high social importance. The educational building cluster is indeed in fifth place in terms of unit number in Italy, but in first place in terms of the total occupied area [9]. As regards the energy performance of

school buildings, the National Register of School Buildings (SNAES - Sistema Nazionale dell'Anagrafe dell'Edilizia Scolastica) [10], introduced in 1996, can be consulted. The database contains information for 61,307 buildings, and points out that 42% of the schools were built before 1976, the year in which the first legislation for the reduction of the energy consumption of buildings was introduced in Italy [11], and only 12% after 1992, the year in which another regulation was introduced [12]. This means that most of the buildings present a very inefficient envelope, and additionally, considering that services and lighting plants are thus more than 12 years old, it can be said that more than 50% of the energy consumption in school buildings can be saved [2].

According to the SNAES database, most of the school buildings are naturally ventilated, and their heating systems are fuelled by fossil fuels. According to Legambiente, moreover, in 2023, only 16% of the buildings were refurbished [13], and the chart in Figure 2 represents the share of school buildings in the different energy classifications (with Class A being the most energy efficient).

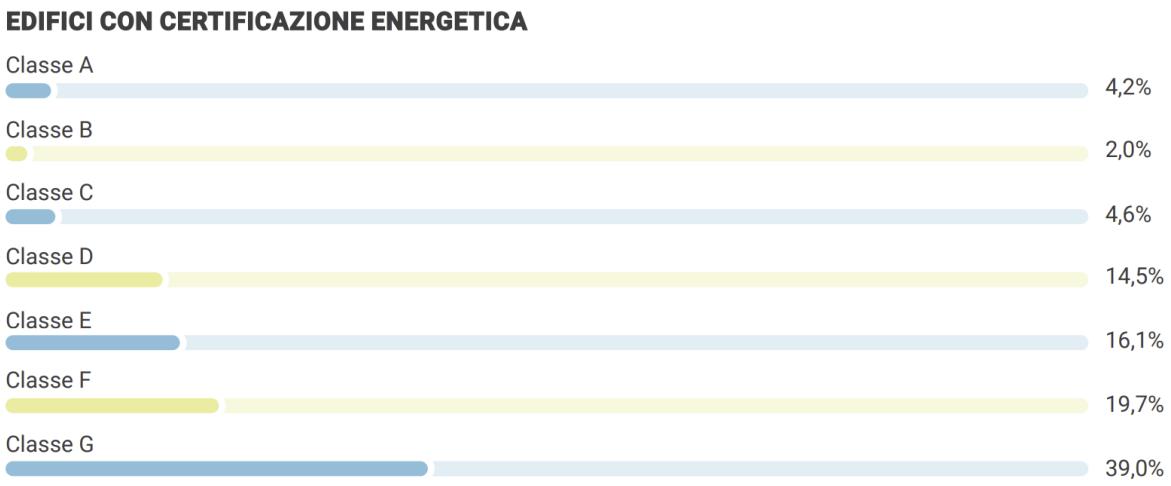

Figure 2 – School buildings with Energy Certificate according to Legambiente Report 2023 [14]

Considering the poor quality and inadequacy of the school buildings stock, it is more and more urgent to renovate it to comply with regulations, as it is also required by the European regulations, that the worst performing buildings must be renovated first, as also mentioned in the previous paragraph.

In addition to the environmental topic, indeed, the renovation of schools is also fundamental to providing the best environment for education. Schools are, in fact, the place where young citizens can learn the importance of sustainability, and the buildings must represent a tangible example of this concept. The renovation of school buildings can contribute to enhancing the wellness of the students and their environmental awareness [2].

Within this scope, the D.M. 18-12-75 [15] sets specific requirements for school constructions, with regulations regarding the minimum area per person, the presence of

spaces for different activities and the habitability conditions. Regarding the latter, requirements are set for acoustics, illumination and colour, thermo-hygrometric and Indoor Air Quality conditions.

2.3 REROADS project

Starting from the need for renovation of the building stock in the European countries and from the considerations presented in the previous paragraph, the RERoadS project [16] focuses on the renovation of school buildings in Italy, in order to provide efficient and safe buildings and improve the functionality and accessibility of educational spaces, which are recognised to play a fundamental role in the growth and development of the sustainability concept of future generations.

Figure 3 – RERoadS logo

The project aims at creating a specific Buildings Passport for schools, completed by educational programmes for the sensitisation about sustainability, as required by the European directives. The present thesis is developed in the scope of the creation of the Building Renovation Passport (BRP), which includes two main elements: the Digital Building Logbook (DBL) and the Renovation Roadmap (RR). The methodology comprehends the writing of a renovation plan, the use of energy simulations and the validation of the results in some test buildings, with the monitoring of Indoor Environmental Quality (IEQ).

The project is developed to comprehend building technologies, sustainability, energy and Indoor Environmental Quality, and is planned in four main Work Packages (WP). The first package, WP1 – Project Coordination, Management and Monitoring, is created to ensure the respect of the requirements of the MUR, the Ministry of University and Research, to identify and solve possible activation problems and to create the School Advisory Board. In the WP2 – Definition of the Methodological Framework for the School Building Renovation Passport, data from the buildings is gathered, and the overall methodology for the development of the Digital Building Logbook and the Renovation Roadmap is defined. During the third phase, WP3 – Development and Performance Assessment of Scenarios for the School Renovation Roadmap, the Elementary Renovation Actions (ERAS) are defined for the different building typologies, previously grouped in Reference Educational Buildings (REB) according to a geo-clustering process. The ERAS, for which cost and energy saving are defined, are then combined in renovation packages for the increase of the performance and related to the REB. After this, in WP4 – Validation and demonstration of the School BRP, sensors are used to monitor the IEQ and the users' behaviour, the project is validated and applied to the whole Italian school building stock. In the end, WP5 – Communication, Dissemination, Training and Education, deals with the communication and the creation of courses.

2.4 Energy efficiency strategies

After describing the aim for which the present research is developed, it is also necessary to delineate the possible strategies that can be used to reach the scope. In the ENEA document for the renovation of school buildings, some key aspects are listed referring to the energy retrofit of buildings [2]:

1. The building envelope – a high-performance building envelope can be achieved by insulating the walls and roof and by improving the transparent parts' performance, with insulating glass and frame, shadings and films, to minimise the heat losses in the cold season and the overheating risk in summer.

2. Daylighting – high-performance windows allow to exploit natural light to the maximum, minimising the use of artificial light.

3. Artificial lighting – LED lights and control systems allow for the energy consumption for the provision of the necessary lighting in indoor spaces.

4. Ventilation, heating and cooling systems – the systems must present the highest performance and be equipped with control systems to reduce their use in function of the needs of the users.

5. Renewable energies – on-site exploitation of renewable energy, such as solar and geothermal help improve the performance of the building and reduce the energy consumption from the grid.

6. Water management systems – rain and grey water reuse systems allow to reduce waste of water and energy.

In the same document, a possible workflow for the renovation of buildings is presented: the process must start from the selection of the building to be renovated, through the energetic diagnosis to select the most convenient solution, the finding of fundings and the monitoring of results.

According to the ENEA guide for the renovation of schools, all the buildings from before 2006 do not respect the present regulations on the reduction of energetic consumption and are thus to be refurbished. The most appropriate retrofit action has to be determined based on the energy consumption, on the building's characteristics and on the climatic zone. The possible actions include modifying the energy supply contracts, improving the management of systems, the refurbishment of parts of the building envelope, or the substitution of the building system. The choice of the action will be based on the condition of the building, on the economic availability and on the energy saving potential. ENEA also lists some possible interventions, with their energy saving potential and economic return time. From the data presented by ENEA, it is possible to conclude that the economic return of the actions is usually related to the climatic zone, with an increase in the convenience, and thus a decrease

in the return period, in the colder climatic zones. Moreover, renovation actions on windows and roofs present a higher convenience than the insulation of walls and floors.

As regards building services, ENEA lists different possibilities, mostly concerning winter climatisation, that control internal temperature, relative humidity and indoor air quality. The different typologies of building services described in the document are summarised in Chapter 3, along with the possible renovation strategies, which range from the maintenance of the system and the introduction of control systems to optimise the energy consumption, to the substitution of components.

2.5 Summer season energy efficiency

This thesis aims to analyse the necessity of retrofitting buildings with optimised summer performance as an objective, to respond to two main needs of the school building stock. The first one is the need for energy renovation, which was deeply described in the previous paragraphs, and for which one of the solutions is the introduction and optimisation of ventilation, heating and cooling systems. The second problem is the almost total absence of cooling systems in Italian schools, which are, also for this reason, closed for a long period in summer. It is thus believed that studying the summer performance of buildings would improve the thermal and overall comfort of students in schools, and also the energy value of the buildings.

As concerns the first topic, as seen in the previous chapter, the addition and optimisation of ventilation, heating and cooling systems is one of the main strategies to improve energy efficiency, as suggested by the ENEA document for energy efficiency of schools [2]. Mechanical ventilation is recognised as one of the most important factors for the well-being of students in schools, as confirmed by the study “Mechanical ventilation for Italian school classrooms” [17] and presented in a related article [18]. According to Cardelli, mechanical ventilation is fundamental to providing comfort in schools. The study starts from the observation that, especially after the COVID-19 pandemic, air renovation in classrooms is needed to provide a safe environment to students. Among the different ventilation strategies, mechanical ventilation is identified as the most efficient one to combine energy savings and Indoor Environmental Comfort, as it can be coupled with heat recovery systems and thus also provide heating and cooling. The study also concludes that the use of mechanical ventilation would guarantee primary energy savings by 30%, with more than 70% of the savings associated with the northern regions. The impact of the use of mechanical ventilation was thus mainly linked with the heating of schools, as this is the major energy need at the present time in schools, which are closed during the summer period. Mechanical ventilation can nevertheless also be used for cooling, and this could be a winning strategy to improve the role of schools also during summer, considering the current climatic trend and the increasing global temperatures.

On the other hand, according to the Tortuga think-tank, only 10% of Italian schools currently present a cooling system [19], with this percentage decreasing with the increase of the age of the buildings. This means that in most cases, the only way of cooling the rooms in the hotter months is just opening the windows. Moreover, according to a study from the National Bureau of Economic Research, for each degree Celsius increase in the temperature, the performance of scholars decreases of 2% [20]. Until now, the main solution to this problem has been a long summer break in Italian schools, which is 14 weeks long, and is the second longest among European countries. Applying retrofit strategies that are aimed at decreasing overheated hours in the schools that are most affected by warm summer months could help to extend the lectures in June and September, increasing the holidays during the academic year and decreasing the need for summer camps, which are often not enough and not affordable for all families [19].

In the next chapters, the state of the art concerning the installed building services in the Italian schools' building stock is presented, with a particular focus on the presence and dimensions of the cooling systems. Then, the methodology used to assess the research questions is presented, and in the end, the results are presented and discussed.

Chapter 3 – State of the Art

In this chapter, the state of the art concerning the topic of overheating in Italian classrooms is presented. First, overheating assessment strategies from the literature and regulations are listed, then possible retrofit strategies for the reduction of overheating in the summer season are presented, starting from the passive techniques, which rely on modifications of the building envelope and of its usage, and also presenting the active ones, which are mainly based on the use of conditioning systems.

3.1 Overheating assessment

In the next decades, temperatures at the global scale are expected to increase substantially according to climate projections [21], with an increase in severe heat waves and with the Mediterranean region particularly being affected by this phenomenon [22]. This is the reason why overheating assessment strategies are acknowledged to be more and more necessary for the modelling of efficient and comfortable buildings, and to improve health conditions and decrease mortality ratios, which are worsened by extreme weather conditions [23]. In this framework, building design's effectiveness is two-fold: designing more efficient buildings reduces their environmental impact, which is known to be at present very high [1], and at the same time improves the comfort of the users, providing better conditions inside the spaces. This is moreover particularly urgent for school buildings, which usually do not provide suitable temperatures in the summer periods [24], mainly because of poor ventilation and conditioning of spaces, which does not allow for the removal of the excessive heat load produced by densely populated classrooms, and of high solar gains due to poor performance glazing [25].

In the next paragraphs, different overheating assessment strategies that are used at present and that will be used throughout the study for the evaluation of different scenarios are listed, starting with the definition of adaptive comfort, through CIBSE's documents for the assessment of overheating, to other techniques that include the comparison of high temperatures with day-night temperature differences, in combination with heat waves studies. In general terms, overheating is defined mainly in two ways: a static threshold one, which applies fixed temperature limits, and an adaptive threshold one, which considers the adaptation of occupants to higher temperatures, setting the threshold based on outdoor temperatures and occupant behaviour. First of all, adaptive comfort thresholds and methodologies are described, then the overheating strategies defined by the CIBSE are outlined, and in the end, a literature review of other overheating assessment strategies is summarised.

3.1.1 Adaptive comfort thresholds

Adaptive comfort considers the power of occupants to adapt to different conditions based on the outdoor conditions. First of all, the comfort temperature is defined based on the running mean outdoor temperature, which is calculated as the weighted average of the mean outdoor daily temperature of the recent 7 days, according to EN 16798-2:2019 [26]:

$$T_{rm} = (T_{-1} + 0.8 \cdot T_{-2} + 0.6 \cdot T_{-3} + 0.5 \cdot T_{-4} + 0.4 \cdot T_{-5} + 0.3 \cdot T_{-6} + 0.2 \cdot T_{-7})/3.8$$

The comfort temperature can thus be calculated as [26]:

$$T_{comfort} = 0.33 \cdot T_{rm} + 18.8°C$$

Three acceptable comfort bands are defined in Table 1:

Table 1 – Comfort categories

Category		**Acceptable range**	**Comfort band**
I	High level of expectation (sensitive occupants)	90% satisfied	$T_{comf} + 2°C$ $T_{comf} - 3°C$
II	Normal level of expectation (typical buildings)	80% satisfied	$T_{comf} + 3°C$ $T_{comf} - 4°C$
III	Moderate level (only acceptable for limited use)	65% satisfied	$T_{comf} + 4°C$ $T_{comf} - 5°C$

Moreover, according to the ASHRAE 55 [27] regulations, when increasing the air speed, for example, with the use of fans, the upper limit of the comfort band can be shifted up to 2.2°C maximum (corresponding to an air speed of 1.6 m/s or higher) above the previous limit.

The presented formulas can, however, be used only when the outdoor running mean temperatures are between 10°C and 30°C, and for naturally ventilated buildings. In case these limits are not met, alternative formulas have to be used. For example, Barbadilla et al. [28] proposed a formula that can be used in Mediterranean climate for hybrid buildings (with intermittent use of air conditioning):

$$T_{comfort,Barbadilla} = 0.24 \cdot T_{rm} + 19.3°C$$

3.1.2 CIBSE's overheating assessment

The most complete methodology for the assessment of overheating is outlined by the CIBSE, the Chartered Institution of Building Services Engineers [29], mainly in the following documents:

- TM52 – "The limits of thermal comfort: avoiding overheating in European buildings" [30]
- TM59 – "Design methodology for the assessment of overheating risk in homes" [31]

TM52 defines three criteria, which are summarised as follows:

1. The number of hours during which the operative temperature exceeds the upper limit of the comfort band by more than 1°C shall not be more than 3% of the occupied summer hours (from the 1st of May to the 30th of September).

2. The weighted exceedance – defined as the sum over all occupied hours of the difference between the operative temperature and the upper limit of the comfort band – shall not exceed 6 degree-hours on any day during the summer period.

3. The operative temperature shall never exceed the upper limit of the comfort band by more than 4°C during the occupied hours.

A building is considered in overheating if it fails two or more criteria. The criteria are based on the comparison between the operative temperature inside the building and the upper limit of the comfort band, which is calculated based on the outdoor running mean temperature. The criteria are intended to be used for adaptive comfort evaluations in naturally ventilated or free-running buildings.

TM59, on the other hand, specifically describes the design methodologies for preventing overheating in residential units, outlining specific criteria for homes depending on the ventilation type.

For naturally ventilated homes, the criteria are:

1. For living rooms, kitchens, and bedrooms: the number of hours during May-to-September during which the internal temperature exceeds the comfort threshold by more than 1°C shall not exceed 3% of occupied hours.

2. During sleeping hours (10:00 pm to 7:00 am), the operative temperature in bedrooms must not exceed 26 °C for more than 1% of annual hours.

For mechanically ventilated homes, there is only one criterion, which requires a fixed maximum temperature of 26°C, that cannot be exceeded for more than 3% of annual occupied hours.

The CIBSE also published an additional document, the TM56 – "Resource efficiency of building services" [32] in which some overheating assessment strategies are presented in the scope of reducing the embodied and operational resource use for building services. Taking this into account, passive cooling and natural ventilation strategies are suggested in order to prevent overheating in buildings, but no specific assessment methodology is provided.

3.1.3 Heat waves and day-night temperature differences

Other overheating assessment strategies consider the response of the occupants to high peaks of temperature, related to the presence of low peaks on the same day and to the occurrence of multiple days of high peaks. The overheating stress is indeed higher if high temperatures are registered over multiple days, but it is lower when the high temperature day is isolated and when the cooler night temperatures allow the system to cool down. Two concepts can thus be related to this: the heat wave concept and the day-night temperature difference concept.

A heat wave is defined as several consecutive days during which the maximum temperatures exceed a high threshold. The number of days and the temperature threshold can be defined differently by different organisations, as summarised in Table 2.

Table 2 – Heat wave definitions in the literature

Organisation/paper	**Temperature threshold**	**Number of days**
WMO – World Meteorological Organisation [33]	$T_{max} > T_{max,avg} + 5°C$	≥ 5
UNDRR – United Nations Office for Disaster Risk Reduction [34]		≥ 2/3
IPCC AR6 WG1 Chapter 11 [35]	$T_{max} > T_{90th/95th/99th\ percentile}$	≥ 2/3
Climate-ADAPT [36]	$T_{max} > T_{max,\ 99th\ percentile\ May\text{-}September}$	≥ 3
Copernicus [37]	$T_{max} > T_{max,\ 90th\ percentile}$ $T_{min} > T_{min,\ 90th\ percentile}$	≥ 3

The day-night temperature difference improves the comfort, as the low night temperatures help occupants and buildings to cool down and reduce the stress caused by the high day temperatures. Night outdoor temperatures must fall below 24°C to provide this effect, according to a study by AIVC, the Air Ventilation and Infiltration Centre [38].

It can thus be concluded that a combination of high maximum temperatures over multiple days and of low temperature difference between day and night can highly impact the overheating stress of the occupants, and the number of days that belong to this definition can be used as a metric to quantify the overheating risk.

3.2 Overheating reduction passive retrofit strategies

In this paragraph, possible passive strategies for the reduction of overheating in indoor spaces are presented. Passive strategies include modifications of the building envelope components, such as the insulation of the opaque components or the improvement of the performance of the glazed part, through the use of double or triple glazing and of higher solar performance glasses, and of their usage, for example, connected with the opening of windows to increase natural ventilation. For the reduction of overheating, insulation of the building is usually not relevant, while strategies such as the decrease of the solar heat gain coefficient, the use of shadings or the increase of the natural ventilation are highly impactful methods, and will thus be described in the following sub-chapters.

3.2.1 Solar heat gain coefficient

Solar heat gain coefficient is the parameter that describes the summation of the solar transmitted and re-emitted from absorption radiation through a glass. Lowering this value thus reduces the solar gains in the room and has a positive effect in the summer season [39]. At the national level, the DM 26-06-2015 [7] sets a maximum value of 0.35 for the total glazing plus shading solar factor value.

The reduction in the solar heat gain coefficient can be achieved mainly in two ways: by reducing the SHGC value of the glazing itself or by adding shading devices. The latter will be more deeply analysed in the following sub-chapter, while as far as the glazing SHGC value is concerned, its reduction can be achieved by substituting the whole glazing system or by adding films on the existing glazing, which is particularly favourable for retrofit projects. Compared to the use of movable shadings to reduce the solar transmission, on the other hand, using glazing with reduced SHGC value or applying a low emissive film reduces the solar gains also in the winter season and might lower the satisfaction of the occupants in terms of visual comfort, as usually also the visible radiation is reduced with these technologies [40], [41].

3.2.2 Shading devices

Another option for reducing the solar gains in the summer season is the use of shading, which, as already mentioned in the previous paragraph, can also be movable and allow solar gains in the colder seasons. In general terms, shadings can be fixed or movable, and internal or external. There are then different kinds of shadings depending on the material and geometry. Movable shadings can also be manually or automatically activated, in the latter case by automated systems that follow specific schedules or rules. A high reduction of the solar gains can thus be achieved thanks to the use of shading devices, which are taken into account in the calculation of the total SHGC value [40].

3.2.3 Natural ventilation

Natural ventilation is another key passive technique for the reduction of overheating in internal spaces. Natural ventilation is the effect of exchanging air between the internal and external environment, thanks to buoyancy and wind-driven effects and provides multiple advantages in terms of thermal and Indoor Air Quality comfort. Natural ventilation can be used for conditioning the spaces, generating a saving in terms of energy consumption and cost and an improvement in the comfort of the users [42]. Studies on natural ventilation demonstrate that this technique allows for energy savings between 17% and 30% while maintaining comfort levels [25], [43].

Classrooms in southern European countries are usually naturally ventilated, but this results generally in poor ventilation rates [44], often below the requirements of 8 l/s/person set by

the EN 16798-1 regulation [45], especially during cold hours, which could be, on the contrary, exploited to cool down the spaces. A particular and very effective way of naturally ventilating buildings is indeed night-time ventilation, which allows the building's thermal mass to cool down during the night, colder hours, in order to provide a more comfortable environment during the day. Night-time ventilation is usually more effective in climates and seasons that present night temperatures around 20°C and a day-to-night temperature difference higher than 10°C, according to Givoni [46], who also determined the maximum external temperature for day-time ventilation to be around 28-32°C, and that day-time ventilation is more effective, thus in milder climates. When considering the implementation of night-time ventilation, the practical aspect also has to be considered, examining whether it is more convenient to implement an automated system for opening and closing the windows in the desired range of temperatures, or if other solutions provide the same effect in a more cost-effective way.

3.3 Overheating reduction active strategies

Active overheating reduction strategies include the use of active systems to cool down the spaces, for example, with the use of fans or other more energy-intensive systems.

3.3.1 Fan use and air movement

Air movement can be used as a strategy to improve the comfort of users in the hot periods, thanks to the improvement in the perception of the thermal environment connected to the increase in air speed. Different sources indeed confirm that increasing the air speed with the same temperature has a positive impact on the comfort of the users and also provides savings in the energy consumption and costs with respect to other cooling systems [47], [48]. According to Miller et al. [48] using ceiling fans can provide comfort to the users even with higher internal temperatures compared to usual air conditioning temperatures, and decrease the energy use, as summarised in Figure 4.

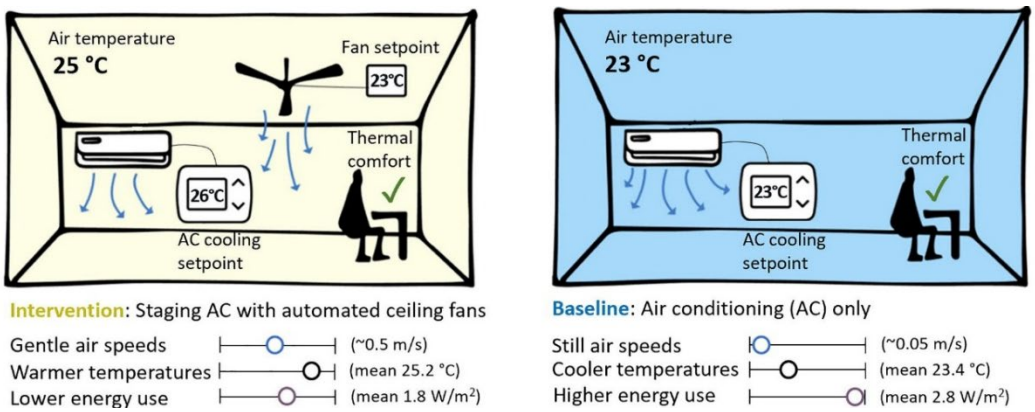

Figure 4 – Fan use advantages according to [48]

The energy savings are estimated at around 32% by a study from Kent et al. [47] (Figure 5).

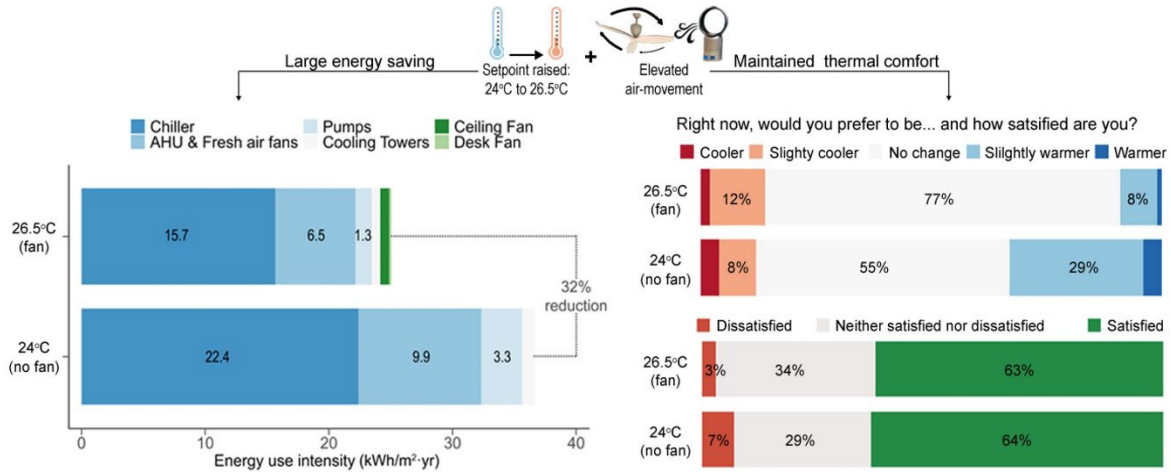

Figure 5 – Energy savings and comfort improvement with fan use according to [36]

3.3.2 Building systems for the reduction of overheating

In this sub-chapter, the state of the art for what concerns active building systems for the cooling of internal spaces is presented. The typologies of services that are present in the current school building stock are studied in order to estimate their performance and compare it to the performance of a possible improved system.

Building services typologies in the current school building stock are listed in the SNAES (Sistema Nazionale dell'Anagrafe dell'Edilizia Scolastica) open database [10], published by the Ministry of Education and Merit, that collects all data about the geographical localisation of schools, on their construction year and on some characteristics such as the dimensions, destination of use of spaces, accessibility and typology of heating system. The latter is used as a starting point to analyse the distribution of building systems typologies in Italian schools, and the results are described in the following paragraphs. The data for school systems, as presented in the following analysis, point out how active systems are usually present only for heating in school buildings, while cooling systems are often missing.

The SNAES database contains data from 61,307 State schools of all levels, encompassing the autonomous region of Valle d'Aosta. Data is provided by the local owner institution or managers, and the last update is from the scholastic year 2021-2022. The schools are classified with a code, and several files are provided for the different topics. As concerns the building services, and in particular the heating and conditioning systems, the database provides information that is summarised in the following chart (Figure 6). It can be seen that most of the buildings (88.6%) present a heating system, while only 1.3% does not have one, and for the rest (10.1%) this information is "not defined". Among the buildings that present a heating system, the typology of heating system can be selected. Most of them have a

methane plant, while other sources like diesel, district heating, GPL, solar thermal, and fuel oil are also used in smaller amounts, and some buildings are heated with electric heaters. Only 7.3% of the buildings present a conditioning and ventilation system. All the data is registered only if heating is registered: buildings without or with a "not defined" heating system don't present a definition of the type of system, with the only exception of the ventilation and conditioning system, which is present in four cases in which the heating system is not present or "not defined". Moreover, some buildings present multiple systems at the same time, probably meaning that parts of the school are served by different systems, or that, for example, the solar thermal plant is used in addition to another plant for backup.

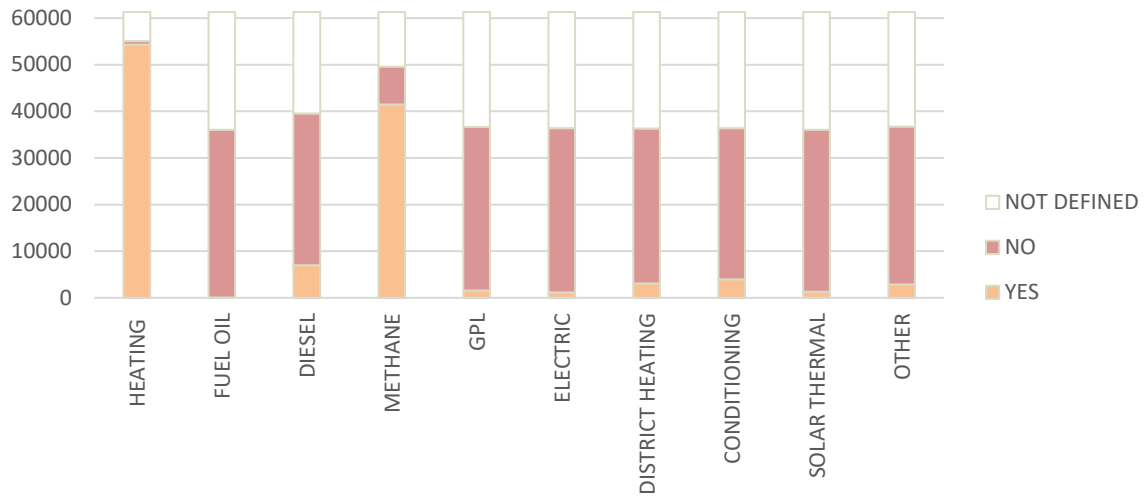

Figure 6 – Data for heating and conditioning systems for Italian schools according to SNAES [10]

The next chart (Figure 7) represents the intersection between the different features, clearly underlining that methane is the most used fuel for heating, but also that there are still intersections between the different fuel types, meaning that for some buildings, two or more fuels are declared.

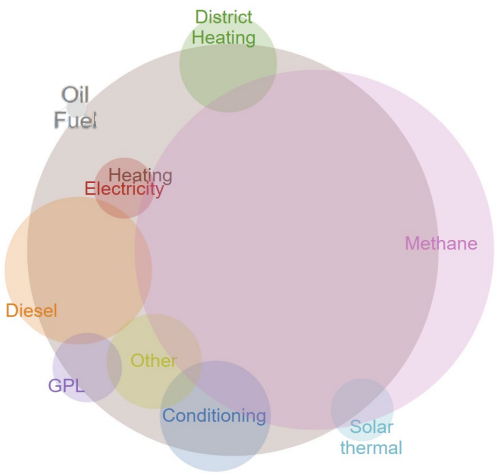

Figure 7 – Venn chart for the SNAES [10] data

The different heating sources are unevenly spread across the country's regions, as can be seen in Figure 8, which summarises the share of schools that adopt a certain heating source in the parts of Italy. It can be easily seen that the use of diesel fuel and of electric heating increases, both in absolute and relative value, in the southern regions and in the islands, and that District Heating is only present in the northern and central regions.

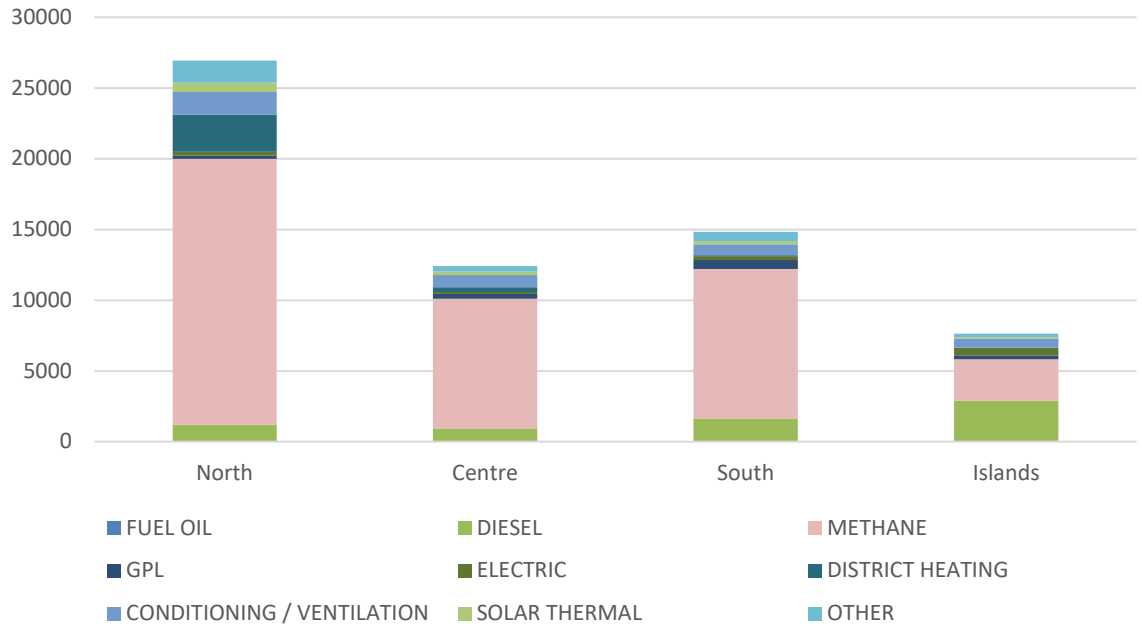

Figure 8 – Share of heating systems in the different parts of Italy

The next charts (Figures 9 and 10) show data for each heating system, presented as a share over the total number of heated schools, in each region. Again, the charts confirm that GPL and electricity are used primarily in the southern regions, that diesel is used mainly in the islands, and that district heating is used only in the north.

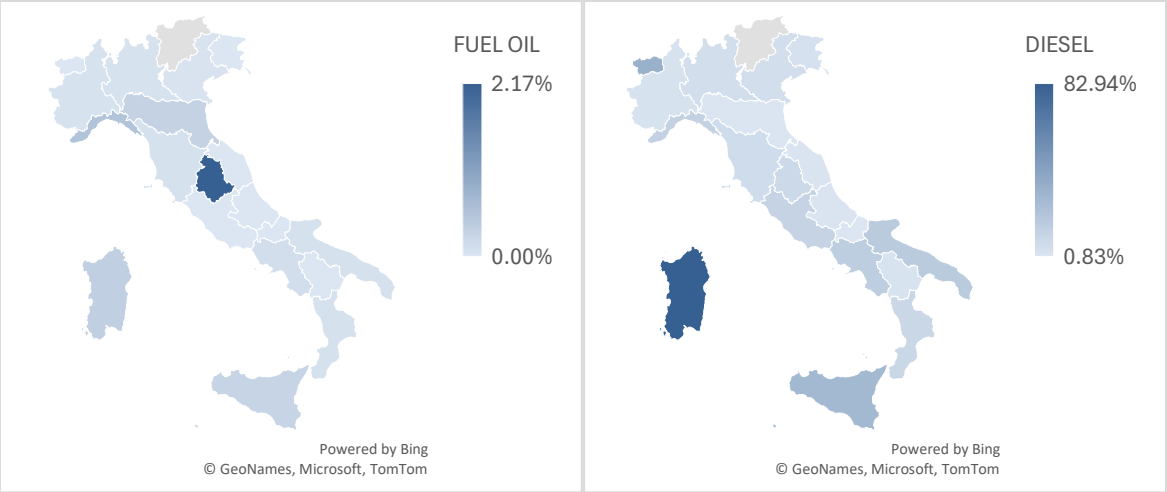

Figure 9 – Share of fuel oil and diesel heating systems per region

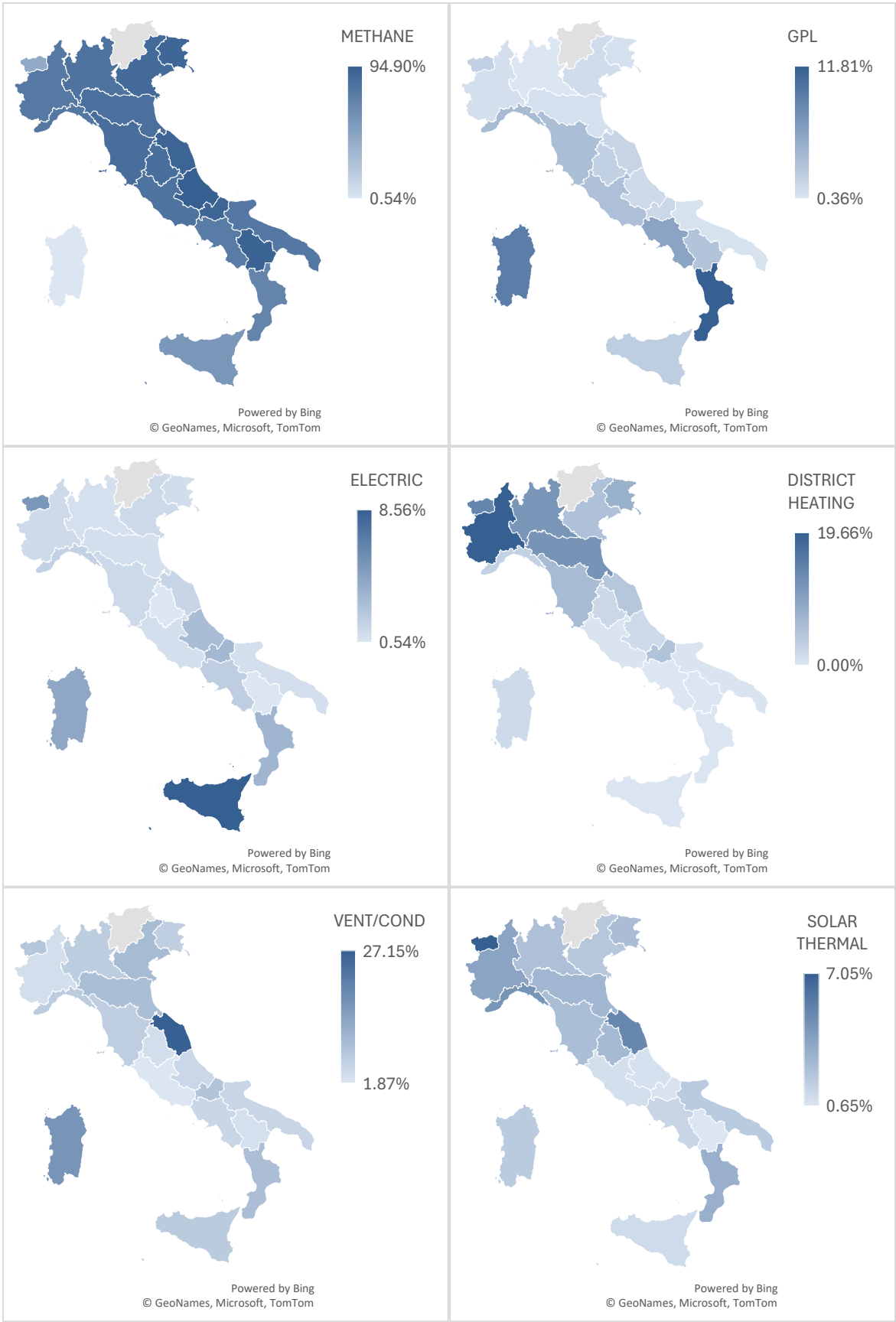

Figure 10 – Share of methane, GPL, electric, DH, ventilation and solar thermal systems per region

3.3.2.1 Building services typologies and dimensions at the regional level for Lombardy and Liguria

As the national database presented so far does not contain any information on the dimensions and consumption of the school building services, two regional datasets were analysed, in particular for the schools in Lombardy and Liguria, with data concerning the installed power in relation to the dimensions of the schools. The results of this preliminary assessment were included in deliverable 3.2 of the mentioned ReRoadS project.

In the next paragraphs, the characteristics of the two datasets, the cleaning process and the analysis results are presented.

Description of the datasets

The Lombardy dataset is downloaded from the CENED website, which collects information for all the buildings that undergo an Energetic Performance Certification (APE, Attestato di Prestazione Energetica), and that can be filtered for destination of use – E.7 is the label for educational buildings. This dataset contains all the geometric characteristics of the building (floor surface, volume, envelope surface), the climatic region, the energetic classification, the description of the renovation interventions and the description of the installed services, separated into winter climatisation, summer climatisation, domestic hot water, illumination, and renewable sources production.

Liguria's dataset contains the geometric characteristics, the climatic region, the energetic classification and the installed power of the services.

Datasets cleaning

First of all, the two datasets were cleaned following the same rules:

- Only unique buildings were considered (as some of the buildings were registered twice in the datasets)
- As far as the database for Liguria is concerned, only the buildings classified as active school buildings were considered
- The geometric characteristics were filtered, deleting the zeros and outliers about the volume, the floor surface, the floor height and the number of floors
- The buildings without a construction date were deleted
- The outliers for the installed power were deleted

Following these rules, the datasets were reduced from a total of 4478 school buildings to 2710 for Lombardy and from 1679 to 547 for Liguria.

Datasets analysis

For both datasets, the installed power of the systems was analysed, first of all, by describing the average of all the considered schools.

Lombardy's database presents the distinction between the summer and winter climatisation plants, and also the possibility of two different plants for each category. The installed power can thus be analysed considering the average power per unit of heated floor area, and the chart in Figure 11 is created. It can be clearly seen that cooling is only provided through heat pumps, while the other plant types are only used for heating.

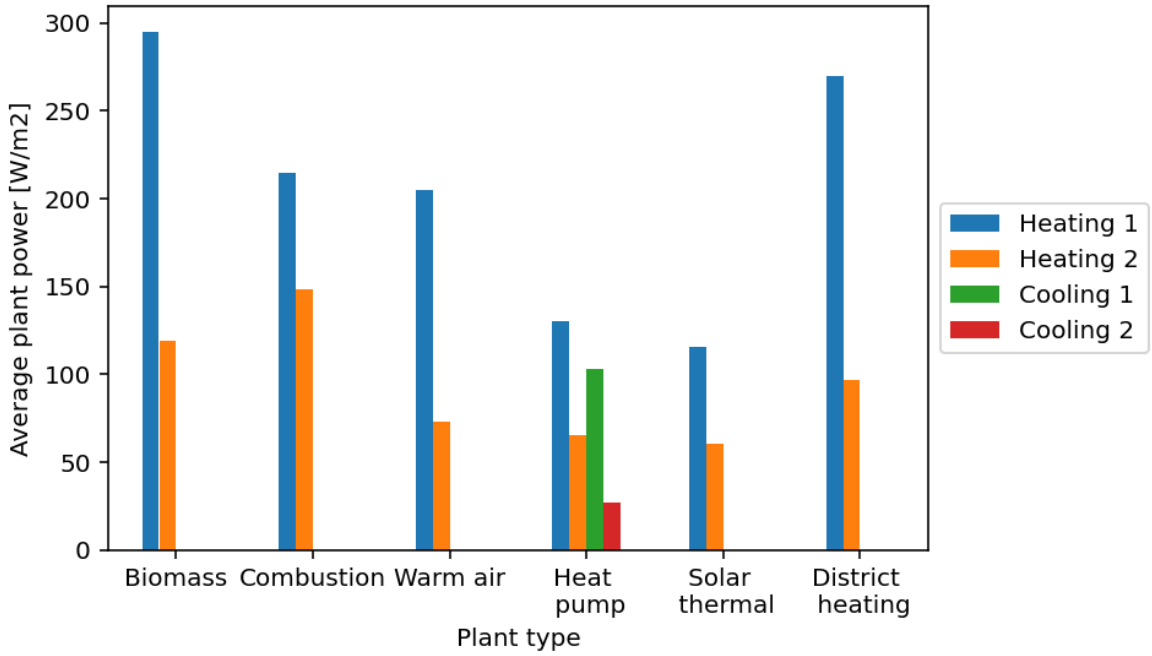

Figure 11 – Average plant power per plant type (Lombardy)

As only a few buildings present cooling plants, and as in Liguria's dataset, this data is not provided, the two pieces of information are separated, and first, the heating plant is analysed.

Dataset analysis – Heating plants

In general, the distribution of the power per unit of heated floor area is described in the following chart (Figure 12). In comparison, Liguria's heating power median (147.23 W/m^2) is similar to Lombardy's heating power median (148.36 W/m^2), and the same can be said for the second and third quartile distribution, but data from Liguria presents a wider distribution for what concerns the fourth quartile distribution, with some cases that reach values three times higher than the third quartile limit.

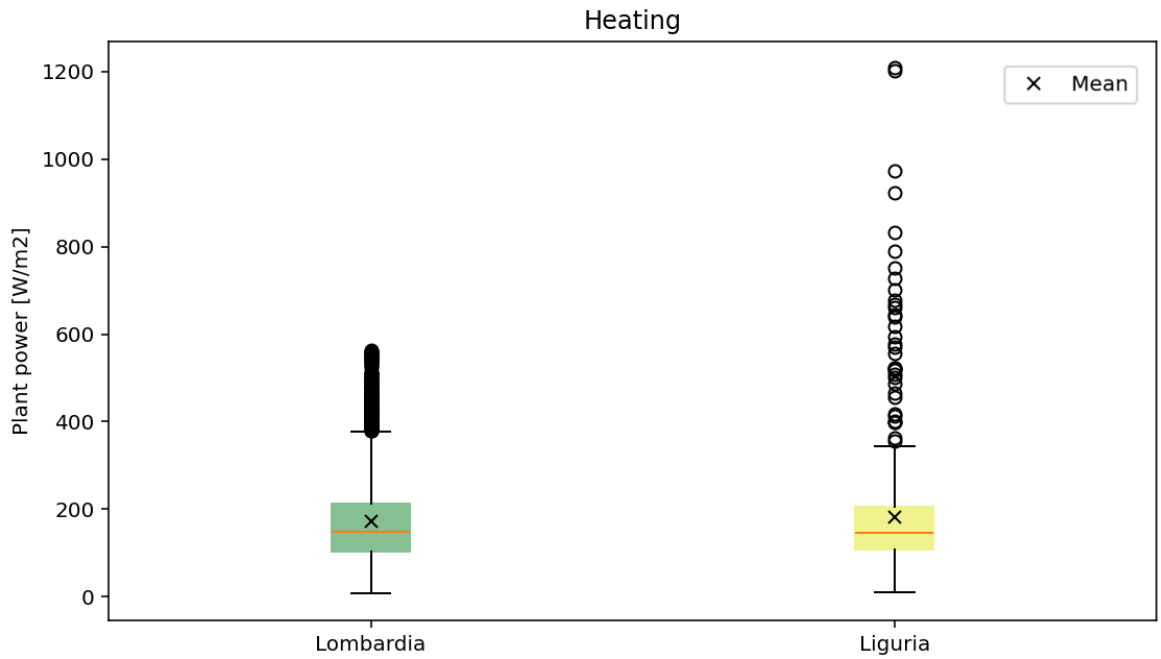

Figure 12 – Plant power distribution for school heating plants in Lombardy and Liguria

Figure 13 shows the relationship between the heating power and the heated surface for the two regions.

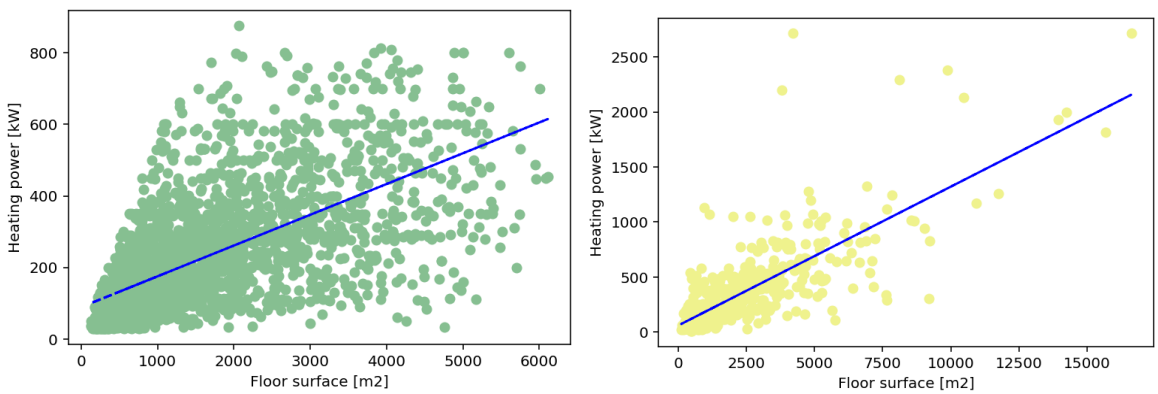

Figure 13 – Heating power per floor surface in Lombardy (left) and Liguria (right)

It is nevertheless useful to further filter the considered dataset, as the power of the installed plants strongly depends on the performance of the building, which is described by the energetic class. Some of the factors that influence this are also the year of construction and the climatic zone.

In the next chart (Figure 14), the distribution of buildings in the different energy classes for the Lombard and Ligurian dataset is displayed. Most of the Lombard schools are classified in the C, D and E categories, while the vast majority of schools in Liguria belong to energetic classes lower than D and especially to class G. This can be because the Lombard dataset is downloaded from the CENED website and thus represents the buildings that have undergone

an energy certification, and that hence improved their performance. It is decided to concentrate on the F and G categories, to which most of the Italian school buildings belong.

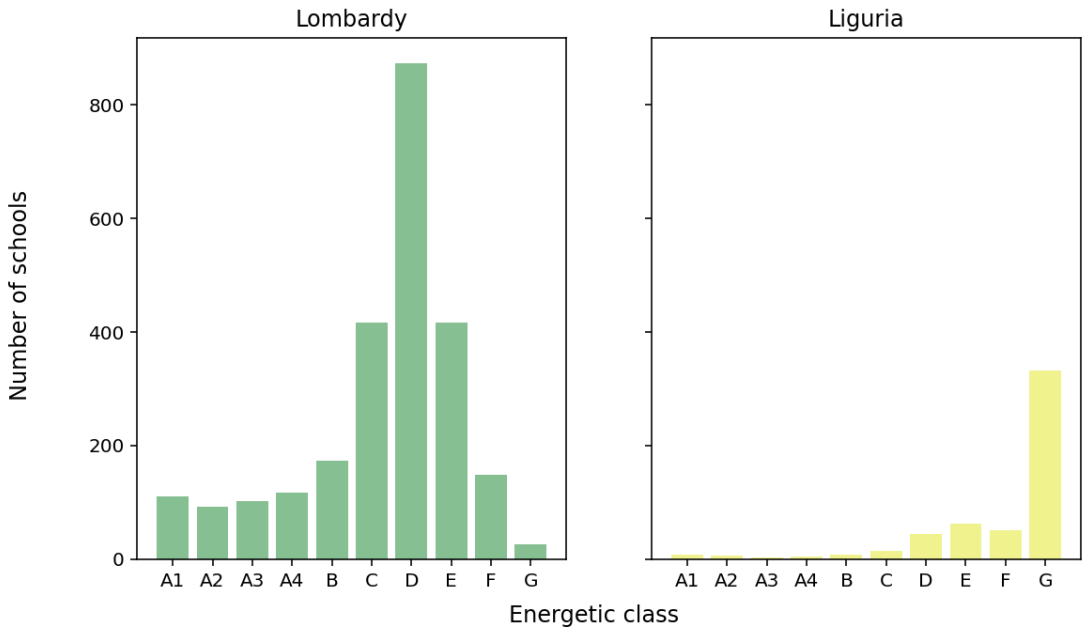

Figure 14 – Energetic class distribution of school buildings in Lombardy (left) and Liguria (right)

As concerns the climatic region, the distribution is displayed in Figure 15. Schools in Lombardy are only located in zone E and F, while in Liguria they are mainly located in zone D, with some in zones C and E and very few (6) in zone F. This also justifies the different distribution in the energetic classification seen in the previous chart, as buildings in colder climates are more probable to be refurbished than the ones in milder climates.

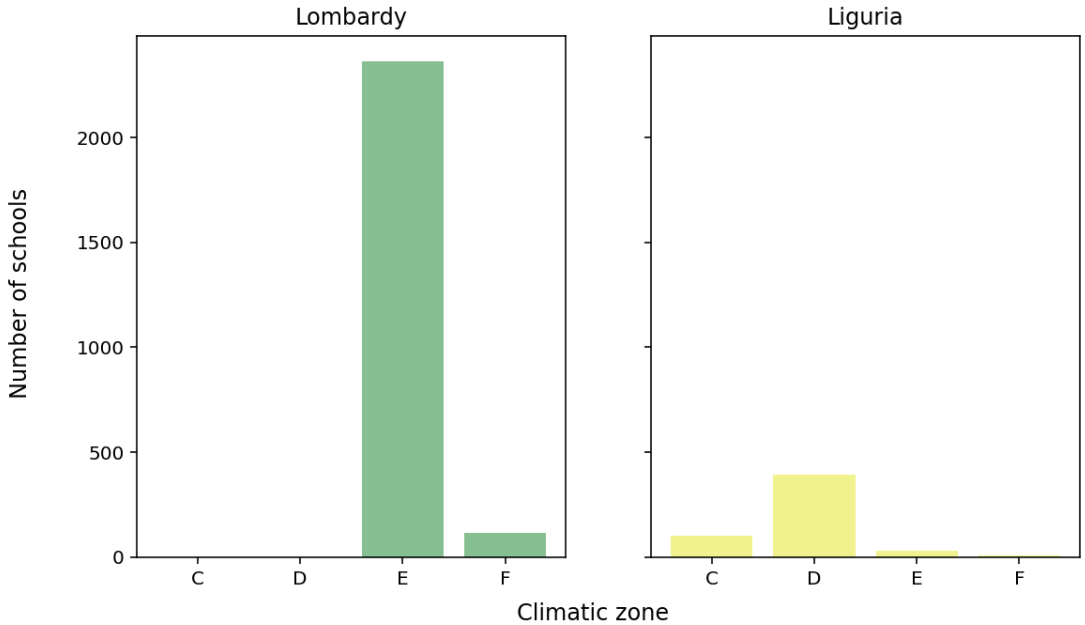

Figure 15 – Climatic zone distribution of school buildings in Lombardy (left) and Liguria (right)

As concerns the year of construction, the following plots (Figure 16) describe the distribution of schools based on the year of construction, dividing them into seven main categories, which are defined in the CENED database and represent important changes in the Italian built environment: 1976, 1992 and 2006 are the years in which building performance regulations were published ([11], [49], [50]), while the previous three categories are defined based on the relation with the historical events.

- schools built before 1930,
- schools built in the period 1930-1945,
- schools built in the period 1946-1960,
- schools built in the period 1961-1976,
- schools built in the period 1977-1992,
- schools built in the period 1993-2006,
- schools built after 2006

It can be seen that schools in Lombardy were mostly built in the periods 1961-1976 and 1977-1992. On the other hand, in Liguria, a lot of schools were built before 1930 and then in the 1961-1976 period.

In the charts, the histogram represents the number of buildings with the same year of construction, and the blue line represents the cumulative percentage of buildings built in each period, while on top of the chart, the number of schools built in each period is displayed.

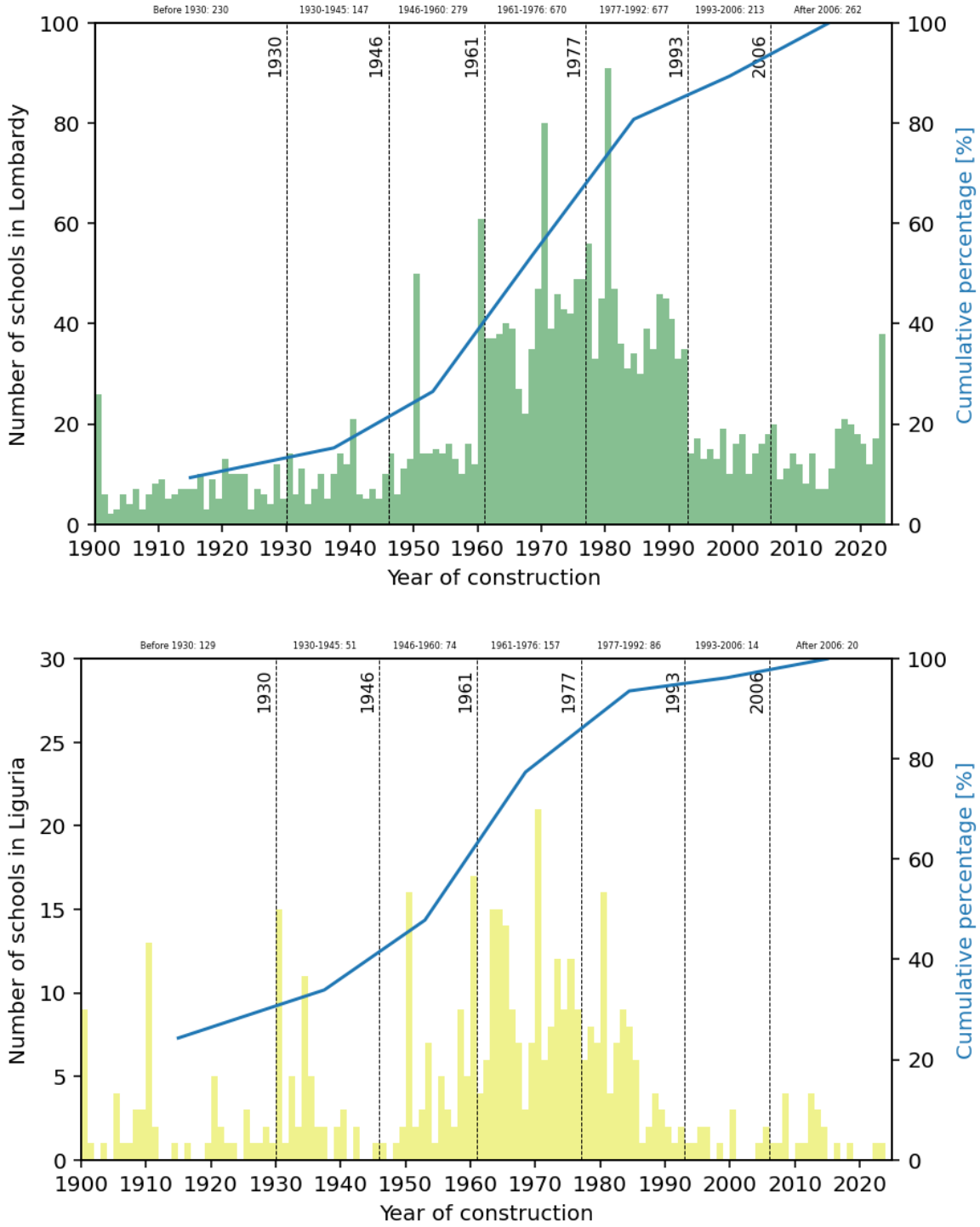

Figure 16 – Year of construction distribution of school buildings in Lombardy (top) and Liguria (bottom)

Considering only the F and G categories and separating for climatic region, the power data presented in the first chart is updated as follows (Figure 17). Comparing the data from Lombardy with the one from Liguria, it can be seen that the power per unit of surface for climatic zones E and F are similar, but with a narrower distribution for Liguria. It can be seen that, as regards buildings in Liguria, the median heating power per heated surface

increases in the colder climatic zones, but it decreases in climatic zone F, and the same happens also for the buildings in Lombardy.

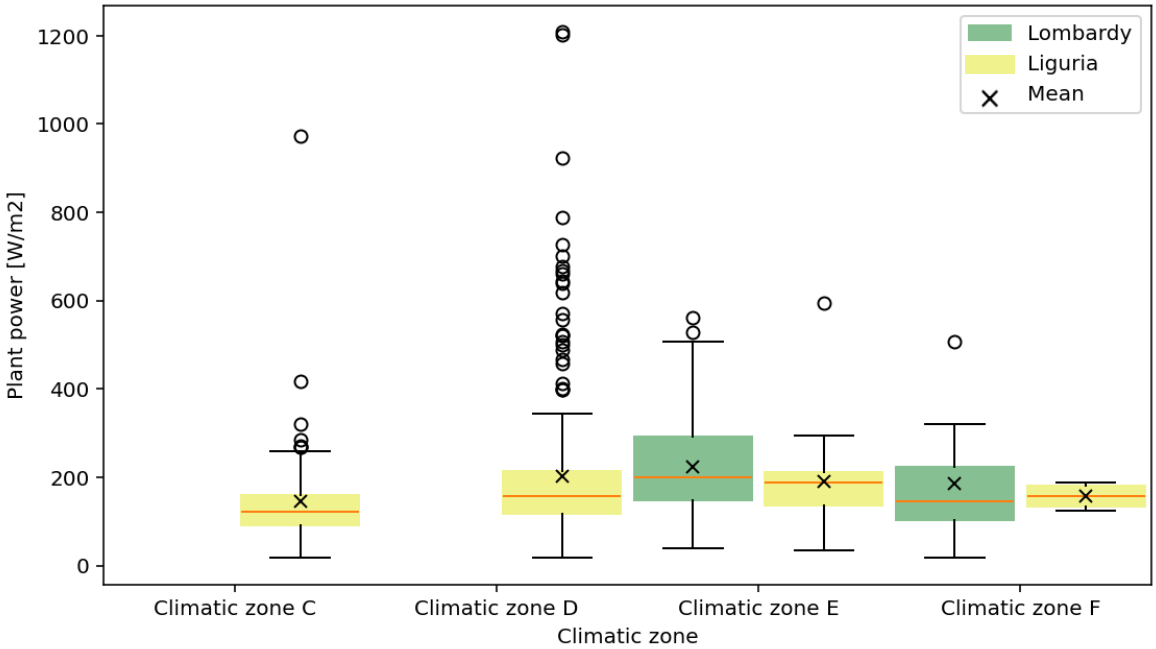

Figure 17 – Heating plant power per climatic zone in Lombardy and Liguria

The slight decrease in the heating power per surface in the colder climatic zone can be justified if it is considered that probably the buildings in climatic zone F present a better insulated envelope, which allows for a decrease in the heating emitted by the plant. This could be demonstrated by looking at the year of construction of the buildings, as schools built in more recent years present a better performance of the envelope, or, if the buildings have been renovated in recent years, looking at the average transmittance of the envelope, which should be lower for the schools in a colder climate. The reduced dimensions of the dataset and the availability of data, though, didn't allow us to obtain this information.

As concerns the year of construction, as seen in Figure 18, the heating power seems to be quite stable through the years, with some variations in the last period, in which, though, the number of buildings is very limited.

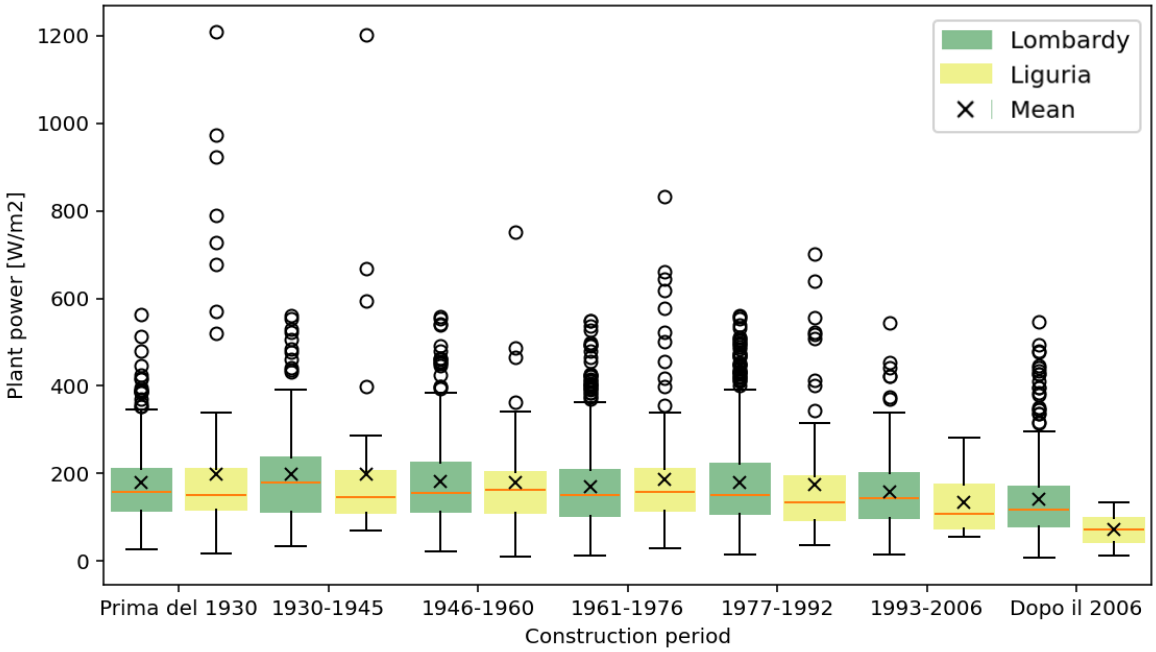

Figure 18 – Heating plant power per period of construction in Lombardy and Liguria

Dataset analysis – Cooling plants

In this paragraph, only data for Lombardy is analysed, as Liguria's dataset does not provide any data for cooling plants. In Lombardy, just 8.7% of the schools do not have a heating plant, while 84% do not have a cooling plant, with power distribution shown in Figure 19.

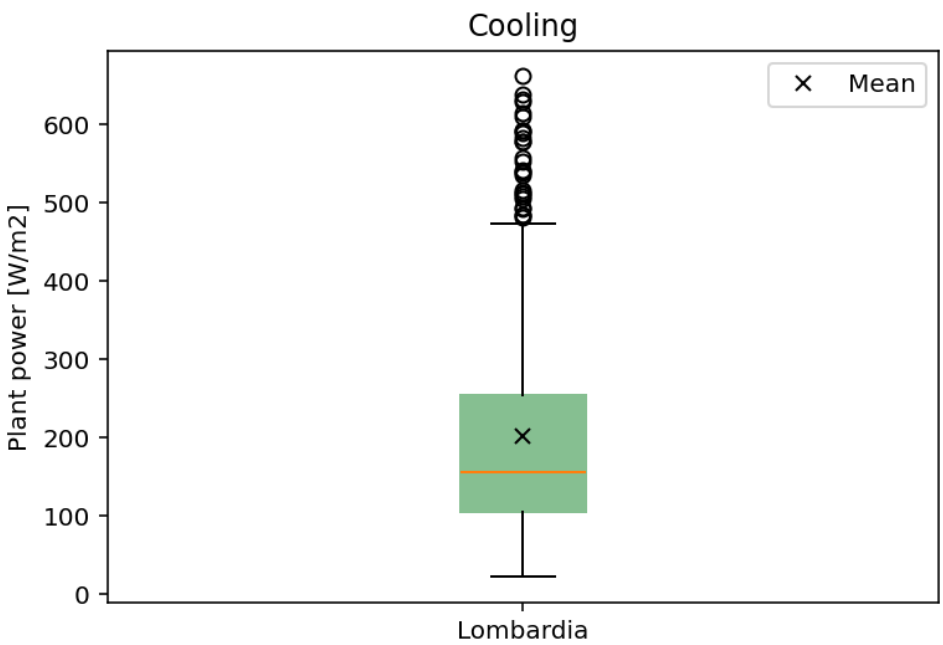

Figure 19 – Cooling plant power distribution for Lombardy

The following chart (Figure 20) shows the relationship between the cooling power and the cooled floor area.

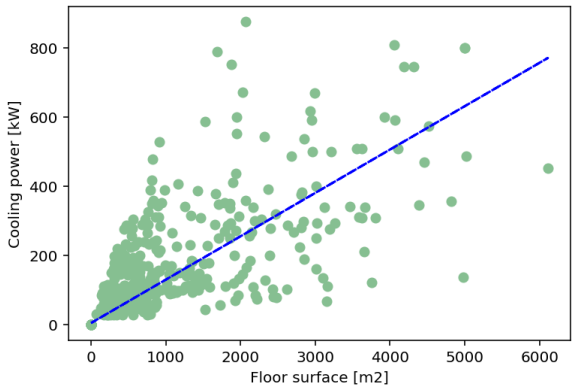

Figure 20 – Cooling power per floor surface in Lombardy

Considering only the F and G categories and separating for climatic region, the power data presented in the first chart is updated as follows (Figure 21). As it is seen clearly in the graph, none of the schools located in climatic zone F presents a cooling plant, while it is present only in a few of the schools located in climatic zone E.

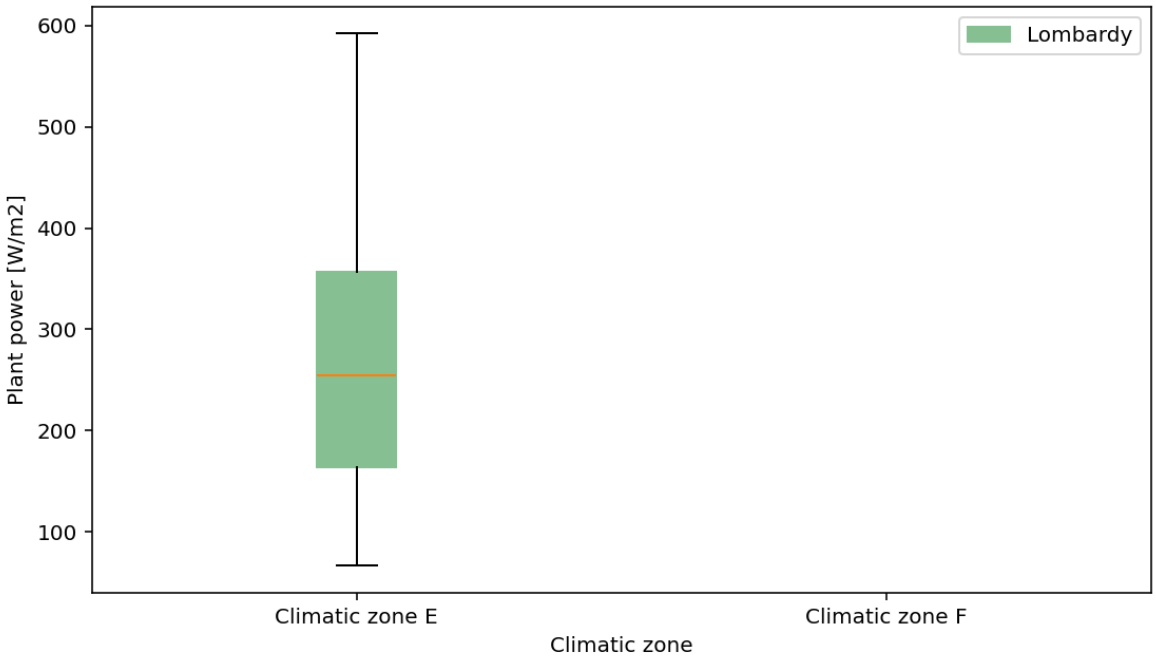

Figure 21 – Cooling plant power per climatic zone in Lombardy

3.3.2.2 Retrofit building services typologies

The possible strategies that can be used to retrofit building services are described in this paragraph, following the guidelines published by ENEA [2]. The potential interventions range from the maintenance to the introduction or improvement of the control system, or to the partial or complete substitution of the plant. The strategies are listed and described in the

following paragraphs, starting from the most economical one and moving towards the more expensive ones.

Maintenance of the system

To improve the efficiency of a system, it is often sufficient to just ensure the correct maintenance and cleaning of the components. Replacing leaking ducts and cleaning filters can improve both the efficiency and the users' comfort in an indoor environment, as the systems can work at maximum performance and provide the service they were designed for, improving the satisfaction of the occupants [51].

Control systems

Usually, the control systems used in school buildings are thermostatic valves that regulate the sending of heat based on the requirement of the user, with a very simple physical mechanism. The introduction of those systems can greatly improve the energy efficiency of the heating system, as well as the comfort of the users. It is seen that just regulating the setpoint temperature allows a reduction of at least 40% for heating (with a decrease of 3°C in the setpoint, from 22°C to 19°C) and of approximately 50% for cooling (with an increase from 23°C to 26°C in the setpoint) [52].

Another option presented by the ENEA guidelines [2] is to add a Building Energy Management System (BEMS), as it has been proven by different studies that it helps to drastically reduce the energy consumption, for example, with an estimated reduction of the energy consumption of 50% by Kamali et al. [53]. The BEMS can control the heating and cooling plants, the ventilation system, the domestic hot water production and the lighting, and are particularly effective to guarantee comfort and optimise the performance, especially in refurbished buildings.

BEMS use sensors that detect the temperature of the room, along with other parameters like the relative humidity and the quality of the air. Those systems can also be connected through the Internet of Things (IoT), and machine learning models can be trained in order to derive the response of the users and their comfort state based on a variety of variables, and thus act on the heating and conditioning system to regulate the comfort. It has been demonstrated in different studies that this strategy not only improves the comfort, which in school buildings is a fundamental requirement, but also increases the energy efficiency by an average of 15% and up to 50%, as found in a literature review work by the author [54].

When considering the addition of control systems, the education of the users, who in the case of schools are teachers but also students, must be taken into account, to allow a correct use of those systems.

The improvement due to the addition of a control system can be evaluated with the UNI EN ISO 52120-1:2022 ("Energy performance of buildings. Contribution of building automation,

controls and building management. General framework and procedures") [55], which presents a simplified and a detailed method for the evaluation of control systems' impact on building performance.

Replacement or addition of system components

It is also possible to replace or add some of the components of the heating plant. Replacements can be operated at the generation, distribution and emission systems, while changes in the control system have already been discussed. These changes are discussed in the next paragraphs.

1. Replacement in the generation system

It is possible to substitute the main heating system, e.g. the boiler, with a more efficient plant. Some of the options are represented by condensing boilers, which also retrieve heat from the water vapour in the exhaust fumes, or heat pumps. Substituting the generation plant in an existing building, nevertheless, requires the renovation of the thermal and electrical systems and thus high costs, especially when a boiler is substituted by a heat pump.

If a condensing boiler is used, higher performances (106-107% [2]) can be reached. In addition to this, solar thermal plants can be added to the system to contribute to the heating of water with a renewable energy source and thus consume less energy. De Santoli et al. [56] report a calculation of payback time for the replacement of the boiler with condensing boilers in some case study schools in Rome, concluding that the payback time depends on the share of volume of retrofitted plant.

For the same purpose, heat pumps can be employed, also coupled with renewable energy exploitation plants such as PV [57]. Usually, heat pumps are electricity-powered, and the most common ones use air as a cold source, even if water and soil can also be used, with a consequent minor dependence on the climatic conditions. The heat pump can be used, besides heating and DHW, also for cooling, and in this way, the return time of the investment is shortened. To optimise the use of heat pumps in a school building, Deng et al. [58] identify some possible typical problems and solutions by studying the operation of two school buildings in China. It is seen that the main methods to optimise the heat pump performance are applying control strategies, adding a storage system to decouple demand and supply, adding frequency converters for water pumps to increase their efficiency and bypasses for unused heat pumps.

If heating is provided with a ventilation system, some improvements can be made, for example, adding a heat exchanger to the outlet system, to retrieve part of the heat, with efficiencies that can reach 80-90%.

If the electrical plant is also considered, cogeneration plants (CHP – Combined Heat and Power) can become an option, as the combined production of heat and electricity enhances

the efficiency of the whole building system. Cogeneration plants provide the production of electricity as a primary output and heat as a byproduct of the enthalpy of the waste gases. It is indeed clear that this process is very efficient and reduces the emissions of additional gases. The heat can be used both in the winter season for heating and in the summer season, as trigeneration (CCHP – Combined Cooling, Heat and Power) can be implemented for the absorption of heat and consequent production of cooling energy. This technology is particularly effective for big schools with pools and gyms that are also used outside of school hours.

In the end, the generation systems can be enhanced with the production of renewable sources. In the case of schools, the most suitable renewable energies are photovoltaic, solar thermal and wind power. Photovoltaic systems are more efficient in the southern regions and with specific tilt angles, and can be easily integrated on the roofs of buildings, or sometimes also on the façades. Solar thermal plants are, on the other hand, capable of transforming solar energy directly into thermal energy; they are cheaper than photovoltaic systems and have a short return period.

2. Addition of a summer cooling system

As presented in the introduction of the thesis and demonstrated with some analysis on the considered datasets in the previous subchapter, only 10% of Italian schools currently present a cooling system [19]. The addition of a summer climatisation plant would improve both the air quality management, with a reduction in the heat gains, and the thermal comfort of students during the hotter months, which are constantly growing due to global warming.

3. Replacement in the distribution system

Apart from maintaining the pipes and ducts, the distribution system can be improved by adding valves and circulation pumps with inverters to regulate the mass flow based on the requested heat load.

4. Replacement in the emission system

The efficiency of a heating system can also be improved by substituting the emission plant with a lower operating temperature one, for example, with floor heating. Reducing the temperature of the radiant element, indeed, enhances the performance of the generation plant, as for example, heat pumps work better with lower emission temperatures, boiler systems consume less to heat up water at a lower temperature and also district heating is more efficient at lower temperatures. It is nevertheless true that changing the emission system is highly expensive, as it requires massive work on the building, and this can be done only if it implies major improvements.

Chapter 4 – Methodology

In this chapter, the methodology used to develop and test the tool is presented. The tool aims at studying the phenomenon of overheating in Italian schools, identifying the key parameters that affect it and the possible mitigation strategies. The tool can be used to identify the schools that cannot guarantee comfort during the summer period, and to what extent, also considering the variations that our climate is currently undergoing and that will tend to increase the mean temperatures in the coming years.

The tool is built thanks to simulations performed with the IESVE environment and its Python API, in order to simulate a batch of files in which the key parameters are changed. In the following paragraphs, the model used to carry out the simulations is described, both in terms of the IESVE model and of Python code. The IESVE shoebox model is described, along with the variations that are performed on the envelope characteristics and the results extraction and elaboration. Additionally, the methodology used to analyse the impact of certain passive strategies and of different weather scenarios is described, and then, the methodology used to prepare the results visualisation tool is provided. In the end, the model is validated through the comparison of the results with other simulation software results and a sensitivity analysis and an analysis on the impact that changing a model assumption, specifically the starting day of the year for the simulations, are performed.

4.1 Model description

First of all, a shoebox classroom is created in IES-VE, with dimensions 9x6 meters, for a resulting floor area of 54 m^2, and with a height of 3.5 meters. The classroom is located in a building, composed of three floors, with total dimensions of 27x12 meters, 9 meters high. The insertion of the room in the building is done to make sure that, during the variations done through the API, the window area is set only on one side of the classroom. The whole building, except for the classroom, is modelled in IESVE as an "Adjacent building", and there are thus no heat exchanges between the room and the rest of the building, as this definition determines adiabatic conditions between the spaces – the temperature is always equal, and there are thus no heat exchanges. Six cases are considered mainly, varying the position of the classroom with respect to the building: classroom at the ground level, in the middle and on the top floor, both in the middle and corner positions. The corner position cases present windows on both of the exposed sides, but with the same window-to-floor ratios as in the middle cases. For the corner classrooms, the exposition is classified based on the main window's exposition, considered the one on the largest side, and with the other window placed as follows (main/second window): south/east, west/south, north/west,

east/north. The corner configuration is simulated even though it is not very diffused in the Italian building stock, being usually the corner classrooms configured as the middle position ones, only with one window.

The overall layout of the test reference building for the middle floor, middle position classroom is displayed in Figure 22.

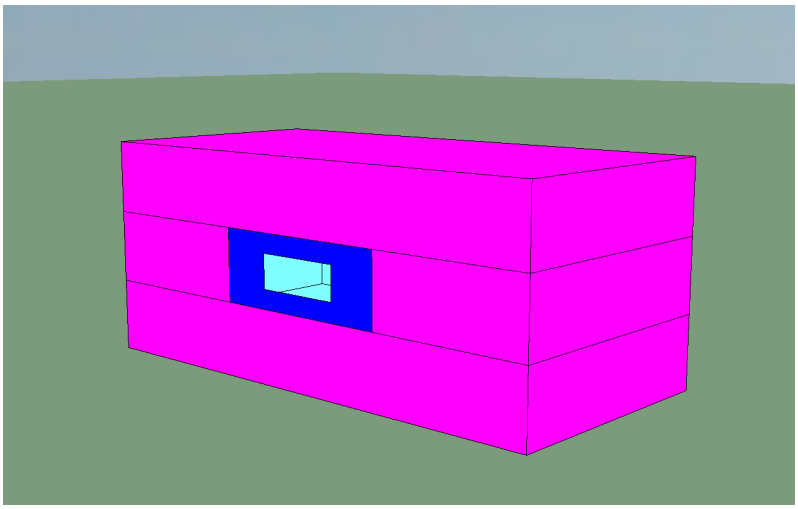

Figure 22 – IES-VE model

4.1.1 Loads

The model is defined by setting the following characteristics:

- No heating/cooling loads, the building is modelled as a free float building, and internal temperatures are not affected by any kind of building service
- Occupancy load is defined according to EN ISO 7730, setting an occupancy rate of 2 m^2/person, sensible gain 90 W/person, latent gain 60 W/person and an occupancy profile that follows the working hours, from Monday to Friday, 8 AM through 6 PM
- Lighting load is set to 10 W/m^2, with a profile that follows the occupancy profile
- Ventilation rate is set to 8 l/s/person, according to EN 16798-1 [45], with a profile that follows the occupancy profile. A second set of simulations is also run with a lower ventilation rate, corresponding to 1.20 ACH, as it is seen that in most of the cases the required levels of natural ventilation are not accomplished, especially in the cold periods.
- Infiltration rate is set to 0.5 air changes per hour, with a constantly ON profile. In the cases with refurbished windows, this value is reduced to 0.25 ACH.

4.1.2 Constructions

The constructions used in the model are specified in this sub-chapter. For both internal partitions and envelope constructions, the stratigraphies are created taking into account the state of the art of the Italian school building stock. In the first paragraph, the internal partitions and ceiling/floor constructions are described, then the base-case and the improved case envelope stratigraphies are discussed. Different envelope configurations are indeed simulated, considering a base-case modelled with simple stratigraphies without insulation and a single-glazed window, and some improved cases, with the addition of insulation on the external wall and roof or with the substitution of the glass with double-glazing. The base-case model is defined with basic constructions, modelled according to UNI TR 11552 [59], to reach the conduction values summarised in Figure 23, which contains the typical values of insulation of basic stratigraphies in the state of the art of the buildings, elaborated from UNI TS 11300 [60] values comparing the transmittance values indicated by TABULA [61] and URBEM [62] projects.

	Typology	Insulation	U-value [W/m² K].
Walls	Cavity wall	Not insulated	1.10
Roof	Flat roof	Not insulated	1.35
	Reinforced concrete-brick	Insulated	1.01
Internal slab	Reinforced concrete-brick	Not insulated	1.30
Ground floor slab	Ground floor on pilotis or ventilated crawl space	Not insulated	1.30
Window	Single glazing	-	6.00
	Double glazing Air filled	-	3.60

Figure 23 – Conduction values table

4.1.2.1 Internal partitions and ceiling/floors stratigraphies

The internal partitions of the building are modelled with a single layer of 100 mm bricks, with plaster on both sides. The internal floor slab is modelled as a SOL04 (Figure 24 [59]), with a U-value of 1.30 W/m^{2}K. In the figure, as also in the figures reported for the envelope constructions, the thickness combination that allows reaching the desired U-value is highlighted. Table 3 summarises the stratigraphy of the internal partitions and their characteristics. The thickness of the layers has been determined in order to satisfy the U-value requirements specified in Figure 23, using the thicknesses highlighted in each figure. In some cases, the conductivity of the layer had to be set according to the layer's resistance specified in the UNI TR 11552. In these cases, the conductivity was determined in order to get the desired U-value of the finished stratigraphy. Those values are highlighted in red. It must be in the end noted that, for the materials for which a Specific Heat Capacity was not determined, UNI TR 11552 assumed a value of 1000 J/kgK, and thus the same value is used for the modelling of the stratigraphies in this study, but it has to be taken into account that this has consequences on the thermal mass of the building.

Table 3 – Internal partitions stratigraphy

	Thickness	Conductivity	Density	Specific Heat Capacity
	mm	W/mK	kg/m³	J/kgK
XXX – Internal partition				
Int. plaster	20	0.700	1400	1000
Hollow brick	120	0.600	800	1000
Int. plaster	20	0.700	1400	1000
SOL04 – Internal floor/ceiling				
Int. flooring	15	1.470	1700	1000
Grout	20	1.400	2000	1000
Cast concrete	120	0.580	900	1000
Grout	20	0.700	2000	1000
Cast concrete	40	0.700	2400	1000
Brick + concrete	240	0.700	900	1000
Plaster	20	0.900	1800	1000

SOL04 - Solaio in laterocemento – blocchi non collaboranti, esempio 1- [3]

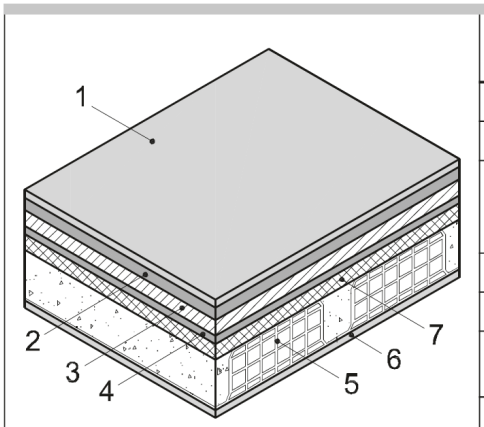

Strato	d [cm]	ρ [kg/m³]	c [J/(kg K)]	λ [W/m K]	R [m²K/W]
1 Pavimentazione interna - gres	1,5	1700	1000	1,470	-
2 Malta di cemento	2	2000	1000	1,400	-
3 Massetto in calcestruzzo alleggerito	2 6 12	400 900 1400	1000	0,580	-
4 Malta di cemento	2	2000	1000	-	0,330-0,370 a)
5 Calcestruzzo armato	4	2400	1000		
6 Soletta (blocchi di laterizio+travetti in calcestruzzo)	16-24	900	1000		
7 Intonaco esterno	2	1800	1000	0,900	-

Descrizione (spessori in cm)	U [W/(m² K)]			κ_i [kJ/(m² K)]	Y_{ie} [W/(m²K)]
	Fl.ascendente	Fl.discendente	Fl.orizzontale		
1,5 - 2 - 2 – (2 + 4 + 16) - 2	1,81	1,61	1,72		
1,5 - 2 - 2 –(2 + 4 + 24) - 2	1,69	1,51	1,61		
1,5 - 2 - 6 – (2 + 4 + 16) - 2	1,61	1,45	1,54		
1,5 - 2 - 6 –(2 + 4 + 24)- 2	1,51	1,37	1,45		
1,5 - 2 -12 – (2 + 4 + 16) - 2	1,38	1,26	1,33		
1,5 - 2 -12 – (2 + 4 + 24) - 2	1,31	1,20	1,26		

NOTA 1 A titolo esemplificativo si ipotizza una pavimentazione in gres ceramico.

a) Resistenza termica ricavata secondo la norma UNI 10355.

Figure 24 – SOL04 stratigraphy

The internal partitions are considered adiabatic, and this is achieved in the IESVE model through the introduction of the surrounding building, defined as “adjacent building”.

4.1.2.1 Base-case envelope stratigraphies

In the base-case, the wall stratigraphy MCV01 is chosen, as in Figure 25 [59] with a U-value of 1.10 W/m^{2}K, and the roof is modelled as COP01 (Figure 26 [59]), with a U-value of 1.35 W/m^{2}K. The ground floor is modelled as SOL04 (Figure 24 [59]), with a U-value of 1.30 W/m^{2}K, to which an equivalent insulation layer is added to model the effect of the ground, calculated according to EN ISO 13370 [63].

MCV01 - Muratura a cassa vuota in laterizio forato, esempio 1- [1]

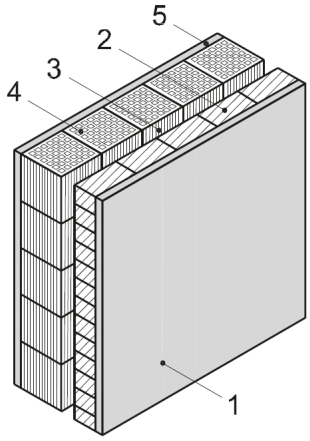

Strato	d [cm]	ρ [kg/m^3]	c [J/(kg K)]	λ [W/m K]	R [m^{2}K/W]
1 Intonaco interno	2	1400	1000	0,700	-
2 Mattoni forati	8 12	800	1000	-	0,200 a) 0,310 a)
3 Intercapedine d'aria	2,5/30	-	-	-	0,180 b)
4 Mattoni forati	12 25	800	1000	-	0,310 a) 0,890 a)
5 Intonaco esterno	2	1800	1000	0,900	-

Descrizione (spessori in cm)	U [W/(m^2 K)]	κ_i [kJ/(m^2 K)]	Y_{ie} [W/(m^{2}K)]
2 – 8 – 2,5/30 – 25 – 2	0,67	**52,5**	**0,127**
2 - 12 - 2,5/30 - 25 - 2	0,62	**52,4**	**0,089**
2 - 8 - 2,5/30 - 12 - 2	1,10	**57,9**	**0,594**
2 - 12 - 2,5/30 - 12 - 2	0,98	**57,4**	**0,417**

a) Resistenza termica ricavata secondo la norma UNI 10355.

b) Resistenza termica ricavata secondo la norma UNI EN ISO 6946.

Figure 25 – MCV01 stratigraphy

COP01 – Copertura piana non praticabile, esempio 1- [3]

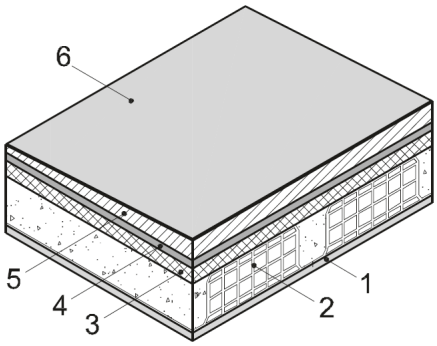

Strato	d [cm]	ρ [kg/m³]	c [J/(kg K)]	λ [W/m K]	R [m²K/W]
1 Intonaco interno	2	1400	1000	0,700	-
2 Soletta (blocchi di laterizio+travetti in calcestruzzo)	16 24	900	1000	-	0,330-0,370[a)]
3 Calcestruzzo armato	4	2400	1000		
4 Malta di cemento	2	2000	1000		
5 Massetto in calcestruzzo ordinario	2-12	2000	1000	1,060	-
6 Membrana impermeabilizzante bituminosa	1	1200	1000	0,170	-

Descrizione (spessori in cm)	U [W/(m² K)]			κ_i [kJ/(m² K)]	Y_{ie} [W/(m²K)]
	Fl.ascendente	Fl.discendente	Fl.orizzontale		
2 – 16 – 4 – 2 – 2 – 1	1,74	1,55	1,65		
2 – 16 – 4 – 2 – 6 – 1	1,63	1,46	1,55		
2 – 16 – 4 – 2 – 12 – 1	1,49	1,35	1,43		
2 – 24 – 4 – 2 – 2 – 1	1,62	1,46	1,55		
2 – 24 – 4 – 2 – 6 – 1	1,53	1,38	1,46		
2 – 24 – 4 – 2 – 12 – 1	1,41	1,28	1,35		

a) Resistenza termica ricavata secondo la norma UNI 10355.

Figure 26 – COP01 stratigraphy

The stratigraphies used in the base-case model are thus summarised in Table 4, with the layers listed from the outside to the inside. The stratigraphies are reported from the external to the internal layer, and the same clarifications of Table 3 are applicable.

Table 4 – Base-case stratigraphies

	Thickness	Conductivity	Density	Specific Heat Capacity
	mm	W/mK	kg/m³	J/kgK
MCV01 – External cavity wall				
Ext. plaster	20	0.900	1800	1000
Hollow brick	120	0.600	800	1000
Air gap	120	-	-	-
Hollow brick	80	0.260	800	1000
Int. plaster	20	0.700	1400	1000
COP01 - Roof				
Bitumen	10	0.170	1200	1000
Cast concrete	120	0.380	2000	1000
Grout	20	1.400	2000	1000
Cast concrete	40	1.700	2400	1000
Brick + concrete	240	1.500	900	1000
Int. plaster	20	0.700	1400	1000
SOL04 – GROUND FLOOR				
U-value correction	116.4	0.050	550	1000
Cast concrete	10	1.400	2000	1000
Cavity				
Brick + concrete	240	1.900	900	1000
Cast concrete	20	1.400	2000	1000
Cast concrete	120	0.580	1400	1000
Cast concrete	20	1.400	2000	1000
Gres	15	1.470	1700	1000

4.1.2.2 Improved envelope stratigraphies

Then, improved cases are also modelled, considering the addition of an insulation layer to the external walls and to the roof, with a thickness that enables reaching the limit U-value, according to the Decreto Requisiti Minimi 2025 [64], that reports different requirements for each climatic zone. The requirements are reported in Table 5, while Table 6 reporst the improved stratigraphy of the constructions with the insulation layer thickness for climatic zones A+B/C/D/E/F. The insulation layer is highlighted in red for clarity. For the improved cases, only the refurbishment of walls and roofs was considered, as the ground one is less diffused.

Table 5 – U-values [W/m²K] requirements for building envelope components according to DM 28-10-2025 [64]

Climatic zone	External walls	Roofs	External floor slabs
A and B	0.43	0.35	0.44
C	0.34	0.33	0.38
D	0.29	0.26	0.29
E	0.26	0.22	0.26
F	0.24	0.20	0.24

Table 6 – Improved stratigraphies

	Thickness	Conductivity	Density	Specific Heat Capacity
	mm	W/mK	kg/m³	J/kgK
MCV01b – External cavity wall with external insulation				
Ext. Insulation	48/70/85/100/110	0.034	200	840
Ext. plaster	20	0.900	1800	1000
Hollow brick	120	0.600	800	1000
Air gap	120	-	-	-
Hollow brick	80	0.260	800	1000
Int. plaster	20	0.700	1400	1000
COP01b – Roof with external insulation				
Ext. Insulation	73/80/105/130/145	0.034	200	840
Bitumen	10	0.170	1200	1000
Cast concrete	120	0.380	2000	1000
Grout	20	1.400	2000	1000
Cast concrete	40	1.700	2400	1000
Brick + concrete	240	1.500	900	1000
Int. plaster	20	0.700	1400	1000
SOL04b – Ground floor with insulation				
Ext. Insulation	50/65/90/105/115	0.034	200	840
U-value correction	116.4	0.050	550	1000
Cast concrete	10	1.400	2000	1000
Cavity				
Brick + concrete	240	1.900	900	1000
Cast concrete	20	1.400	2000	1000
Cast concrete	120	0.580	1400	1000
Cast concrete	20	1.400	2000	1000
Gres	15	1.470	1700	1000

4.1.2.3 Window stratigraphies – base-case and improved case

In the base-case, the window glazing is modelled as single-glazed, while in the improved case it is modelled as double-glazed.

The base-case single glazing is modelled as a "PLANILUX 4mm.SGG" glass from WINDOW LBNL 7.8 [65], with the characteristics described in Figure 27, resulting in a U-value of 5.75 W/m²K and a Solar Heat Gain Coefficient of 0.87.

	ID	Name	Mode	Thick	Flip	Tsol	Rsol1	Rsol2	Tvis	Rvis1	Rvis2	Tir	E1	E2	Cond	Comment
Glass 1	21021	PLANILUX 4mm.SGG	#	4.0	☐	0.849	0.076	0.076	0.900	0.081	0.081	0.000	0.840	0.840	1.000	

Figure 27 – Base-case single glass characteristics

The improved case glazing is modelled as a double-glazing, with two clear float glasses and an argon cavity, with the characteristics described in Figure 28, resulting in a U-value of 2.59 W/m²K and a Solar Heat Gain Coefficient of 0.75.

	ID	Name	Mode	Thick	Flip	Tsol	Rsol1	Rsol2	Tvis	Rvis1	Rvis2	Tir	E1	E2	Cond	Comment
Glass 1	21023	PLANILUX 6mm.SGG	#	6.0	☐	0.817	0.074	0.074	0.892	0.081	0.081	0.000	0.840	0.840	1.000	
Gap 1	2	Argon		16.0												
Glass 2	21023	PLANILUX 6mm.SGG	#	6.0	☐	0.817	0.074	0.074	0.892	0.081	0.081	0.000	0.840	0.840	1.000	

Figure 28 – Improved case double-glazing system characteristics

In the following paragraph, the parametric tool is described, and the variations on the emissivity of the glazing system are specified.

4.2 Parametric tool script

The tool VEScripts is used to write a Python code, accessible in a few months at the link https://github.com/biancavigioli/Overheating-parametric-tool, that accesses the IES-VE model, modifies some parameters according to defined rules, simulates the model, extracts the results in terms of indoor and outdoor temperature and elaborates the data to identify overheating situations. The IESVE 2024 version is used, as the 2025 version returns an error when trying to run SunCast simulations through the VEScripts tool.

4.2.1 Model variations

To study the effect of overheating in different school configurations, three main characteristics are identified to be the most impactful: the window-to-floor ratio, the orientation of the window and the window glazing's solar heat gain coefficient. These parameters have to be changed for each of the combinations listed in the previous sub-chapter and for a set of chosen locations. Moreover, all the simulations are performed for two natural ventilation scenarios, considering in one case the minimum required ventilation (8 l/s/person) and in the other case a value of 1.2 ACH, as presented in the Loads subchapter. Therefore, four nested *for* loops are created, in the order:

- Location loop
    - Natural ventilation loop
        - Envelope construction loop (base, wall refurbishment, window refurbishment and roof refurbishment only for top floor rooms)
            - Simulation parameters loop

Each batch of simulations includes the 2 ventilation cases, the 3 or 4 (in the case of the top floor rooms) envelope configurations and the 48 parameter configurations (6 window-to-floor ratio values, 4 orientations and 2 solar performance values). Each simulation lasts around 10 seconds, and with the simulations being 288 (2x3x48) or 384 (2x4x48), the duration of each batch run is around 48 or 64 minutes. In total, 36 batches are simulated, corresponding to the 6 geometric cases and the 6 locations. Indeed, each geometric case has to be created as a separate model in IESVE, and for what concerns the location it was noticed

that a change in the location operated thanks to the method described in the following paragraph has an effect on the thermal simulation (Apache) but does not propagate to the Suncast simulation, returning an error for the mismatch between the two simulations that have to be run each time.

4.2.1.1 Location loop

The location is changed through the VELocate.set(location_dictionary) method, with the latitude, longitude, altitude, location denomination and weather file defined in a location dictionary. The locations are selected to represent the six Italian climatic zones (Table 7 and Figure 29). Weather files are considered from the closest airports to the selected city, with the 2009-2023 time-period.

Table 7 – Climatic zones and locations

Climatic zone	City	Latitude	Longitude	Elevation	Weather file
A	Lampedusa	35.50°	12.62°	21 m	Lampedusa
B	Palermo	38.18°	13.10°	34 m	Palermo Falcone e Borsellino
C	Napoli	40.88°	14.29°	72 m	Napoli Capodichino
D	Roma	41.95°	12.50°	24 m	Roma Urbe
E	Milano	45.44°	9.28°	108 m	Milan Linate
F	Cuneo	44.38°	7.54°	534 m	Cuneo Levaldigi

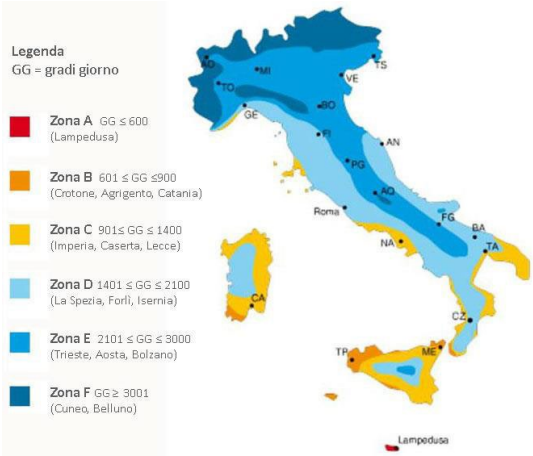

Figure 29 – Italian climatic zones based on the Degree-Days

4.2.1.2 Natural ventilation loop

In the second layer of iterations, the natural ventilation rate is accessed and modified to simulate two different scenarios. To modify the ventilation rate, first of all two ventilation profiles are created in the thermal template, and during the simulation the ventilation is changed by adding the new profile and removing the old one, with the VETemplate.add_air_exchange(project.air_exchange[NEW]), for adding the new profile, and the VETemplate.remove_air_exchange(project.air_exchange[OLD]) for removing the old one.

4.2.1.3 Envelope construction loop

The opaque envelope constructions (walls and roof) are assigned through the VEBody.assign_construction(construction, surface) method, which requires the desired construction ID and the surface to which the construction has to be assigned to. The construction has to be already created in the IES-VE model, and it is assigned according to the required refurbishment. The window construction is assigned in the simulation parameters loop, as the Solar Heat Gain Coefficient is one of the variables to be analysed. In this external loop, only the number of glass layers is determined, and this information is then used in the internal loop, coupled with the information about the SHGC value. The possible window constructions are indeed 4:

- Single glazing → clear glass
  → low-emissive glass
- Double glazing → clear glass
  → low-emissive glass

4.2.1.4 Simulation parameters loop

The simulation parameters, namely the orientation, the window-to-floor ratio and the window solar heat gain coefficient, are then accessed through a VEScript method, and have to be processed as follows:

- The window-to-floor ratio must be expressed in terms of window-to-wall ratio, as this parameter can be changed through the API. It is thus necessary to calculate the window-to-wall ratio according to the following formulas, starting from the given window-to-floor ratio:

$$WWR = \frac{window\ area}{wall\ area} = \frac{WFR \cdot floor\ area}{wall\ area}$$

The floor and wall areas are extracted from the model through the VEBody.get_areas() method. Window-to-wall ratio is assigned with VEGeometry.set_percent_wall_glazing(#).

- The orientation of the window can be changed by changing the orientation of the whole building, using the VEGeometry.set_building_orientation(value) method.

- The window glazing's solar heat gain coefficient can be changed by changing the whole window construction, assigning to each case a window construction that presents the required SHGC and glazing stratigraphy (single or double). The method VEBody.assign_construction_to_opening(construction, wall, opening) is used to assign the window construction. The construction to be assigned has to be already created in the IES-VE model, and it is assigned according to the desired SHGC value.

Moreover, when changing the glazing construction, the infiltration rate also has to be changed, as a lower infiltration rate corresponds to the double-glazing technology. This change is operated in a similar way with respect to the change in natural ventilation rate, using the VETemplate.add_air_exchange(project.air_exchange[NEW]), for adding the new infiltration profile, and the VETemplate.remove_air_exchange(project.air_exchange[OLD]) for the old infiltration profile. Both the profiles need to be previously created in the IESVE template manager. At this stage, the possible values that the input parameters can assume are also defined, and those are presented as follows, also with the corresponding meaning in terms of simulation.

As far as the window-to-floor ratio is concerned, values between 1/8 (12.5%) and 22% have been chosen, as the 1/8 value is the one required in the regulations (DM 5/7/1975 [66]), with an interval of 2%. As the IES-VE API only accepts integer percentage values, the following array of possible values has been selected: [0.12, 0.14, 0.16, 0.18, 0.20, 0.22]. For the orientation, the four cardinal directions are chosen. In IES-VE, the orientation of the building can be set by specifying an angle of rotation of the north. In the considered case, the value 0° corresponds to the north pointing in the opposite direction with respect to the position of the room and of the window, and the other cases are described in Table 8.

Table 8 – Orientation values

Orientation in the IES-VE model [°]	Cardinal direction of the window
0	S
90	W
180	N
270	E

For what concerns the SHGC values, a high (around 0.8) and a low (around 0.35, value required by the regulations) value are chosen. These are obtained by creating two stratigraphies for each configuration (single and double-glazed), and those are summarised in Table 9.

Table 9 – Glazing stratigraphies

	Thick. [mm]	Cond. [W/mK]	Gas	Tsol [-]	Rsol1 [-]	Rsol2 [-]	E1 [-]	E2 [-]	SHGC [-]	U-value [W/m²K]
Single Clear	4	1		0.849	0.076	0.076	0.840	0.840	0.87	5.75
Single LowE	4	1		0.241	0.463	0.441	0.840	0.840	0.35	5.76
Double clear	6	1		0.817	0.074	0.074	0.840	0.840	0.75	2.59
	16		Argon							
	6	1		0.817	0.074	0.074	0.840	0.840		
Double LowE	6	1		0.360	0.200	0.239	0.840	0.840	0.33	1.22
	16		Argon							
	6	1		0.664	0.142	0.128	0.081	0.846		

In the end, thus, for each of the geometrical cases defined at the start, all the possible combinations of location, model configurations (refurbished or not) and simulation parameters (WFR, orientation and SHGC) are assigned one by one to the model and simulated as explained in the following chapters. The assigned variables are:

- Location → climatic zone
- Model configurations:
    - Wall: base-case or insulated
    - Roof: base-case or insulated (only in cases in which the room is on the top floor)
    - Ground floor: base-case or insulated (only in the cases in which the room is on the bottom floor)
    - Window: single or double
- Simulation parameters:
    - Window-to-floor ratio: 0.12 / 0.14 / 0.16 / 0.18 / 0.20 / 0.22
    - Orientation: south, east, north, west
    - Solar Heat Gain Coefficient: low (0.33 / 0.35) or high (0.75 / 0.87)

4.2.2 Model simulation

After defining the parameters, first a SunCast simulation is run in order to redefine the shadows and solar incidence after the changes in the geometry and orientation. Then, the Apache simulation is also run, with the SunCast link enabled in order to take into account the performed simulation.

4.2.3 Results extraction

The results are then extracted in terms of indoor and outdoor temperatures, with the get_weather_results("Temperature", "Dry-bulb temperature) method for the outdoor temperature and get_room_results(VEBody.id, "Room air temperature&Room radiant temperature", "Operative temperature (TM 52/CIBSE)", "z") method for the indoor operative temperature.

4.2.4 Results elaboration

The results are, in the end, elaborated to obtain a final output in terms of temperature and overheating risk. The main analyses represent the frequency and the cumulative frequency distribution of temperatures, the share of hours in the comfort bands, the compliance with the TM52 criteria and the share of heat stress days calculated according to the definition of heat wave and of day-night temperature difference. These parameters are described in the next paragraphs.

4.2.4.1 Comfort bands

The share of hours in the different comfort category bands, calculated according to EN 16798-2:2019 [26], is plotted. Starting from the outdoor temperature in the seven previous days, the running mean temperature is calculated with the formula:

$$T_{rm} = (1-\alpha) \cdot (T_{-1} + \alpha \cdot T_{-2} + \alpha^2 \cdot T_{-3} + \alpha^3 \cdot T_{-4} + \alpha^4 \cdot T_{-5} + \alpha^5 \cdot T_{-6} + \alpha^6 \cdot T_{-7})$$

That, using α = 0.8, as in EN 16798-2:2019 [26], results to be:

$$T_{rm} = (T_{-1} + 0.8 \cdot T_{-2} + 0.6 \cdot T_{-3} + 0.5 \cdot T_{-4} + 0.4 \cdot T_{-5} + 0.3 \cdot T_{-6} + 0.2 \cdot T_{-7})/3.8$$

The comfort temperature is calculated as:

$$T_{comfort} = 0.33 \cdot T_{rm} + 18.8°C$$

And the number and share of hours that belong to each comfort band, calculated as in Table 10, are assessed.

Table 10 – Comfort categories equations

Category	Lower boundary	Upper boundary
Low		$T_{comfort} - 5°C$
Lower III	$T_{comfort} - 5°C$	$T_{comfort} - 4°C$
Lower II	$T_{comfort} - 4°C$	$T_{comfort} - 3°C$
I	$T_{comfort} - 3°C$	$T_{comfort} + 2°C$
Higher II	$T_{comfort} + 2°C$	$T_{comfort} + 3°C$
Higher III	$T_{comfort} + 3°C$	$T_{comfort} + 4°C$
High	$T_{comfort} + 4°C$	

According to the regulations [26], at least 95% of the hours must be in a comfort category for the building to be classified in that category.

The comfort categories are calculated for separate periods of the year, in order to identify the possible issues in the thermal behaviour or the building and provide the user with possible strategies to tackle the overheating problem in the different periods, and define the necessary actions. Considering that the study is carried out and the tool is built for use in Italian schools, and considering that in Italy heating is allowed only in certain periods and that school buildings present a particular occupational schedule over the year, the following periods are considered:

- From the beginning of January to the end of the heating season (that is different for each climatic zone)
- From the end of the heating season to the end of the school period (usually at the beginning of June)
- From the end of the school year to the beginning of the school year, during summer (usually from June to September)
- From the beginning of the school year to the beginning of the heating season (that is different for each climatic zone)
- From the beginning of the heating season to the end of the year

The end and beginning of the heating season for each climatic zone are summarised in Table 11.

Table 11 – End and start of the heating season for each climatic zone

Climatic zone	End of the heating season	Start of the heating season
A	15th of March	1st of December
B	31st of March	1st of December
C	31st of March	15th of November
D	15th of April	1st of November
E	15th of April	15th of October
F	-	-

As no limits are provided for climatic zone F, the same dates as for climatic zone E are assumed, in a conservative approach. For what concerns the start and end of the summer break, the 15th of June and the 15th of September are used, based on the current school calendar in Italy.

For each of those periods, the share of hours in the comfort bands is calculated and plotted.

4.2.4.2 Frequency and cumulative frequency of temperatures

The difference in temperature between indoor and outdoor is computed to create its cumulative frequency chart, and to be able to compare different scenarios from a graphical point of view. In this way, the comparison between the different case studies results in being easier, as well as the one between ventilated and non-ventilated buildings, and possible renovation strategies and their impact can be evaluated.

4.2.4.3 TM52 compliance criteria

A function, moreover, is created to identify the hours in which the indoor temperature exceeds the maximum comfortable temperature and calculate the overheating risk in the selected scenario according to TM52.

The maximum temperature allowed is calculated for each day, considering the second category of comfort, which corresponds to "Normal level of expectation" and is usually used for typical buildings:

$$T_{max} = 0.33 \cdot T_{rm} + 18.8°C + 3°C$$

Then, the indoor operative temperature is compared to the maximum allowed temperature and the three criteria defined in the TM52 are evaluated as follows:

1. For the first criterion, the percentage of hours in which $T_{op} > T_{max} + 1°C$ is calculated. Only non-heating occupied hours are considered, filtering the temperature array and considering only the values that correspond to months between the end and beginning of the heating season, except for August, days from Monday to Friday and hours from 8 AM to 6 PM.

2. For the second criterion, for the occupied non-heating days in which the operative temperature is higher than the maximum temperature, daily degree hours of exceedance are calculated, and the percentage of days in which this value is higher than 6°C is calculated.

3. For the third criterion, the number of non-heating occupied hours in which the operative temperature is higher than the maximum temperature by more than 4°C is calculated, and its percentage over the non-heating occupied hours is computed.

In the end, the overheating risk is evaluated, considering that if two or more of the criteria are not met, the room is in overheating. The first criterion is not met if the calculated percentage is above 3%, while the second and third ones if the calculated percentage is not null.

The calculated percentages for the three criteria are exported along with the identification of the overheating possibility, in order to highlight the possible reduction of the overheating risk in the different scenarios.

Moreover, the same evaluation is also performed considering a higher air speed in the building (1.2 m/s), increasing the maximum acceptable temperature by 2 °C.

4.2.4.4 Heat stress days evaluation

In the end, an assessment of the heat stress days is performed, according to the definition of heat wave defined in the previous chapters. The building is considered to be in overheating according to the heat wave definition if the following conditions are met:

- The registered temperature exceeds the limit:
    - The internal temperature exceeds the threshold value according to the adaptive calculations (considering the II category of comfort)

    OR

    - The external running mean temperature exceeds the 30°C limit, above which the adaptive comfort equation can't be used

AND

- Ventilation is not feasible to cool down the internal spaces, meaning that, at each timestep of the considered day:
    - The external temperature is higher than the internal one
    - The external temperature is higher than the minimum threshold for the category (II)

AND

- The described conditions are met for at least three consecutive days

To identify the overheated days, thus, first of all, the days in which the temperature threshold is exceeded are identified based on the first two conditions. On an hourly basis, then, the timesteps at which the ventilation can be useful to cool down the building are identified, and the relative day is removed from the overheated ones if ventilation is feasible at all timesteps. Among those, the isolated heat stress days or the two-consecutive days are removed, and according to this definition, the share of heat stress days is calculated over the different periods.

4.3 Additional passive strategies analysis

Some additional passive strategies are also added to the study, in order to verify the potential overheating lowering and provide schools with data regarding the possible increase in the comfort of the users with the use of those strategies. Two main additional strategies, shadings and night-time natural ventilation, are considered, and the methodology regarding their study is described in the following sub-chapters.

For these additional cases, only part of the configurations is analysed. Simulations are performed only for the cases of classroom in the central position of the floor, avoiding the ones with classroom at the angle, which is much less diffused, and only for two extreme cases of window-to-floor ratio, 12% and 22%, as it is seen from the sensitivity analysis that this parameter is the least influencing one and that changing this value at a 2 percentage

points step is redundant. The total number of simulations for the 6 climatic zones is thus 1920 for each of the cases (2 shading cases and 1 night-ventilation case).

4.3.1 Shadings

As regards the shading analysis, the ERA_6 (Elementary Renovation Actions) shadings were used. This ERA considers the installation of externally mounted louvres for the reduction of solar gains. Two inclination configurations are simulated, with 0° and 45° inclination, with the solar transmission factors summarised in Table 12.

Table 12 – Transmission factor values for 0° and 45° inclinations

Incident angle	**0°**	**15°**	**30°**	**45°**	**60°**	**75°**	**90°**
0° louvres (%)	100	78	52	19	15	7	7
45° louvres (%)	35	20	9	8	7	7	7

The louvres are automatically activated with an incident irradiance-based rule, described as follows:

$$irradiance\ incident\ variable\ (ii) > 250\ W/m^2$$

4.3.2 Night-time natural ventilation

As concerns night-time ventilation, a rule-based additional ventilation flow is added to the model. The additional ventilation is modelled for the two levels of ventilation – 8 l/s/person and 1.2 ACH, as for the natural ventilation. It must be specified that, like the whole thesis's process, the ventilation strategies study is a comparative evaluation process that focuses on considering extreme values for comparison, as it is not possible to simulate all the different scenarios. The low ventilation rate value, 1.2 ACH, represents the extreme winter configuration, applied to the whole year, while the 8 l/s/person scenario represents the effective value for ventilation and for the removal of people's heat load, which is aligned with the one requested by the regulations and is feasible with high stack effect conditions. The additional ventilation is activated with a schedule from 6 PM to 8 AM (the non-occupied hours) in the non-heating period of the hottest climatic zone, with a rule that allows the ventilation only when the temperature is between 15°C and 26°C. The effect of night ventilation is thus studied in the hotter months, comparing different solutions. The possibility of low and uncomfortable morning temperatures because of too intensive night ventilation is thus present, but the simulations are performed to demonstrate the reduction potential of the overheated hours in the summer period.

Moreover, the used rule is simplified and does not take into account the difference between the internal and external temperature, only considering the outside air temperature and not the operative one. It was nevertheless seen from the analysis of a specific case that the operative and air temperature are very close in most of the cases, and that the use of night-

time ventilation with the presented rule yields the same reduction for both quantities, as seen in Figure 30.

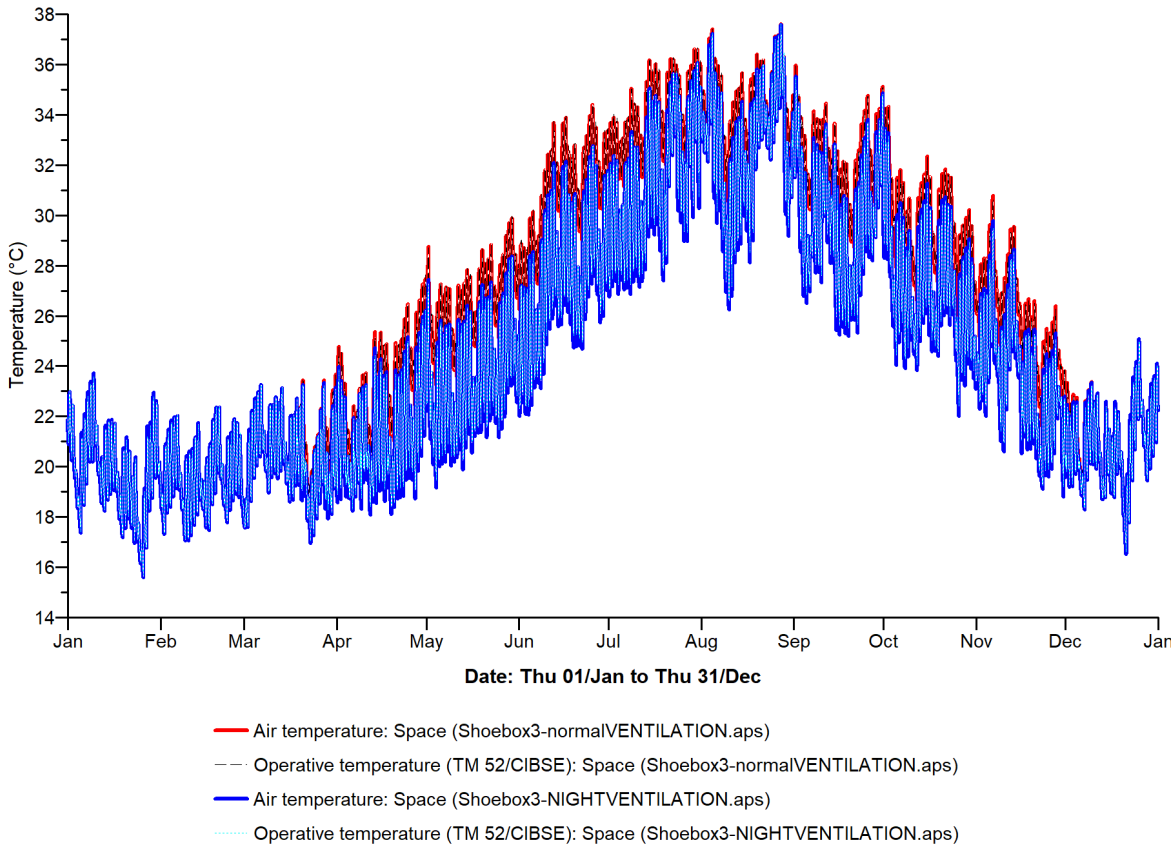

Figure 30 – Air and operative temperature for an example case located in climatic zone A, with base-case ventilation and with the addition of night-time ventilation

4.4 Overheating drivers analysis

In the end, additional simulations are also performed to analyse the response of the case studies to higher temperatures with respect to the ones currently simulated with the TMY (Typical Meteorological Year), which represents the average weather over the last 20-year timespan. This underlies a strong assumption, as usually the building is not located in the same position where the variables were registered, and moreover, it is going to be operated in the future period, with life expectancies that can reach 50 years or more. The retrofit process of a building cannot avoid taking into account this variability of conditions, and the designed building should be able to adapt to future variations of climate and to urban and local climate effects. This is particularly true in the scope of this research, which studies the overheating effects that can be highly increased by these weather variations.

Two scenarios of higher weather temperature are considered: future climate scenarios and the Urban Heat Island effect. For both cases, the Future Weather Generator 4.0.2 [67] tool is used. Also for these cases, the same reduced number of simulations is performed as for the additional passive strategies described in the previous sub-chapter.

4.4.1 Future climate scenarios

Future Weather Generator morphs present-day EPW files to represent climate change scenarios, considering different CMIP6 GCM Models (Couples Model Intercomparison Project Phase 6 – including Global Climate Models) [68]. The models can also be combined to create an ensemble, and the tool returns a set of files for two time-frames (2050 for 2035-2065 and 2080 for 2066-2095) and for each of the IPCC scenarios, the SSP (Shared Socioeconomic Pathways). The SSPs are representations of future emissions scenarios that also consider the socio-economic trends, characterised by a number (2.6, 4.5, 7.0, 8.5) that represents the different possible radiative forcing scenarios in W/m^2, with this parameter indicating the intensity of the greenhouse effect by the year 2100 [69].

For this analysis, the following models were selected for the creation of the ensemble: CNRM-CM6.1, MRI-ESM2.0, EC-Earth3-Veg, UKESM1.0-LL, CMCC-ESM2. “Inverse distance weighting” was selected as the interpolation method, 48h as month transition smoothness, “Engerer (2015) – Method 2” as diffuse radiation model, “By Month” as solar hour adjustment and no shift of temperature for winter and summer. The ensemble file for each location in the different SSP scenarios and time-frames were created, and the worst case scenarios (SSP5-8.5) were simulated both for the short-term prediction (2050) and for the long-term one (2080).

4.4.2 Urban Heat Island effect

As concerns the Urban Heat Island effect (UHI), Future Weather Generator requests as input the EPW weather file of the location to be studied and the Local Climate Zones (LCZ) for the source EPW and for the EPW to be created. For these parameters, choices are provided among the 17 possibles [70]. The Local Climate Zone of the desired location can be derived from the LCZ Generator [71], an online global map of Local Climate Zones. When uploading a weather file in Future Weather Generator, though, the choices listed for the source and target LCZ are based on which LCZ are close to the EPW’s coordinates within a certain distance. Therefore, the EPW’s coordinates need to be modified in order to allow the software to provide both the source and target Local Climate Zones.

The UHI morphing is performed by Future Weather Generator, which affects three variables: the dry-bulb temperature, the relative humidity and the horizontal infrared radiation intensity. According to the Future Weather Generator documentation available about the UHI morphing, the dry-bulb temperature (N6) is modified based on the temperature

differences between the source and target LCZs, while relative humidity (N8) is recalculated using psychrometric functions, and horizontal infrared radiation intensity (N12) is recalculated by multiplying the dry-bulb temperature to the power of 4 by the Stefan-Boltzmann constant and by the atmospheric emissivity, that depends on the dry-bulb temperature, on the sky cover and on the partial pressure of water vapour. The temperature difference applied to the EPW file, though, does not depend only on the difference between source and target LCZs, but also on the geographic location and on the Köppen climate classification. It is thus possible to modify the coordinates, applying fictitious ones in the EPW to be morphed, only if the new coordinates are placed at a reasonable distance from the selected city.

For each city representing the 6 climatic zones, fictitious coordinates are pasted in the EPW file, and the desired source and target LCZs are selected. In the cases in which it was possible, namely Lampedusa, Napoli and Cuneo, the coordinates are selected in the correct city, in a place that allows for the selection of both LCZs. In the other cases, though, the two LCZs are too far apart and cannot be detected by Future Weather Generator simultaneously. To obtain the desired output, thus, coordinates from other cities are used, in particular for Roma and Palermo the same coordinates of Napoli are used, as the source and target LCZs are the same, while for Milano, as it is not possible to find in Italy a location with LCZ 14 and 1 close enough, it is decided to use coordinates from Milano that allow for choosing LCZs 14 and 2, also considering that the areas of Milan that belong to LCZ 1 (compact high-rise buildings) are not spread. In Table 13, the source EPW's and the target's Local Climate Zone for each city are reported, along with the coordinates used in the EPW to create the UHI weather file and the reference coordinates. In the table, the highlighted coordinates represent the coordinates that are not in the correct city.

Table 13 – Local Climate Zones for the source and target EPWs for each city

Zone	City	Source LCZ	Target LCZ	EPW coordinates	New coordinates
A	Lampedusa	16 – Bare soil or sand	3 – Compact low-rise	35.498, 12.618	35.501, 12.605
B	Palermo	14 – Low plants	2 – Compact mid-rise	38.182, 13.099	40.884, 14.291
C	Napoli	14 – Low plants	2 – Compact mid-rise	40.884, 14.291	40.884, 14.291
D	Roma	14 – Low plants	2 – Compact mid-rise	41.952, 12.501	40.884, 14.291
E	Milano	14 – Low plants	2 – Compact mid-rise	45.449, 9.278	45.47, 9.18
F	Cuneo	14 – Low plants	2 – Compact mid-rise	44.553, 7.625	44.389, 7.534

The UHI weather files are thus created through Future Weather Generator, and the same set of simulations described in the previous paragraphs is simulated for the different locations and configurations.

Figure 31 displays the hourly average of the differences between the source and UHI weather files, on a monthly basis, for the three affected variables: the dry-bulb temperature, the relative humidity and the horizontal infrared radiation intensity.

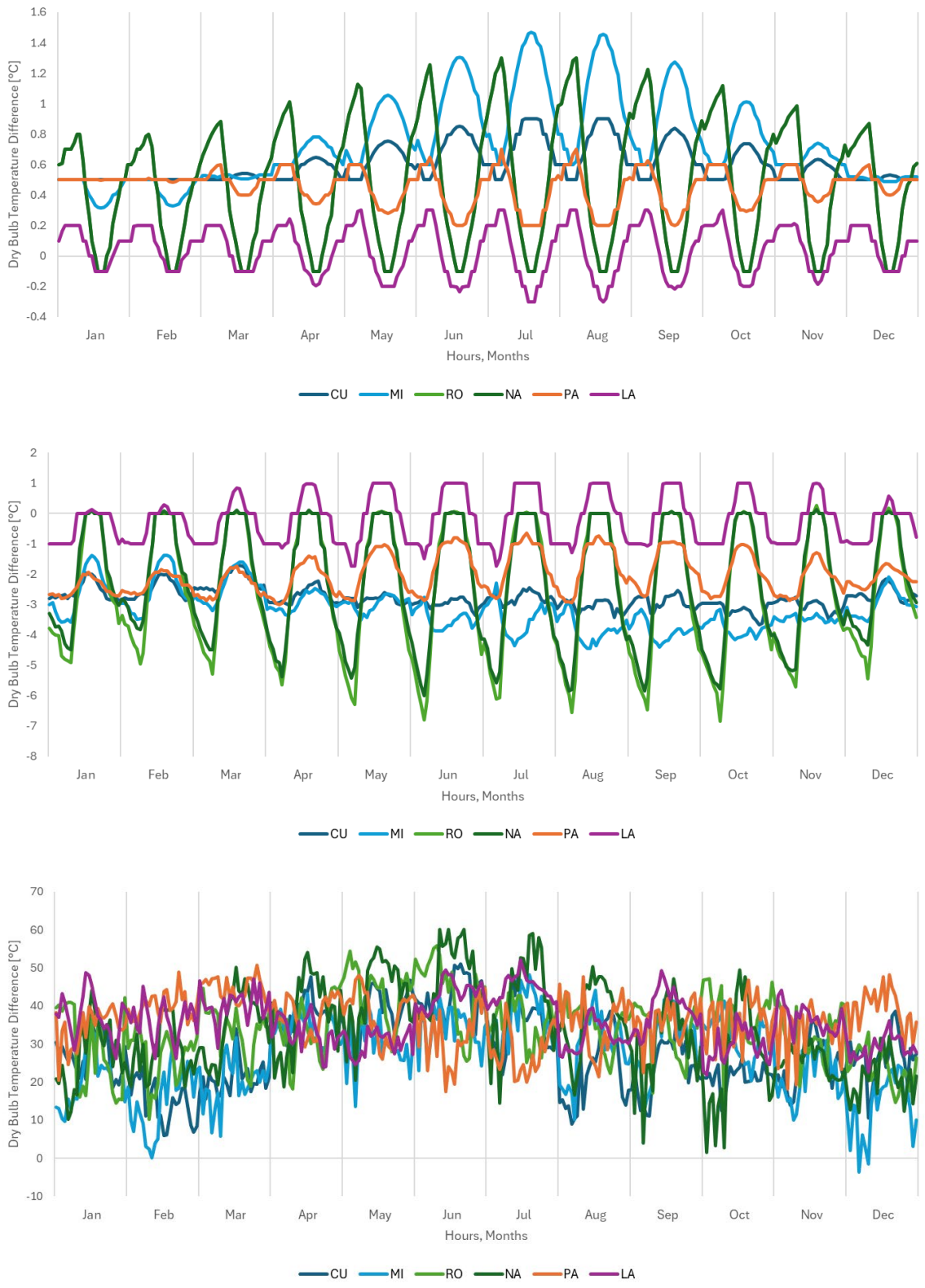

Figure 31 – UHI to base-case EPW file temperature difference in the three cases of source to target LCZs

It can be clearly seen how the dry-bulb temperature is the primarily affected variable, with fixed temperature deltas based on the hour, season and source-target LCZs, while relative humidity and horizontal infrared radiation intensity are affected consequently. Observing the temperature chart, it can be seen that on average, temperature increases of around 0.5°C in the urban settlements in the wintertime, with higher variability during summer. The city with the strongest influence of the UHI effect is Milan, with summer day-time peaks that reach differences of 1.4°C with respect to the source EPW temperatures. On the other hand, cities such as Roma, Napoli, Palermo and Lampedusa present higher temperature differences during the night-time. This effect is a direct consequence of one of the biggest issues of Urban Heat Island, that is, the thermal mass of the urban settlement. The materials that are more diffused in the cities, indeed, present a lower albedo and tend to absorb more heat than vegetation, moreover presenting higher thermal mass and thus maintaining high temperatures for a longer time and dispersing it during the night, thus increasing the temperature of the air during the night. For this reason, the UHI simulations are performed for both the base ventilation case and the night-time ventilation case, in order to compare the results and assess the decrease in the effectiveness of night ventilation with the UHI effect.

Relative humidity decreases in all cases almost over the entire year, with some low increase peaks in summer for the case of Lampedusa, which is the only case in which “bare soil and sand” is used as a source Local Climate Zone, while horizontal infrared radiation intensity always increases with average increases of 8-11%.

4.5 Overheating evaluation

In total, 24,768 simulations were run. The parameter combinations are summarised in Figure 32, with the number of possible values assumed by each parameter and variation described in the previous paragraphs and the total number of simulations. It must be taken into account that the total number of simulations does not correspond to the product of all the single parameter values, as some combinations are not simulated. The roof retrofit condition is indeed only simulated in the top floor configuration, and moreover, in the additional simulations (night ventilation, shadings, future weather and UHI), only two extreme window-to-floor ratio values and only the middle position classrooms are considered, reducing the number of simulations considerably.

In this section, the results elaboration tool is described, starting with the description of the necessary input and then describing the output and the methodology used to identify the overheating condition. Two different tools for the visualisation of the results are created, one for the assessment of the overheating condition of a single classroom, with the comparison between different retrofit strategies, and the second for the assessment of the whole school based on the condition of each classroom group.

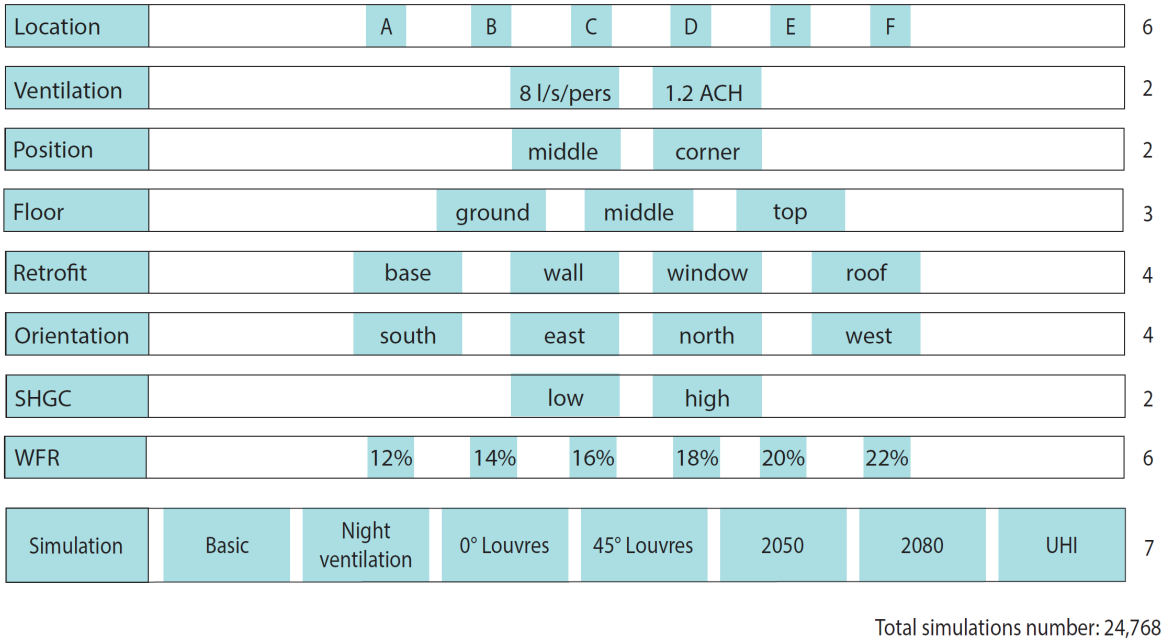

Figure 32 – Simulation parameters combination diagram

4.5.1 Classroom overheating evaluation

This tool is intended to be used to compare specific passive strategies for the reduction of overheating in particular classroom configurations. In this sub-chapter, the usage of the tool for the assessment of overheating in Italian school classrooms is presented. The tool gets as input from the user the following data:

- Climatic zone: A, B, C, D, E, F
- Floor: Ground, Middle, Top
- Position on the floor: Middle, Corner
- Classroom orientation: south, east, north, west
- Window-to-floor ratio: with a slider from 0 to 100%
- Solar heat gain coefficient: with a slider from 0 to 1
- Condition of natural ventilation: 8 l/s/person or less (1.2 ACH)
- Retrofit condition: no retrofit, wall retrofit, roof retrofit, window retrofit

The numerical inputs are rounded to the simulated values, with the following rules:

- For the WFR, the values below 13% are approximated to 12%, then the values between 13% and 21% are approximated to the nearest even number, while the values above 21% are approximated to 22%
- For the solar heat gain coefficient, all the values below 0.5 are considered low values, while all the values above 0.5 are considered high

As output, the tool proposes first of all the results for the specific configuration, then a comparison between different retrofit conditions, and in the end, a comparison with the use of additional passive strategies and with the consideration of different climate scenarios. For each of these sections, the results are presented in terms of share of comfort hours in the different seasons, of distribution of temperatures, of compliance with the TM52 regulation and of share of heat stress days. For what concerns the different retrofit strategies comparison, the tool requests that the user select from a multiple selection list the configurations that the user wants to compare. The list of possible comparisons is:

- Reduce the solar heat gain coefficient (only if the initial condition presents a high SHGC)
- Walls retrofit (only if not considered in the initial condition)
- Roof retrofit (only if not considered in the initial condition and for the top floor room)
- Double glazing or window retrofit (only if not considered in the initial condition)
- Increase of the ventilation rate (only if the initial condition considers a low value)
- Increase in the air speed thanks to fans

For this section, the following labels are used to identify the different strategies:

- BASE = base-case
- WALL = wall retrofit
- ROOF = roof retrofit
- WINDOW = window retrofit
- G-VALUE = solar heat gain coefficient decrease
- 8 l/s/person = increase in the natural ventilation rate
- 1.2 m/s = increase in the speed of the air thanks to fans

As concerns the passive strategies comparison section, the comparison is provided for the base-case condition with shading devices and night ventilation results, with the same plots described above. The used labels are presented as follows:

- BASE = Initial configuration
- 0° = Louvres 0°
- 45° = Louvres 45°
- NIGHT = Night ventilation

In the end, two future weather scenarios and the Urban Heat Island scenario are compared, using the following labels:

- BASE = Initial configuration
- 2050 = 2050 future weather projections for the SSP5-8.5 scenario
- 2080 = 2080 future weather projections for the SSP5-8.5 scenario
- UHI = Urban Heat Island effect

4.5.2 School overheating evaluation tool

In this sub-chapter, the usage of the tool for the assessment of overheating in Italian schools is presented. The tool gets as input from the user the following data:

- Climatic zone: A, B, C, D, E, F
- Window-to-floor ratio for the whole school: with a slider from 0 to 100%
- Solar heat gain coefficient for the whole school: with a slider from 0 to 1
- Condition of natural ventilation for the whole school: 8 l/s/person or less (1.2 ACH)
- Retrofit condition for the whole school: no retrofit, wall retrofit, roof retrofit, window retrofit
- Number of classroom groups: slider from 1 to 10, determining the number of times the following inputs are requested
- Number of classes in group #
- Floor of classroom group #: Ground, Middle, Top
- Position on the floor of classroom group #: Middle, Corner
- Classroom orientation of classroom group #: south, east, north, west

With these inputs, a report regarding the overheating condition of each type of classroom and the evaluation of the whole overheating condition of the school is created.

The output of the tool is reported in the form of four table plots, indicating the percentage of hours with temperature above the maximum threshold in the different periods, the number of hours with temperature above the limits, the TM52 compliance and the share of heat stress days for each group of classes.

At the end of the report, for each group of classrooms, two indicators of the overheating risk are calculated, respectively in the intermediate (spring and autumn, between the end/beginning of the heating season and the end/beginning of the school period) and summer seasons. If the share of hours above the threshold is above 5%, if the condition of overheating is verified according to the TM52, and if the share of heat stress days during the school non-heating period is above 10%, the case is considered at overheating risk. If the share of hours above the threshold is above 5% but the share of hours with temperature above 2°C over the limit is lower than 5%, then the overheating risk is classified as middle risk. If the TM52 returns a "no overheating" condition, the case is automatically considered not overheated. Thanks to these evaluations, each group of classrooms is classified on a low-middle-high overheating risk scale, and a summary is reported.

In the end, according to the number of classrooms that are considered at high overheating risk, the total overheating risk of the whole school building is assessed, referring to the share of classrooms at high overheating risk and considering the two main objectives of the present research: the comfort condition during the non-heating school season and the possibility of using the school also during the summer break. As regards the intermediate seasons, the school is considered in overheating condition if more than 25% of the classrooms are in a discomfort condition, with the suggestion of applying possible retrofit strategies or temporarily shifting the didactic schedules to cooler hours. For what concerns the summer break period, three levels of usability of the building are defined. If less than 25% of the classrooms are at high overheating risk, the school has a good potential for usage also in the summer period, while 60% is used as an acceptability threshold for sporadic and low attendance use. Shares between 25% and 60% make the school usable discontinuously with low attendance. The use of the second tool, for the assessment of single classrooms, is suggested at the end of the report, to analyse more in-depth the behaviour of single classroom groups and to compare different retrofit and overheating reduction strategies for each group.

Figure 33 summarises the assessment of the overheating condition of the single classroom and of the whole school building, based on the share of overheated classrooms, in the intermediate and summer seasons.

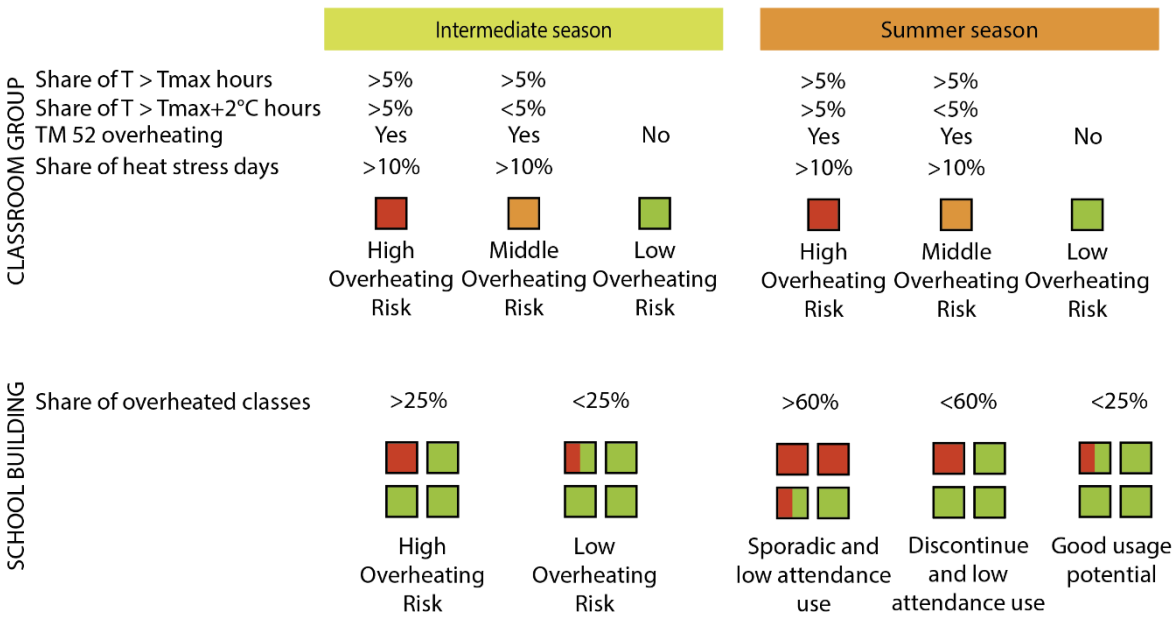

Figure 33 – Classroom and whole school overheating evaluation for the intermediate and summer season diagram

4.6 Simulations tool validation

To validate the used methodology, first of all, the tool is applied to a limited number of cases, to study the output and compare the results for extreme conditions with the expected outcome, then, the results for the simulated cases are compared with the same results extracted from another simulation software, to detect possible wrong assumptions. The following sub-chapters display the methodology and results for the two analyses.

4.6.1 Test simulations

All the simulations are performed on a basic model case, with the room in the middle position of the middle floor and with the base-case stratigraphy. The three parameters are varied over the hypothesised range, letting each parameter assume the two extreme values of the range. The combinations of parameters are thus resumed in Table 14.

Table 14 – Validation model scenarios parameter values

Case	WFR	Orientation	SHGC
1	0.12	S	0.35
2	0.12	S	0.87
3	0.12	N	0.35
4	0.12	N	0.87
5	0.22	S	0.35
6	0.22	S	0.87
7	0.22	N	0.35
8	0.22	N	0.87

The test simulations output for two locations is contained in Appendix A. The analysis of this small set of data aimed at determining the behaviour of the model as a consequence of the study parameters variations – the location and climatic zone, the orientation and dimension of the window and its solar performance. The results were extracted and commented for combinations of extreme values, and the simulations are thus verified, since they return reasonable results, consistent with the expected ones.

4.6.2 Different software results comparison

The presented methodology lays its foundations on the use of computer simulation tools, which are widely used in the present research scene, but that yield results that are not tested in reality, and this is especially true when dealing with future weather scenarios [72]. One of the possible validation strategies for simulation-based research is the use of other simulation software, which allows to identify possible misleading assumptions made during the simulation process.

To validate the defined model, a comparison with another building simulation software, EnergyPlus, is performed. EnergyPlus is an open-source simulation platform, validated thanks to the widespread use and the feedback of the users. The same case study shoebox building is thus simulated in the same conditions, including geometry, stratigraphy, weather and location data, and the output is compared for 8 case studies in which the window-to-floor ratio, the orientation and the solar heat gain coefficient of the window are changed and combined using the extreme values defined in the previous paragraphs. Moreover, the same simulations are also performed with the latest version of IESVE, IESVE 2025, in order to detect possible improvements that were introduced in the software's calculation methods.

The comparison is performed on the simulated indoor operative temperature with the model characteristics described above (middle floor middle classroom, base-case stratigraphies), considering the weather conditions of Milan and the 8 cases that are defined from the combination of the extreme values of the 3 considered variables.

4.6.1.1 EnergyPlus batch simulations setup

To perform a batch simulation with EnergyPlus, first of all, a base file is created with the geometric definition of the shoebox model, then a Python code is run to create the batch of modified files, and in the end, the files are simulated simultaneously, and the results are extracted and compared to the other software's results.

The base shoebox file is created with geometric characteristics and all the necessary construction types to match the ones created in IESVE. In the IDF file, the desired output variable, the indoor operative temperature, is specified.

The Python code that creates the batch of files accesses the IDF text version and splits it into lines. Then, a *for* loop is created to generate the number of different files that have to be

simulated, which in this case is 8. In the *for* loop, according to the values assumed by the three variables in the different scenarios, the geometry of the building and of the window and the construction of the window are accessed and modified as follows:

- The window-to-floor ratio must be expressed in terms of window coordinates in EnergyPlus. It is thus necessary first of all to calculate the window area as the product of the WFR and of the floor area. Then, the dimensions of the window are calculated starting from the area, making sure that the geometry of the window in EnergyPlus matches the one in IESVE, which is created by setting the WWR and presents the same proportions as the wall that it is applied to, and is centred on the wall. Then, the vertical and horizontal coordinates are calculated, making sure it is centred on the wall in both directions. The horizontal coordinates will be used as x or y coordinates, depending on the orientation of the window.

- The orientation of the window can be changed by setting the horizontal coordinates of the window in the correct order. Moreover, as the room presents different dimensions in the two directions, based on the orientation of the window, the coordinates of the walls also need to be changed, making sure that the bigger wall corresponds to the window. In the IESVE model, only the surface with the window is exposed to the outdoor environment, as the other surfaces are surrounded by adjacent buildings and are considered adiabatic. To reproduce the same situation in EnergyPlus, in which the model is formed only by the classroom and does not include the rest of the building, for each of the building surfaces that do not host the window, the outdoor conditions are set to adiabatic and the exposition of sun and wind is neglected, while the surface that presents the window is connected to the outdoor environment and is considered sun and wind exposed. The ceiling and floor are always considered adiabatic and not exposed to the sun and wind, but their coordinates are also changed based on the orientation of the building.

- The window glazing's solar heat gain coefficient can be changed by changing the whole window construction, assigning to each case a window construction that presents the required SHGC and glazing stratigraphy (single or double).

The modified IDF files are then saved in a separate folder, along with the "RunDirMulti.bat" with the specifications of the EnergyPlus version used for the simulation, the number of cores to be used to simultaneously simulate the batch of files, and the weather file to be used for the simulation. The batch simulation is then started, and a set of .csv result files is generated. Those are then merged into a single results file through a Python code, and in the end, the results are compared using the matplotlib library, with the output presented in the following sub-chapters.

4.6.1.2 Settings alignment

To get comparable results, different model settings had to be checked and aligned in the two software, IESVE (both 2024 and 2025 versions) and EnergyPlus, in order to avoid discrepancies caused by different default settings. The main parameters that were checked are listed and explained as follows. Some of the parameters that are listed were fundamental to achieve a correct comparison, as the default settings of the two software determine the calculation of highly different values for the internal operative temperature, which is the compared result. In order to identify the issues, other results were also analysed, such as the internal (people and lighting) gains, the ventilation gains, the solar gains and incident fluxes on the surface. At the end of the list, some additional fixings that were taken into account for the comparison between the two software are reported, as, even if they did not return a great improvement in the model comparison, they are worth being checked for this type of analysis.

- People gain: the default settings in the two software for what concerns the people load yield different results in terms of people gain. Indeed, IESVE sets a fixed value for the sensible and the latent load, while EnergyPlus's default is to auto-calculate the Sensible Heat Fraction. Thus, setting the field "Sensible Heat Fraction" of the "People" object to 0.6 in EnergyPlus allows for matching the people gain values, as the values in IESVE are 90 W/person sensible load and 60 W/person latent load, which yields 90/(90+60) = 0.6 as a sensible heat fraction.

- Warmup period: the two software approach the warmup period differently, and this can cause high differences in the simulation, especially in the first days of the year. Indeed, IESVE uses a "preconditioning period", whose length can be customised, that starts with a fixed initial temperature and after which the real simulation and the reported results start. On the other hand, EnergyPlus uses the fields "Minimum Warmup Days" and "Maximum Warmup Days", and tolerances for the convergence of loads and temperature. In order to avoid problems due to the mismatch between the warmup periods, the EnergyPlus simulation is forced to run on a two-year weather file (a doubled version of the weather file used for IESVE), and then only the results of the second year are considered.

- Day of the week for start of the simulation: some of the heat loads that act in the model are governed by weekly schedules, in particular those depending on the occupancy hours, namely the occupants' presence, the lighting profile and the ventilation profile. It is thus fundamental that the weekdays are aligned between the two software. In IESVE, the calendar is set from ApLocate, and the day of the week for January 1st is set according to the real day corresponding to the year taken from the weather files' January month. In EnergyPlus, on the other hand, if no year is input, the field "Day of the Week for Start Day" of the "RunPeriod" object will default to Sunday, while if a year is input and the field is blank, the correct weekday

will be set. In this specific case, the simulation is performed with the Milan Linate 2009-2023 weather file, in which January is represented by 2021's January. IESVE will thus set Friday as the weekday of the first day of the year, taking it from 2021's actual first weekday. In EnergyPlus, as already mentioned, the simulation is run for two years, to avoid mismatches due to the warmup period, and the results are analysed only for the second year of simulation. The "Start of the simulation year" field would thus need to be set to 2020, but 2020 is a leap year, and this would determine the second year's weekdays to be misaligned. To fix this, the "Start of the simulation year" field is thus set to 2015, and thus the results are taken from year 2016, which starts with a Friday.

- Daylight Saving Time: in this comparison, the Daylight Saving Time is neglected in both software, to avoid problems of peak misalignment during the summer days and to facilitate the reading of the azimuth and solar altitude during the whole year.

- Convection algorithm: the convection algorithm's default values are different in the two software, and they do not present the same options for these parameters, but similar ones were chosen. This is one of the most impactful adjustments to match the results between the two software. The default settings in IESVE use the "McAdams" algorithm for the external convection and the "CIBSE fixed values" for the internal convection. On the other hand, the default algorithms used in EnergyPlus are the "DOE-2" for the external convection and the "TARP" for the internal convection. The results are thus very different, and to solve the issue, the external convection is set to "ASHRAE simple" in IESVE and "SimpleCombined" in EnergyPlus, being the latter described as "combined radiation and convection coefficient using simple ASHRAE method", and the internal one is set to "CIBSE fixed values" in IESVE and "Simple" in EnergyPlus, being the latter described as "constant value natural convection". Taking as a test example the 6th case (highest WFR, window exposed south and clear glass), in which the solar gains are the highest and in which thus the temperature differences between the two models are higher, with the default settings for both the software, the share of hours in which the operative internal temperature difference between the two software is higher than 2°C is higher than 50%, while setting the algorithms as explained in the present paragraph reduces this share to 1.66%.

- Solar absorptance: the solar absorptance is set to 0.7 on all surfaces, internal and external, as this is the default value in EnergyPlus, while IESVE assigns by default a value of 0.7 for the external surfaces and 0.55 for the internal ones.

- Frame factor: the frame factor is set to 0 in both software.

- Window-to-wall ratio: as IESVE only accepts rounded values, it is fundamental to round the WWR value in the same way before calculating the area of the window and its coordinates.
- Furniture mass factor: furniture mass factor must be set to 0 in IESVE, while by default it is set to 1, as no furniture is modelled in the shoebox room, and as EnergyPlus does not consider furniture presence by default.
- Stratigraphy thermal mass: the correct order of the layers in the stratigraphy of the constructions has to be checked. In both software, the layers are listed from the outside to the inside, and the specific heat capacity of the different layers is determinant for the analysis. This is important even when considering adiabatic boundary conditions, as both software consider half of the stratigraphy to be part of the thermal mass of the considered zone.
- Glazing angular properties: the glazing properties can be set in both software in different ways, and the angular properties can have a determining effect. In IESVE, for each glass layer, the "Angular dependence" can be defined as "Fresnel", "Explicit", in which the values associated with all the variables at the different incidence angles can be manually set, "Constant" or "LBNL", which uses the values from Window LBNL. In EnergyPlus, the glazing can be defined through the "WindowMaterial: SimpleMaterialGlazing", in which the U-value and SHGC value of the whole glazing are specified, or with the "WindowMaterial: Glazing" and "WindowMaterial: Gas" objects, which are then combined through the "Construction" object. The "WindowMaterial: Glazing" requires specifications in the "MaterialProperties: GlazingSpectralData", which contains the transmittance and reflectance values corresponding to an array of discrete wavelengths. These objects can be derived from the Window LBNL software, and thus the characteristics of the glazing can be matched between the two software.

4.6.1.3 Results comparison

After fixing the differences between the two models, the simulations are launched, and the results are extracted and compared. In all the descriptions and charts hereafter, the SHGC values are rounded to 0.9 and 0.3 for the sake of simplicity, but these values represent the values determined in the Model description paragraph, where the window stratigraphy was defined.

First of all, the temperature is plotted over the whole year, in comparison with the running mean temperature (Trm) and with the maximum acceptable temperature according to the II comfort band. The latter presents two values, one corresponding to air speed equal to 0 (Tmax) and the second that originates from the increase of the air speed to 1.2 m/s, which generates an increase in the acceptable temperature of 2°C (TmaxVent). Observing the charts

in Figure 34, it can be seen that the temperatures simulated by the 3 software are quite similar, with the one from EnergyPlus being on average slightly higher in some summer months. To further analyse this difference, a frequency distribution and cumulative distribution chart is plotted for each case in Figure 35, where it can be seen that, while the range of temperatures is the same in all the software, the higher temperatures occur with a higher frequency in EnergyPlus with respect to the two versions of IESVE, resulting in higher peaks in the chart. In this second chart, the similarity between the two versions of IESVE is even clearer, with the cumulative frequency line being almost overlapping.

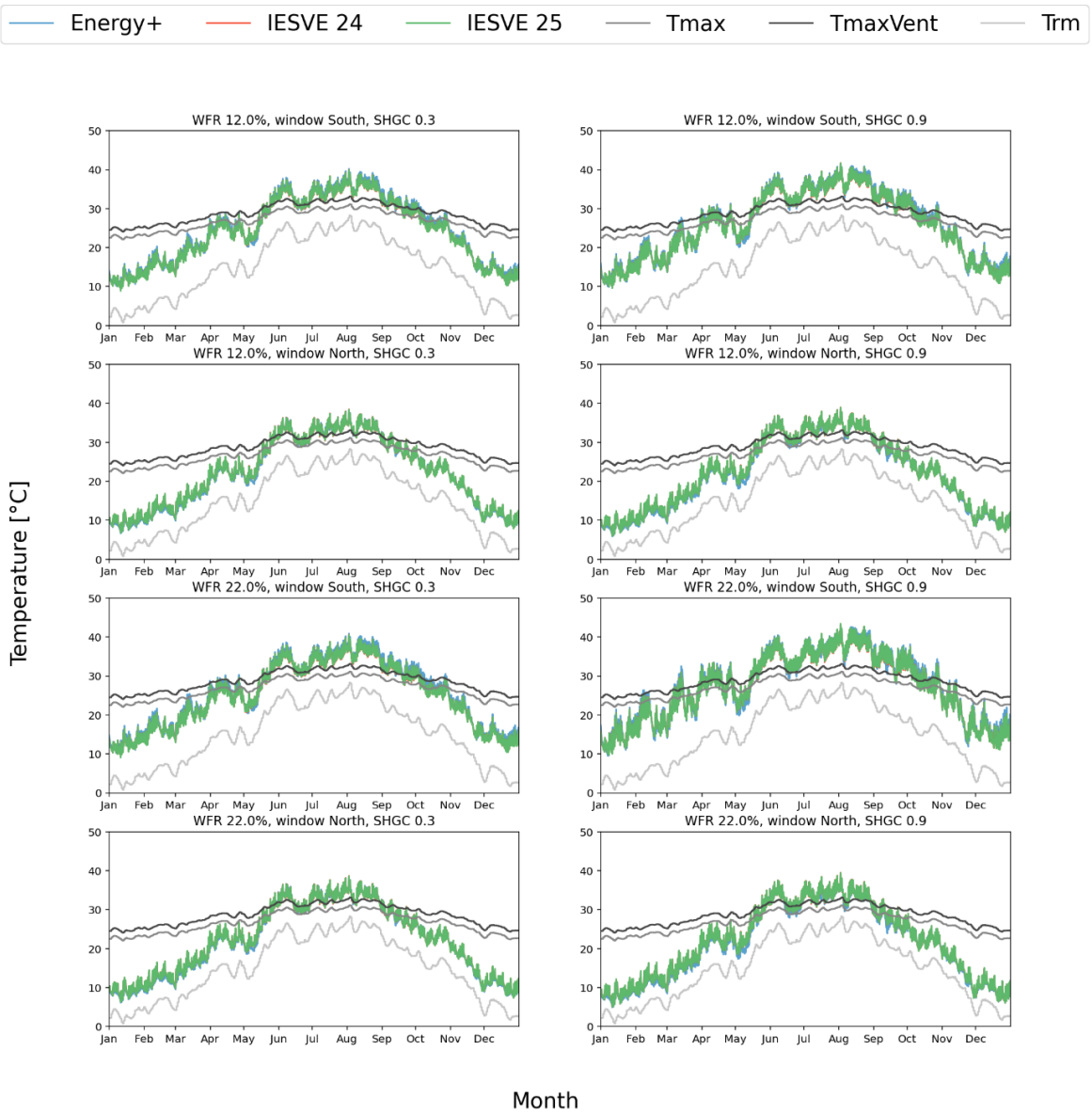

Figure 34 – Indoor operative temperature over the year simulated in the three software and compared to running mean temperature (Trm), maximum temperature with zero air speed (Tmax), and higher air speed (TmaxVent)

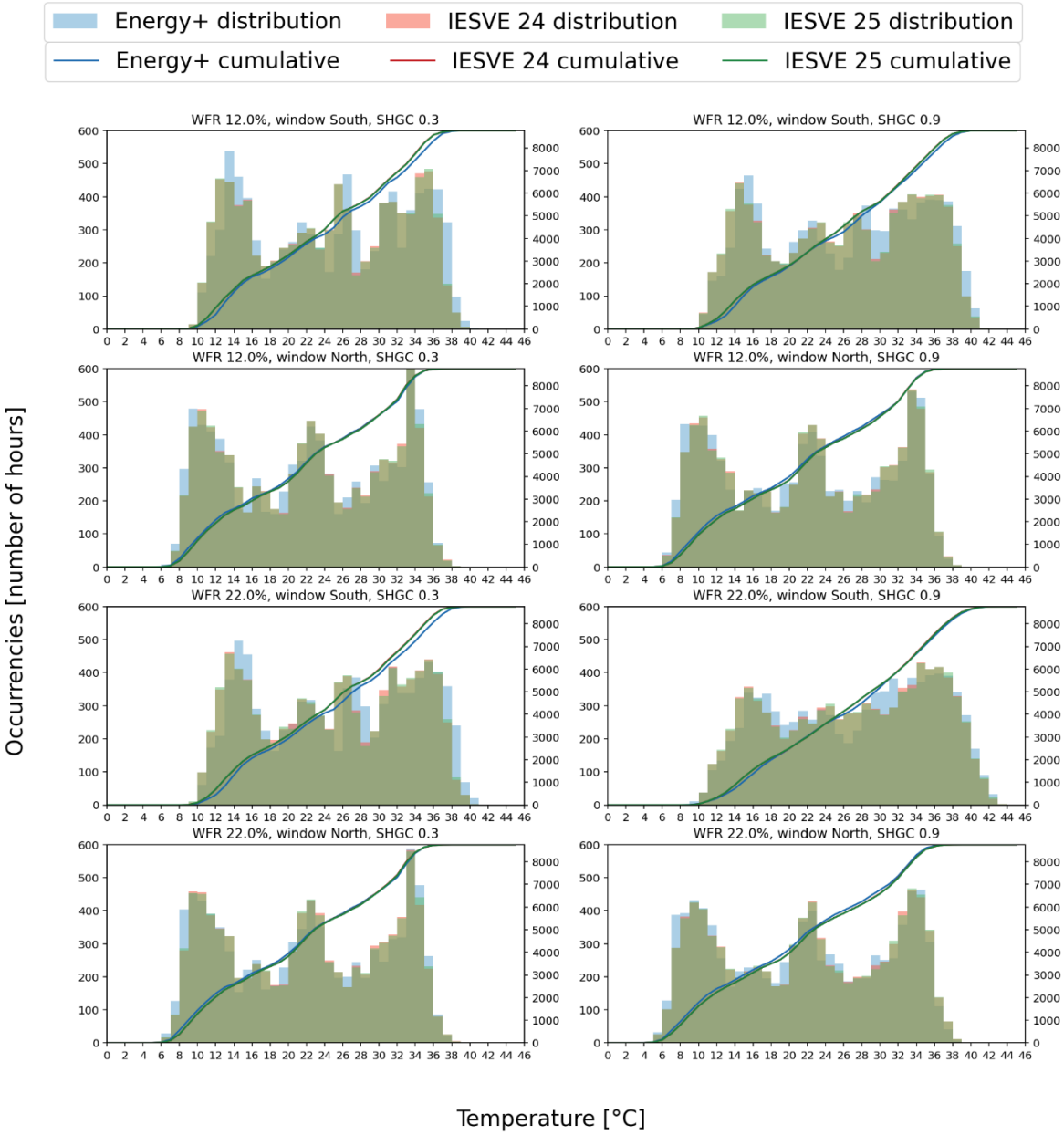

Figure 35 – Indoor operative temperature frequency charts and cumulative frequency plots for the 8 considered cases simulated with the three software

The minimum, average and maximum temperatures for the 8 cases simulated in the three software are summarised in Table 15. On average, the difference between the two IESVE versions is 0.004°C for the average temperature, 0.075°C for the minimum and 0.046°C for the maximum. The difference between the EnergyPlus simulation and the IESVE (version 24/25) ones is 0.096/0.092°C for the average temperature, 0.027/0.047°C for the minimum temperature and 0.065/0.019°C for the maximum one. Al-janabi et al. [73] reports differences of 1°C for the average and minimum temperatures and of 1.5°C for the maximum temperature, so the results reported in this study can be considered acceptable.

Table 15 – Minimum, average and maximum temperature for all the simulations

	Case 1			Case 2		
	EnergyPlus	**IESVE24**	**IESVE25**	**EnergyPlus**	**IESVE24**	**IESVE25**
Minimum	9.25	8.95	8.85	9.87	9.64	9.54
Average	24.91	24.37	24.37	26.25	25.88	25.89
Maximum	40.25	39.93	39.89	41.65	41.70	41.68
	Case 3			**Case 4**		
	EnergyPlus	**IESVE24**	**IESVE25**	**EnergyPlus**	**IESVE24**	**IESVE25**
Minimum	6.58	6.82	6.75	5.81	6.03	5.97
Average	22.11	22.26	22.27	21.78	22.08	22.09
Maximum	38.40	38.47	38.38	38.78	39.00	38.93
	Case 5			**Case 6**		
	EnergyPlus	**IESVE24**	**IESVE25**	**EnergyPlus**	**IESVE24**	**IESVE25**
Minimum	9.56	9.15	9.03	9.49	9.75	9.68
Average	25.62	24.93	24.94	27.36	27.11	27.11
Maximum	40.94	40.62	40.57	43.06	43.43	43.46
	Case 7			**Case 8**		
	EnergyPlus	**IESVE24**	**IESVE25**	**EnergyPlus**	**IESVE24**	**IESVE25**
Minimum	6.11	6.40	6.32	4.92	5.06	5.06
Average	21.93	22.12	22.13	21.42	21.84	21.84
Maximum	38.59	38.68	38.61	39.17	39.52	39.46

To better visualise the difference between the results simulated by EnergyPlus and IESVE, a comparison chart is plotted, with a scatter plot relating the EnergyPlus results on the x-axis and the IESVE 24 results on the y-axis. Only the IESVE 24 results are compared in this case, as it is seen that the 24 and 25 version results are similar. As seen in Figure 36, the trend line almost always overlaps the bisector, with angular coefficients that range from 0.978 to 1.000 and r^2 values that range from 0.991 to 0.999. The cases in which the r^2 value is lower are the ones with the window exposed south and with a poor performance of the glazing, while the best cases are the ones with the window on the north side and the best performance glazing.

Figure 37, moreover, displays the temperature difference distribution between the IESVE and the EnergyPlus simulations, marking in addition the 98th percentile value of this difference. The 98th percentile value always lies between 1°C and 2°C, being even lower than 1°C in the best cases (with a window on the north and best performance glazing). Only a few values exceed 2°C in the 6th case, while the values exceeding 1°C are 1.66% in the 6th case, and values lower than 0.5% or null in the other cases.

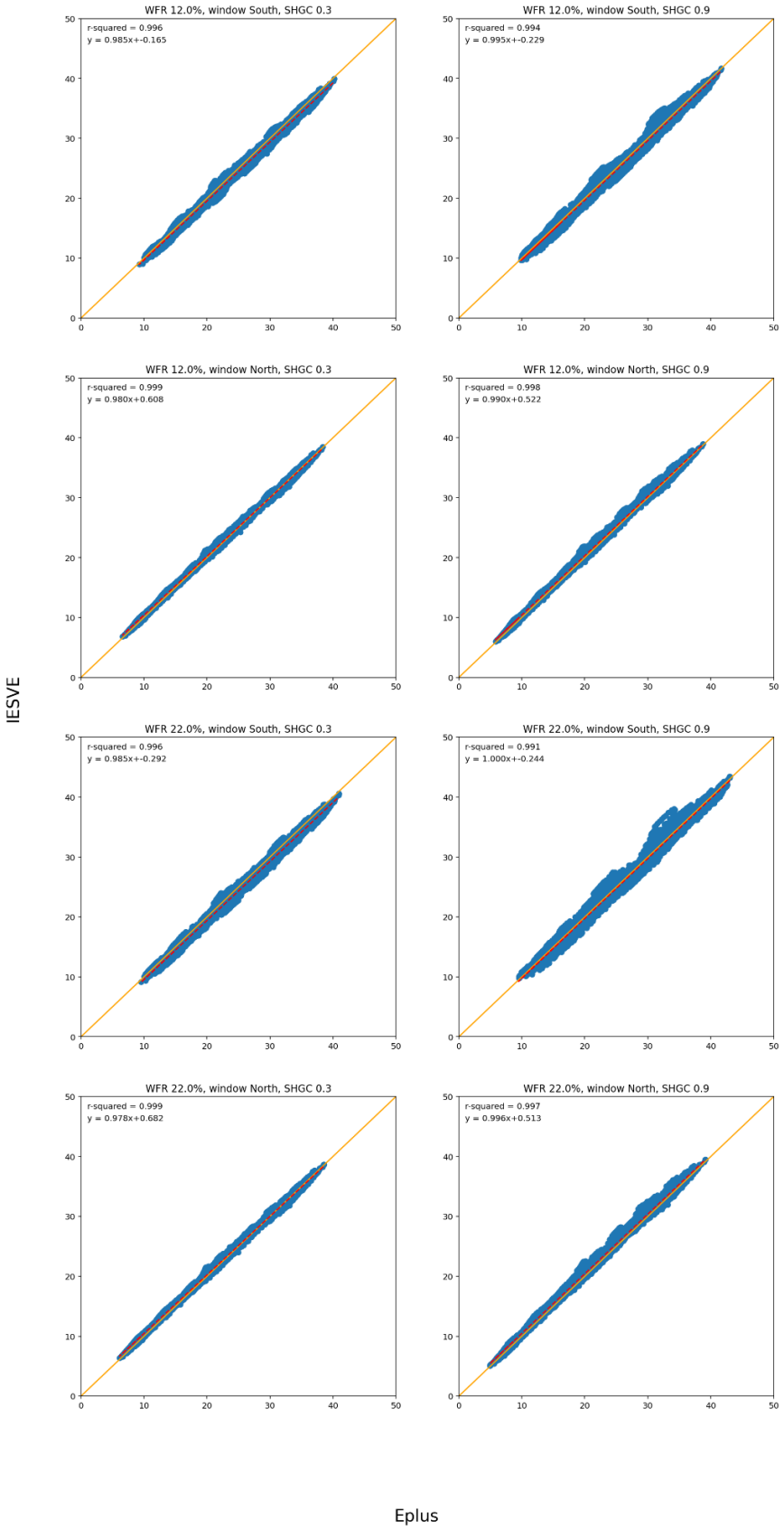

Figure 36 – Comparison plot between the EnergyPlus and IESVE operative temperatures for the 8 cases

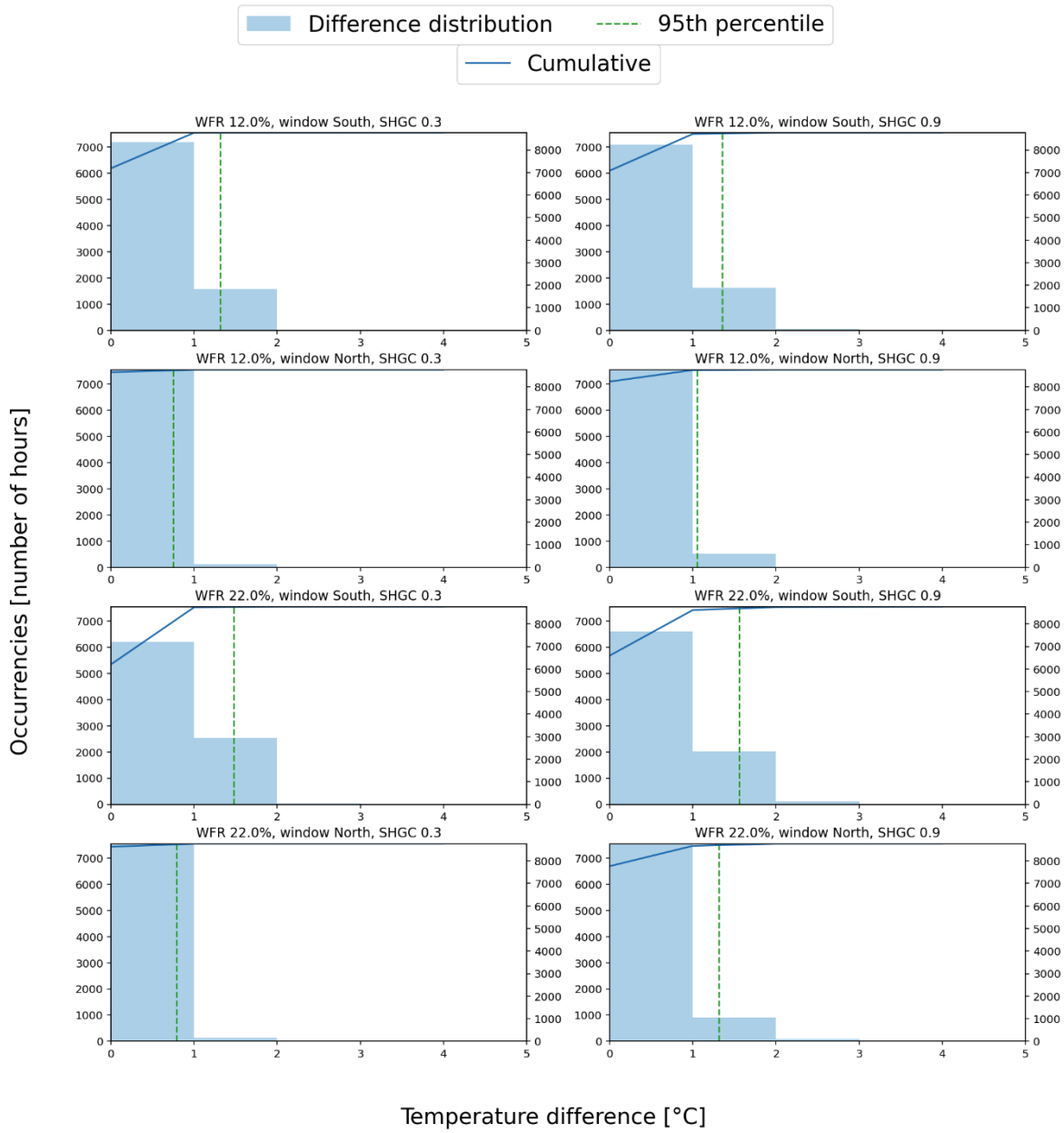

Figure 37 – Operative temperature difference between the IESVE and EnergyPlus simulations distribution plot for the 8 cases

As it is seen in the first chart (Figure 36) that the bigger difference between the software occurs in the summer months – when the temperatures are higher – and as the present study aims at analysing the summer performance of different envelope configurations, a focus on the day with the highest temperature is carried out and presented in Figure 38, where the temperature over the day with the highest peak is plotted. First of all, it can be confirmed again that the difference between the two versions of IESVE is very small. As regards the comparison with EnergyPlus, it can be seen that, as already mentioned, EnergyPlus registers higher temperatures on average, with an average difference of 0.19°C for IESVE 24 and of 0.18°C for IESVE 25, but that the peak temperature is similar in terms of value, with average

differences of 0.07°C for IESVE 24 and of 0.02°C for IESVE 25. The peak temperature and the time at which it occurs is also marked in the plot, making it clear that the two IESVE version perfectly coincide, while that, mainly in the cases of the window facing south and with a low performance of the glazing, EnergyPlus records the peak in advance of 1 hour respect to IESVE, even though this peak is not clearly determined, as it belongs to a plateau.

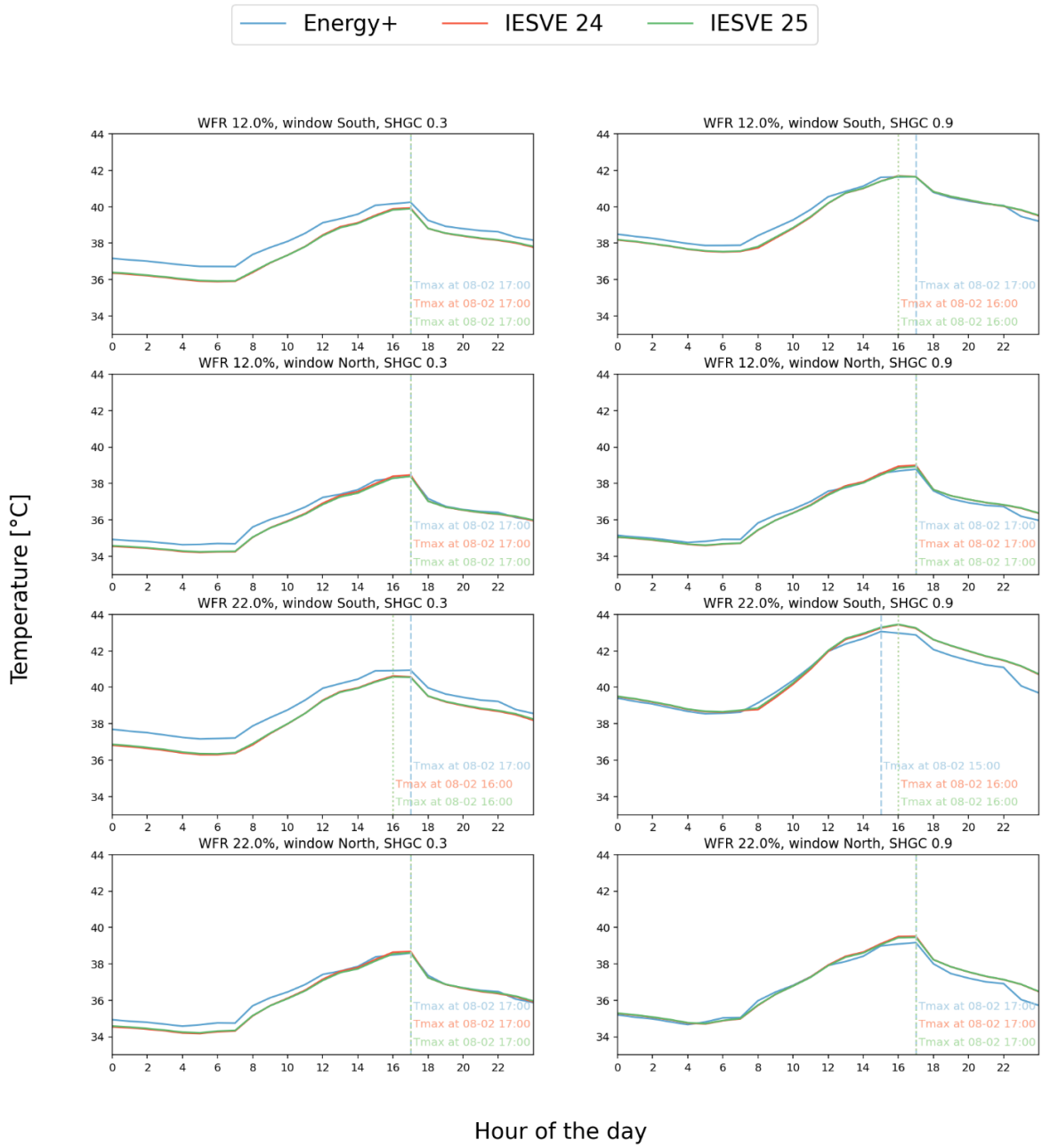

Figure 38 – Indoor operative temperature simulated in the 3 software over the day with the highest temperature for the 8 cases

Also the day with the lowest temperature is plotted, and the results are visible in Figure 39. In these charts, the temperatures simulated by the two IESVE versions are identical, while the difference with the EnergyPlus simulation returns similar conclusions as in the previous

discussion. In this case, the day with the lowest temperature varies in the different cases and is sometimes different for the same case in EnergyPlus respect to IESVE, but the hour at which it occurs is always the same except for two cases in which there is a 1-hour delay, but also in this case the minimum belongs to a plateau and it is very hardly placeable.

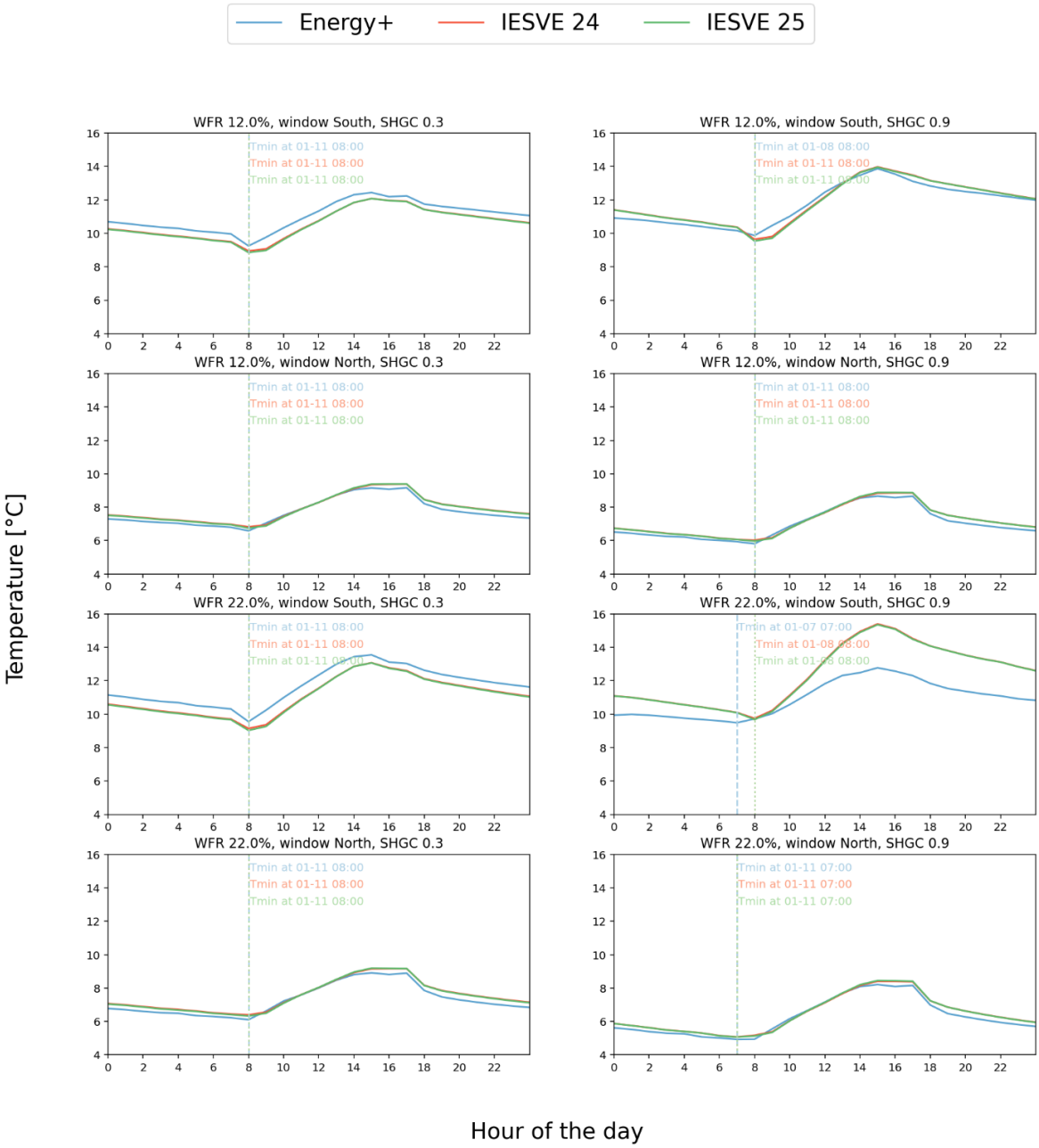

Figure 39 – Indoor operative temperature simulated in the 3 software over the day with the lowest temperature for the 8 cases

The percentage of summer occupied hours that belong to each comfort band, as defined in the EN 16798 for the adaptive comfort, is calculated and presented in the charts in Figures 40 and 41. The first figure corresponds to the case with null air speed, while the second figure corresponds to the case with an increase in the air speed, which expands the comfort

band of 2°C towards the higher temperatures. Comparing the 3 simulations for each case, it can be seen that the two versions of IESVE return almost identical results (with a difference of 0.17 and 0.22 absolute percentage points, respectively, in the not ventilated and in the ventilated case), while the EnergyPlus results present, on average, a slightly higher share of hours in the hot discomfort region. On average, this difference is 1.63 absolute percentage points for the case without ventilation and 2.35 absolute percentage points for the case with ventilation. In general, all the cases present very low performances, with discomfort hours share almost always above 50%. Comparing the two charts, though, it can be seen how, introducing ventilation, an average of 19 percentage points decrease in the hours of discomfort is registered. In both cases, however, as the charts refer to the summer occupied hours, in no case except for the last one (higher window area on the north side with poor glass stratigraphy) too low temperatures are registered.

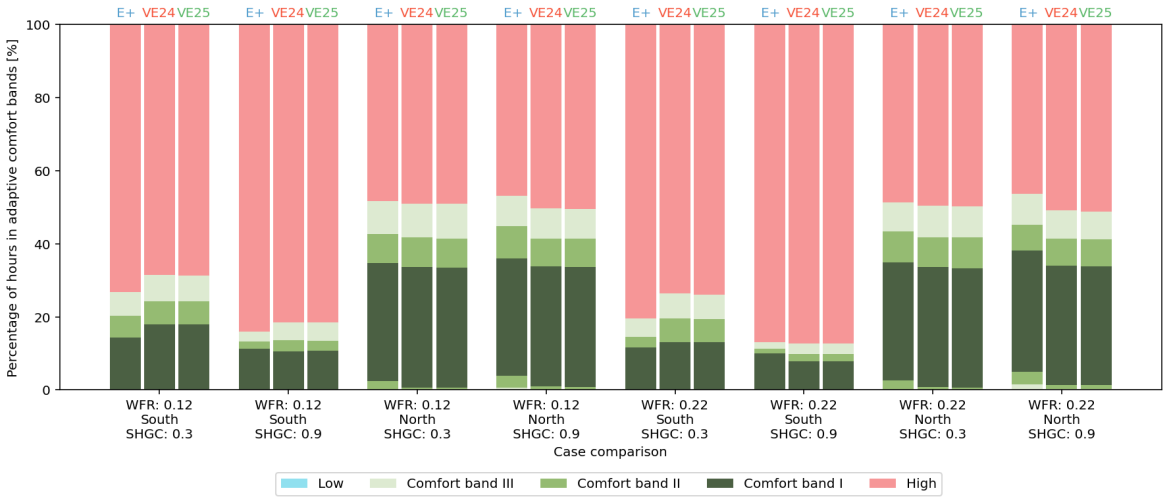

Figure 40 – Comfort hours for the 8 cases simulated with the 3 software in the case of no air speed

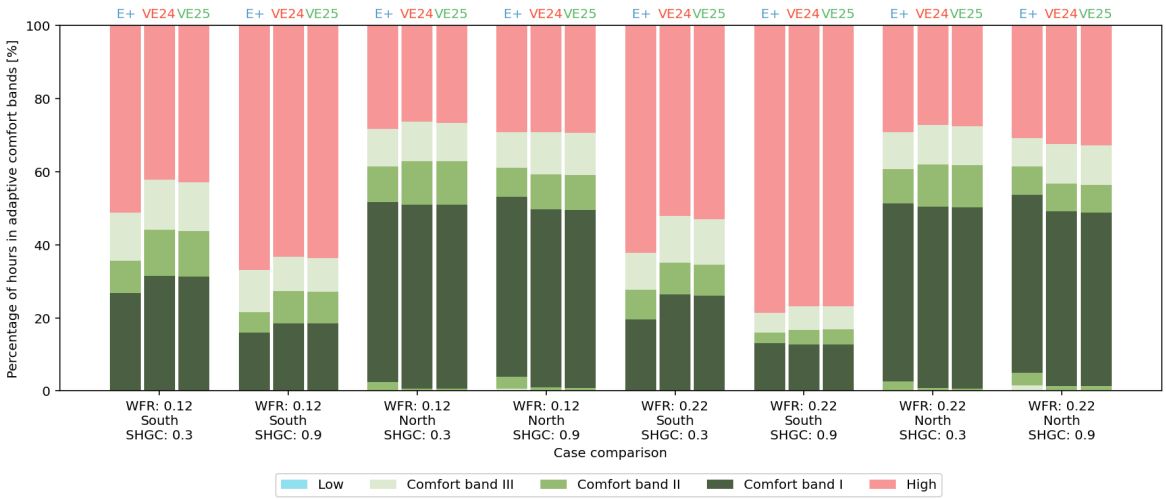

Figure 41 – Comfort hours for the 8 cases simulated with the 3 software in the case of air speed equal to 1.2 m/s

4.7 Sensitivity analysis

In order to study the impact of the different variables on the temperature outcome, a sensitivity analysis is performed on an example case. The tornado chart is used as an instrument for the sensitivity analysis, listing variables in descending order from the most impactful to the least impactful one, creating a funnel shape that highlights key drivers. A base-case is defined, and simulations are performed for the base-case and for configurations in which one variable at a time is increased or decreased of the 30% of its base-case value. The base-case is a middle-floor middle-position classroom located in Rome (climatic zone D), with average values for each of the parameters: 0.5 as a solar heat gain coefficient, 17% as a window-to-floor ratio (resulting in a 30% WWR), 8 l/s/person as a natural ventilation rate and 0.6 m/s as air speed from the fans. The room is south-exposed, as this configuration amplifies the results variation. The values assumed by the parameters are summarised in Table 16.

Table 16 – Parameter values for the base-case configuration and the ±30% variations

Parameter	Low	Mid	High
Location	Rome – zone D		
Orientation	South		
Position	Middle floor – middle position		
WFR	12%	17%	22%
SHGC	0.35	0.50	0.65
Natural ventilation rate	5.6 l/s/pers	8 l/s/pers	10.4 l/s/pers
Air speed	0.42 m/s	0.6 m/s	0.78 m/s
Retrofit condition	base-case		

As concerns the window-to-floor ratio, the value is converted to window-to-wall ratio (obtaining 21%, 30% and 38% respectively). To change the SHGC value, three different glazing types are created, and their characteristic values are summarised in Table 17. As can be seen, the thickness of the glass is kept equal to maintain the same U-value, while the transmission and outside reflection values are changed to reach the desired values of solar heat gain coefficient.

Table 17 – Glazing properties for the sensitivity analysis

	Thick. [mm]	Cond. [W/mK]	Tsol [-]	Rsol1 [-]	Rsol2 [-]	E1 [-]	E2 [-]	SHGC [-]	U-value [W/m^{2}K]
Low	8	1	0.299	0.544	0.432	0.019	0.840	0.35	5.63
Mid	8	1	0.335	0.049	0.047	0.840	0.840	0.50	5.63
High	8	1	0.551	0.070	0.070	0.840	0.840	0.65	5.63

The air speed change is not used as an input in the IES-VE simulation, but to calculate the upper temperature threshold for the second comfort band. Indeed, increasing the air speed allows the occupants to adapt to higher temperatures, and the relationship between the air speed and the maximum acceptable temperature for comfort band II is derived from the EN 16798 regulations [45], and these values are interpolated through a polynomial equation to

obtain the temperature threshold values for the desired air speeds. Figure 42 presents the data for the temperature threshold correction related to the air speeds according to the regulation.

Table B.4 — Indoor operative temperature correction ($\Delta\Theta_o$) applicable for buildings equipped with fans or personal systems providing building occupants with personal control over air speed at occupant level

Average Air Speed (v_a) 0,6 m/s	Average Air Speed (v_a) 0,9 m/s	Average Air Speed (v_a) 1,2 m/s
1,2 °C	1,8 °C	2,2 °C

Figure 42 – Temperature thresholds correction according to the air speed from EN 16798 [45]

From this data, the interpolation returns the following trendline equation:

$$T = (-2.3611 \cdot v_{air}^2 + 5.7583 \cdot v_{air} + 22.487)°C$$

Thus, the temperature threshold increases corresponding to air speeds of 0.42 m/s and 0.78 m/s are respectively 0.5°C and 1.5°C.

The internal operative temperature is extracted from the results for each simulation, and from its comparison with the external temperature and the derived metrics (running mean temperature and consequently maximum comfort band temperature), the indicators used for the evaluation of all the configurations are derived:

- Share of hours above the comfort temperature threshold (%)
- Share of occupied hours with temperature higher than 2°C above the maximum one
- Share of hours not complying with each criterion from the TM52 regulations
- Number of heat stress days

The results are then proposed in the following tornado charts (Figures 43, 44 and 45), listing the parameters from the most to the least impacting ones. In all the plots, the orange bars indicate the value assumed by the metric when increasing the value of the parameter of the 30%, while the light blue bars indicate the value reached when decreasing the value of the parameter by the 30%. As can be seen, the increase in the air speed and in the ventilation rate decreases the measured value in all the cases, as of course it decreases the internal operative temperature. Comparing all the considered metrics, it is seen that the ventilation rate has the highest impact on the measured temperature, while the window-to-floor ratio is the least impacting one, with impacts that can be almost considered linear, as the difference between the results in the low and high case respect to the mid one is almost always equal. Solar heat gain coefficient and air speed present similar impacts on the considered metrics.

The results are thus particularly encouraging, as natural ventilation, solar heat gain coefficient and air speed are easily modifiable parameters, while window-to-floor ratio is usually a fixed value for classrooms. In most cases, thus, it will be sufficient to activate fans to increase air speed or to increase the natural ventilation rate to obtain a drastic increase in the comfort of the users.

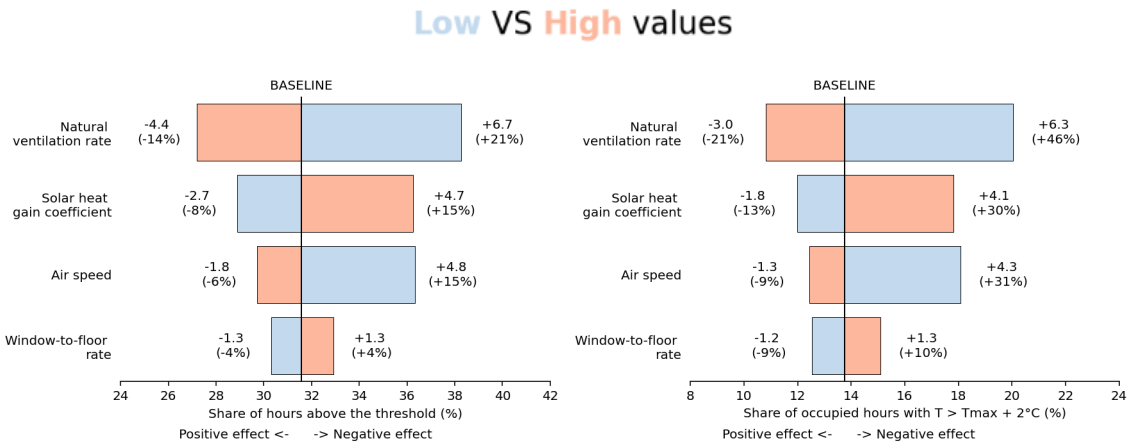

Figure 43 – Tornado chart for the share of hours above the threshold and above 2°C over the threshold

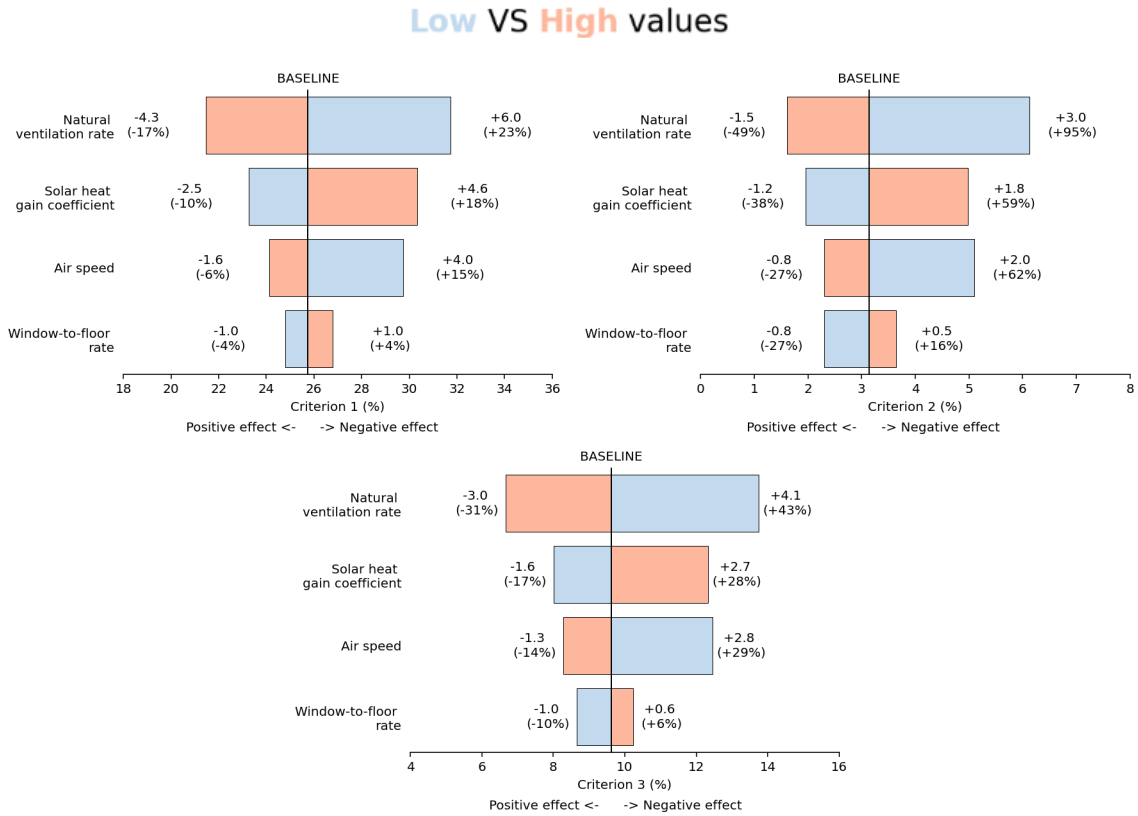

Figure 44 – Tornado chart for the share of hours that do not meet each of the TM52 criteria

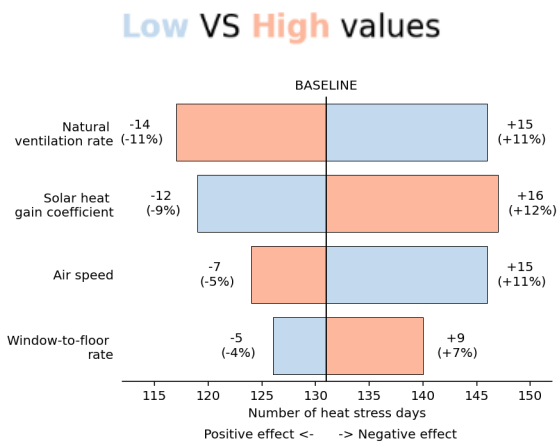

Figure 45 – Tornado chart for the number of heat stress days

In Appendix B, moreover, an analysis of the impact that the alignment between the internal loads and the solar gains has is discussed, changing the starting weekday in the simulations and analysing the impact that this variation determines. It is seen that the variation determines a higher impact in the cases in which solar gains are less important than internal ones, causing higher standard deviations of the share of discomfort hours.

Chapter 5 – Results

In the following chapter, the results of the research are presented. In the first part of the chapter, the results obtained thanks to the simulations of all the cases are summarised and commented on. In total, 24,768 simulations were run, for a total of 68 hours, with 11,520 initial simulations and the rest for additional passive strategies and future weather simulation analysis. The results cannot be presented in a comprehensive way in the text. For this reason, first of all, some examples for specific cases are reported, then some comparative results are presented. These discussions can be used as a guide for the interpretation of the results provided for the specific cases. Moreover, the results for the additional simulations regarding the passive strategies implementation (shadings and night ventilation) and the future weather and Urban Heat Island effect are reported, in comparison with the previously simulated cases. In the second part of the chapter, the output of the study, a parametric tool for the identification of overheating in Italian classrooms and for the comparison of different retrofit strategies, is presented, and in the end, the tool is applied to an existing school.

5.1 Simulation results

In this sub-chapter, the numerical results obtained for all the sets of simulations are presented and discussed. First of all, a restricted set of simulations is presented, then multiple cases are aggregated to compare the variation of different variables.

5.1.1 Example results

In this sub-chapter, the results for the middle floor middle position classroom, for location Milan and base case stratigraphies are displayed.

5.1.1.1 Comfort bands

The comfort bands charts divided per period are displayed in Figure 46, with a chart that encompasses the results for the 48 cases that originate from the combination of the 2 SHGC values, the 4 orientations and the 6 WFRs, with a ventilation rate set to 8 l/s/person. The two SHGC values are compared on the same line in two separate subplots, in which 4 clusters of columns (for each orientation) represent the different WFRs, from the lowest (12%) to the highest value (22%), with a step of 2%. It can be seen that decreasing the SHGC has a positive effect in all the cases, decreasing the hours outside the comfort bands, except for increasing the cold discomfort hours in the winter period. Moreover, rooms with a lower WFR present, in most cases, a better performance, and in all cases, the effects of these variables are intensified when the window is exposed south.

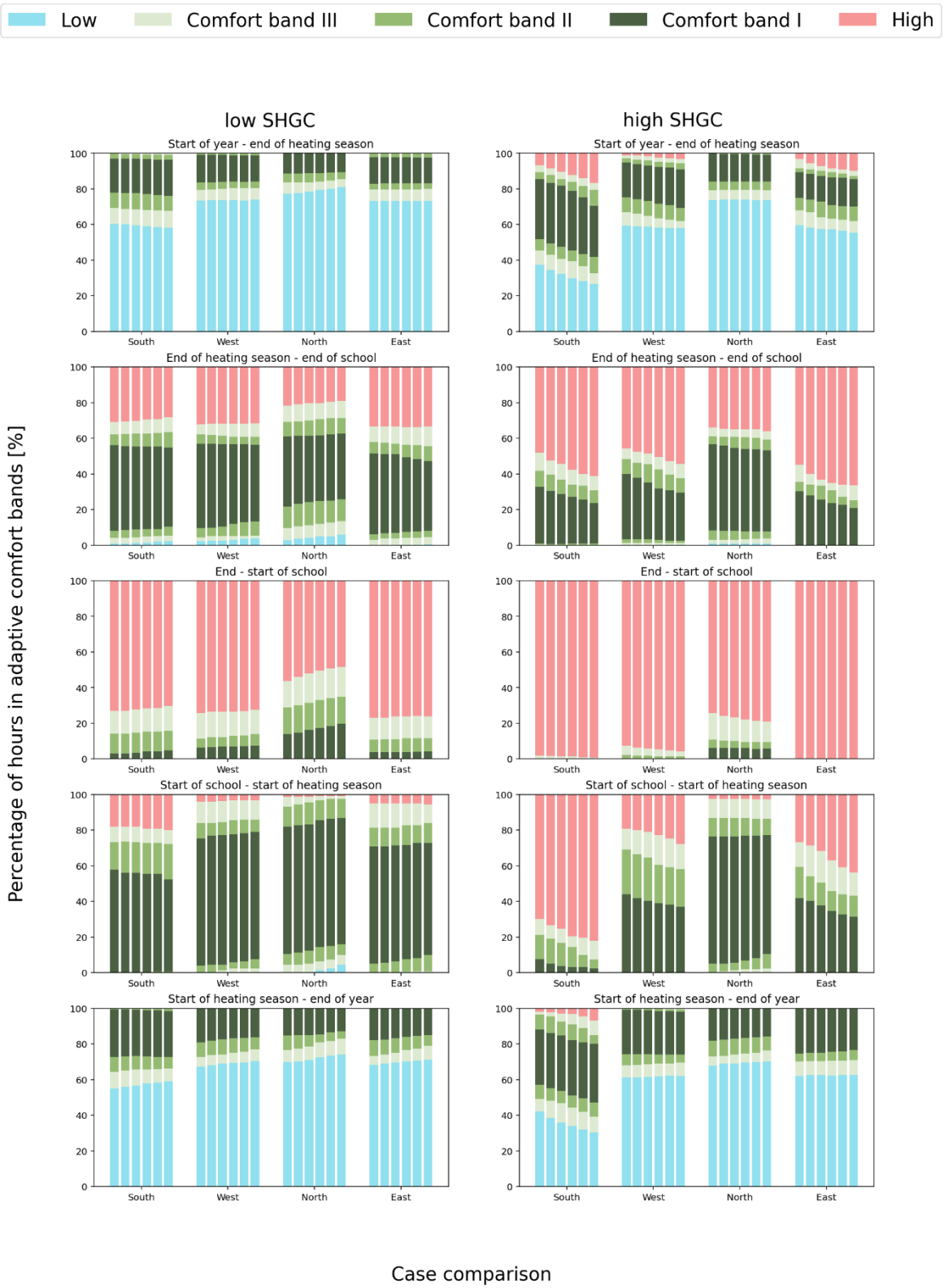

Figure 46 – Comfort bands per period in the case of Milan, with the base-case configuration and room in the middle floor and middle position, with all the combinations of SHGC, exposition and WFR

5.1.1.2 Frequency and cumulative frequency of temperatures

As concerns Figure 47, the distribution of temperatures outside the comfort ranges is plotted. The charts on the left represent the ones with low SHGC, and the ones on the right the ones with high SHGC, while on each row, results for the different orientations of the window are reported, and in each chart, different lines represent different WFR, with the blue-scale lines representing the cases with an increase in the air speed with respect to the red-scale ones. It can be seen that in the cases of window facing north, almost no effect is visible with the different changes of the configuration, except for adding ventilation, which shifts all the cases uniformly towards the comfort zone. On the other hand, the cases with window facing south are more affected by the change in WWR, especially for the low performance glazing cases, while cases with window facing east and west present an average trend, with an higher effect for the east exposition, in which the sun hits the window in the morning hours and affects the zone temperature for the whole day, while if the window is exposed west, the higher gains, that are numerically comparable with the ones for the east exposition, are received in the afternoon and can be dissipated in the night. It can be seen that, moreover, decreasing the SHGC, the variation of response with the variation of the window area decreases.

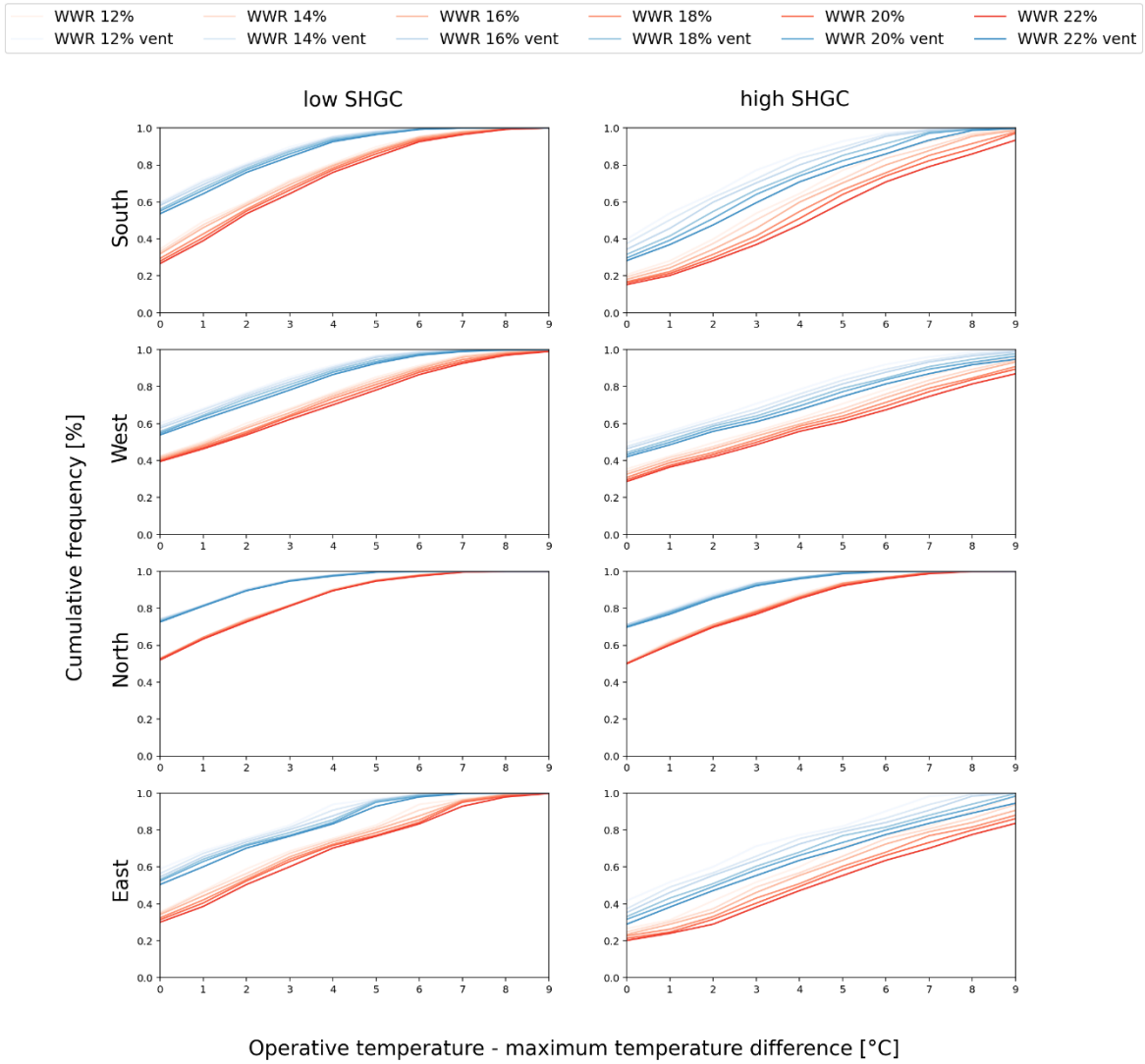

Figure 47 – Cumulative frequency of temperature exceedance for Milan with the base-case configuration and room on the middle floor and middle position (blue for zero and red for higher air speed)

5.1.1.3 TM52 compliance criteria

As already observed in the preliminary analysis, none of the cases reach condition of no overheating according to TM52, except for the cases with the increase of the air speed, in which the second criterion is met for the cases of window exposed south, north and east for the high performance glazing and for the cases of window exposed north for the low performance window, as seen in Figure 48, where the red and green cells indicate if the condition of overheating is respectively met or not for each configuration.

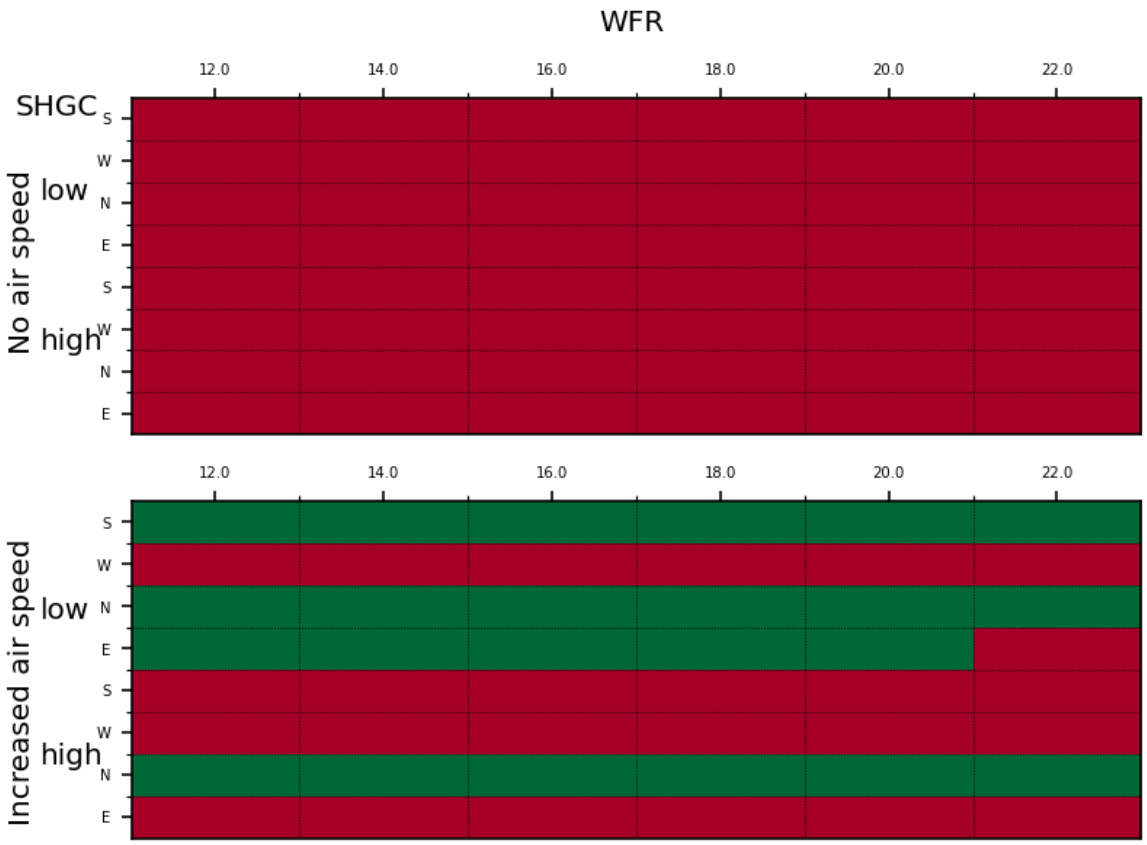

Figure 48 – TM52 compliance for all the combinations in the case of Milan with the base-case configuration and room on the middle floor and middle position

This figure only displays the final result in terms of risk of overheating according to the TM52 regulations, which is false only if at least one of the criteria is met. It is thus not useful to detect what cases are more at risk with respect to the others, and therefore, a similar plot with the values for each criterion (Figure 49) and a parallel plot are created (Figure 50), in order to visualise the values for the three criteria. From the first chart (Figure 51), it can be seen that the cases with a window facing north and a good glazing performance present criterion 2 values very close to zero and approximated to zero. In general terms, the north-facing classrooms present better results, while the south and east ones represent the worst cases.

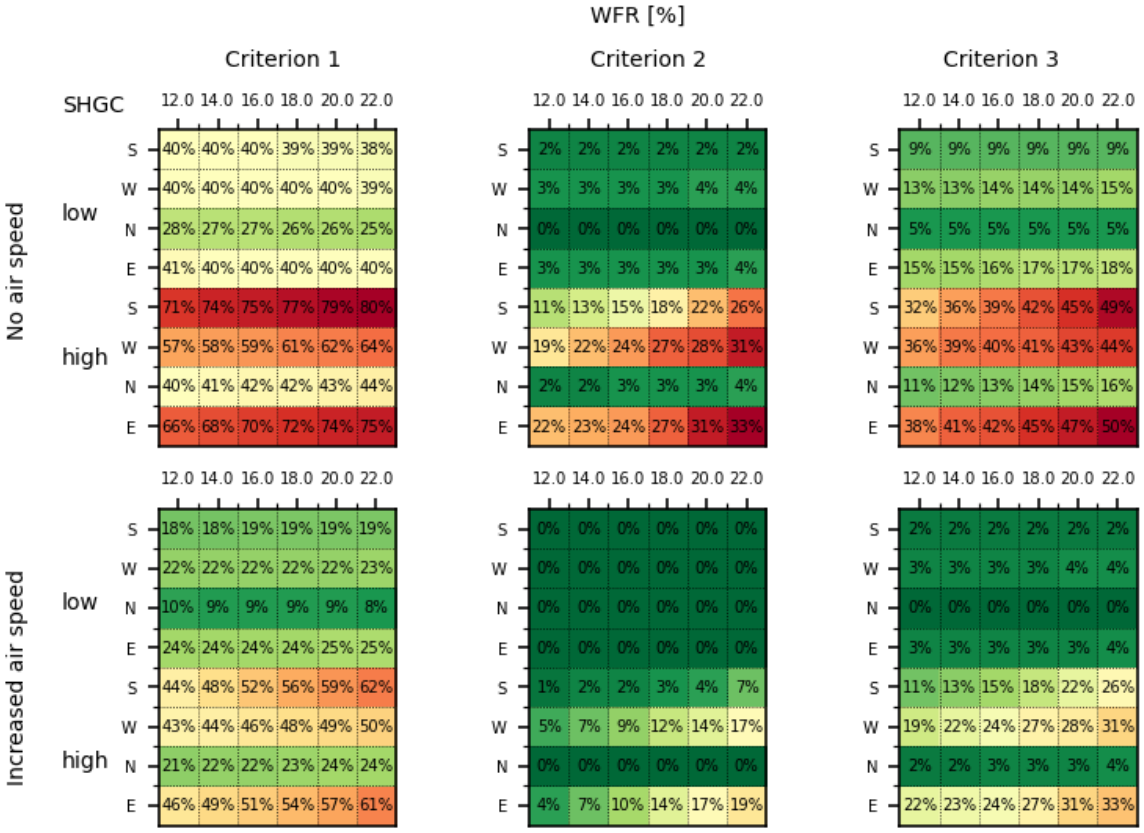

Figure 49 – TM52 compliance for each criterion for all the combinations in the case of Milan, with the base-case configuration and room in the middle floor and middle position

In the parallel plot (Figure 50), the blue lines represent the cases with an increase in the air speed with respect to the red ones, as in the chart of Figure 47. For criteria 2 and 3, the threshold is 0%, while for criterion 1, it is 3%, according to how these criteria are defined. It can be easily seen that the criterion for which the best conditions are reached is the second one, with all the cases presenting values below 35%, while for criterion 1, values are higher than 10% and can reach also 80%. The plot, created with the plotly library from Python [74], is interactive and can be used to identify the cases for which some parameters are contained in a range. Figure 51 displays the cases with criterion 2 equal to zero or close to it. Most of those cases present higher air speed, while the ones that do not are the ones that are north exposed and with a good glazing performance. On the other hand, the cases with the worst performance (with the highest values for criterion 1 and, as a consequence, also for the other criteria) are the ones without the increase in the air speed, with a poor glazing performance and exposed east or south, as seen in Figure 52, in accordance with what was already noticed when discussing Figure 49.

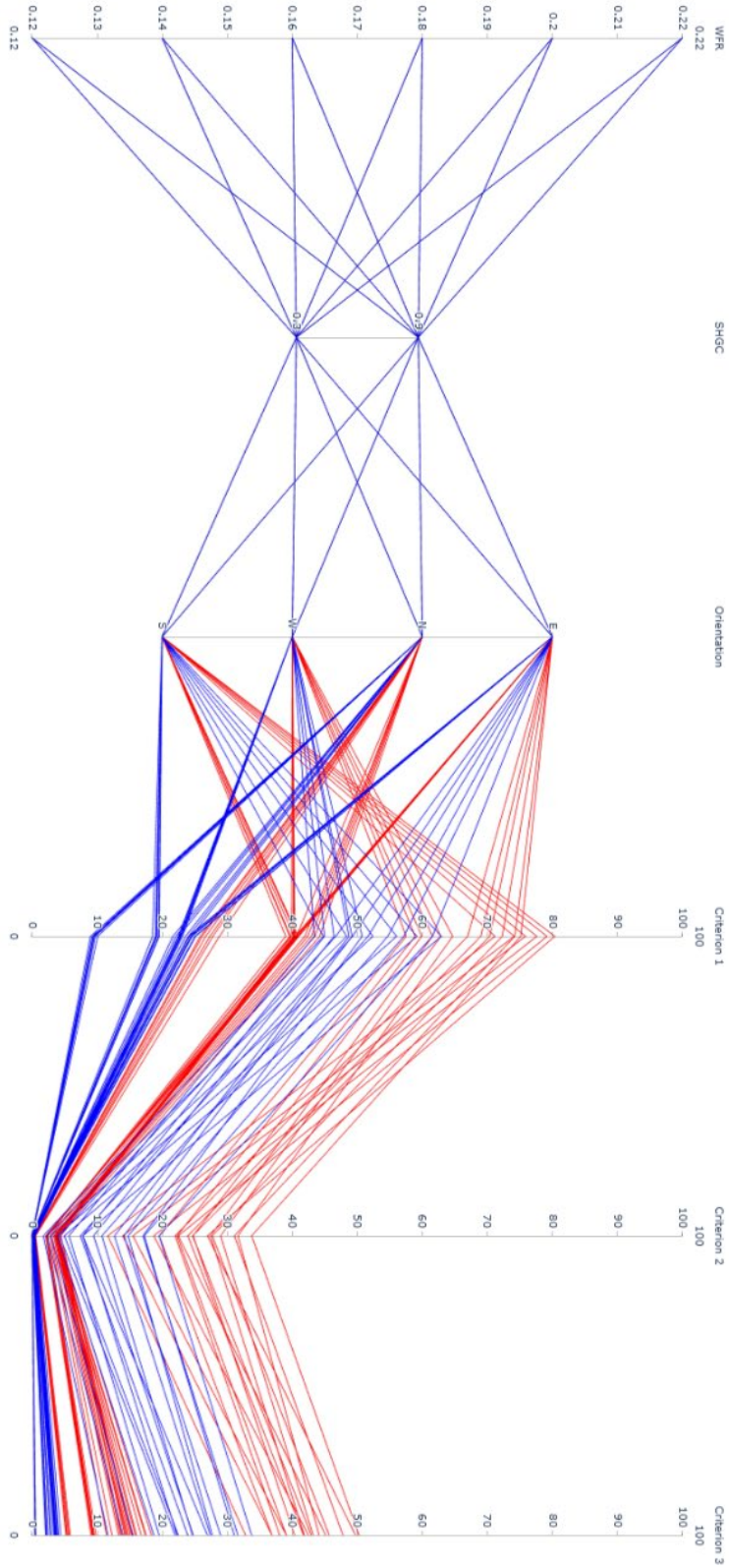

Figure 50 – Parallel plot for the TM52 criteria in the case of Milan with the base-case configuration and room on the middle floor and middle position

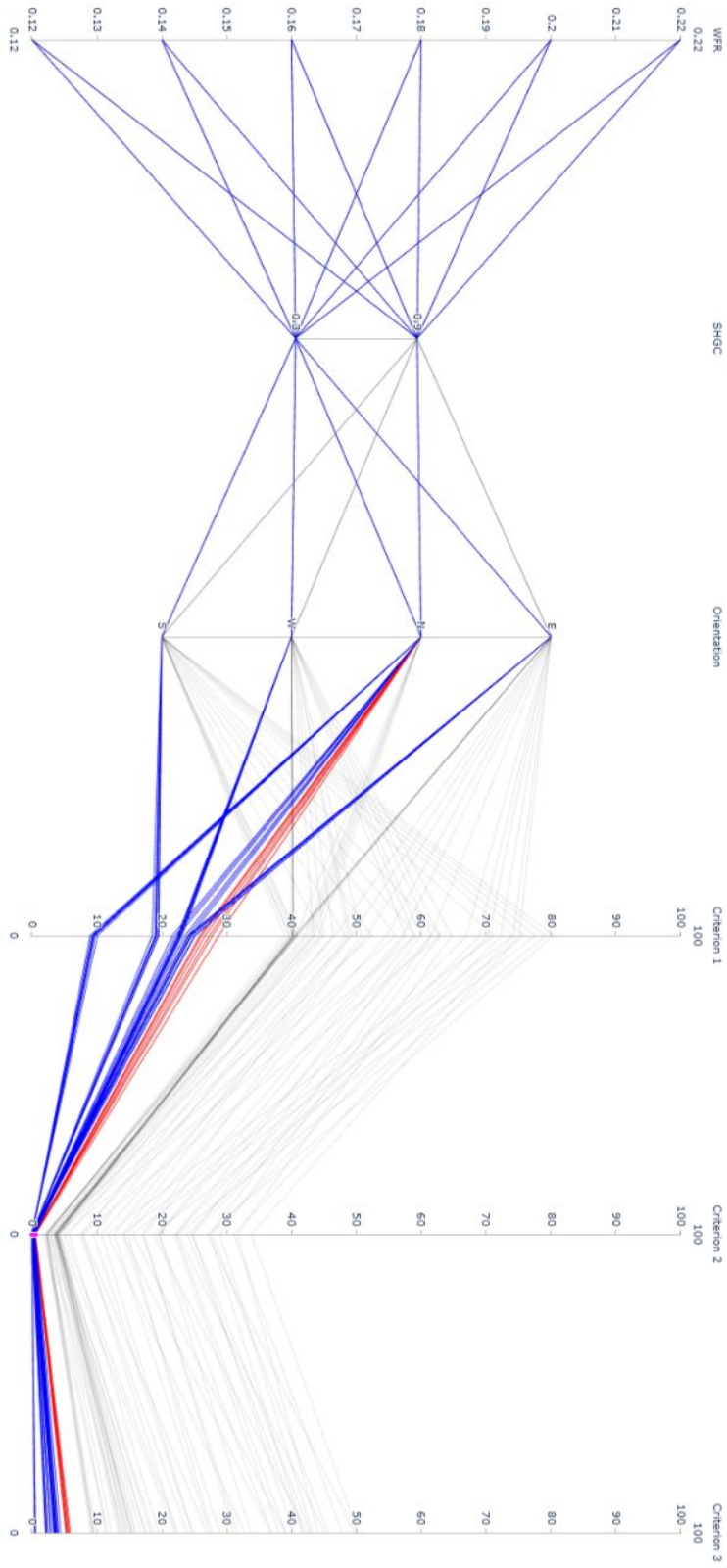

Figure 51 – Parallel plot for the TM52 criteria in the case of Milan with the base-case configuration and room in the middle floor and middle position, with highlighting of the cases with criterion 2 equal or close to zero

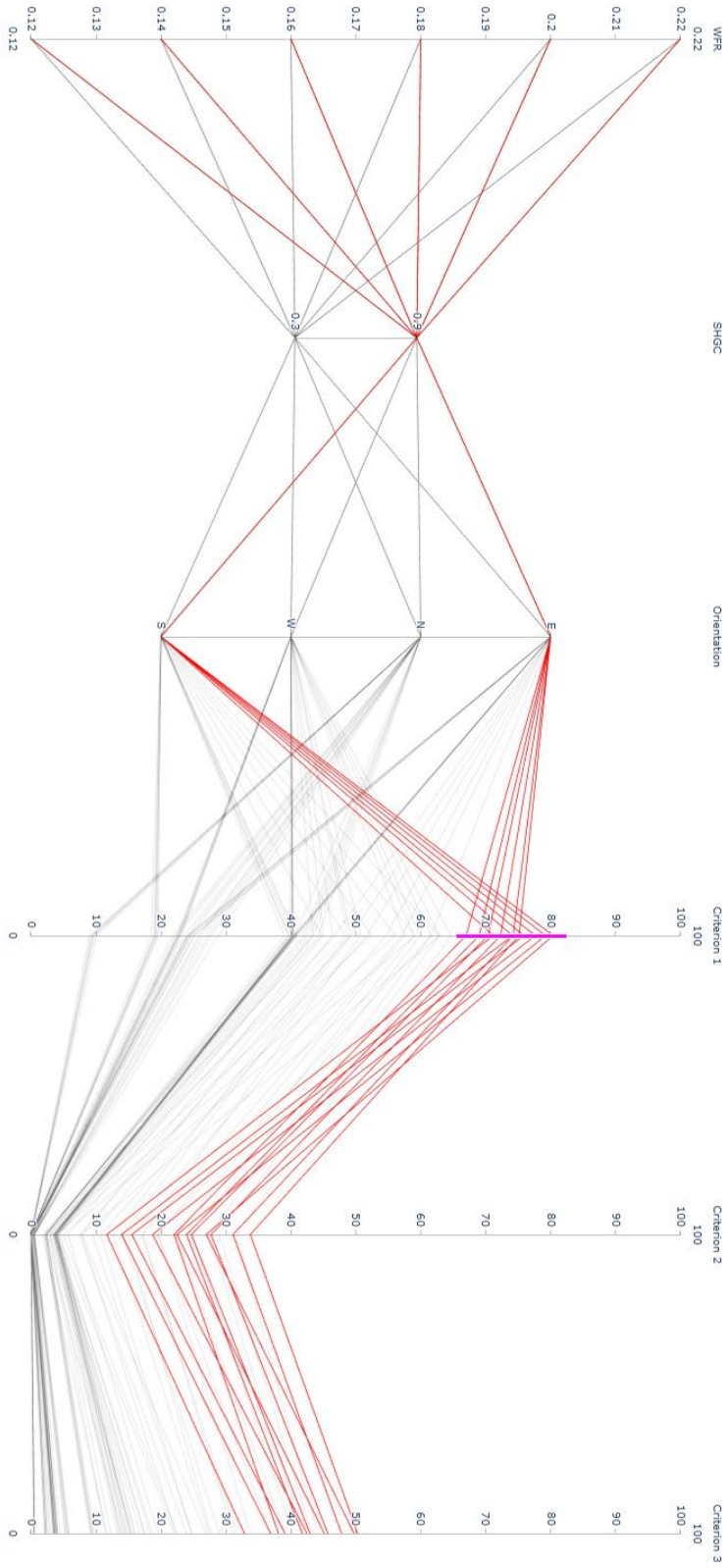

Figure 52 – Parallel plot for the TM52 criteria in the case of Milan with the base-case configuration and room in the middle floor and middle position, with highlighting of the cases with the worst values for criterion 1

5.1.1.4 Heat stress days evaluation

In the end, the overheated days share is calculated, according to the heat wave definitions and to the methodology described in the previous chapter, and plotted in Figure 53. As already mentioned when commenting on the other metrics, the classrooms with north exposition, with an increase in the air speed and with better glazing performance present better results, with a low variability for what concerns the window-to-floor ratio. The shares range from 18% in the best cases to 42% in the worst ones. Figure 54 displays the same results divided by period, based on the start and end of the heating season and of the school period. It can be seen that most of the overheated days belong to the summer period, and that thus the classroom's thermal performance should be improved if use in the summer period is needed. Figure 55 displays an example of the distribution of the days for one specific case (located in Milan, with the classroom in the centre of the middle floor, with WFR 12%, south exposition and SHGC 0.3). The internal operative temperature is plotted against the running mean outdoor temperature, and the comfort categories are displayed for the range of use of the equation (from 10°C to 30°C). The dark red dots represent the days classified as overheated, the medium ones the non-consecutive days and the light red ones the days in which ventilation can be performed.

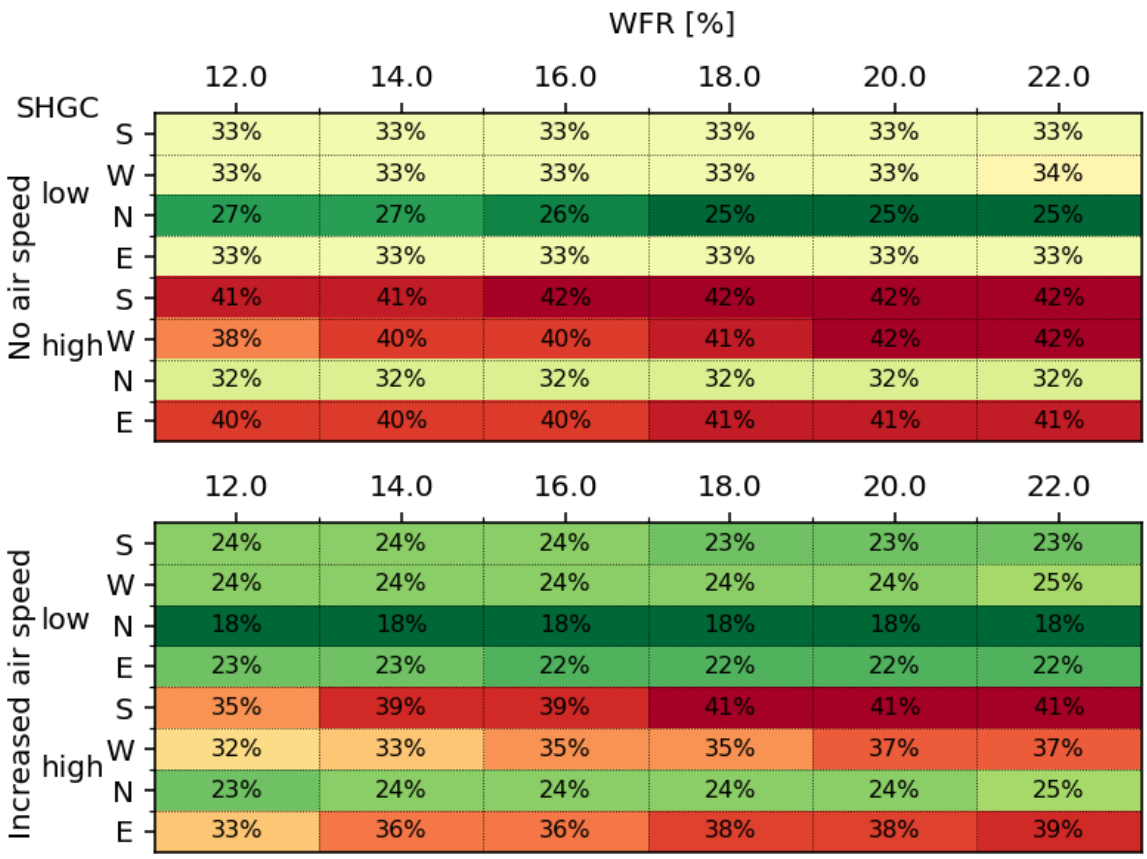

Figure 53 – Share of heat wave days for Milan with base-case configuration and room on the middle floor, middle position

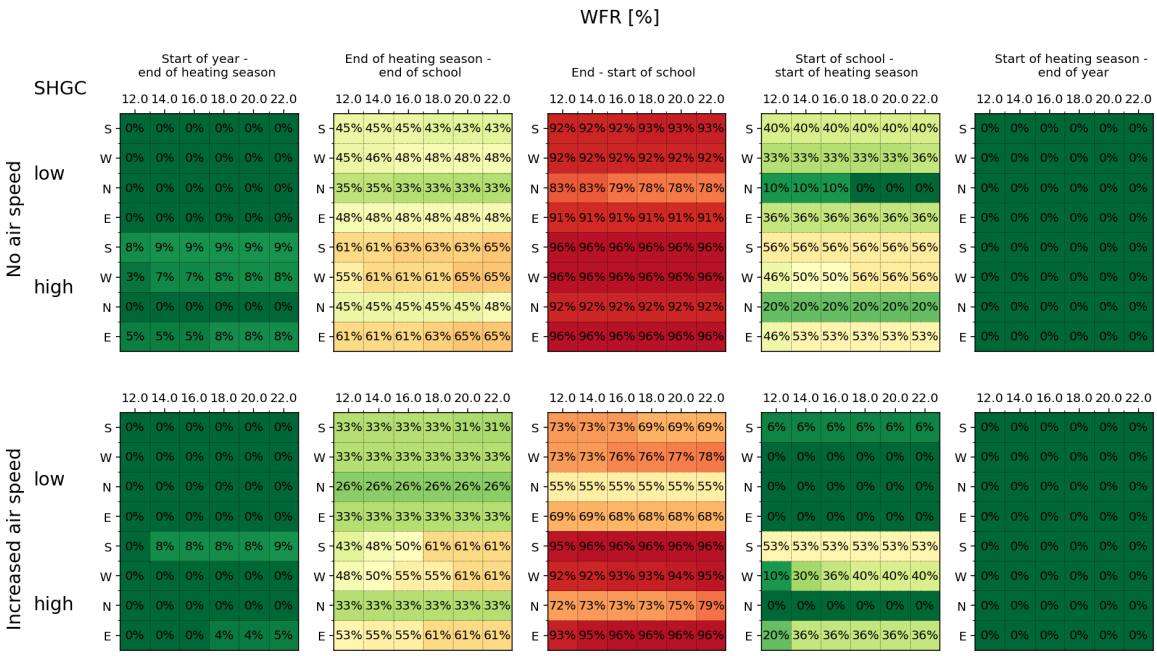

Figure 54 - Share of heat wave days in the five periods for the Milan base-case configuration and room in the middle floor, middle position

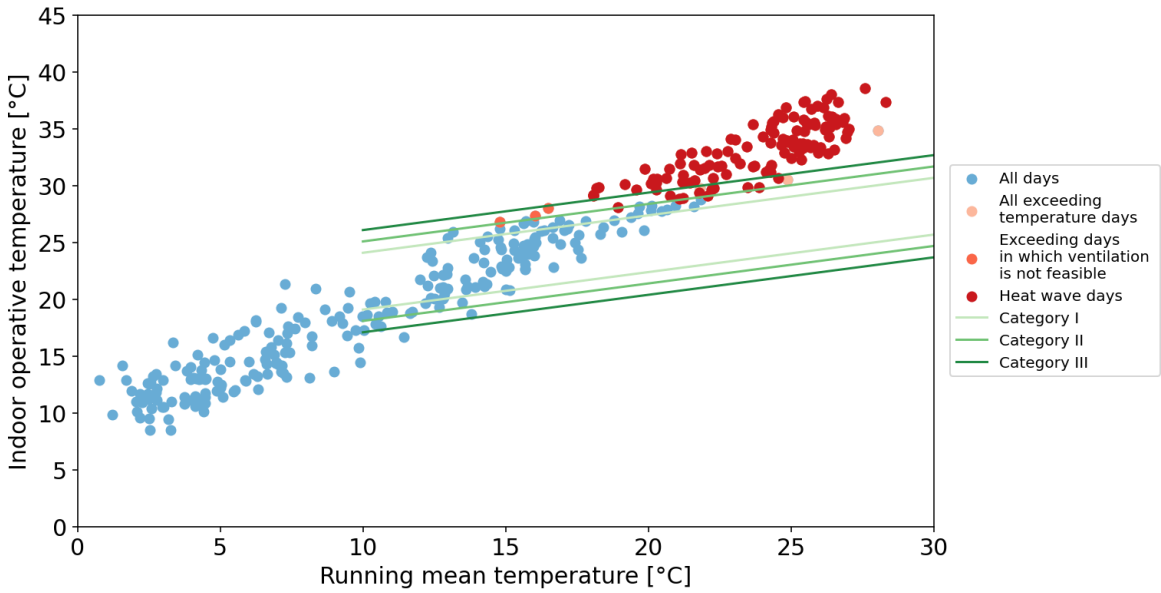

Figure 55 – Example distribution of heat wave days for the case Top Centre Base 12% WFR, south, 0.3 SHGC

5.1.2 Configurations comparison

In this chapter, the results for sets of simulations are gathered and compared. Heatmaps are created for the principal metrics that are being used as an output in the analysis, to compare the different configurations on several axes: the retrofit configuration (base-case, wall retrofit, roof retrofit, window retrofit), the location of the building (represented by the 6 climatic zones), the position of the classroom (Ground, Middle or Top floor and Middle or

Corner position) and the ventilation rate (8 l/s/person as prescribed by the regulations or a lower value of 1.2 ACH). The classroom positions are coded as follows:

- G-M: Ground floor, Middle position
- G-C: Ground floor, Corner position
- M-M: Middle floor, Middle position
- M-C: Middle floor, Corner position
- T-M: Top floor, Middle position
- T-C: Top floor, Corner position

For all the plots, the "ROOF" retrofit case is present only in the top-floor scenarios.

The results are compared considering the average values for each location, position of the classroom and retrofit case of the following quantities:

- Comfort bands: share of hours with temperature higher than the comfort threshold (Figure 56).
- Distribution of temperatures above the comfort threshold: share of hours with temperature higher than 2°C above the comfort threshold (Figure 57), as this is the value over which the discomfort condition is considered excessive. The colour scale in this plot is the same as in the previous one, to highlight the decrease in the share of hours in unacceptable discomfort conditions.
- TM52 compliance: cases that are not compliant with the regulation (Figure 58). This plot presents a higher share of "red" cells, as the TM52 compliance does not detect the shades of cases that are closer to the thresholds.
- Heat stress days: share of heat stress days, for both cases of zero air speed (Figure 59) and increased air speed (Figure 60)

The first two charts present the same colour scale, in order to compare the reduction in the share of hours above the two limits. The same happens for the last two plots regarding the heat stress days, while the plot for the TM52 compliance presents a colour scale from 0 to 100%.

5.1.2.1 Retrofit condition comparison

Observing all the plots, it can be seen that the retrofit of the building in most cases worsens the situation in terms of overheating metrics, especially when replacing the glazing with double-glazing ("WINDOW" retrofit case). On the other hand, the roof and wall insulation do not yield such bad consequences, even if they still, on average, worsen the result. It must

be specified that the window retrofit also affects the infiltration rate, reducing it from 0.5 ACH of the base-case and of all the other cases to 0.25 ACH, and this is probably the cause of such a high increase in the values for what concerns the window retrofit cases respect to the, other retrofit scenarios, in addition to the increased insulating performance, of the glazing.

5.1.2.2 Classroom position comparison

Comparing the different classroom positions, it can be seen that the ground (G) classrooms present better values, especially in climatic zones A and F, while the top floor (T) classrooms only present better results in some of the cases. The ground floor classrooms owe their low temperatures to the contact with the ground, while the top floor ones to the high emissivity that allows for good night cooling conditions. The corner position (C) determines, on average, a slight improvement in the results. This effect has to be justified, keeping in mind that the corner position classrooms do not present higher window areas, as they present the same window-to-floor ratios, with the area of the window split on the two walls, and they present a higher façade dispersing area.

5.1.2.3 Climatic zone comparison

As concerns the comparison between different climatic zones, it can be seen that zone F presents better results than the others, which are quite homogeneous. Also climatic zone A presents good results, and it has to be kept in mind that the definition of the comfort bands also takes into account the external running mean temperature, and thus the discomfort hours share and the other considered metrics are affected by this. As far as the heat stress days are considered, a neater correlation can be identified, observing that the colder the climate is, the smaller is the share of heat stress days. This metric is indeed calculated taking into account the possibility of ventilating the room thanks to the difference of temperature between the indoor and outdoor spaces, along with the consecutiveness of high temperature days, thus not only considering the adaptive temperature thresholds. It can be concluded thus that in the colder climates, there is a greater possibility of ventilating the rooms even on the hot days, which are more isolated.

5.1.2.4 Ventilation rate comparison

In conclusion, comparing the two subplots that in each figure represent the different ventilation scenarios, it can be seen that respecting the regulations' minimum ventilation rate of 8 l/s/person can determine a considerable decrease in the share of discomfort hours.

Comparing the two heat stress days' figures, it can be seen that increasing the air speed also provides a positive effect.

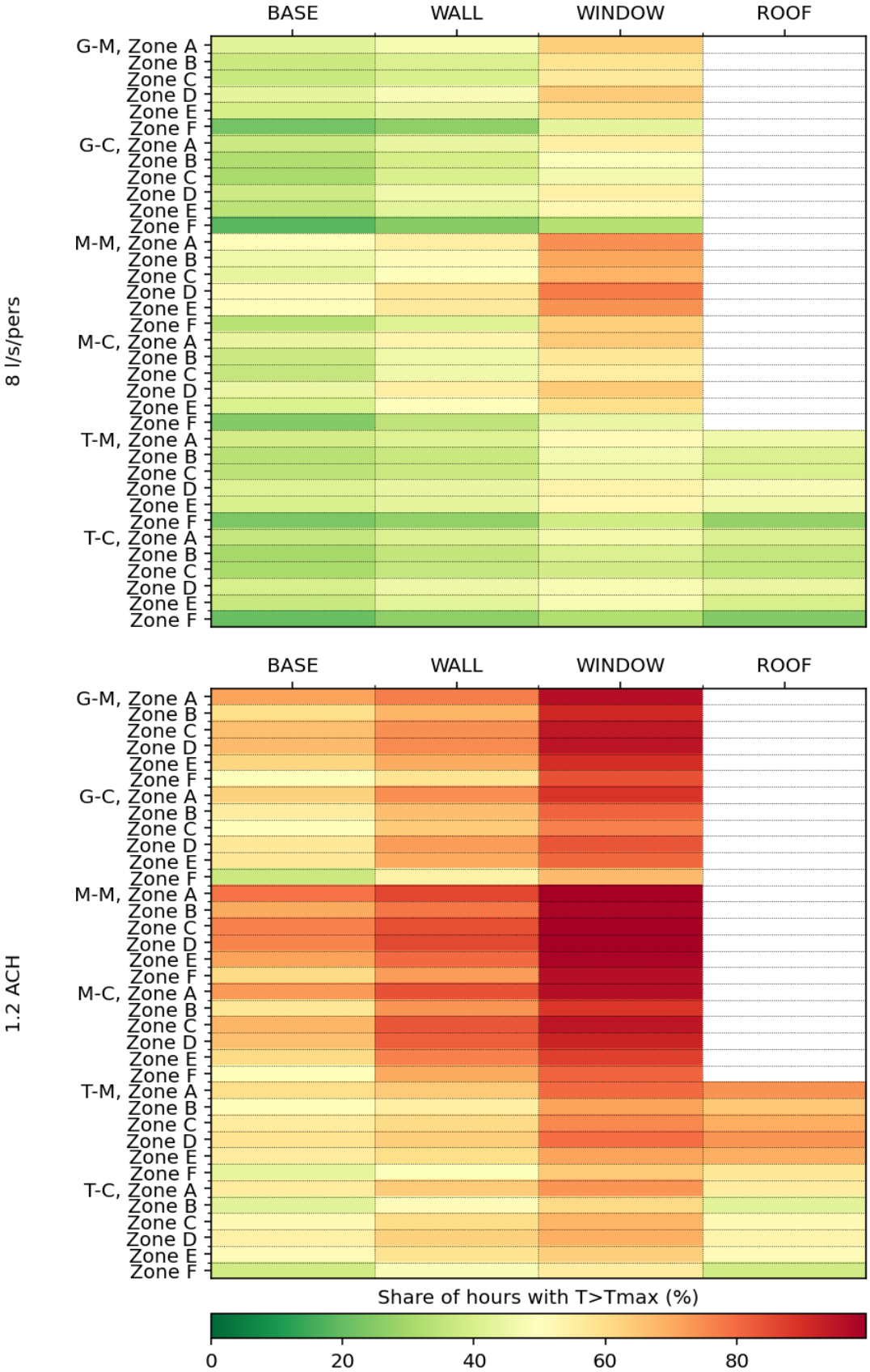

Figure 56 – Average of the share of hours outside the comfort bands heatmap

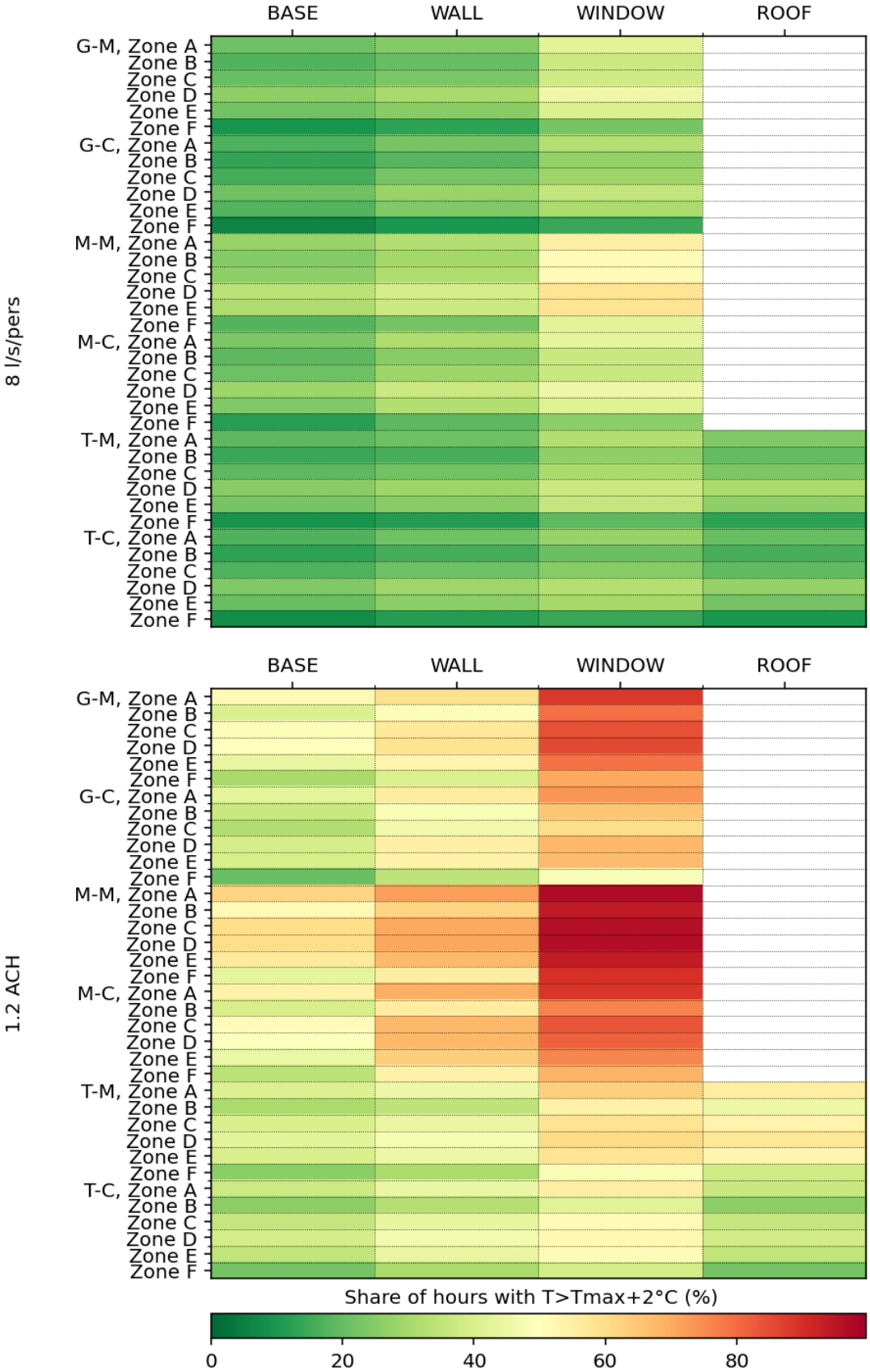

Figure 57 – Average of the share of hours with temperature higher than 2°C above the maximum temperature heatmap

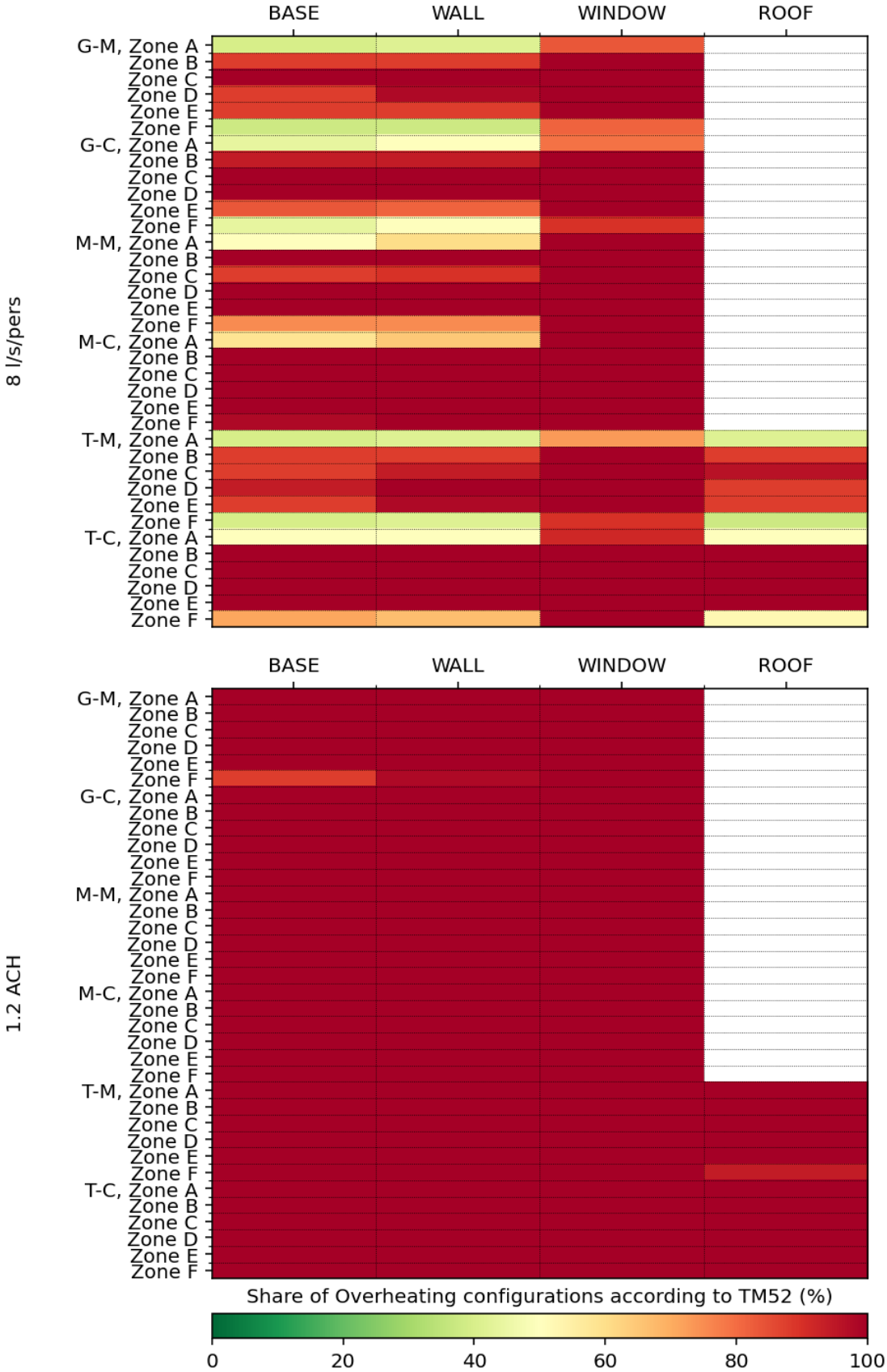

Figure 58 – Share of cases that are not compliant with the TM52 heatmap

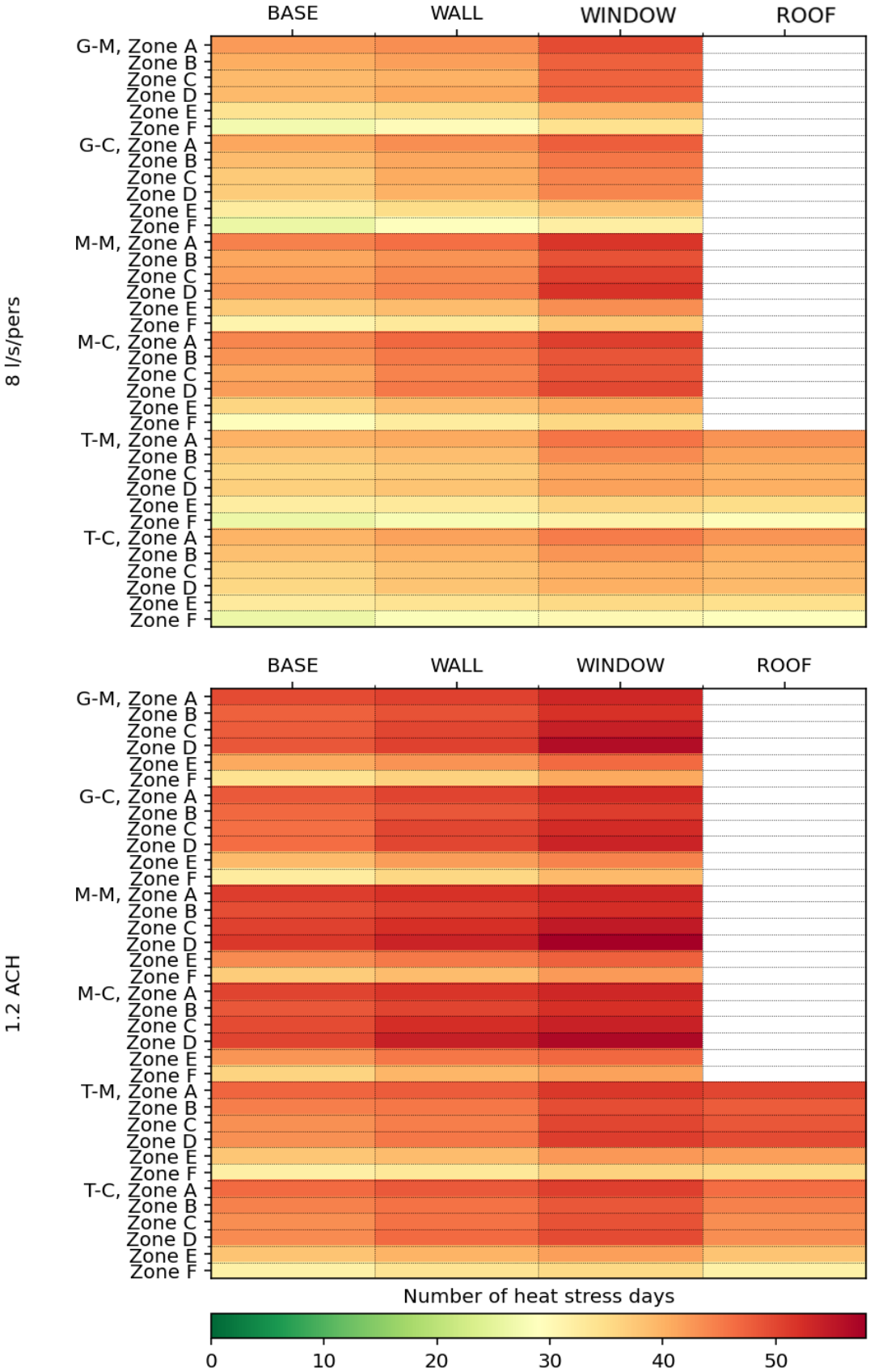

Figure 59 – Average number of heat stress days heatmap

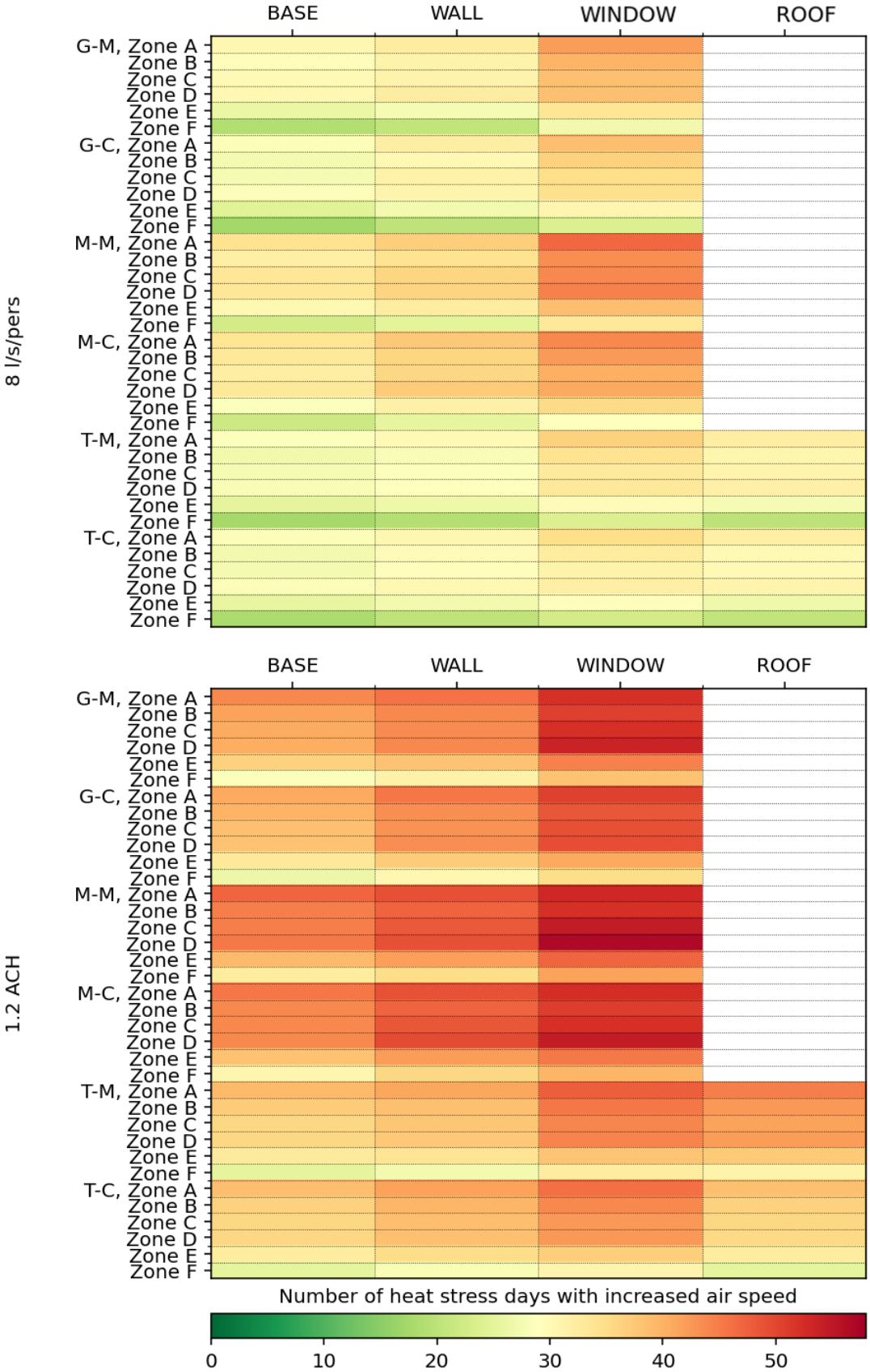

Figure 60 – Average number of heat stress days heatmap for increased air speed cases

5.1.3 Additional passive strategies simulation results

In the following paragraphs, the results in terms of share of hours with temperature above the comfort threshold are reported for comparing the passive strategies that were implemented, namely adding the shadings and activating night ventilation.

5.1.3.1 Shadings simulations results

Figures 61 and 62 display the average values of the share of hours with temperature above the comfort threshold, comparing the three shading scenarios: no shading, louvres at 0° and louvres at 45°. The results are moreover divided for the solar heat gain coefficient values, low and high, respectively, at the left and right of each figure, and for the two ventilation rate scenarios, 8 l/s/person and 1.2 ACH, in the two different plots. The subplots separate the different retrofit scenarios, gathering classrooms on the same floor in different climatic zones. The roof retrofit values are only reported for classrooms on the top floor, as the roof retrofit does not influence the other cases.

It can be seen that adding shading devices provides a high impact on the reduction of discomfort hours, reducing them to values lower than 20% in the cases of low SHGC value and without window retrofit. Moreover, it is clearly visible how the reduction in the discomfort hours is higher for the configurations with a high SHGC value, as those are the cases in which discomfort is higher without any shading device.

On average, the highest decrease is obtained in the cases with window retrofit, with averages of 8 and 15 percentage points decrease in the 0° and 45° louvres configurations, respectively.

The plots can be used to identify whether it is more convenient to apply shading devices or to reduce the SHGC value of the window, comparing the reduction in the overheated hours and, additionally, the costs connected to the two different solutions.

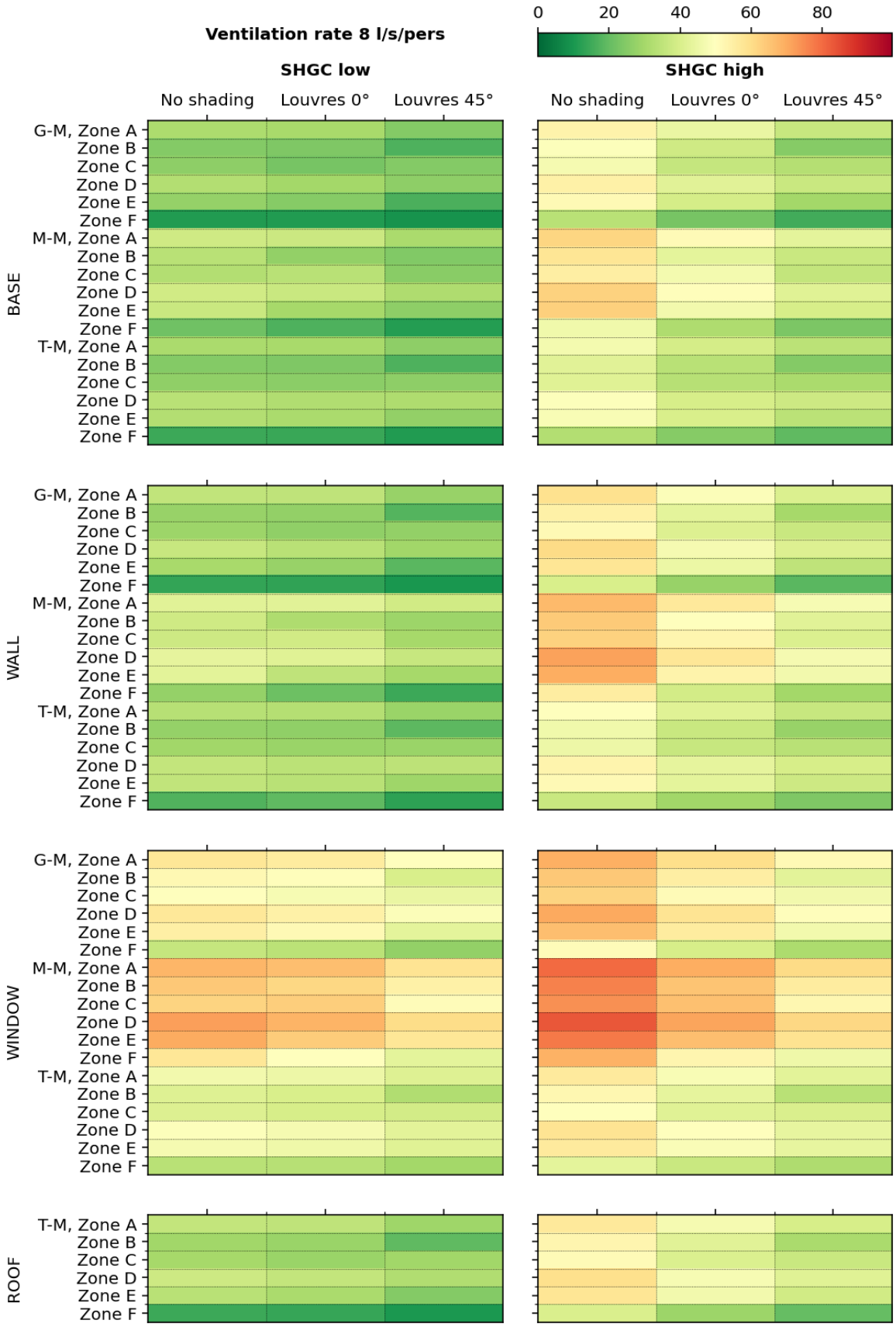

Figure 61 – Different shading configuration comparison for high and low SHGC for the 8 l/s/person ventilation scenario

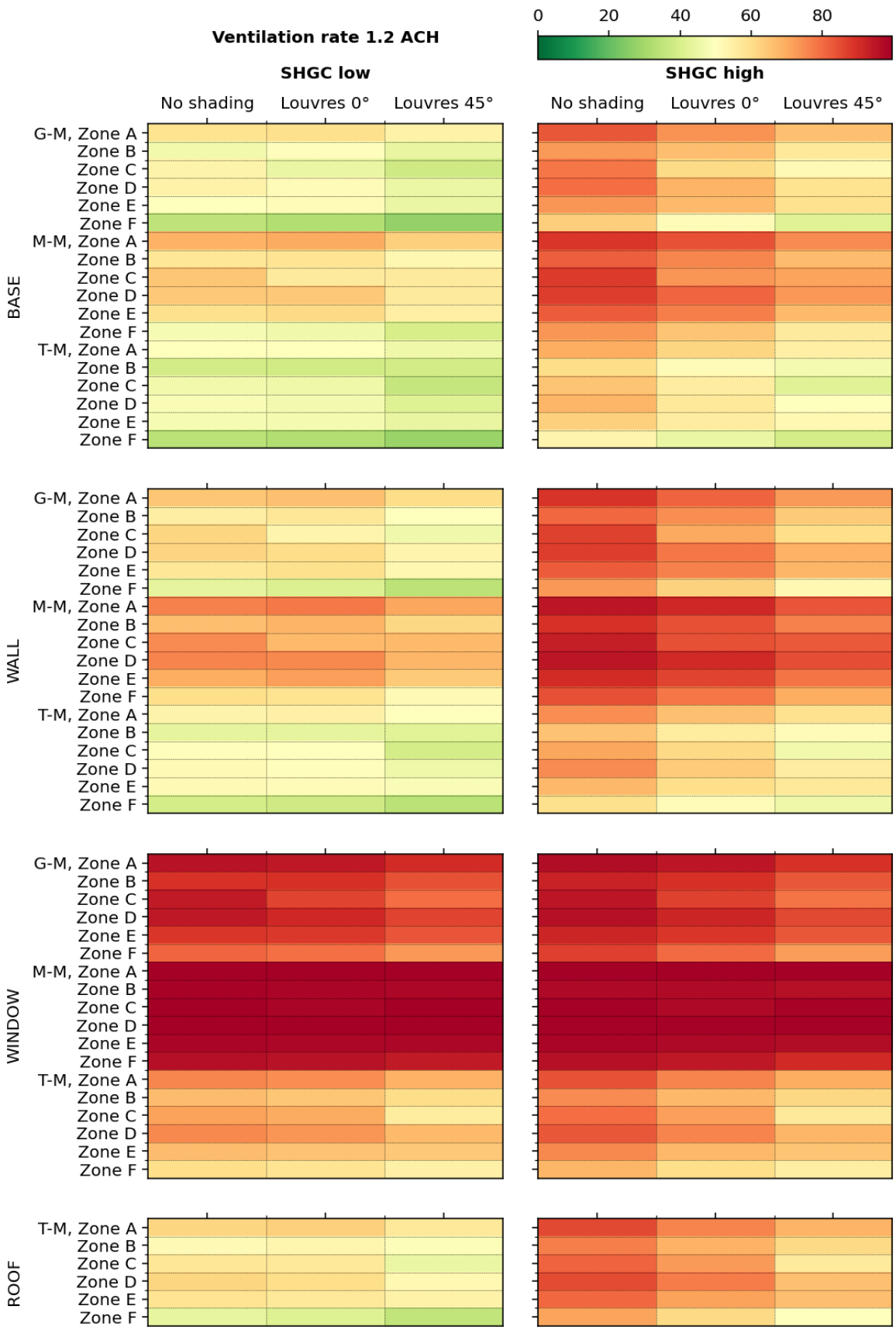

Figure 62 – Different shading configuration comparison for high and low SHGC for the 1.2 ACH ventilation scenario

5.1.3.2 Night-time ventilation simulation results

Figures 63 and 64 display the average values of the share of hours with temperature above the comfort threshold, comparing the night ventilation scenario with the base-case scenarios. In the same way as for the shading plots, the results are moreover divided for the solar heat gain coefficient values, low and high, respectively, at the left and right of each figure, and for the two ventilation rate scenarios, 8 l/s/person and 1.2 ACH, in the two different plots. The subplots separate the different retrofit scenarios, gathering classrooms on the same floor in different climatic zones. The roof retrofit values are only reported for classrooms on the top floor, as the roof retrofit does not influence the other cases.

In both cases, it can be clearly seen how adding the night ventilation strategy provides a sharp decrease in the hours with temperature above the discomfort temperature, with better results compared to the results associated with the use of shading devices. Moreover, comparing the two SHGC scenarios, different retrofit strategies can be compared, for example, considering that with a high SHGC value for the window and the addition of night-time ventilation, similar results to the case of low SHGC can be reached. For what concerns the scenarios with ventilation rates of 1.2 ACH, it can be seen how even adding the night-time ventilation has a very poor positive effect, bringing the share of discomfort hours below 40% only in the cases of low SHGC and not in the case of refurbished windows, cases in which also the infiltration rate is reduced and thus cooling the space is harder.

The very high influence of ventilation on the reduction of overheated hours, already presented with the sensitivity analysis, observed with the comparison of all the plots with the two ventilation flow rates scenarios and now confirmed observing the sharp reduction of the parameter with the addition of night ventilation, has to be thus carefully taken into account, as this passive strategy can be implemented in more or less automated manners and can provide a good improvement to the quality of indoor classroom spaces.

On average, a stable decrease in the discomfort hours between 14 and 24 percentage points is registered in all configurations with the addition of night ventilation.

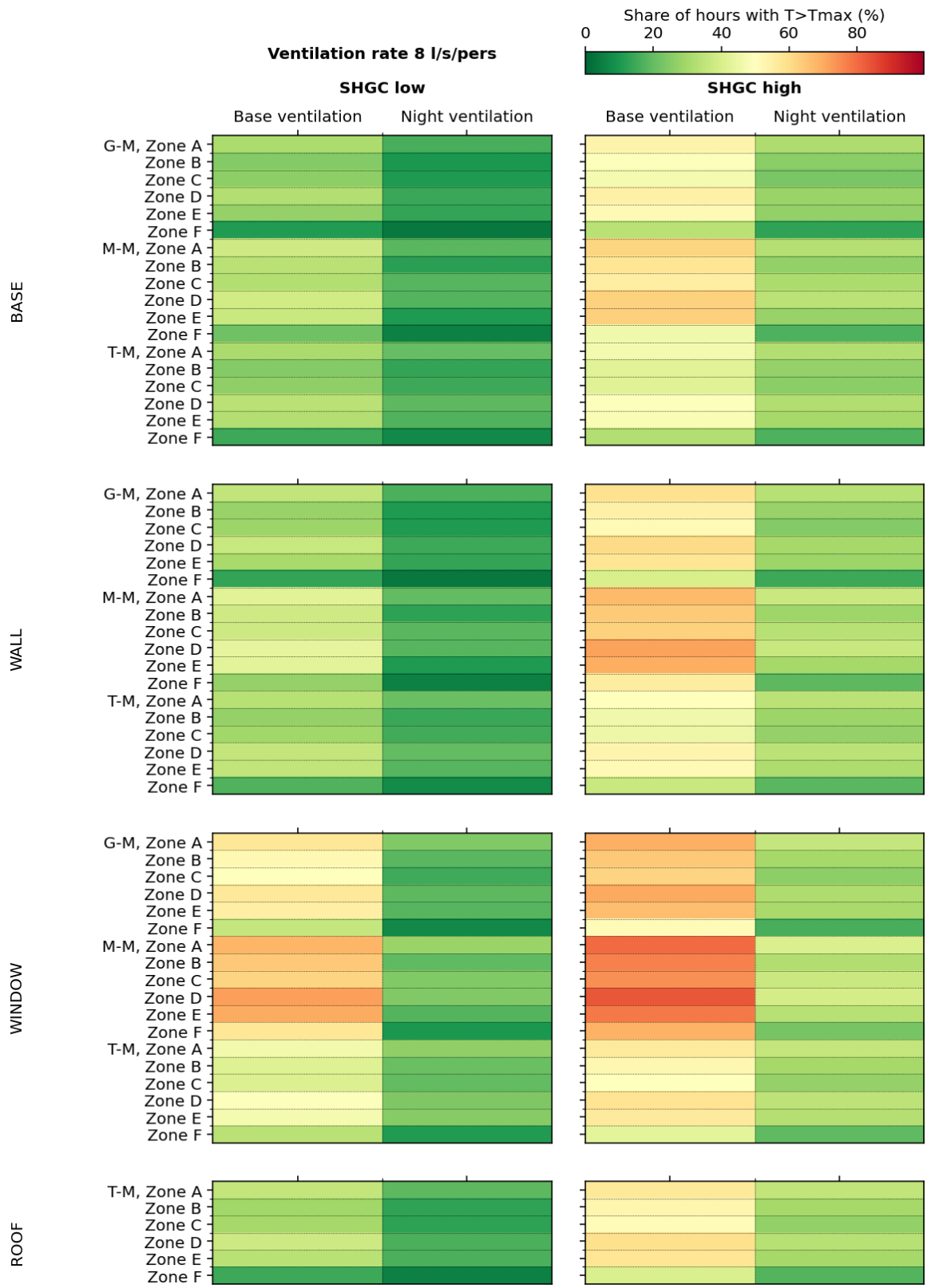

Figure 63 – Night ventilation with respect to normal ventilation configurations comparison for high and low SHGC for the 8 l/s/person ventilation scenario

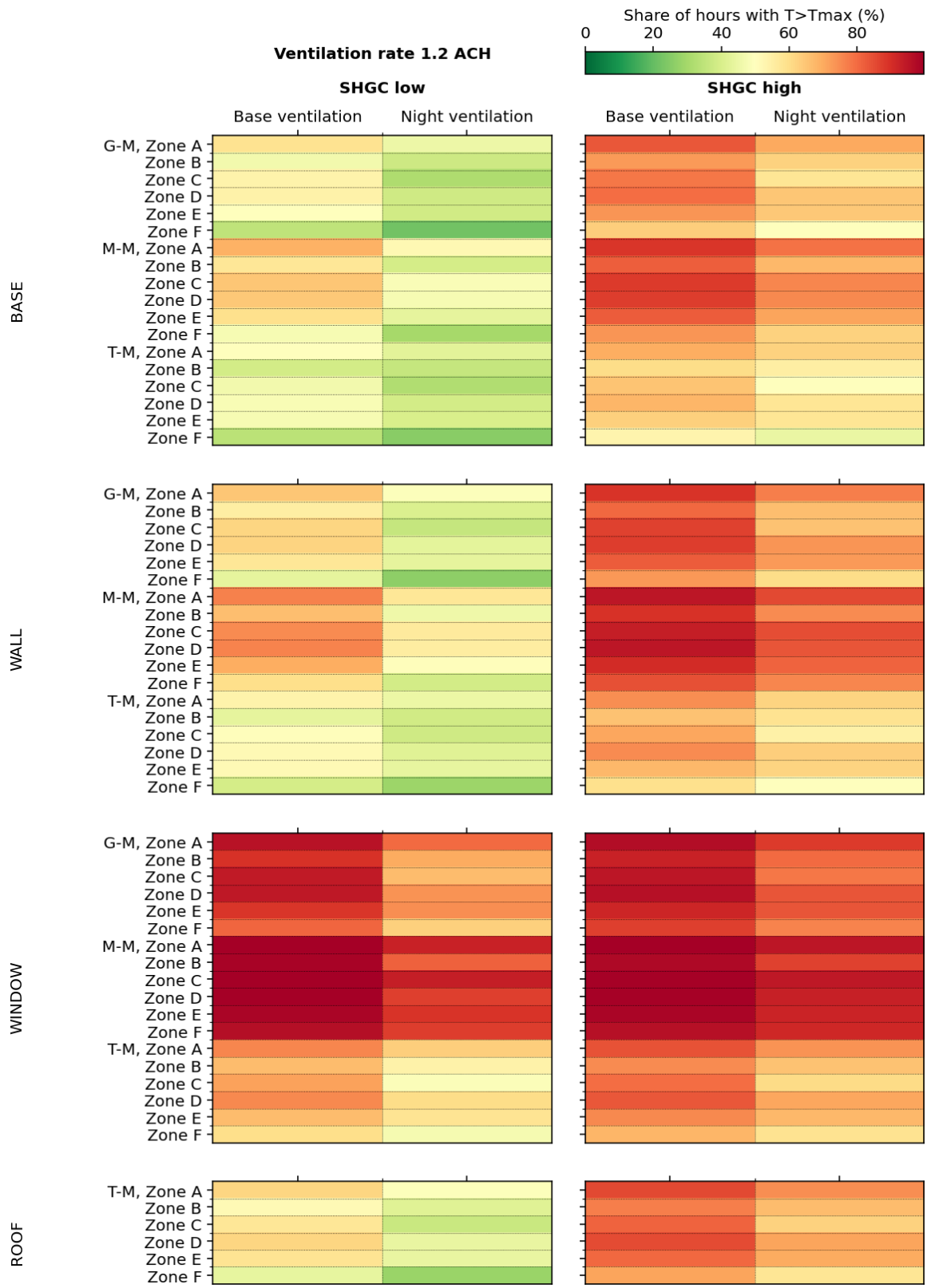

Figure 64 – Night ventilation with respect to normal ventilation configurations comparison for high and low SHGC for the 1.2 ACH ventilation scenario

5.1.4 Overheating drivers' simulation results

In the following paragraphs, the results in terms of share of hours with temperature above the comfort threshold are reported for comparing two additional weather scenario phenomena: the increase of temperatures in the future weather scenarios and the increase of temperatures as a consequence of the Urban Heat Island effect.

5.1.4.1 Future weather simulation results

Figures 65 and 66 display the average values of the share of hours with temperature above the comfort threshold, comparing the three weather scenarios: the historical weather file, used until now for all the simulations, the 2050 SSP585 weather file and the 2080 SSP585 weather file. The results are moreover divided for the solar heat gain coefficient values, low and high, respectively, at the left and right of each figure, and for the two ventilation rate scenarios, 8 l/s/person and 1.2 ACH, in the two different plots. The subplots separate the different retrofit scenarios, gathering classrooms on the same floor in different climatic zones. The roof retrofit values are only reported for classrooms on the top floor, as the roof retrofit does not influence the other cases.

From the plots it can be observed how with the future climate weather files, a very high increase in the discomfort hours is detected, with higher increases, around 15 and 27 percentage points for the 2050 and 2080 scenarios, for the base case configurations, and lower increases, around 10 and 17 percentage points for the 2050 and 2080 scenarios, for the window retrofit configurations.

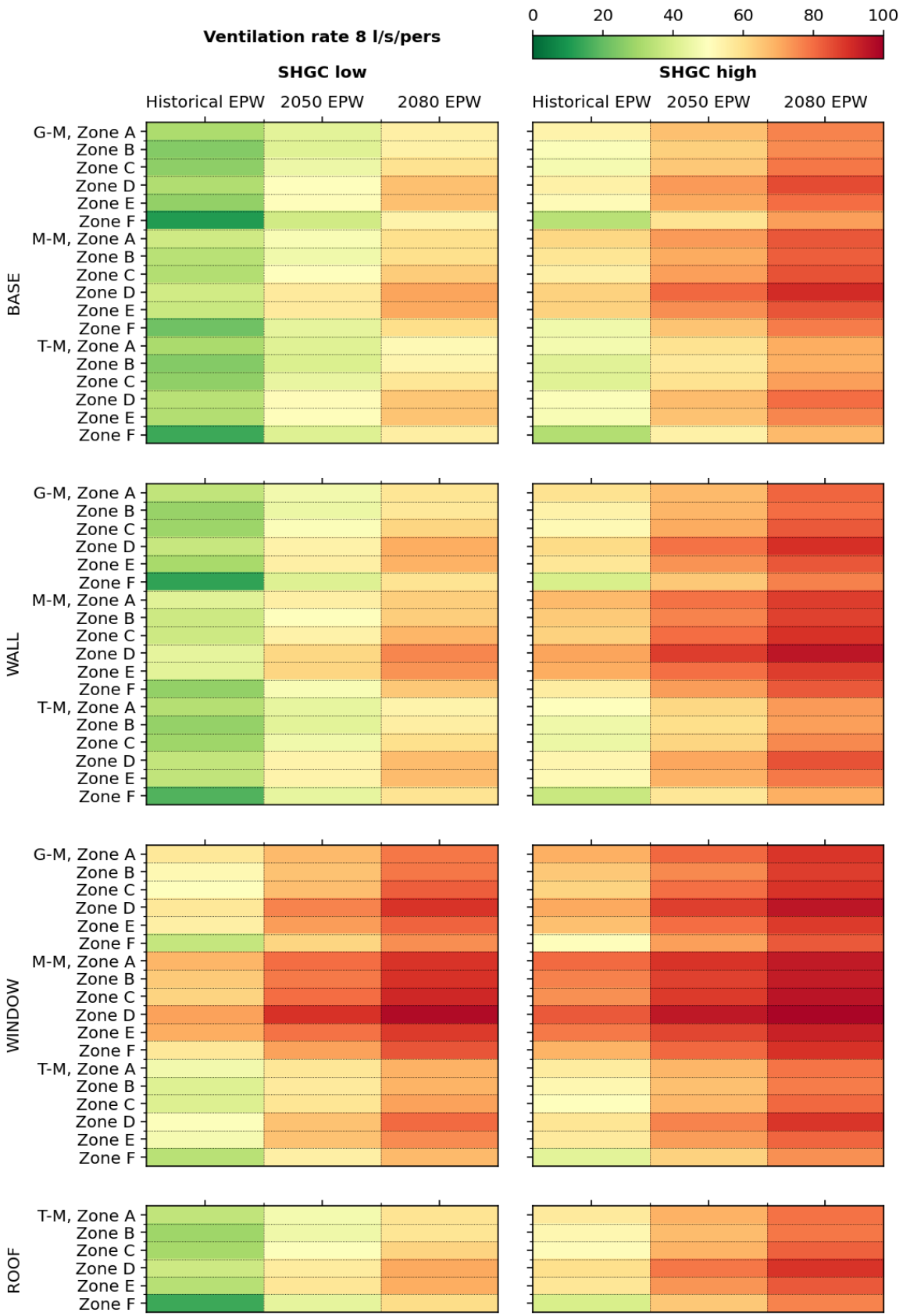

Figure 65 – Future weather results comparison for high and low SHGC for the 8 l/s/person ventilation scenario

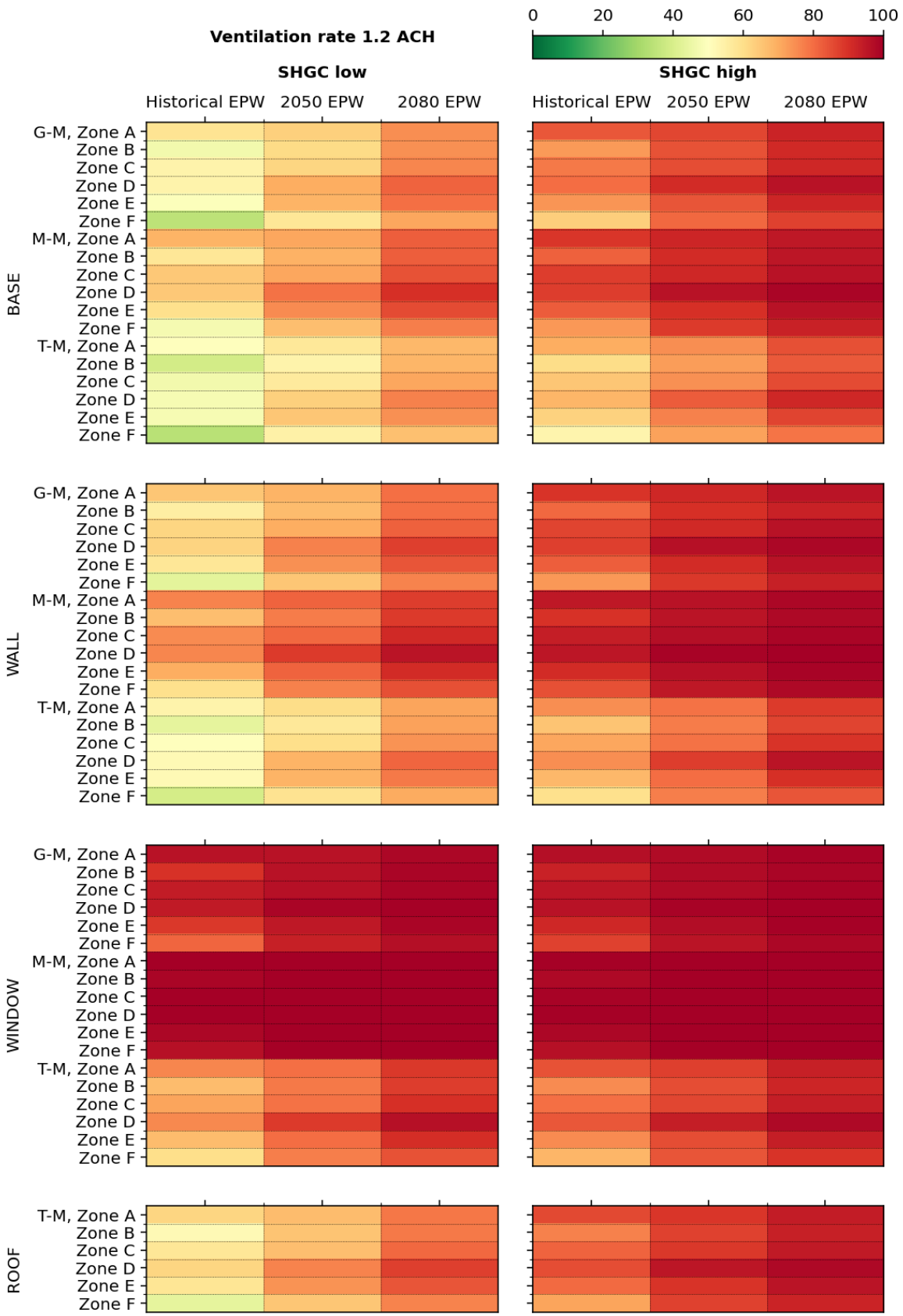

Figure 66 – Future weather results comparison for high and low SHGC for the 1.2 ACH ventilation scenario

5.1.4.2 Urban Heat Island simulation results

Figures 67, 68, 69 and 70 display the average values of the share of hours with temperature above the comfort threshold, comparing the Urban Heat Island weather file results with the base-case scenarios results. In the same way as in the other plots, the results are moreover divided for the solar heat gain coefficient values, low and high, respectively, at the left and right of each figure, and for the two ventilation rate scenarios, 8 l/s/person and 1.2 ACH, in the two different plots. The subplots separate the different retrofit scenarios, gathering classrooms on the same floor in different climatic zones. The roof retrofit values are only reported for classrooms on the top floor, as the roof retrofit does not influence the other cases.

As seen in the plots (Figures 67 and 68), the increase in temperatures due to the Urban Heat Island effect, as simulated in the present study, is not significant, with increases in the share of hours above the maximum temperature threshold of around 1% or less. This very low increase in the discomfort hours demonstrates that a slight increase in the external temperatures, that is around 1°C, does not considerably affect the operative internal temperature, demonstrating the stronger influence of the building's envelope on the internal comfort. Moreover, the presented metric refers to the share of hours above the comfort threshold, which is defined according to the running mean temperature, and that thus is increased in the UHI cases.

Figures 69 and 70 display the same results for the cases with the addition of night ventilation. In these cases, UHI is slightly more visible, as the increase in temperatures due to this effect usually determines higher temperature increases during the night hours, when the heat that was absorbed by the thermal mass of the urban settlements is re-emitted. In these cases, thus, night ventilation results in being less effective than in the countryside, as higher outdoor temperatures determine a lower night purge effect. The increase in the share of discomfort hours is nevertheless around 2%, also in this case, since the temperature threshold depends on the running mean outdoor temperature, and moreover, due to the simplification of the night-ventilation modelling, which sets a fixed ventilation rate when temperatures are in a certain range, without modulating it to take into account the stack effect.

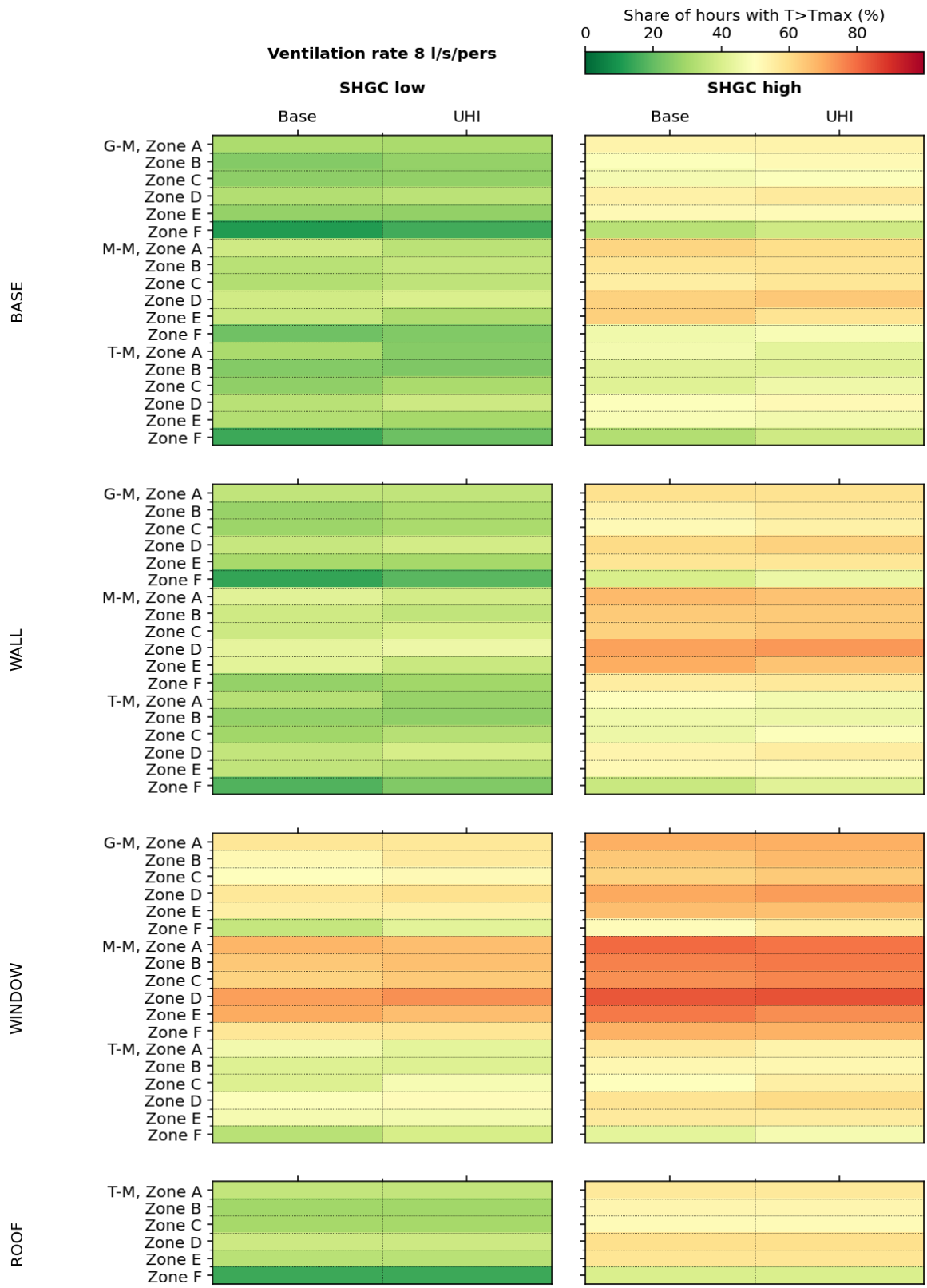

Figure 67 – UHI weather results comparison for high and low SHGC for the 8 l/s/pers ventilation scenario

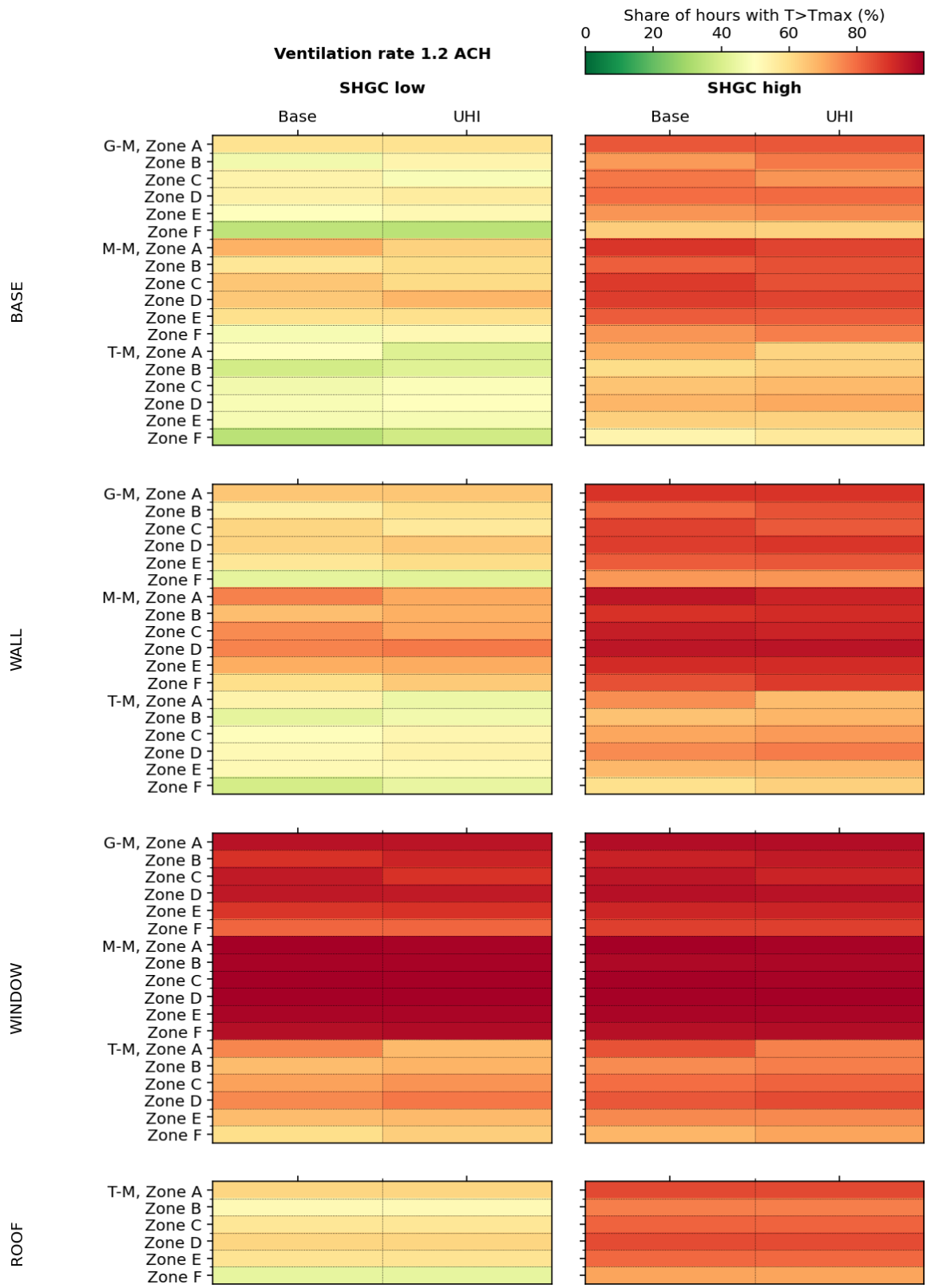

Figure 68 – UHI weather results comparison for high and low SHGC for the 1.2 ACH ventilation scenario

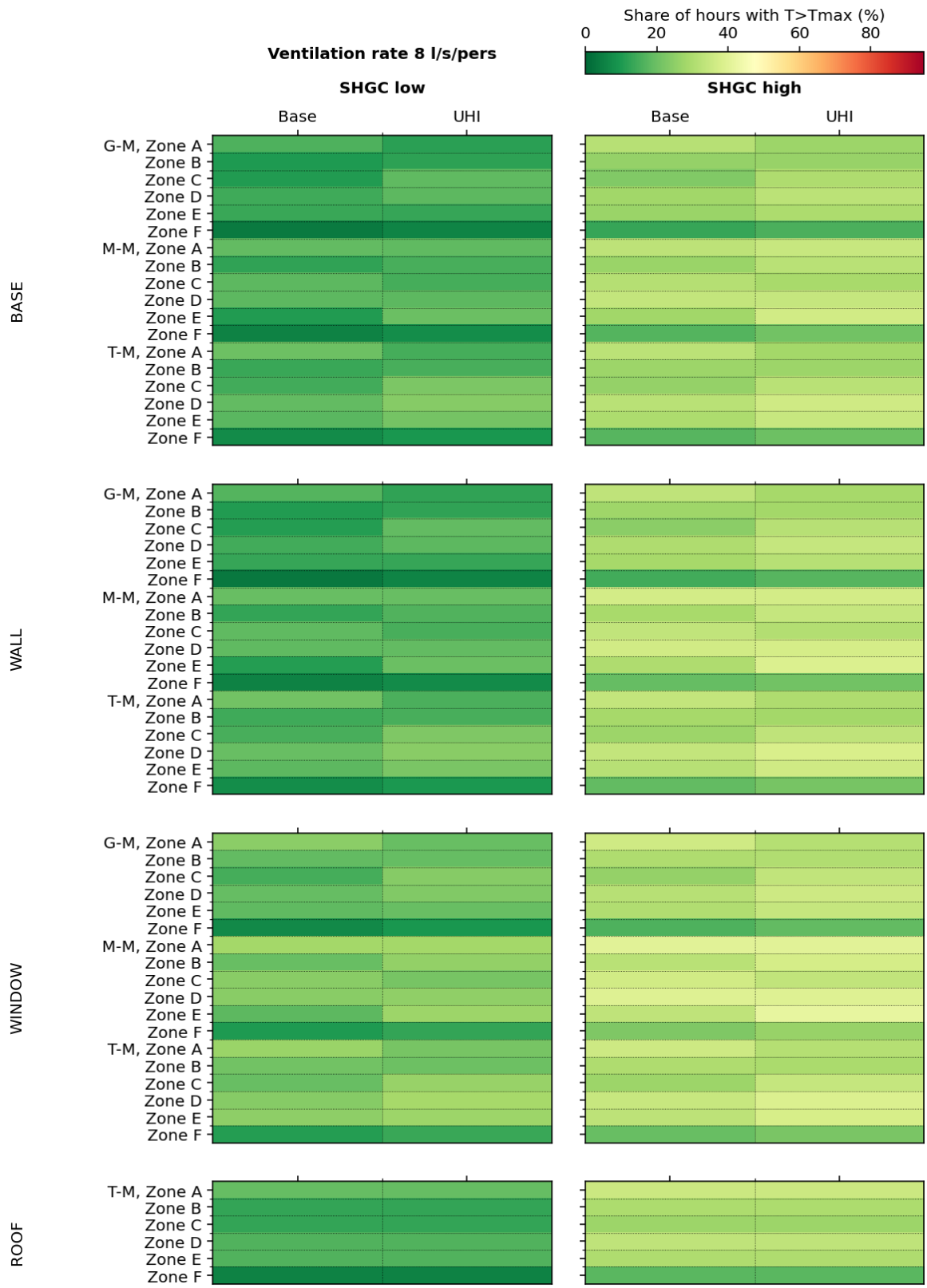

Figure 69 – UHI weather results comparison for high and low SHGC for the 8 l/s/person ventilation plus night ventilation scenario

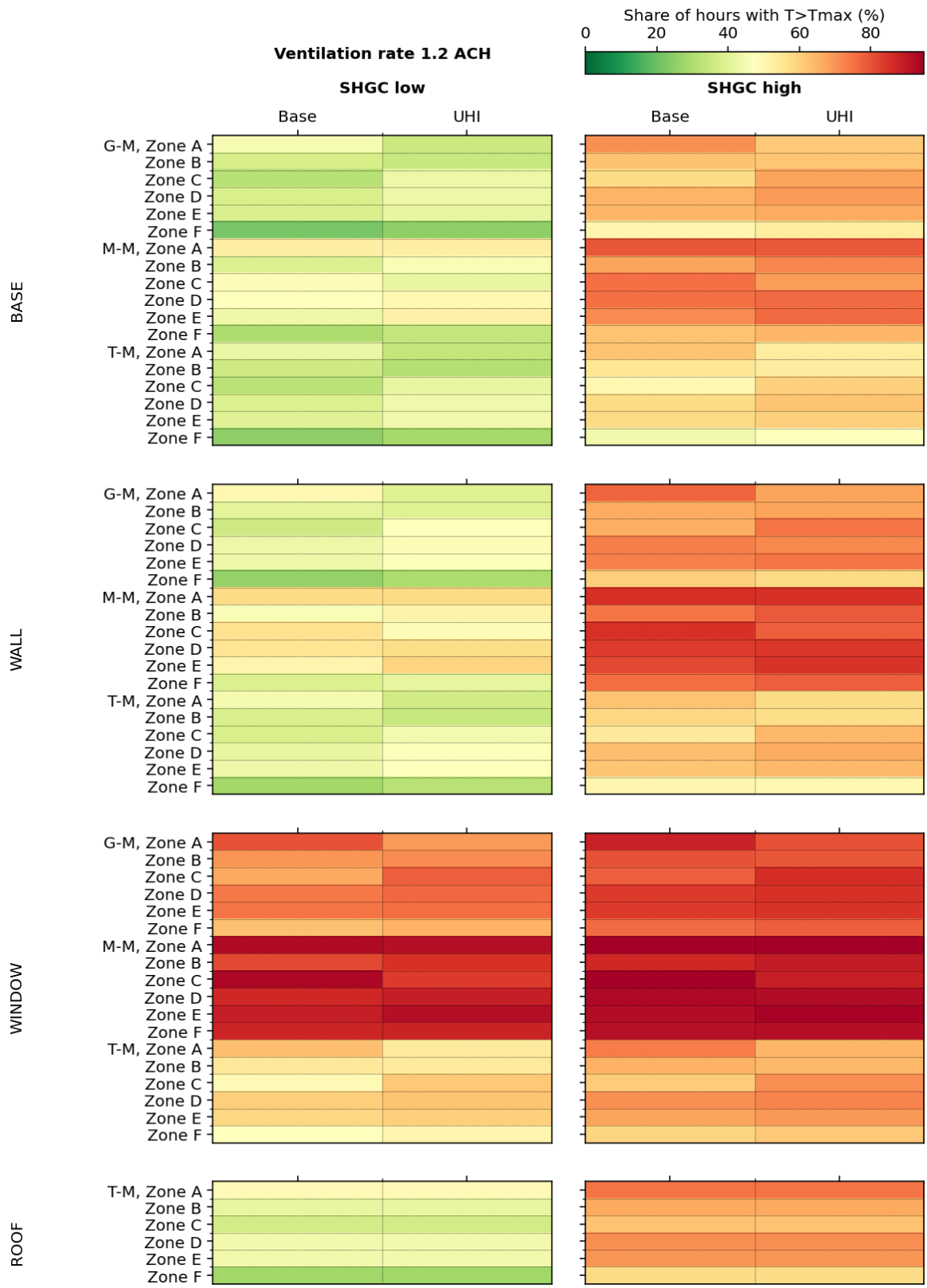

Figure 70 – UHI weather results comparison for high and low SHGC for the 1.2 ACH ventilation plus night ventilation scenario

5.2 Tool usage examples

The tool for assessing overheating in school buildings and classrooms will be available in a few months at this link: https://github.com/biancavigioli/Overheating-in-schools-tool. At the link, the instructions for running the tool are described. In this section, two examples of the tool's use are presented: one for assessing the whole school building, and the other for a single classroom and possible improvement strategies. The two tools are presented for two different example cases to highlight their characteristics.

5.1.2 School overheating evaluation

The results provided by the tool for the assessment of the overheating condition of the whole school are presented in Appendix C for a specific case, with climatic zone E, 12% as a window-to-floor ratio and a low value of solar heat gain coefficient, a high value of natural ventilation and without any retrofit interventions. The example school is built on three floors and presents 30 rooms in total, with exposures south/north and all central positions. Six classroom groups are thus created, with 5 rooms in each group.

The first heatmap presents the percentage of hours with temperature above the maximum threshold in the different periods for each group of classes. The second and third heatmaps represent the number of hours with temperature above the limit over the total number of hours. The metric is presented for the whole non-heating season and for the non-heating season during the school months. The second table presents the same results for hours exceeding the temperature threshold of more than 2°C. Then, the results for each of the TM52 criteria and the overall result in terms of compliance with the regulation for each group of classrooms are displayed. In the end, the last heatmap displays the number of days of heat stress in the non-heating period and in the school non-heating period for all the groups of classrooms.

Thanks to these evaluations, each group of classrooms is classified on a low-middle-high overheating risk scale, as summarised at the end of the report. The school is thus considered to be at high overheating risk in the intermediate seasons, as more than 25% of the rooms are at high overheating risk, while it is classified to be in middle risk and can be used discontinuously with low affluence in the summer season. In the end, the tool suggests using the classroom tool to compare various improvement possibilities for the overheating mitigation of the different classroom groups.

5.2.2 Classroom overheating evaluation

The results provided by the classroom tool are presented in Appendix C for a specific case, with climatic zone C, classroom placed at the central floor in middle position, north exposition, 12% as a window-to-floor ratio and a high value of solar heat gain coefficient, high value of natural ventilation and without any retrofit interventions.

First of all, the share of hours in the comfort bands is presented, divided into periods according to the heating and non-heating periods and on the summer break. The plot also indicates which months belong to each period, depending on the climatic zone. The second plot shows the distribution of temperatures above the maximum temperature, with data referring to the non-heating period and only to the occupied hours. The coloured areas on the plot indicate the acceptability of the overheating conditions: over 2°C above the maximum allowed temperature, the condition is considered seriously unacceptable, while below this limit and with a cumulative frequency of temperatures below the maximum threshold above 95%, the condition is considered almost acceptable. The chart presents the results for the base case and for the case with increased air speed (achieved with fans). On the side of the chart, the table indicates the number of hours in which the temperature is above the limit over the total number of hours, for two periods: the whole non-heating period and the school non-heating period, excluding the summer break. The same metric is also displayed for the number of hours above 2°C over the maximum temperature. The following tables represent the compliance with each of the TM52 criteria and the total result. Also in this case, the results are displayed for both the zero and the increased air speed. In the end, the adaptive chart plot is displayed, with the indoor operative temperature related to the running mean outdoor temperature. The comfort bands are drawn for the interval 10°C – 30°C for which the adaptive formula is valid. In the chart, the heat stress days are highlighted in red. Those are the days in which, for at least 3 consecutive days, the temperature is above the maximum threshold one (corresponding to the second category of comfort) and in which ventilation is not feasible. At the top of the plot, the total number of heat stress days is reported, along with the number of heat stress days registered during the school period, neglecting the summer break.

The same plots that were created for the initial condition are then displayed for the comparison between different retrofit strategies, which can be chosen from a drop-down menu.

As regards the addition of passive strategies such as shadings or night ventilation, which are resumed in the same plots, it is interesting to observe that the addition of night-time ventilation significantly improves the comfort conditions of the users, especially in the summer period, while shadings are more effective in the transition seasons.

In the end, as concerns the different climatic scenarios comparison, it can be seen how the future weather scenarios significantly reduce the comfort of the users, while the UHI scenario presents a much lower effect on the summer comfort of the users.

5.3 Tool application

In this final section of the results chapter, the results obtained from applying the tool to a real case building are presented. A real school building in the Varese Province, in the north

of Italy, is considered as example school, and all the steps to simplify its structure and apply the methodology are described.

Starting from the school's floor plans, the groups of classrooms are identified, with the number of rooms that belong to each of them and their common characteristics. Then, the "school" tool is applied to identify the most critical areas of the building, and in the end, the "room" tool is applied to the critical room groups, in order to compare passive strategies and identify possible improvements.

The example school is located in climatic zone E and is composed of three above-ground floors and one below-ground floor, with technical spaces and rooms for special didactic activities. The typical floor plan presents a longitudinal shape, with an atrium in the central part. The orientation of the building, as seen in the simplified floor plans, makes the classrooms groupable in two groups: a mainly west-exposed side and a mainly east-exposed one. In Figure 71, the floor plans of the ground, first and second levels of the school are schematized, and the classrooms belonging to the different groups are highlighted in different colours. The below-ground floor is not considered, as this category was not part of the study. The average classroom dimension is 55 square meters, with two 335x200 cm windows, for a total window area of 13.4 square meters and thus a window-to-floor ratio of 24%. It is considered that the glazing presents a low solar heat gain coefficient and that no retrofit interventions were applied to the envelope, while a ventilation of 8 l/s/person is used.

From the figure, it can be seen that the school presents 9 clusters of classrooms, for a total of 44 classrooms, excluding the personnel's offices and the rooms used for other purposes such as laboratories. The 9 classroom clusters are listed as follows:

- Group 1: ground floor, central, west-exposed classrooms → 8 classrooms
- Group 2: ground floor, corner, west-exposed classrooms → 1 classroom
- Group 3: ground floor, central, east-exposed classroom → 4 classrooms
- Group 4: first floor (middle), central, west-exposed classroom → 10 classrooms
- Group 5: first floor (middle), corner, west-exposed classroom → 1 classroom
- Group 6: first floor (middle), central, east-exposed classroom → 8 classrooms
- Group 7: second floor (top), central, west-exposed classroom → 10 classrooms
- Group 8: second floor (top), corner, west-exposed classroom → 1 classroom
- Group 9: second floor (top), corner, east-exposed classroom → 1 classroom

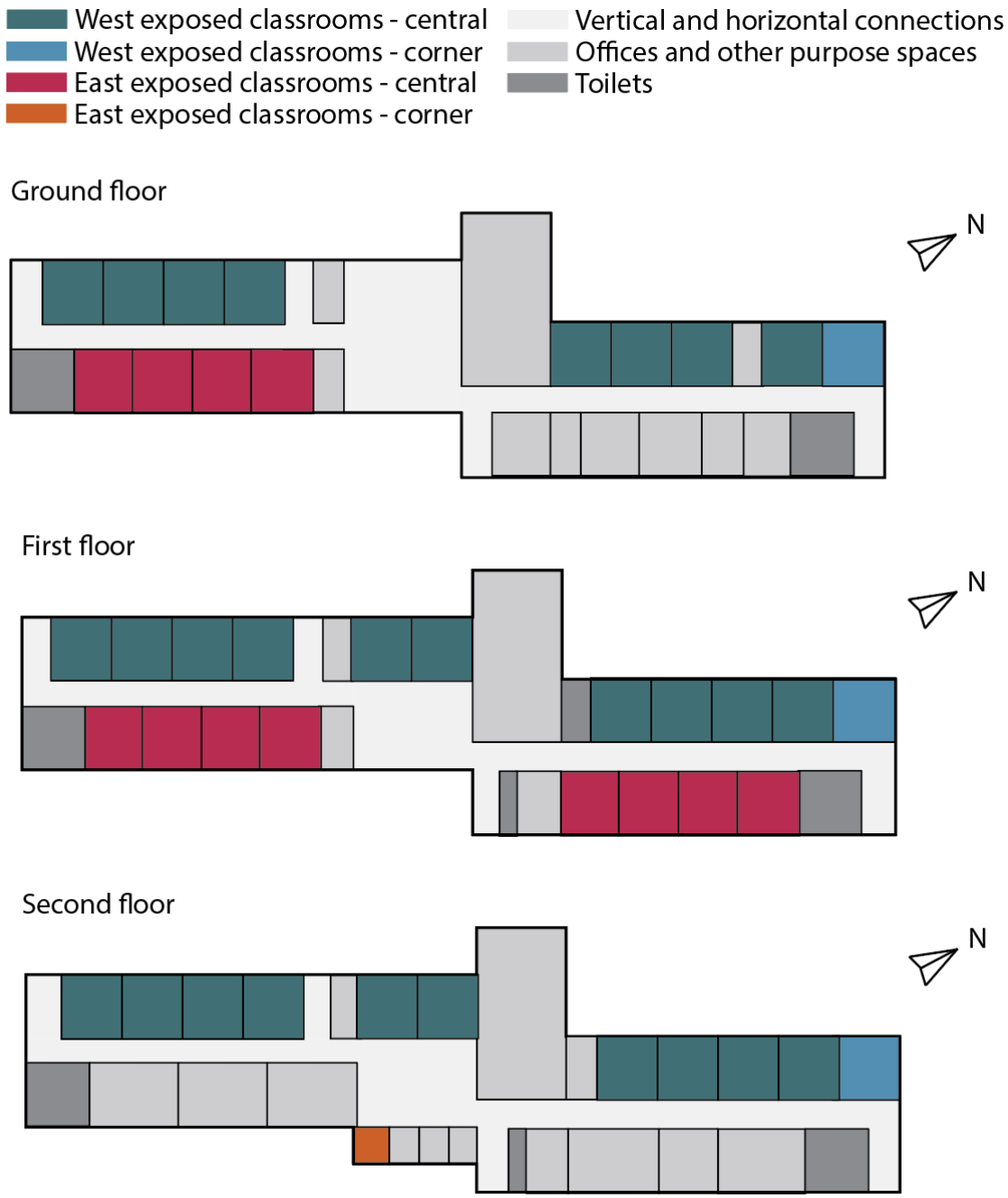

Figure 71 – Floor plans scheme for the example school

The complete results from the two tools for the assessment of the overheating potential of the whole building and of an example classroom are reported in Appendix C. As can be easily seen by observing Figure 72, all the classrooms are at high overheating risk in the intermediate seasons and during summer, probably because of the high window-to-wall ratio. Between the end of the heating season and the end of the school and during the summer break the classrooms always exceed the 5% acceptability threshold, while in the period between the start of the school and the start of the heating season most of the classes do not present overheated hours, with only the middle floor east exposed classrooms exceeding the

5% threshold, representing the worst case results. In Appendix C and in the following charts, a more specific analysis is performed on this classroom case.

	Start of year - end of heating season	End of heating season - end of school	End - start of school	Start of school - start of heating season	Start of heating season - end of year
Classrooms at Ground floor, Central, West exposed	0.0%	26.28%	58.31%	0.0%	0.0%
Classrooms at Ground floor, Angular, West exposed	0.0%	22.33%	50.31%	0.0%	0.0%
Classrooms at Ground floor, Central, East exposed	0.0%	31.16%	65.54%	0.0%	0.0%
Classrooms at Middle floor, Central, West exposed	0.0%	31.63%	72.46%	3.18%	0.0%
Classrooms at Middle floor, Angular, West exposed	0.0%	27.44%	54.62%	1.82%	0.0%
Classrooms at Middle floor, Central, East exposed	0.0%	33.49%	76.0%	5.45%	0.0%
Classrooms at Top floor, Central, West exposed	0.0%	29.53%	65.54%	0.0%	0.0%
Classrooms at Top floor, Angular, West exposed	0.0%	25.81%	54.92%	0.0%	0.0%
Classrooms at Top floor, Angular, East exposed	0.0%	26.74%	54.31%	0.0%	0.0%

Figure 72 – Share of hours in each comfort band in the different periods for the different classrooms of the example school

The results show how increasing the air speed and adding night ventilation have a positive effect on the overheating condition of the classroom group, decreasing the share of overheated hours considerably in all the seasons and in particular during autumn (Figure 73).

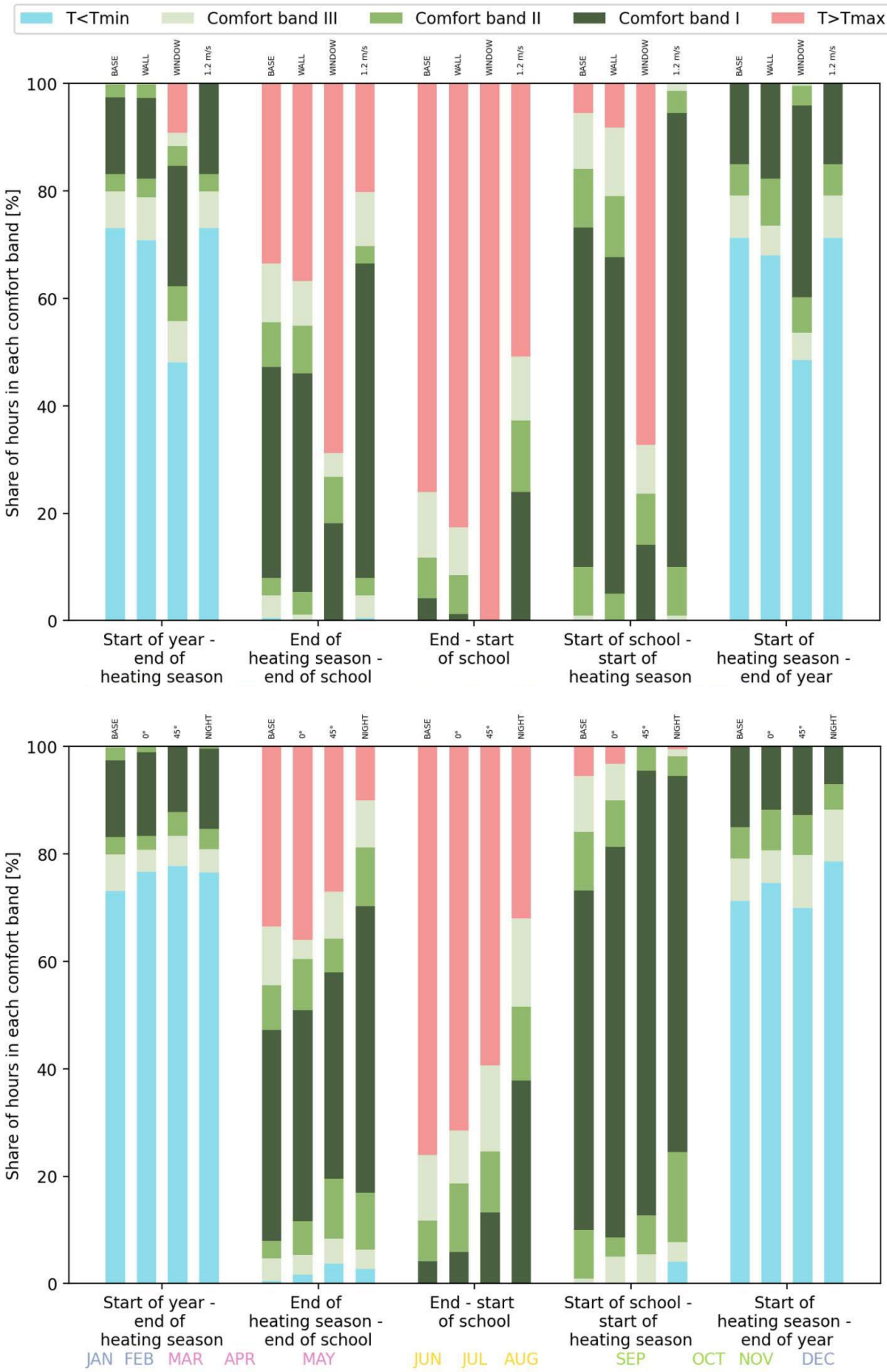

Figure 73 – Comfort bands comparison for the east-exposed middle floor middle position classroom of the example school

Chapter 6 – Limitations & future works

The present thesis has shown the potential of parametric simulations applied to a simplified model for the assessment of overheating and the identification of possible overheating mitigation strategies. Nevertheless, the work presents several limitations connected to the process that affect the conclusions, and can be improved and more deeply developed, especially considering enhancement in the simulations parametric tool, but also considering the expansion of the simulations set and also the usage of the tool to compare different solutions. In the next paragraphs, the limitations are described in detail, also suggesting future works, starting with the model assumptions in terms of geometry, parameters and simulation data, then discussing the limitations in the number of simulations and in the end considering the possibility of adding other comparison metrics to the output, to provide a more complete comparison for the identification of the best mitigation strategy.

First of all, the model used for all the simulations is a simplified shoebox model, and presents several assumptions for what concerns the geometry of the room, the modelling of the loads and of the occupancy rate, which is always fixed, and of the envelope characteristics. The geometry of the model is indeed kept fixed, with dimensions of the room considered as representative of the average school classroom, while, even though the window's dimensions are modified according to the simulations' parameters, the window is always modelled as a single rectangular hole placed in the centre of the wall, with the same proportions and without a frame. The internal loads of the building are always considered equal, with a fixed occupancy rate of 2 m^2/person and a fixed load associated with each person, with the same occupancy profile (8 AM to 6 PM Monday to Friday) over the year. Assumptions are also taken for the lighting load. As concerns the envelope characteristics, representative values for the heat transmission coefficients of the stratigraphies are used, and for the improved cases, target values taken from the regulations for each climatic zone are used. The ground is not modelled, and no consideration of below-ground floors is present. As concerns the roof, a high emissivity coefficient of the external surface, which allows for night cooling and thus reduces the overheating condition of the rooms on the top floor, is used. The infiltration rate is fixed and changes only in the cases with retrofitted windows, and does not take into account the actual dimensions of the cracks or the stack effect.

As for the geometry, moreover, only 6 classroom positions are considered, with three floor possibilities and two positions on the floor, middle and corner. The corner room simulations assume the presence of the windows on both the exposed sides, with a window-to-floor ratio equal to that of the middle position rooms and thus a lower window-to-wall ratio. This configuration is nevertheless less diffused than the one with windows only on the main

exposed wall, as the school buildings are usually built to present the same characteristics for each room. It was not possible, though, to simulate that configuration, as IESVE assigns windows to each exposed wall with the WWR assignment. In addition to this, no consideration of the external environment, in terms of obstructions and shadings, is considered, and the results should be interpreted consequently, as additional shade could highly affect the overheating conditions of classrooms, especially when south exposed.

Additionally, the values assumed by the simulation tool's parameters, like window-to-floor ratio, solar heat gain coefficients and ventilation rates, are based on assumptions as well. It is indeed assumed that the window-to-wall ratio can assume values between 1/8 and 1/4, being 1/8 the minimum required by the regulations. As concerns the solar heat gain coefficient, two values corresponding to low and high glazing performances are considered, assuming values that can be obtained with commercially available glass stratigraphies. In the end, only two ventilation flow rate values are compared, to represent the value that provides the optimal absorption of the heat produced by the occupants in the summer season, that is the value suggested by the regulations, 8 l/s/person, corresponding roughly to 4 ACH, and the value that is assumed to be the operative winter condition value, 1.2 ACH. Additionally, the ventilation schedule is always considered fixed and follows the occupation schedule with a fully open / fully closed operation. These two values, which are usually applied to different seasons, are applied to the whole year to demonstrate the potential increase in the overheating condition when the limits are not respected. The feasibility of these ventilation rates is thus not verified in the different conditions based on the dimensions of the openings and on the stack effect, and this could be implemented in future work through the use of the MacroFlo module of IESVE, to assess whether window opening is enough to provide the necessary ventilation rate or if additional ventilation is needed. The same ventilation rate values are moreover used for the application of night ventilation strategies, for which the opening schedule and strategy are fixed, considering the night opening between 6 PM and 8 AM in the non-heating season and with external air temperature between 15°C and 26°C. These rules could determine temperatures below the lower acceptability threshold in some cases in the morning hours if windows are kept open with low external temperatures. Moreover, these rules assume the possibility of opening and closing the windows during the nighttime, although this possibility is subject to environmental conditions, such as the position of the room and the accessibility from the exterior, and technological or personnel availability to operate the windows in an automated or manual manner. These limitations are taken into account when considering the improvement of the night ventilation strategy and should be coped with in future, even though it must be stressed that the objective of the study is to compare possible mitigation strategies.

As far as the parametric simulation tool developed in the IES VEScripts environment is concerned, many improvements could be applied, especially for what concerns the implementation of the location change. The method to change the location from the python

API, indeed, does not propagate automatically the location change to the Suncast simulation, and this returns an error due to the mismatch between the coordinates in the weather file for the Apache simulation, that have been updated, and the ones used in Suncast, that are not automatically updated, and that moreover report results for a different location. This problem could thus be solved, and a more automated workflow could be implemented, without the need to restart the simulations at each location change. The API can moreover be used to implement further modifications and add multiple parameters to the tool, apart from the ones that were already used, for example, the occupancy rate.

As concerns the simulations' input data, moreover, several assumptions about the climate were made, considering the TMY weather file of 6 Italian cities' airports as representative of the 6 climatic zones. The TMY (Typical Meteorological Year) weather file usually reports the weather variables' values for typical months, thus flattening the possibility of registering extreme weather events such as heat waves. A possible improvement could be the addition of simulations considering extreme weather files, to take into account the hot conditions that are more and more frequent at the present time. The present study, nevertheless, also considered the simulation of future weather and Urban Heat Island morphed weather files, with some assumptions, starting from the fact that both future weather and UHI weather are created with the Future Weather Generator tool, which morphs the temperature and other variables through a stretch procedure. Additionally, the considered future weather files are the 2050 and 2080 files with the SSP5-8.5 scenario, representing the worst case scenario in socioeconomic and environmental terms in the short and long period, considering a life-span of the building of around 25 to 55 years. As concerns the UHI effect, on the other hand, it was seen that the procedure applied to morph the data applies certain temperature differences according to the season and the time of the day, depending on the relation between the source and target Local Climate Zones. Moreover, to be able to select the representative LCZs and obtain the desired effect, the weather file coordinates had to be temporarily modified; a deeper analysis of the UHI effect and of the weather file morphing could thus be implemented, considering the specific conditions of each city.

Another limitation of this research project is the limited number of simulated cases. Even though a high number of simulations was performed, these cases only represent extreme cases that are meant to describe a much wider and denser configuration panorama. The used approach is a comparative evaluation process that thus compares extreme values to demonstrate the possible improvement connected with certain passive mitigation strategies. In this study, the improvement of the ground floor insulation was not implemented, as it was considered to be less diffuse with respect to the walls, roof and windows retrofit in the Italian school building stock. Moreover, the combinations between the retrofitted cases of the different envelope components were not implemented. A future work for the completion of the study could be the addition of other simulation cases, or the trial of machine learning tools for the interpolation of the already simulated cases, to obtain more continuous results instead of discrete and approximated values, for example, for parameters like the location,

the window-to-floor ratio, the solar heat gain coefficient and the orientations. The possibility of using machine learning with these objectives has to be carefully analysed, as the small quantity of data could lead to biased interpolation, as for each parameter, often only two values were considered.

In the end, it must be highlighted that the developed tool returns a comparison between different mitigation strategies with respect to the assessed overheating risk of the base-case, only comparing the reduction in the operative temperature through various indices and criteria. It could be, nevertheless, interesting to add considerations about the Life Cycle Assessment and Return On Investment of the different strategies, to be able to compare them not only on the mitigation effectiveness but also on the environmental and economic costs.

Chapter 7 – Conclusions

The present thesis provides a possible framework for the assessment of overheating in Italian school buildings and classrooms. This issue has become increasingly urgent in the last years due to global and local climate change effects, while the current school building stock is not ready to face it, with renovated buildings that are usually more air-tight and a scarce presence of summer climatisation systems.

Analysing the results that were described in Chapter 5, indeed, it can be seen how refurbished buildings, especially the ones with double-glazed windows, present on average higher risks of overheating, caused by the higher insulation and by the lower infiltration rates. In recent years, indeed, refurbishment of buildings was particularly focused on the improvement of the poor winter performance of the envelope, to decrease the energy consumption, due to a growing awareness of energy efficiency topics. The current climate projections, nevertheless, are pointing to a generalised rise in global temperatures, with an intensification of overheating effects in such buildings. From the analysis of the results obtained in the study, the high importance of coping with the overheating effect is confirmed, along with the proof of its increase in the future years if the future climate projections take place. It is thus necessary to first of all determine the magnitude of this problem in the occupied periods, especially in the late spring and early autumn seasons, when heating, that is often the only active system in Italian schools, is typically turned off and students still go to school, to identify possible mitigation strategies and to improve the resilience of the building to hotter temperatures. In second place, the results also demonstrate that it is possible to increase the comfort of the classrooms also in the summer break, increasing the possibility of using the schools for social activities also during this period, in which usually the buildings are closed. This possibility is especially feasible for classrooms on the ground floor, which, as seen from the results, present considerably lower discomfort hours shares, while rooms at middle floors are usually hotter, because of the smaller dispersive area and the presence of other classrooms on all the other sides.

Analysing and comparing the results from the different simulations, it is seen how the different climatic zones present very similar values of overheating in similar conditions, as the comfort thresholds are defined considering the adaptive comfort formula and are thus based on the external temperature. The colder climatic zones present, nevertheless, slightly lower overheating risks on average, along with much lower shares of heat stress days, which are not only calculated with respect to adaptive comfort thresholds but also on ventilation feasibility and heat stress days' consecutiveness.

In the proposed discussion, a cascade process is suggested for coping with the overheating issue in classrooms, starting from the assessment of its magnitude and listing possible consequent actions to reduce it, starting from the natural ventilation, then adding night-time ventilation, the use of fans to increase the speed of air and thus the maximum acceptability temperature, the application of external shading devices and, in the end, in the cases where the passive strategies are not sufficient to maintain the building in the comfort range temperatures, the addition of a cooling active system, starting from mechanical ventilation. From the analysis of the results, it was indeed observed that increasing the ventilation rates and the air speed substantially decreases the discomfort hours, and moreover, that the night-ventilation strategy is very effective in terms of temperature reduction. It has also to be considered that the lower night temperatures allow for higher ventilation rates because of a higher stack effect, while during the daytime, the higher temperatures might decrease the feasibility of high ventilation rates, and mechanical ventilation could be needed. The effectiveness of night ventilation has been proven to be less effective in urban environments, where UHI effects increase the temperatures, especially during the night, reducing the possibility of night purge effects.

In conclusion, the assessment of the summer performance of school buildings is identified to be of crucial importance for the use of school buildings in the near future, as high temperatures might decrease the learning performance of students and prevent the use of those public buildings during the summer. Some passive strategies are provided as solutions for this issue, with the quantification of their overheating reduction potential, to guide school owners and occupants towards the improvement of school buildings, through simplified actions that can improve their comfort. In future works, this analysis of the comfort improvement could be coupled with a detailed Return On Investment and Life Cycle Analysis, to provide the school owners with all the instruments for the choice of the best mitigation strategy and of the classrooms to be prioritised in this process.

Bibliography

[1] ‘Buildings - Energy System’, IEA. Accessed: Dec. 14, 2024. [Online]. Available: https://www.iea.org/energy-system/buildings

[2] ENEA, ‘Guida all’efficienza energetica negli edifici scolastici’. Jun. 2019.

[3] *TM57: Integrated School Design | CIBSE*. 2015. Accessed: Jun. 14, 2025. [Online]. Available: https://www.cibse.org/knowledge-research/knowledge-portal/tm57-integrated-school-design/

[4] ‘Energy efficiency’, EEA. Accessed: May 22, 2025. [Online]. Available: https://www.eea.europa.eu/en/topics/in-depth/energy-efficiency

[5] ‘Energy Efficiency - Energy System’, IEA. Accessed: May 22, 2025. [Online]. Available: https://www.iea.org/energy-system/energy-efficiency-and-demand/energy-efficiency

[6] ‘Energy Performance of Buildings Directive’, Energy - European Commission. Accessed: May 22, 2025. [Online]. Available: https://energy.ec.europa.eu/topics/energy-efficiency/energy-efficient-buildings/energy-performance-buildings-directive_en

[7] *D.M. 26-06-15 ‘Applicazione delle metodologie di calcolo delle prestazioni energetiche e definizione delle prescrizioni e dei requisiti minimi degli edifici’*, Jun. 2015.

[8] *D.M. 24-11-25 ‘Adozione dei criteri ambientali minimi per l’affidamento di servizi di progettazione e affidamento di lavori per interventi edilizi’*.

[9] ‘Rapporto sui beni immobili delle Amministrazioni Pubbliche’. MEF, 2018.

[10] MIUR, ‘Anagrafe Nazionale Edilizia Scolastica (SNAES)’. Accessed: May 23, 2025. [Online]. Available: https://dati.istruzione.it/opendata/opendata/catalogo/elements1/?area=Edilizia%20Scolastica&&pk_vid=8e3619b0009a8fca1537956759f27725

[11] *LEGGE 30 marzo 1976, n. 373 “Norme per il contenimento del consumo energetico per usi termici negli edifici”*, 1976.

[12] *LEGGE 9 gennaio 1991, n.10 ‘Norme per l’attuazione del Piano energetico nazionale in materia di uso razionale dell’energia, di risparmio energetico e di sviluppo delle fonti rinnovabili di energia’*, 1991.

[13] 'Ecosistema Scuola 2025: i dati del XXV rapporto • Legambiente', Legambiente. Accessed: Feb. 02, 2026. [Online]. Available: https://www.legambiente.it/comunicati-stampa/ecosistema-scuola-2025-i-dati-del-xxv-rapporto/

[14] 'XXII Rapporto nazionale sulla qualità degli edifici e dei servizi scolastici'. Legambiente, Jan. 2023.

[15] *D.M. 18-12-75 'Norme tecniche aggiornate relative all'edilizia scolastica, ivi compresi gli indici di funzionalità didattica, edilizia ed urbanistica, da osservarsi nella esecuzione di opere di edilizia scolastica'*, Dec. 1975.

[16] 'RERoadS project'. Accessed: May 23, 2025. [Online]. Available: https://reroads-project.unibs.it/

[17] R. Cardelli, 'Mechanical ventilation for Italian school classrooms', Politecnico di Milano, 2023. [Online]. Available: https://hdl.handle.net/10589/232552

[18] S. Ferrari, G. Puglisi, and R. Cardelli, 'Heat Recovery Ventilation in School Classrooms Within Mediterranean Europe: A Climate-Sensitive Analysis of the Energy Impact Based on the Italian Building Stock', *Energies*, vol. 18, Sep. 2025, doi: 10.3390/%20en18195069.

[19] T. Tortuga, 'In classe con l'estate addosso (senza aria condizionata)', Domani. Accessed: Jun. 14, 2025. [Online]. Available: https://www.editorialedomani.it/fatti/scuole-aria-condizionata-vacanze-estive-bslntbb0

[20] J. Goodman, M. Hurwitz, J. Park, and J. Smith, 'Heat and Learning', *NBER Work. Pap. Ser.*, no. Working Paper 24639, Nov. 2019.

[21] K. Calvin *et al.*, 'IPCC, 2023: Climate Change 2023: Synthesis Report. Contribution of Working Groups I, II and III to the Sixth Assessment Report of the Intergovernmental Panel on Climate Change [Core Writing Team, H. Lee and J. Romero (eds.)]. IPCC, Geneva, Switzerland.', Intergovernmental Panel on Climate Change (IPCC), Jul. 2023. doi: 10.59327/IPCC/AR6-9789291691647.

[22] 'Cross-Chapter Paper 4: Mediterranean Region'. Accessed: Feb. 05, 2026. [Online]. Available: https://www.ipcc.ch/report/ar6/wg2/chapter/ccp4/

[23] V. Weilnhammer *et al.*, 'Extreme weather events in europe and their health consequences – A systematic review', *Int. J. Hyg. Environ. Health*, vol. 233, p. 113688, Apr. 2021, doi: 10.1016/j.ijheh.2021.113688.

[24] R. M. S. F. Almeida and V. P. de Freitas, 'Indoor environmental quality of classrooms in Southern European climate', *Energy Build.*, vol. 81, pp. 127–140, Oct. 2014, doi: 10.1016/j.enbuild.2014.06.020.

[25] M. Gil-Baez, Á. Barrios-Padura, M. Molina-Huelva, and R. Chacartegui, 'Natural ventilation systems in 21st-century for near zero energy school buildings', *Energy*, vol. 137, pp. 1186–1200, Oct. 2017, doi: 10.1016/j.energy.2017.05.188.

[26] 'EN 16798-2:2019 "Energy performance of buildings - Ventilation for buildings - Part 2: Interpretation of the requirements in EN 16798-1 - Indoor environmental input parameters for design and assessment of energy performance of buildings addressing indoor air quality, thermal environment, lighting and acoustics"'. Accessed: Nov. 26, 2024. [Online]. Available: https://sd.ds.dk/Viewer/Standard?ProjectNr=M297459&Status=90.20&VariantID=41&Page=1

[27] *ASHRAE 55: Thermal environmental Conditions for Human Occupancy*, 2010.

[28] E. Barbadilla-Martín, J. M. Salmerón Lissén, J. Guadix Martín, P. Aparicio-Ruiz, and L. Brotas, 'Field study on adaptive thermal comfort in mixed mode office buildings in southwestern area of Spain', *Build. Environ.*, vol. 123, pp. 163–175, Oct. 2017, doi: 10.1016/j.buildenv.2017.06.042.

[29] 'CIBSE - Chartered Institution of Building Services Engineers'. Accessed: Dec. 08, 2025. [Online]. Available: https://www.cibse.org/

[30] 'TM52: The Limits of Thermal Comfort: Avoiding Overheating in European Buildings | CIBSE'. Accessed: Oct. 31, 2025. [Online]. Available: https://www.cibse.org/knowledge-research/knowledge-portal/tm52-the-limits-of-thermal-comfort-avoiding-overheating-in-european-buildings

[31] 'TM59: Design methodology for the assessment of overheating risk in homes | CIBSE'. Accessed: Oct. 31, 2025. [Online]. Available: https://www.cibse.org/knowledge-research/knowledge-portal/technical-memorandum-59-design-methodology-for-the-assessment-of-overheating-risk-in-homes

[32] 'TM56: Resource Efficiency of Building Services | CIBSE'. Accessed: Nov. 01, 2025. [Online]. Available: https://www.cibse.org/knowledge-research/knowledge-portal/tm56-resource-efficiency-of-building-services/

[33] 'Heat wave | Temperature Extremes, Climate Change, Heat Domes, & Heat Stress | Britannica'. Accessed: Dec. 12, 2025. [Online]. Available: https://www.britannica.com/science/heat-wave-meteorology

[34] 'Heatwave (MH0501) | UNDRR'. Accessed: Dec. 12, 2025. [Online]. Available: https://www.undrr.org/understanding-disaster-risk/terminology/hips/mh0501

[35] 'Chapter 11: Weather and Climate Extreme Events in a Changing Climate'. Accessed: Dec. 12, 2025. [Online]. Available: https://www.ipcc.ch/report/ar6/wg1/chapter/chapter-11/

[36] 'Climatological Heatwave Days'. Accessed: Dec. 12, 2025. [Online]. Available: https://climate-adapt.eea.europa.eu/en/metadata/indicators/climatological-heatwave-days

[37] C. Lavaysse, C. Cammalleri, A. Dosio, G. Van Der Schrier, A. Toreti, and J. Vogt, 'Towards a monitoring system of temperature extremes in Europe', *Nat. Hazards Earth Syst. Sci.*, vol. 18, no. 1, pp. 91–104, Jan. 2018, doi: 10.5194/nhess-18-91-2018.

[38] M. Santamouris, 'Night ventilation strategies', *AIVC Vent. Inf. Pap.*, vol. 4, Mar. 2004.

[39] A. R. Hassani, P. Domenighini, E. Belloni, T. Ihara, and C. Buratti, 'Evaluation of the solar heat gain coefficient of innovative aerogel glazing systems: Experimental campaigns and numerical results', *J. Build. Eng.*, vol. 62, p. 105354, Dec. 2022, doi: 10.1016/j.jobe.2022.105354.

[40] 'Module 125: Applying solar shading to reduce overheating in buildings', CIBSE Journal. Accessed: Feb. 05, 2026. [Online]. Available: https://www.cibsejournal.com/cpd/modules/2018-04-sol/

[41] P. Boyce, N. Eklund, S. Mangum, C. Saalfield, and L. Tang, 'Minimum acceptable transmittance of glazing', *Int. J. Light. Res. Technol.*, vol. 27, no. 3, pp. 145–152, Sep. 1995, doi: 10.1177/14771535950270030201.

[42] H. Zhang *et al.*, 'A critical review of combined natural ventilation techniques in sustainable buildings', *Renew. Sustain. Energy Rev.*, vol. 141, p. 110795, May 2021, doi: 10.1016/j.rser.2021.110795.

[43] R. Becker, I. Goldberger, and M. Paciuk, 'Improving energy performance of school buildings while ensuring indoor air quality ventilation', *Build. Environ.*, vol. 42, no. 9, pp. 3261–3276, Sep. 2007, doi: 10.1016/j.buildenv.2006.08.016.

[44] R. Duarte, M. da Glória Gomes, and A. Moret Rodrigues, 'Classroom ventilation with manual opening of windows: Findings from a two-year-long experimental study of a Portuguese secondary school', *Build. Environ.*, vol. 124, pp. 118–129, Nov. 2017, doi: 10.1016/j.buildenv.2017.07.041.

[45] *EN 16798-1:2019 'Prestazione energetica degli edifici - Ventilazione per gli edifici - Parte 1: Parametri di ingresso dell'ambiente interno per la progettazione e la valutazione della prestazione energetica degli edifici in relazione alla qualità dell'aria interna, all'ambiente termico, all'illuminazione e all'acustica'*.

[46] B. Givoni, *Climate Considerations in Building and Urban Design*. John Wiley & Sons, 1998.

[47] M. Kent *et al.*, 'Energy Savings and Thermal Comfort in a Zero Energy Office Building with Fans in Singapore', Apr. 24, 2023, *Social Science Research Network, Rochester, NY*: 4480684. doi: 10.2139/ssrn.4480684.

[48] D. Miller *et al.*, 'Cooling energy savings and occupant feedback in a two-year retrofit evaluation of 99 automated ceiling fans staged with air conditioning', *Energy Build.*, vol. 251, p. 111319, Nov. 2021, doi: 10.1016/j.enbuild.2021.111319.

[49] *DPR 26 agosto 1993 n. 412 "Regolamento recante norme per la progettazione, l'installazione, l'esercizio e la manutenzione degli impianti termici degli edifici ai fini del contenimento dei consumi di energia, in attuazione dell'art. 4 della legge 9 Gennaio 1991, n°10"*, 1993.

[50] *Decreto Legislativo 192/2005, Attuazione della direttiva 2002/91/CE relativa al rendimento energetico nell'edilizia.*, 2005.

[51] S.-H. Kwon, C. Chun, and R.-Y. Kwak, 'Relationship between quality of building maintenance management services for indoor environmental quality and occupant satisfaction', *Build. Environ.*, vol. 46, no. 11, pp. 2179–2185, Nov. 2011, doi: 10.1016/j.buildenv.2011.04.028.

[52] Y. Wang, J. Kuckelkorn, F.-Y. Zhao, D. Liu, A. Kirschbaum, and J.-L. Zhang, 'Evaluation on classroom thermal comfort and energy performance of passive school building by optimizing HVAC control systems', *Build. Environ.*, vol. 89, pp. 86–106, Jul. 2015, doi: 10.1016/j.buildenv.2015.02.023.

[53] S. Kamali, G. Khakzar, and S. Abdali Hajiabadi, 'Effect of Building Management System on Energy Saving', *Adv. Mater. Res.*, vol. 856, p. 333, Jan. 2014, doi: 10.4028/www.scientific.net/AMR.856.

[54] B. A. Cavigioli, 'Machine learing and data analysis for the Post Occupancy Evaluation of buildings', Politecnico di Milano, 2023.

[55] *UNI EN ISO 52120-1:2022 'Energy performance of buildings. Contribution of building automation, controls and building management. General framework and procedures'*, Mar. 2022.

[56] L. de Santoli, F. Fraticelli, F. Fornari, and C. Calice, 'Energy performance assessment and a retrofit strategies in public school buildings in Rome', *Energy Build.*, vol. 68, pp. 196–202, Jan. 2014, doi: 10.1016/j.enbuild.2013.08.028.

[57] G. Dall'O' and L. Sarto, 'Potential and limits to improve energy efficiency in space heating in existing school buildings in northern Italy', *Energy Build.*, vol. 67, pp. 298–308, Dec. 2013, doi: 10.1016/j.enbuild.2013.08.001.

[58] J. Deng, C. Peng, W. Qiang, Q. Wei, and H. Zhang, 'Can heat pump heat storage system perform better for space heating in China's primary schools? A field test and simulation analysis', *Energy Build.*, vol. 279, p. 112684, Jan. 2023, doi: 10.1016/j.enbuild.2022.112684.

[59] *UNI TR 11552 'Abaco delle strutture costituenti l'involucro opaco degli edifici'*, Oct. 2014.

[60] *UNI TS 11300 'Prestazioni energetiche degli edifici'*.

[61] V. Corrado, I. Ballarini, and S. P. Corgnati, 'National scientific report on the TABULA activities in Italy'.

[62] 'URBEM'. Accessed: Feb. 23, 2026. [Online]. Available: https://www.urbem.polimi.it/en/

[63] *EN ISO 13370 'Prestazione termica degli edifici - Trasferimento di calore attraverso il terreno - Metodi di calcolo'*, 2018.

[64] *D.M. 28-10-25 'Applicazione delle metodologie di calcolo delle prestazioni energetiche e definizione delle prescrizioni e dei requisiti minimi degli edifici'*, Oct. 2025.

[65] 'THERM 7.8 / WINDOWS 7.8 | Windows & Daylighting'. Accessed: Dec. 27, 2025. [Online]. Available: https://windows.lbl.gov/therm-78-windows-78

[66] 'D.M. 5-07-75 "Modificazioni alle istruzioni ministeriali 20 giugno 1896, relativamente all'altezza minima ed ai requisiti igienico-sanitari principali dei locali di abitazione"'. Accessed: Dec. 14, 2025. [Online]. Available: https://www.indicenormativa.it/sites/default/files/Decreto%20Ministero%20della%20Sanita%2005-07-1975.pdf

[67] 'Future Weather Generator – Morphs current weather for performance simulation of buildings in the future'. Accessed: Feb. 06, 2026. [Online]. Available: https://future-weather-generator.adai.pt/

[68] 'CMIP Phase 6 (CMIP6) - Coupled Model Intercomparison Project'. Accessed: Feb. 06, 2026. [Online]. Available: https://wcrp-cmip.org/cmip-phases/cmip6/

[69] 'SSP, gli scenari dell'IPCC - IPCC - Focal Point Italia'. Accessed: Feb. 06, 2026. [Online]. Available: https://ipccitalia.cmcc.it/ssp-gli-scenari-dellipcc/

[70] 'Zone climatiche locali (LCZ)', Zone climatiche locali (LCZ). Accessed: Feb. 06, 2026. [Online]. Available: https://www.cittametropolitana.mi.it/Territori_resilienti/TERRITORI/index.html

[71] M. Demuzere *et al.*, 'Global map of Local Climate Zones'. Zenodo, Oct. 08, 2023. doi: 10.5281/ZENODO.6364593.

[72] Z. J. Zhai, T. Hong, M. Santamouris, and J.-L. Niu, 'Validation practices for simulation-based research', *Energy Build.*, vol. 352, p. 116853, Feb. 2026, doi: 10.1016/j.enbuild.2025.116853.

[73] A. Al-janabi, M. Kavgic, A. Mohammadzadeh, and A. Azzouz, 'Comparison of EnergyPlus and IES to model a complex university building using three scenarios: Free-floating, ideal air load system, and detailed', *J. Build. Eng.*, 2019, doi: 10.1016/j.jobe.2018.12.022.

[74] ‘Data Apps for Production | Plotly’. Accessed: Jan. 13, 2026. [Online]. Available: https://plotly.com/

Acknowledgements

I would like to thank first of all Professor Andrea Giovanni Mainini for his guidance on the topics of the thesis, being of constant help with great experience on all the aspects that I had to cope with, and for being of great inspiration not only for the present work. I also thank Giacomo Caccia, who supported me throughout the whole research period, with valuable advice and attention to the details. Professor Fulvio Re Cecconi also guided me in evaluating the possibility of expanding my work through machine learning techniques, suggesting the initial steps for this operation, and I would like to thank him for that.

I also want to mention all the professors and students that I met at Politecnico di Milano, from whom and with whom I learnt during the five years that I spent in this stimulating, challenging and international environment. The Erasmus experience that I took part in last year at the University of Aarhus, Denmark, also enriched my path to reach this milestone, widening my perspectives in terms of European belonging, internationality and innovative engineering knowledge.

In the end, I would like to thank the team of Edera, where I started to work in the last months, who gave me a glimpse of the application of what I studied at Politecnico and on the implementation of this knowledge for the decarbonisation of the built environment and for making houses affordable for everyone.

All these experiences and stimuli helped me to outline the path that I would like to follow in the next years, combining innovation and respect for the environment, always remembering that buildings are meant to provide comfort and shelter to people.

Appendix A – test simulations

In this Appendix, the results for some test simulations are reported. The tool is applied to two case studies located in two different climatic zones: Milan (climatic zone E) and Palermo (climatic zone B), with the combination of parameters presented in Chapter 4.3.

For the case of Milan, which is located in climatic zone E, the results are presented as follows. Figure 74 represents the temperature and the global solar radiation for the whole year in Milan, according to the 2009-2023 Linate weather file. The average maximum, mean and minimum temperatures are also reported in Table 18.

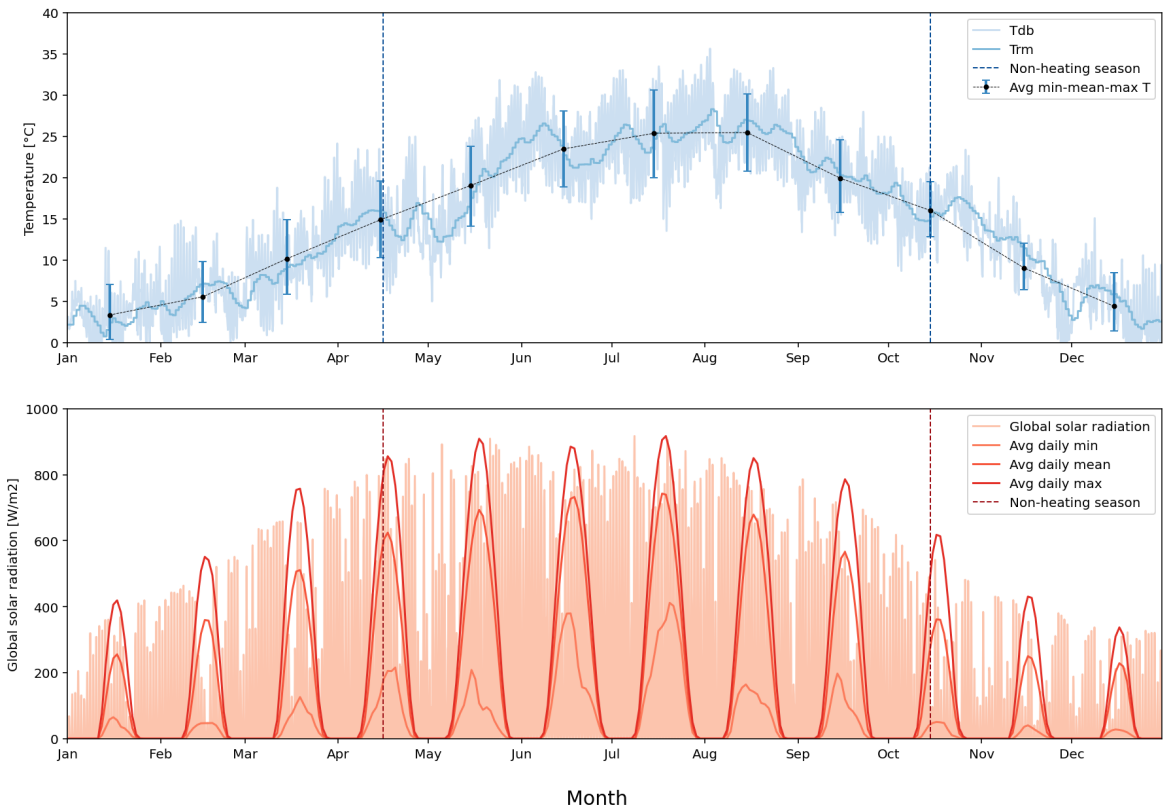

Figure 74 – Temperature and solar radiation plots for Milan

Table 18 – Average monthly maximum, mean, and minimum temperatures for Milan (°C)

	Jan	Feb	Mar	Apr	May	Jun	Jul	Aug	Sep	Oct	Nov	Dec
Max	7.1	9.9	14.9	19.6	23.8	28.1	30.7	30.2	24.6	19.5	12.1	8.5
Mean	3.4	5.6	10.2	14.9	19.1	23.5	25.4	25.5	19.9	16.0	9.1	4.4
Min	0.4	2.5	5.9	10.3	14.1	18.9	20.0	20.8	15.8	12.9	6.4	1.4

After analysing the weather, the simulations are performed for this climate, and the results are extracted first of all in terms of the distribution of temperatures, as reported in Figure 75.

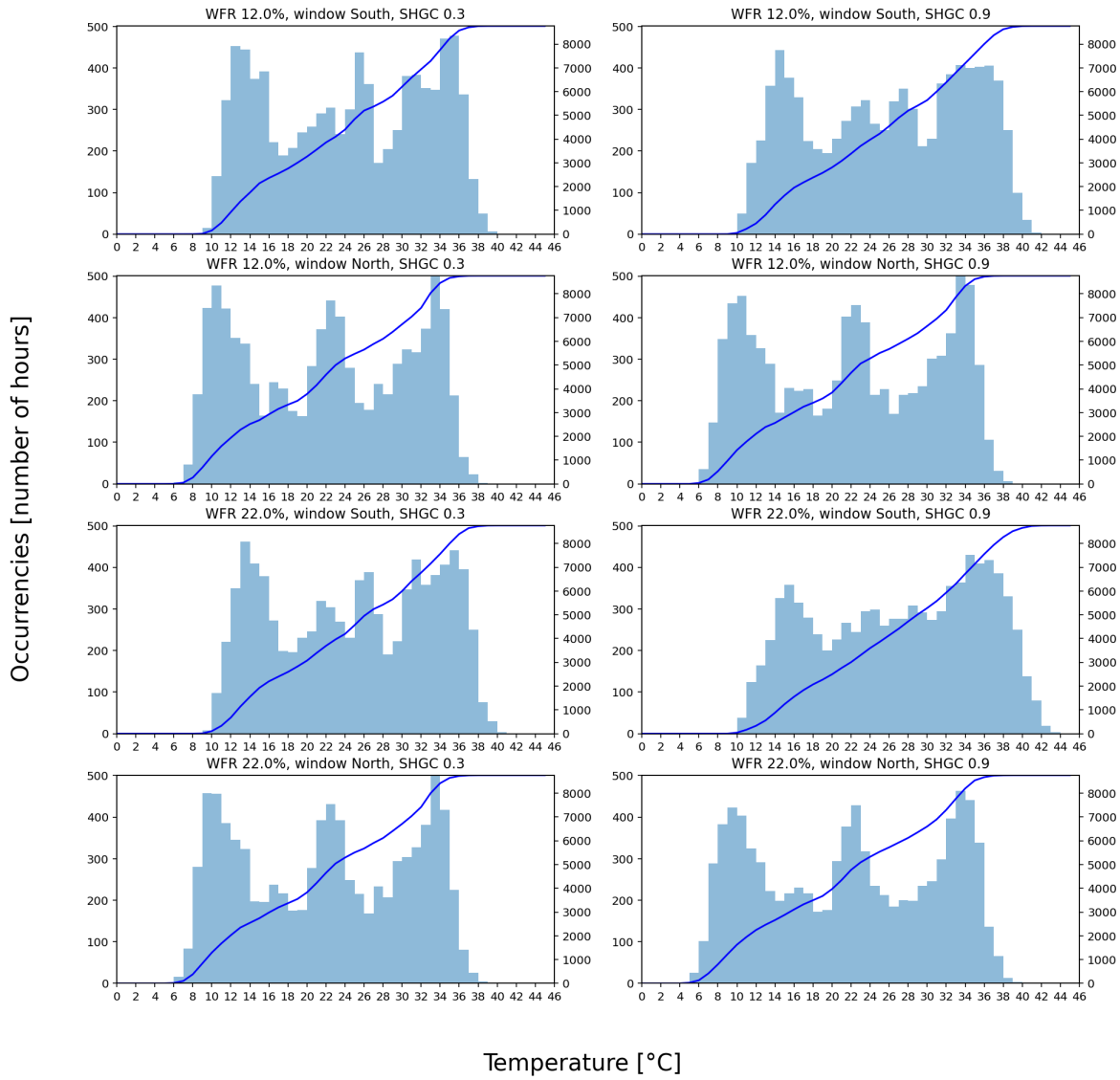

Figure 75 – Temperature frequency chart for Milan cases. Here and in the following charts, all the subplots on the left represent the cases with SHGC equal to 0.3, while the right-side ones represent the 0.9 SHGC cases; the 4 charts on top represent the lower WFR and the lower ones the higher WFR; and among those, the first line corresponds to the window facing south, while the second line corresponds to the window facing north.

As for the cumulative frequency of the difference of temperature between the indoor temperature and the maximum comfort temperature, the chart in Figure 76 displays the results. It can be seen that increasing the air speed shifts the graph towards the left part of the chart, which means that more cases are in the comfort zone.

Figure 77 displays the comparison of the cumulative frequency for cases with equal WFR and orientation with different SHGC, to highlight the possible improvement that the change in the glazing stratigraphy can generate. From the chart, it can be seen that decreasing the SHGC has a positive effect in all the cases, with a lower improvement for the windows facing north.

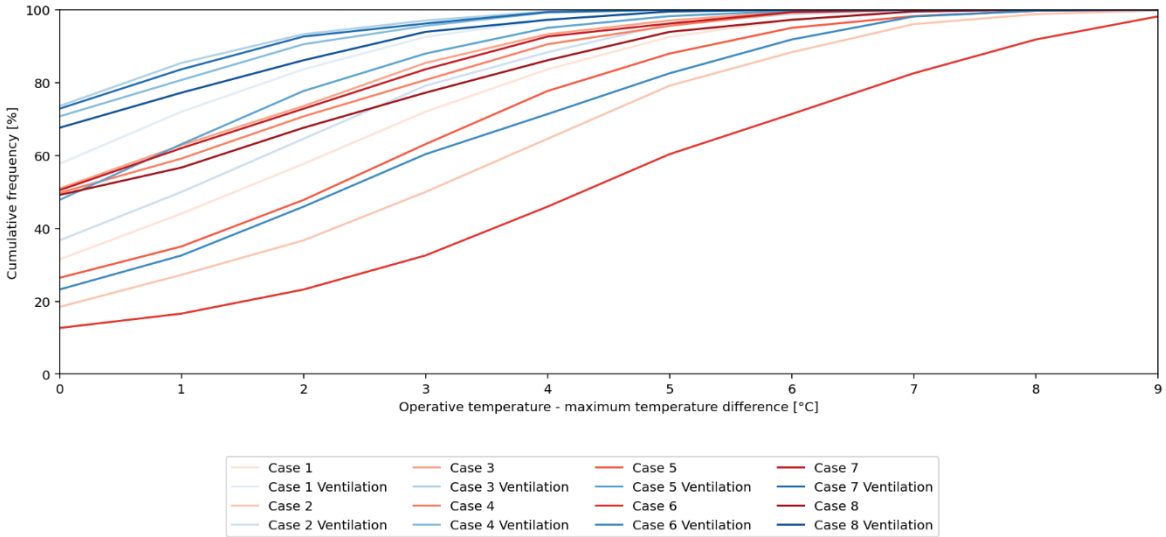

Figure 76 – Cumulative frequency of temperature exceedance for Milan (blue for zero and red for higher air speed)

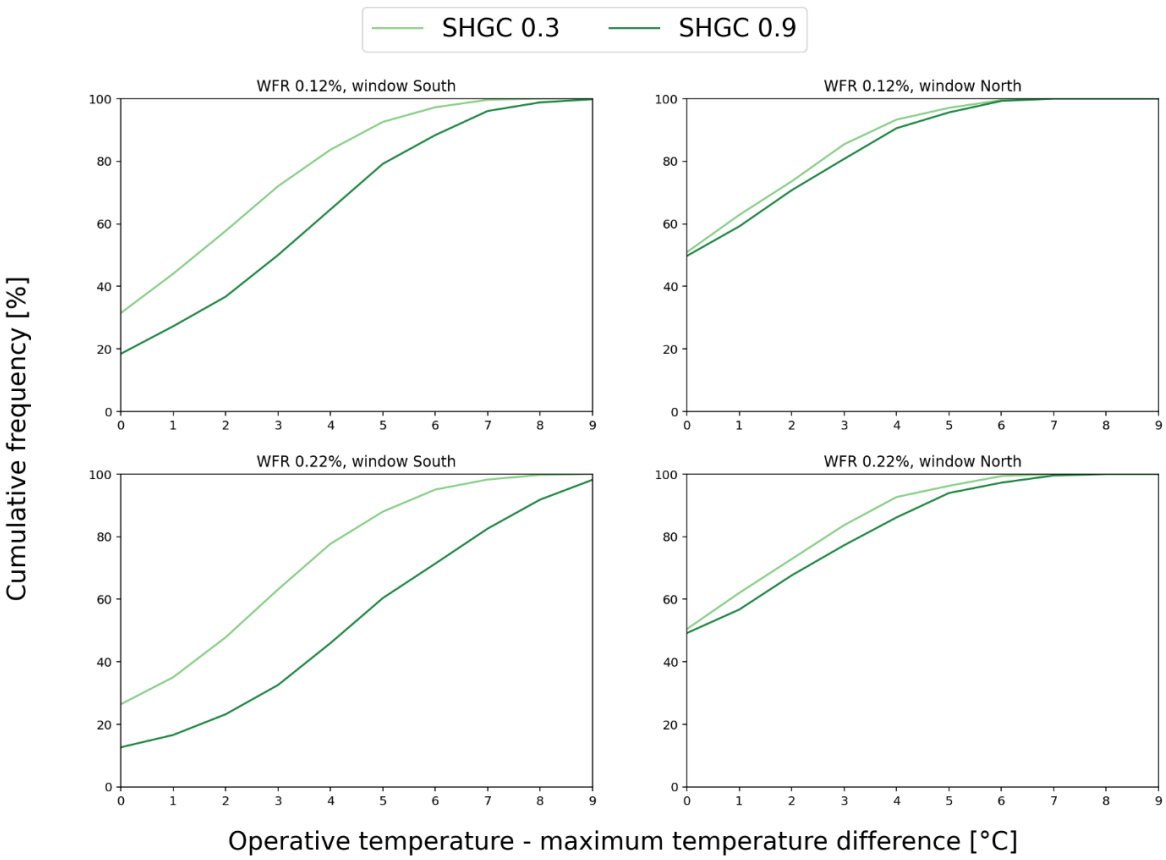

Figure 77 – Cumulative frequency comparison charts for specific cases for Milan

Figure 78 displays the share of summer (non-heating period) hours in the different comfort bands for the different considered cases, with and without mechanical ventilation. It can be seen that, as the air speed increases, the discomfort hours decrease by 15 percentage points.

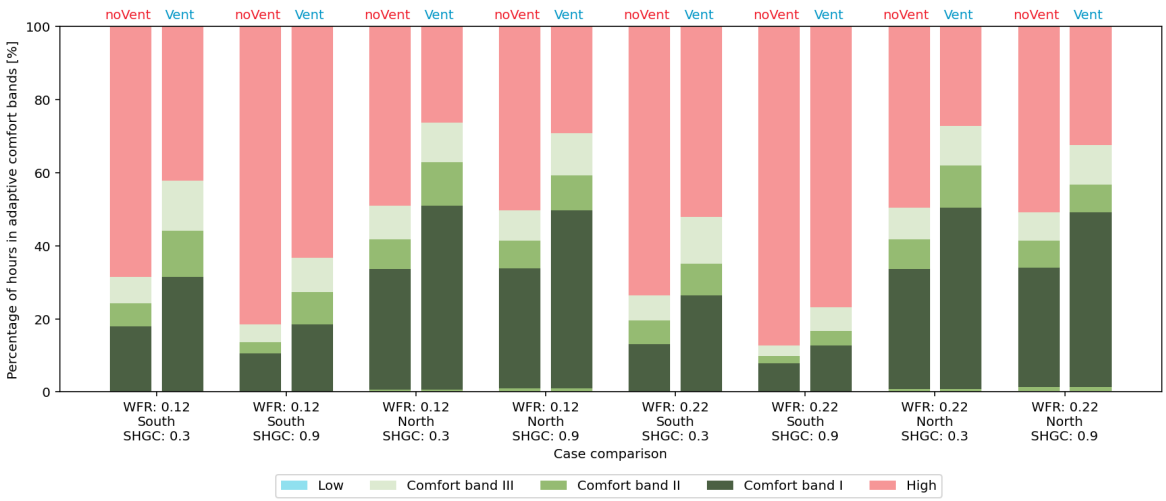

Figure 78 – Comfort bands for the cases of Milan

Additionally, a plot is created separating the different periods (Figure 79), defined according to the start and end of the heating season and of the school period in Italy. Milan is in climatic zone E; thus, the non-heating period runs from the 15th of April to the 15th of October, while the school summer period is considered to start on the 15th of June and end on the 15th of September.

For the north-facing-window cases, in the winter period, from January to the beginning of March and from the end of October to December, the considered classroom does not present overheating hours, and the room requires heating for most of the time. For the south-facing window cases, the scenarios with a good glazing performance present less than 5% of the hours above the upper limit for the comfort categories, while the low-performance glazing ones already require the management of a more consistent share of hours above the comfort limits.

For what concerns the spring period, between the end of the heating season and the end of the school, corresponding to April, May and June, and for the summer period (not considering August, that is considered as not occupied), all the cases require action for the reduction of the overheating hours, that are more than 40% of the hours in spring and 100% in almost all cases in summer.

The autumn period, ranging from mid-September to mid-October, is less critic than the spring period for the north-facing-window cases, even if the requirements are not met, with a share of hours in the II comfort category above 80%, while it results to be more critic for the south-facing-window cases, in which this percentage falls below 20% for the good glazing performance scenarios and below 5% for lower performance glazing ones.

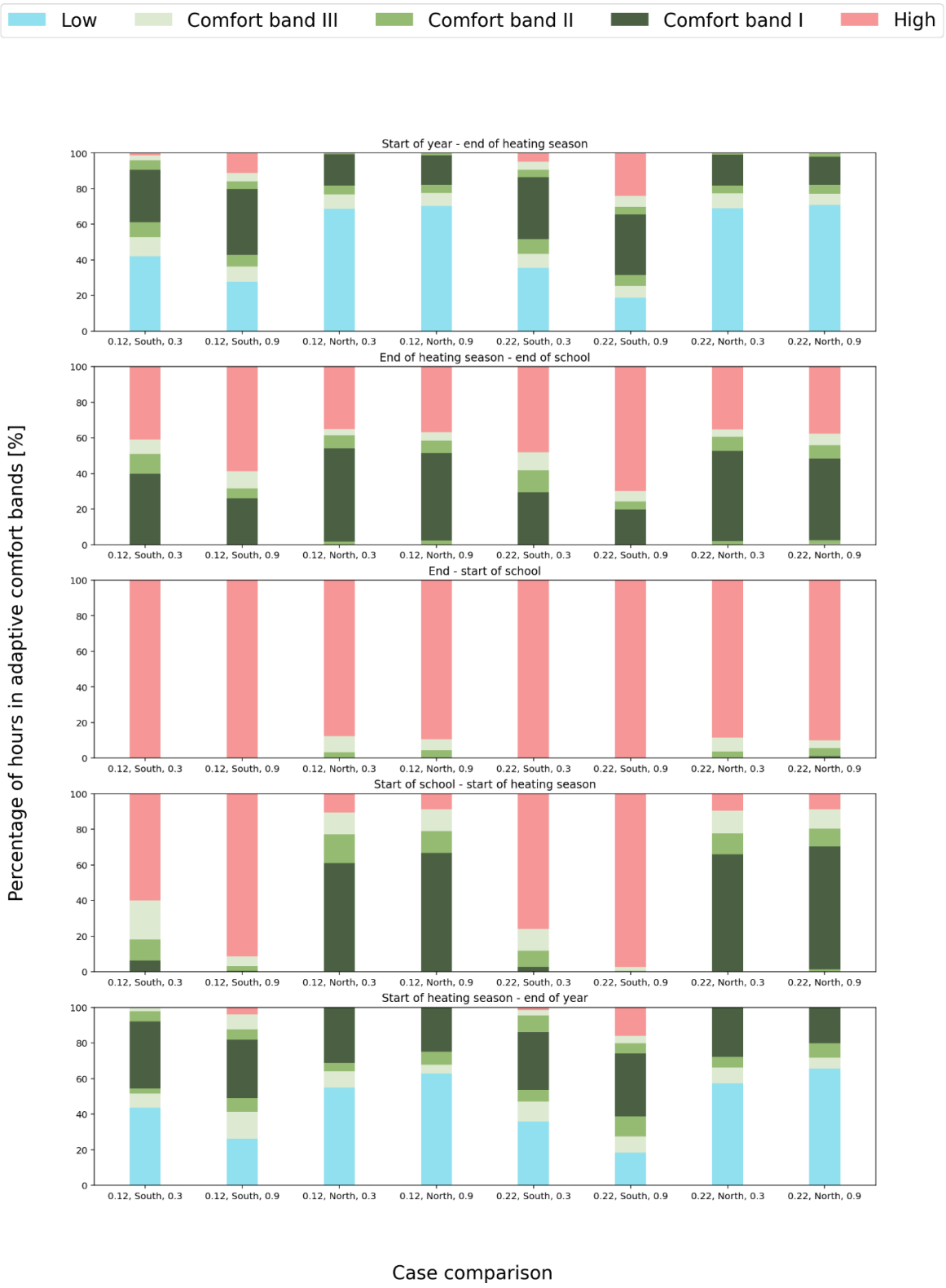

Figure 79 – Comfort bands per period in the case of Milan, with all the cases

As concerns the TM52 criteria compliance, Tables 19 and 20 describe the values of the different criteria for each case. Criterion 1 column displays the share of summer occupied hours during which the operative temperature exceeds the upper II comfort band limit; this

value shall not be higher than 3% for the case to be compliant. Criterion 2 column displays the share of days during which the degree-hours are higher than 6; an acceptable value is 0 in this case. The third criterion column reports the share of hours during which the temperature exceeds the upper II comfort band limit by more than 4°C; also in this case, the acceptable value is 0. The columns are colour formatted for each criterion from the lowest value (green) to the highest one (red) for both tables.

Table 19 – Milan TM52 results for the validation case studies

Case	WFR	Orient-ation	SHGC	C1 [%]	C2 [%]	C3 [%]	Over-heating
1	0.12	S	0.3	68.53	7.43	27.98	True
2	0.12	S	0.9	81.56	20.83	50.00	True
3	0.12	N	0.3	49.08	2.94	14.59	True
4	0.12	N	0.9	50.28	4.40	19.27	True
5	0.22	S	0.3	73.58	12.02	36.88	True
6	0.22	S	0.9	87.34	39.63	67.43	True
7	0.22	N	0.3	49.54	3.76	16.33	True
8	0.22	N	0.9	50.83	6.06	22.75	True

Table 20 – Milan TM52 results for the validation case studies with a higher air speed

Case	WFR	Orient-ation	SHGC	C1 [%]	C2 [%]	C3 [%]	Over-heating
1	0.12	S	0.3	42.29	0.37	7.43	True
2	0.12	S	0.9	63.30	3.94	20.83	True
3	0.12	N	0.3	26.42	0.00	2.94	False
4	0.12	N	0.9	29.27	0.00	4.40	False
5	0.22	S	0.3	52.20	1.74	12.02	True
6	0.22	S	0.9	76.79	17.43	39.63	True
7	0.22	N	0.3	27.16	0.00	3.76	False
8	0.22	N	0.9	32.39	0.46	6.06	True

It can be seen that, as already mentioned, increasing the air speed in the room, the percentage of hours outside the comfort range for the three TM52 criteria decreases considerably. In particular, for the first criterion, a decrease of 20% on average is registered, for the second criterion, the average decrease is worth 9%, while for the third one, it is on average 19%. In some of the cases with high air speed, in the second table, the second criterion values are null, or close to zero, and this puts the case in a condition classified as not overheated. All those cases correspond to the window facing north, as the solar gain in these scenarios decreases considerably.

On average, the most impactful parameter is the orientation, which can determine an increase of about 20% when passing from north to south orientation, while the WFR and the SHGC determine a lower impact, with an average increase of 14% when passing from SHGC 0.3 to 0.9 and of 6% with the increase of the window area.

The same analysis is performed for the city of Palermo, located in climatic zone B, and the results are presented as follows, referring to the use of the weather file of Palermo Falcone e Borsellino 2009-2023. The outdoor dry bulb temperature of Palermo is, on average, higher than that of Milan, as seen in Figure 80. The summer average temperatures are nevertheless similar to those in Milan, while they are higher in winter. On the other hand, the solar radiation is always higher than in Milan. Moreover, the non-heating season, during which the overheating assessment is performed, is longer in Palermo, spanning from the beginning of April to the end of November, while Milan's one is from mid-April to mid-October. The average maximum, mean and minimum temperatures are also reported in Table 21.

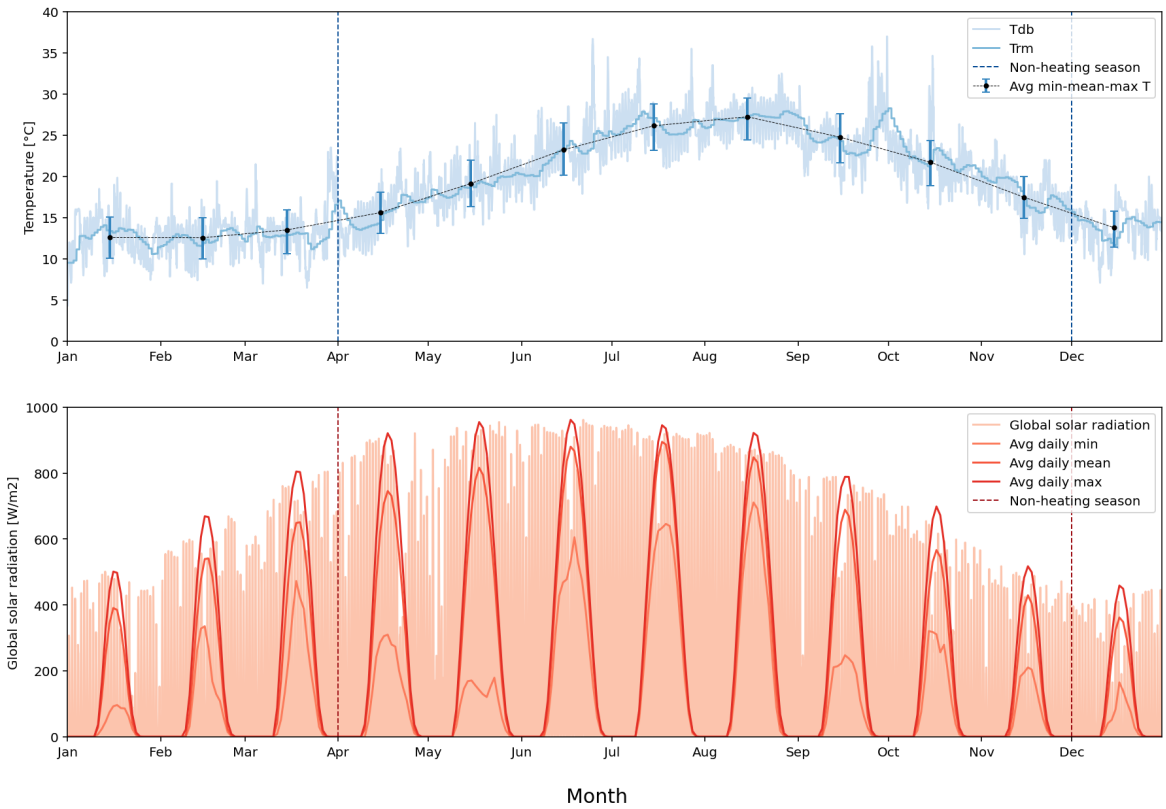

Figure 80 – Temperature and solar radiation plots for Palermo

Table 21 – Average monthly maximum, mean, and minimum temperatures for Palermo (°C)

	Jan	Feb	Mar	Apr	May	Jun	Jul	Aug	Sep	Oct	Nov	Dec
Max	15.1	15.0	16.0	18.1	22.0	26.5	28.8	29.5	27.6	24.4	20.0	15.8
Mean	12.6	12.6	13.5	15.6	19.1	23.2	26.2	27.3	24.8	21.7	17.5	13.8
Min	10.0	10.0	10.7	13.1	16.4	20.1	23.2	24.5	21.7	18.9	14.9	11.4

In the case of Palermo, the indoor operative temperature distribution is more compact than in the previous one, referred to Milan, as it can be seen in Figure 81, where the temperature ranges from 15-19°C as a minimum to 38-44°C as a maximum, in contrast with the temperatures of the Milan case, that range from 6-10°C to 38-44°C. This is due to the higher outdoor temperatures and solar radiation.

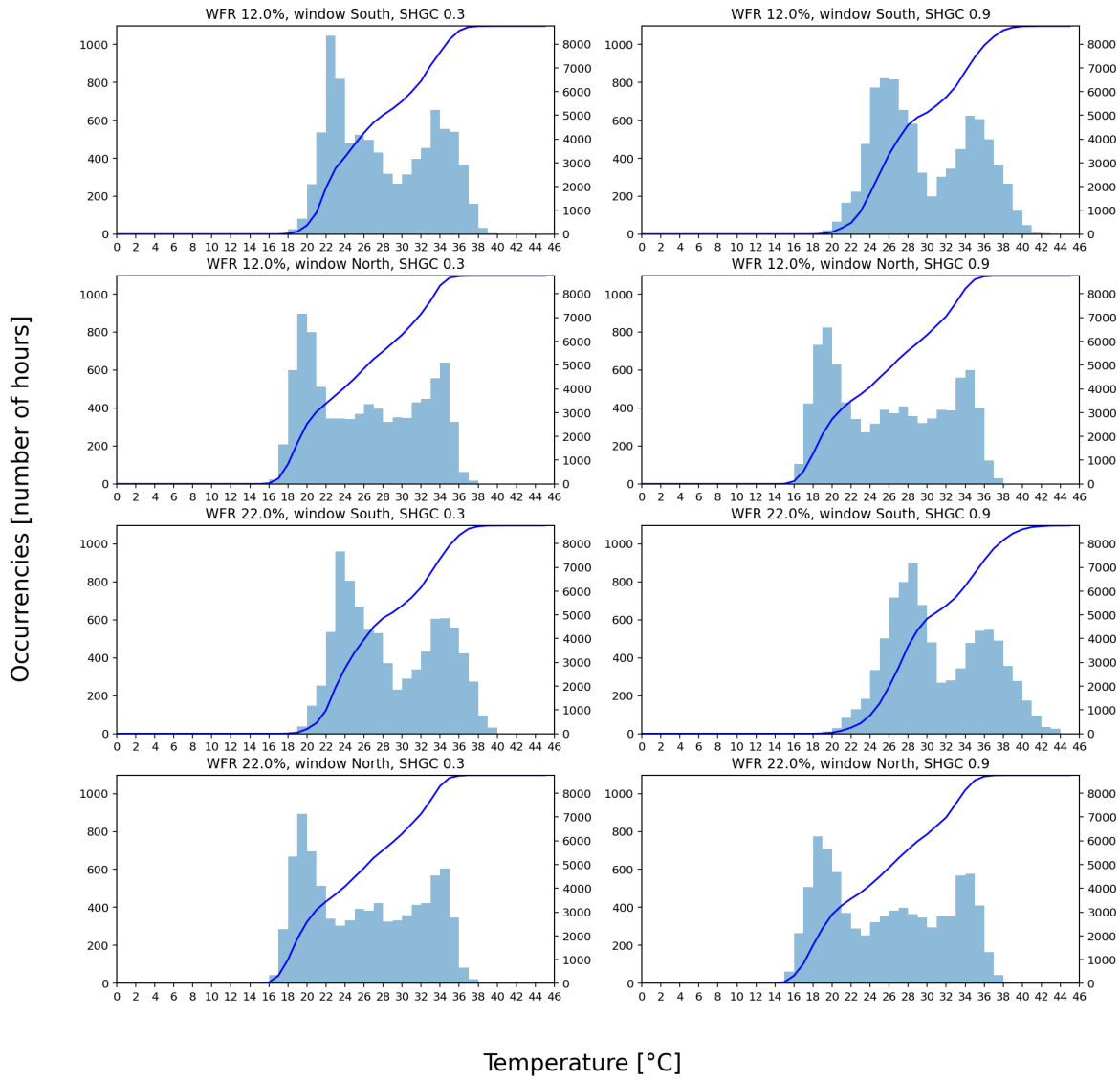

Figure 81 – Temperature frequency chart for Palermo cases

Also in this case, the cumulative frequency of the difference of temperature between the indoor temperature and the maximum comfort temperature is plotted, and similar results with respect to the case of Milan are obtained (Figures 82 and 83). The lines look shifted to the left with respect to the case of Milan, pointing at a higher comfort hours share, and this could be because of the longer span of the non-heating season, which also determines lower temperatures to be included in the calculation.

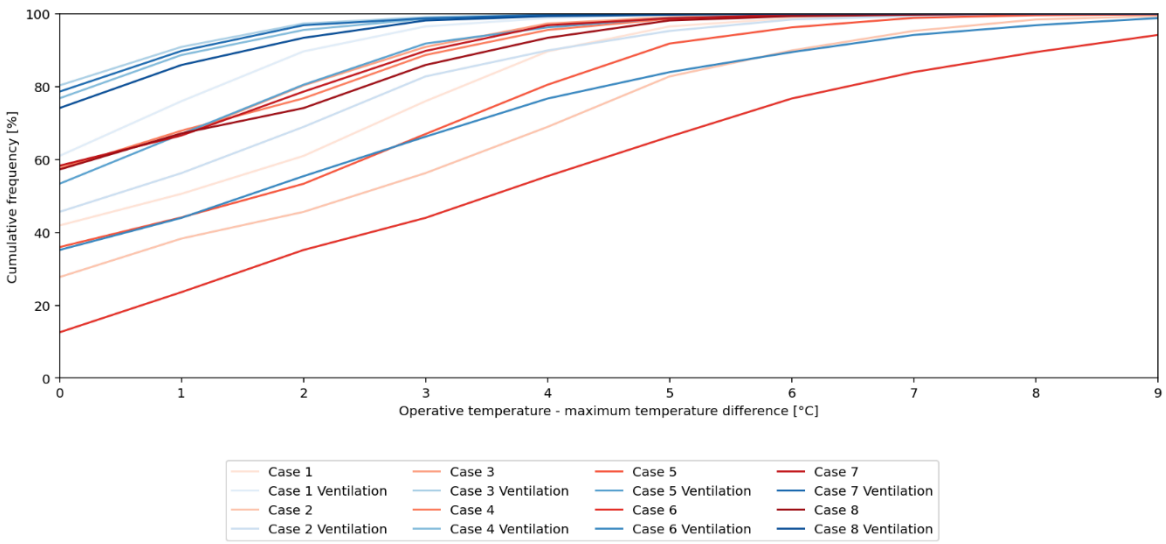

Figure 82 – Cumulative frequency of temperature exceedance for Palermo (blue for zero and red for higher air speed)

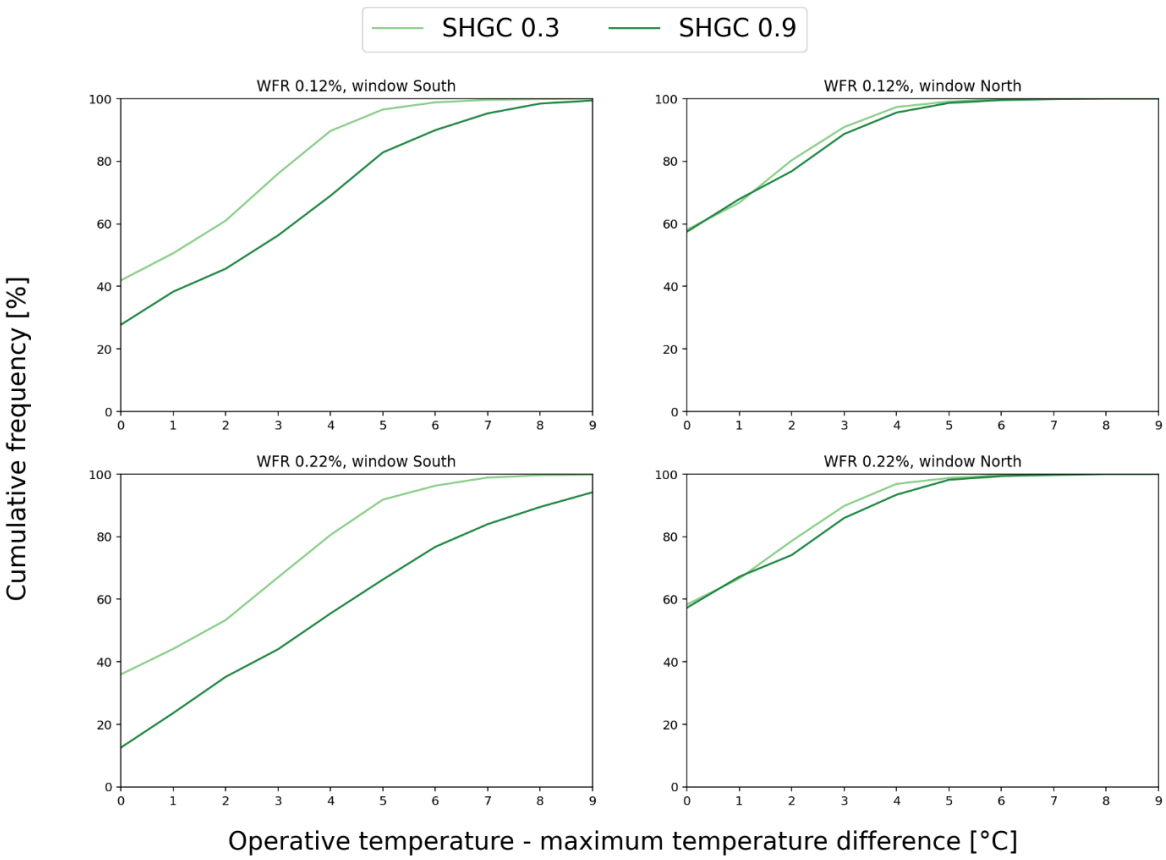

Figure 83 – Cumulative frequency comparison charts for specific cases for Palermo

Figure 84 displays the share of summer (non-heating period) hours in the different comfort bands for the different cases considered, with and without mechanical ventilation. The results are once again similar or even better than the ones of Milan, with wide III category bands, probably because of the longer non-heating period.

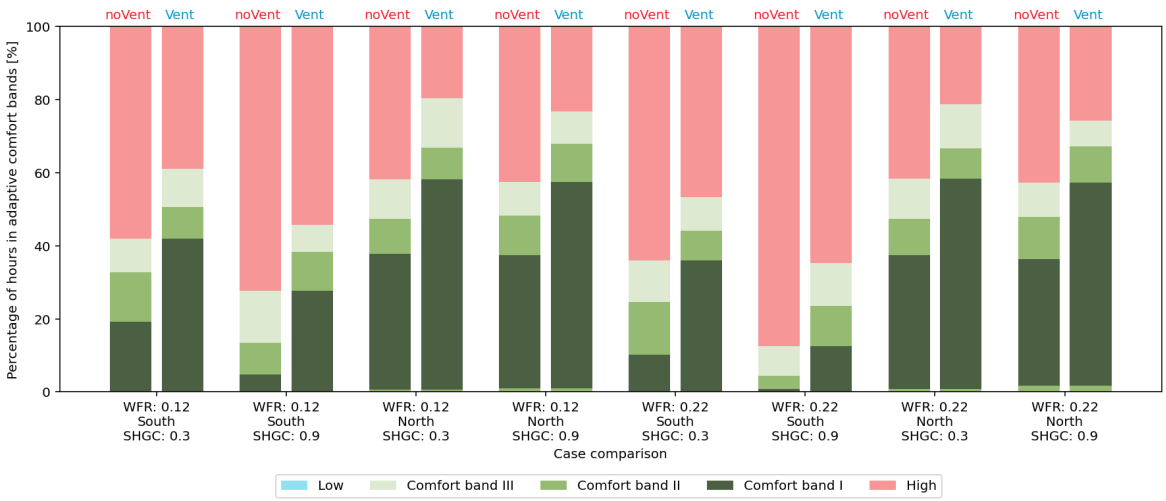

Figure 84 – Comfort bands for the cases of Palermo

The same plot is displayed in Figure 85 with the distinction of the periods defined according to the start and end of the heating season and of the school period in Italy. Palermo is in climatic zone B; thus, the non-heating period runs from the 1st of April to the 1st of November, while the school summer period is considered to start on the 15th of June and end on the 15th of September.

For the good glazing performance cases, in the winter period at the start of the year, from January to the beginning of March, the considered classroom always lies in the comfort bands. For the low-performance glazing cases, on the other hand, the scenarios with the windows facing south present already a risk of overheating, while the scenarios with north facing window require heating in some of the hours.

For what concerns the spring period, between the end of the heating season and the end of the school, corresponding to April, May and June, the summer period (not considering August, that is considered as not occupied) an the autumn one, between September and November, all the cases require action for the reduction of the overheating hours, that are more than 10% of the hours in spring, 100% in all cases in summer and also in autumn except for the north-facing-window cases.

The winter period at the end of the year, ranging from November to December, the north-facing-window cases present most of the hours in the comfort bands, while the south-facing-window cases present a high share of hours above the upper comfort limits.

Compared to the same chart for Milan, it can be seen that in Palermo, heating is rarely needed, also in the winter months. The periods appear shifted with respect to the case of Milan, with the autumn period and winter at the end of the year in Palermo resembling the summer, respectively, and the autumn ones in Milan. The spring period, on the other hand, presents a lower share of overheated hours with respect to the corresponding period in Milan, probably because of the earlier beginning of the non-heating season in Palermo.

Figure 85 – Comfort bands per period in the case of Palermo, with all the cases

For what concerns the TM52 criteria compliance is concerned, Tables 22 and 23 describe the values of the different criteria for each case.

Table 22 – Palermo TM52 results for the validation case studies

Case	WFR [%]	Orient. [-]	SHGC [-]	C1 [%]	C2 [%]	C3 [%]	Over-heating
1	0.12	S	0.3	58.10	3.46	23.99	True
2	0.12	S	0.9	72.29	17.19	43.73	True
3	0.12	N	0.3	41.90	0.92	9.08	True
4	0.12	N	0.9	42.55	1.37	11.31	True
5	0.22	S	0.3	64.05	8.17	33.01	True
6	0.22	S	0.9	87.45	33.73	56.01	True
7	0.22	N	0.3	41.70	1.24	10.20	True
8	0.22	N	0.9	42.75	1.83	14.05	True

Table 23 – Palermo TM52 results for the validation case studies with a higher air speed

Case	WFR [%]	Orient. [-]	SHGC [-]	C1 [%]	C2 [%]	C3 [%]	Over-heating
1	0.12	S	0.3	39.02	0.39	3.46	True
2	0.12	S	0.9	54.38	4.71	17.19	True
3	0.12	N	0.3	19.67	0.00	0.92	False
4	0.12	N	0.9	23.20	0.13	1.37	True
5	0.22	S	0.3	46.67	1.11	8.17	True
6	0.22	S	0.9	64.84	16.01	33.73	True
7	0.22	N	0.3	21.37	0.07	1.24	True
8	0.22	N	0.9	25.88	0.26	1.83	True

The values are quite similar to the ones assumed in the case of Milan. It can be seen that, as already mentioned, increasing the air speed in the room, the percentage of hours outside the comfort range for the three TM52 criteria decreases considerably. In particular, for the first criterion, a decrease of 19% on average is registered, for the second criterion, the average decrease is worth 6%, while for the third one it is on average 17%. In all the cases except for the case with a small window area, low SHGC and north facing window, nevertheless, the condition for overheating is verified, even if in the other north-facing window cases, the second criterion value is very low and a small decrease would determine the classification of the case as a not-overheating one.

In the end, to justify the similarities and differences between the two analysed cases, the chart in Figure 86 is plotted to stress the difference in the trend in the outdoor temperatures of the two locations. It can be clearly seen, indeed, that the running mean temperature in Palermo is almost always higher than the one in Milan, even if in the summer period the hourly temperatures do not reach much higher values. This can be justified by observing that the temperature ranges in Palermo are narrower than the ones in Milan, which, on the other hand, presents very high differences between high and low peaks. This behaviour is the direct cause of the small difference between the data extracted for the two cities in terms of comfort bands hours and TM52 compliance, as those two parameters are defined referring to the running mean outdoor temperature. The temperature difference frequency chart, indeed, presents lower differences between the indoor operative temperature and the maximum II category temperature, as seen in Figure 86, as the running mean temperature is higher in

most cases, and the temperature peaks are smoother. Moreover, the analysis for Palermo includes, apart from the first half of April, also the second half of October and the full month of November, months in which the temperatures are milder and that thus increase the number of hours that are classified as comfort hours.

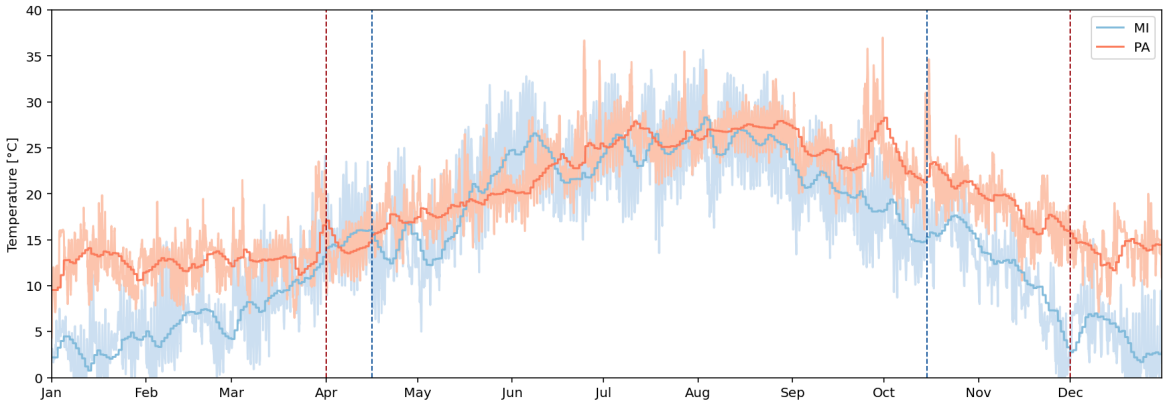

Figure 86 – Milan and Palermo outdoor dry-bulb temperature comparison

Appendix B – day of the week variation study

Changing the initial weekday for the simulation changes the alignment between the peak internal loads, which are determined by the presence of occupants, and the external highest loads, which are fixed by the weather file, and this effect was noticed to impact the comparison between IESVE and EnergyPlus results. An analysis is thus carried out, changing the start weekday in the ApLocate settings in IESVE, and performing the 8 test simulations for each of the seven cases. Figure 87 displays the percentage of hours in the different comfort bands for the 8 test cases in the 7 weekday configurations (M – Monday, T – Tuesday, W – Wednesday, T – Thursday, F – Friday, S – Saturday and S – Sunday). The north-facing and low SHGC cases are the most affected by the change in the weekday alignment, as solar gains have less impact in these configurations. This can be even better seen in Figure 88, which displays the variation of the uncomfortable hours and, on the secondary axis, the standard deviation.

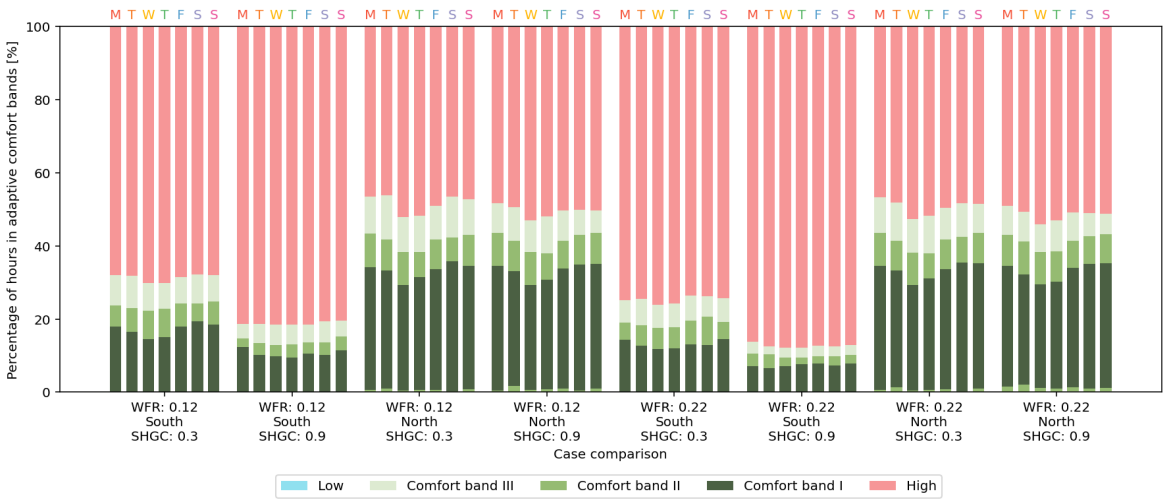

Figure 87 – Comfort hours distribution for the variation of weekdays in the 8 test cases

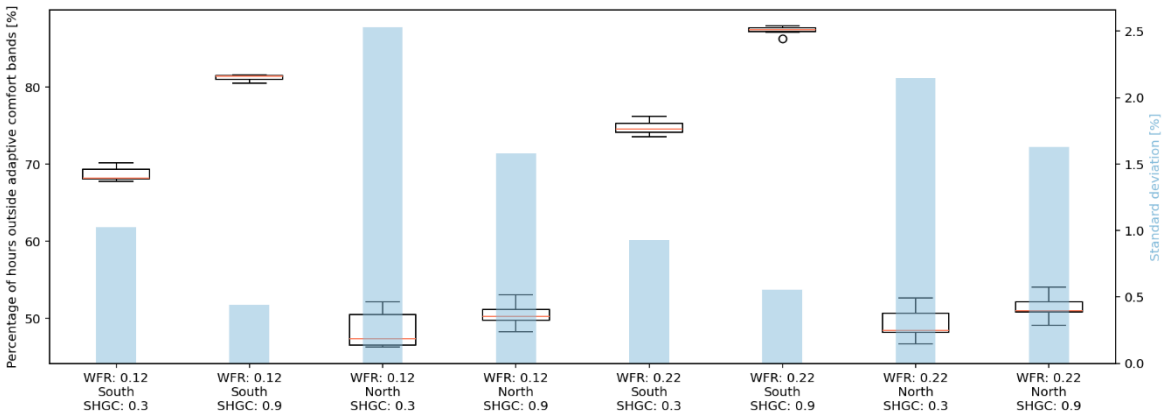

Figure 88 – Variation of discomfort hours for the 8 test cases, with the variation of the day of the week

In Figure 89, which displays the temperature over 24 hours of the hottest day, it can be seen that most of the cases are similar, while the two cases are considerably different from the others. Those are the cases in which the hottest day falls on the weekend, and thus, the temperature is not increased by the internal gains, determining the hottest internal temperature to be registered on a different day. It can be seen indeed that in all cases the hottest day is August the 2nd and corresponds to a day of the week, while that in two cases for each test case, the hottest day is alternatively the 30th of July or the 1st of August, except for the case of window facing south, with high WWR and SHGC, in which the hottest day is still registered on the 2nd of August, as the internal gains play a less important role.

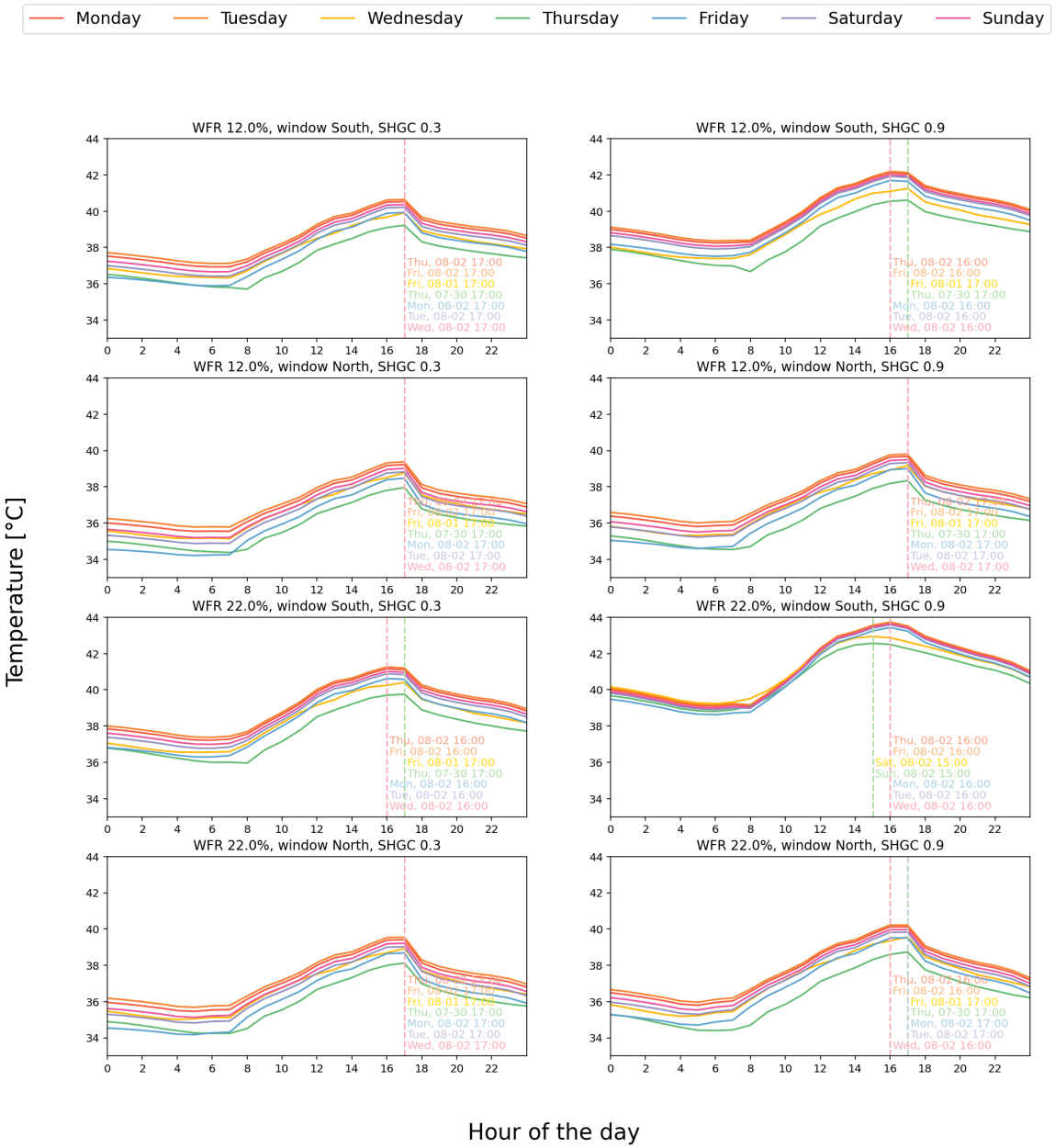

Figure 89 – Indoor operative temperature on the highest temperature day for the seven weekday cases in the 8 test cases

Appendix C – tool reports

In this Appendix, the printed reports that originate from the use of the tool are attached. The reports are ordered as follows:

- C1: School tool application to a fictitious example case
- C2: Classroom tool application to a fictitious example case
- C3: School tool application to the real case school in Varese
- C4: Classroom tool application to one of the classroom groups of the real case school in Varese

C1

Tool for the assessment of overheating in Italian school buildings

This tool allows to analyse the overheating potential of the entire school building, on the basis of the location and of the geometrical, envelope and ventilation characteristics.

School building data

Select a climatic zone

A B C D E F

Insert the total number of classrooms in the school:

30 − +

Select the number of classroom groups, clustered for floor, position and orientation

4

Select the window to wall ratio in %

12

Select the solar heat gain coefficient of the glazings

0.35

Is the 8 l/s/person minimum ventilation flow rate respected?

Yes No

Select the possible retrofit interventions done

No retrofit Walls insulation Roof insulation Double glazings

Confirm

Solution for school in climatic zone E, with WFR 12%, SHGC low and No retrofit

For each group, select the number of classrooms, the postion and the orientation.

Classroom group 1

Select the number of classrooms that belong to the group 1

6

Select the floor of classroom group 1

- (●) Ground
- ( ) Middle
- ( ) Top

Select the position of classroom group 1

- (●) Central
- ( ) Angular

Select the orientation of classroom group 1

- (●) South
- ( ) West
- ( ) North
- ( ) East

[●] Confirm

Classroom group 2

Select the number of classrooms that belong to the group 2

8

Select the floor of classroom group 2

- (●) Ground
- ( ) Middle
- ( ) Top

Select the position of classroom group 2

- (●) Central
- ( ) Angular

Select the orientation of classroom group 2

- ( ) South
- ( ) West
- (●) North
- ( ) East

[●] Confirm

Classroom group 3

Select the number of classrooms that belong to the group 3

8

Select the floor of classroom group 3

Ground Middle Top

Select the position of classroom group 3

Central Angular

Select the orientation of classroom group 3

South West North East

Confirm

Classroom group 4

Number of classrooms that belong to the group 4: 8

Select the floor of classroom group 4

Ground Middle Top

Select the position of classroom group 4

Central Angular

Select the orientation of classroom group 4

South West North East

Confirm

Loading...

Estimated time: 1 min 20 sec

Loading - Group 1...

Loading - Group 2...

Loading - Group 3...

Loading - Group 4...

Results

Share of hours with T>Tmax in the different periods of the year

	Start of year - end of heating season	End of heating season - end of school	End - start of school	Start of school - start of heating season	Start of heating season - end of year
Classrooms at Ground floor, Central, South exposed	0.0%	23.02%	57.54%	0.0%	0.0%
Classrooms at Ground floor, Central, North exposed	0.0%	18.37%	39.69%	0.0%	0.0%
Classrooms at Top floor, Central, South exposed	0.0%	28.37%	65.54%	0.0%	0.0%
Classrooms at Top floor, Central, North exposed	0.0%	24.42%	51.38%	0.0%	0.0%

N° of hours with T>Tmax / N° of hours tot

	non heating	school non heating
Classrooms at Ground floor, Central, South exposed	344 / 1090	114 / 650
Classrooms at Ground floor, Central, North exposed	261 / 1090	93 / 650
Classrooms at Top floor, Central, South exposed	396 / 1090	132 / 650
Classrooms at Top floor, Central, North exposed	340 / 1090	120 / 650

N° of hours with T>Tmax+2°C / N° of hours tot

	non heating	school non heating
Classrooms at Ground floor, Central, South exposed	209 / 1090	72 / 650
Classrooms at Ground floor, Central, North exposed	175 / 1090	59 / 650
Classrooms at Top floor, Central, South exposed	247 / 1090	82 / 650
Classrooms at Top floor, Central, North exposed	209 / 1090	70 / 650

The school presents 14 / 30 classrooms at overheating risk according to TM52

	C1	C2	C3	TOT
Classrooms at Ground floor, Central, South exposed	26.88%	0.09%	5.96%	Overheating
Classrooms at Ground floor, Central, North exposed	20.28%	0.0%	2.84%	No overheating
Classrooms at Top floor, Central, South exposed	32.48%	0.83%	8.72%	Overheating
Classrooms at Top floor, Central, North exposed	26.7%	0.0%	5.87%	No overheating

Total heat stress days and heat stress days for the non heating school period.

	total	school non heating
Classrooms at Ground floor, Central, South exposed	105 / 365	26 / 89
Classrooms at Ground floor, Central, North exposed	88 / 365	21 / 89
Classrooms at Top floor, Central, South exposed	102 / 365	27 / 89
Classrooms at Top floor, Central, North exposed	92 / 365	23 / 89

Group 1: 6 Classrooms at Ground floor, Central, South exposed --> high overheating risk in the intermediate seasons

Group 2: 8 Classrooms at Ground floor, Central, North exposed --> low overheating risk in the intermediate seasons

Group 3: 8 Classrooms at Top floor, Central, South exposed --> high overheating risk in the intermediate seasons

Group 4: 8 Classrooms at Top floor, Central, North exposed --> low overheating risk in the intermediate seasons

The school is considered to be at high overheating risk in the intermediate seasons

Group 1: 6 Classrooms at Ground floor, Central, South exposed --> high overheating risk in summer

Group 2: 8 Classrooms at Ground floor, Central, North exposed --> low overheating risk in summer

Group 3: 8 Classrooms at Top floor, Central, South exposed --> high overheating risk in summer

Group 4: 8 Classrooms at Top floor, Central, North exposed --> low overheating risk in summer

The school is considered to be at middle overheating risk and can be used discontinuously with low attendance in the summer season

To compare various improvement possibilities for the overheating of the different classroom groups, use the classroom tool

C2

Tool for the assessment of overheating in Italian school classrooms

This tool allows to analyse the overheating reduction potential of classrooms, on the basis of the location and of the geometrical, envelope and ventilation characteristics

Select the climatic zone

○ A ○ B ◉ C ○ D ○ E ○ F

Select the floor

○ Ground ◉ Middle ○ Top

Select the postion

◉ Central ○ Angular

Select the orientation

○ South ○ West ◉ North ○ East

Select the window to wall ratio in %

12

Select the solar heat gain coefficient of the glazings

0.75

Is the 8 l/s/person minimum ventilation flow rate respected?

◉ Yes ○ No

Select the possible retrofit interventions done

◉ No retrofit ○ Walls insulation ○ Roof insulation ○ Double glazings

Confirm

Solution for classroom in climatic zone C, at floor Middle, Central, North exposed, with WFR 12%, SHGC high, and No retrofit

Loading...

Estimated time: 20 sec

Results

Share of hours in the comfort categories, represented per period based on the heating and school period.

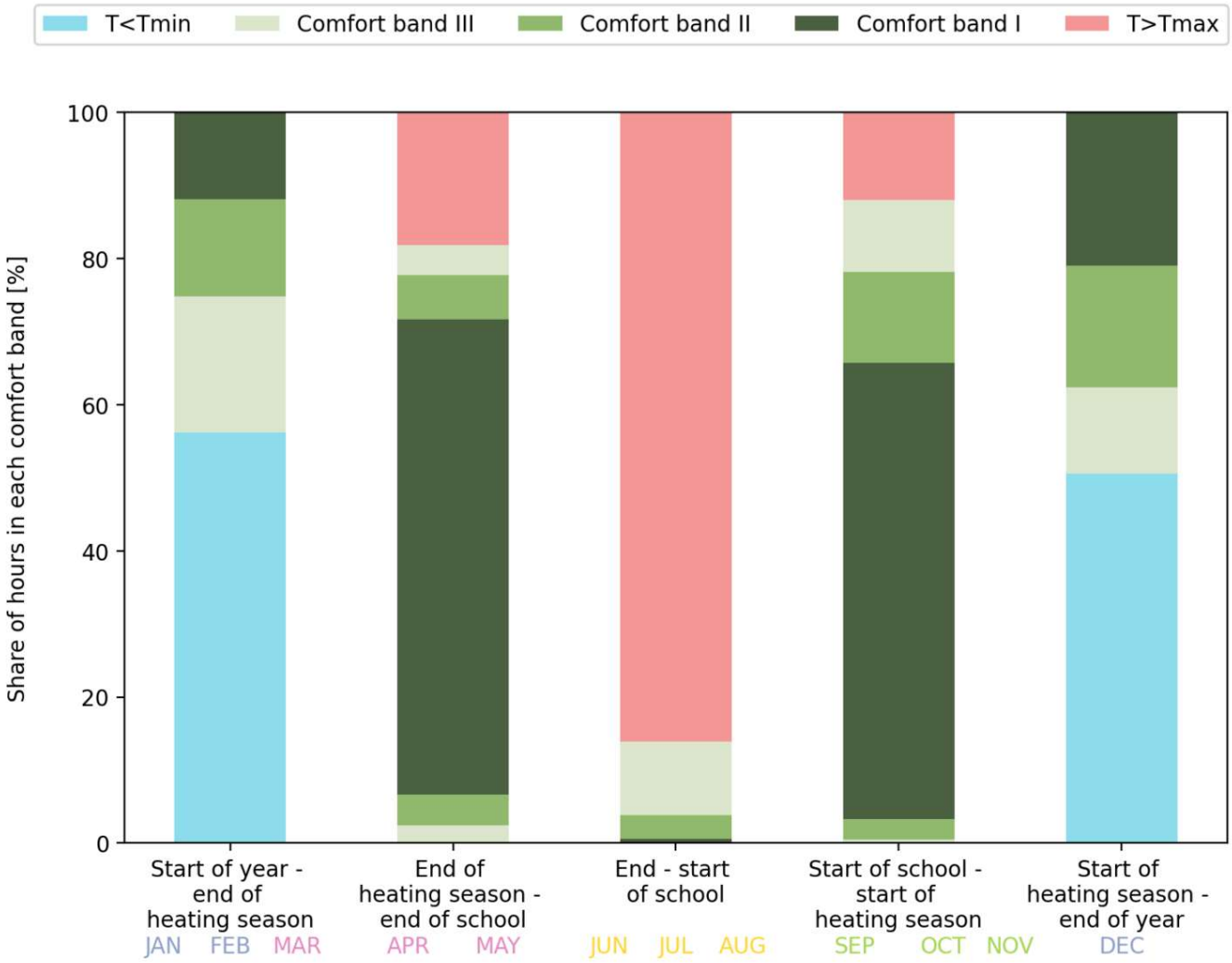

Distribution of temperatures above the Tmax. Data for the non heating period in the occupied hours

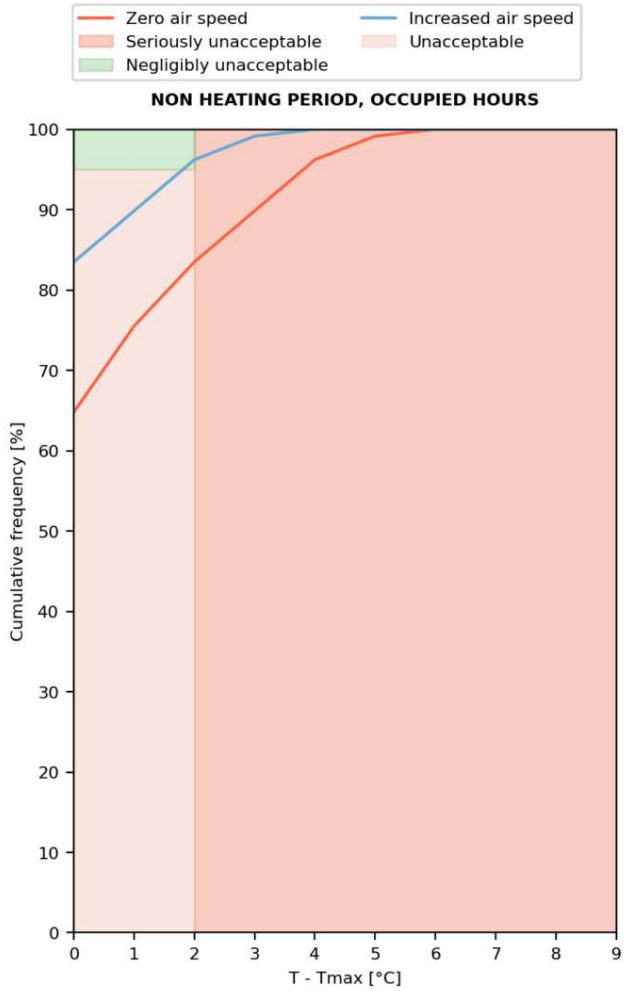

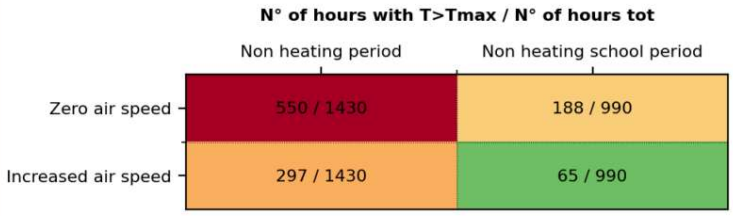

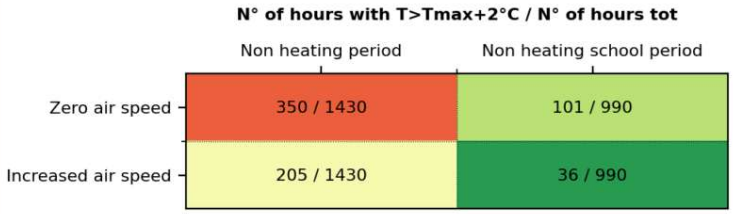

TM52 compliance criteria. Overheating risk if failure of 2 or more criteria.

- Criterion 1: share of hours with T > Tmax+1°C shall be ≤ 3%
- Criterion 2: share of days with CDH > 6 degree hours shall be null (Cooling Degree Hours = sum of T-Tmax at each hour)
- Criterion 3: share of hours with T > Tmax + 4°C shall be null

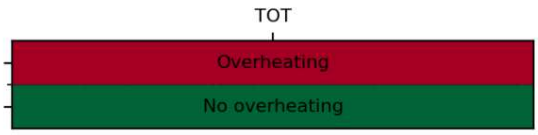

Heat stress days, calculated as days in which for at least 3 consecutive days the temperature exceeds the Tmax, and in which ventilation cannot be activated to decrease the temperature.

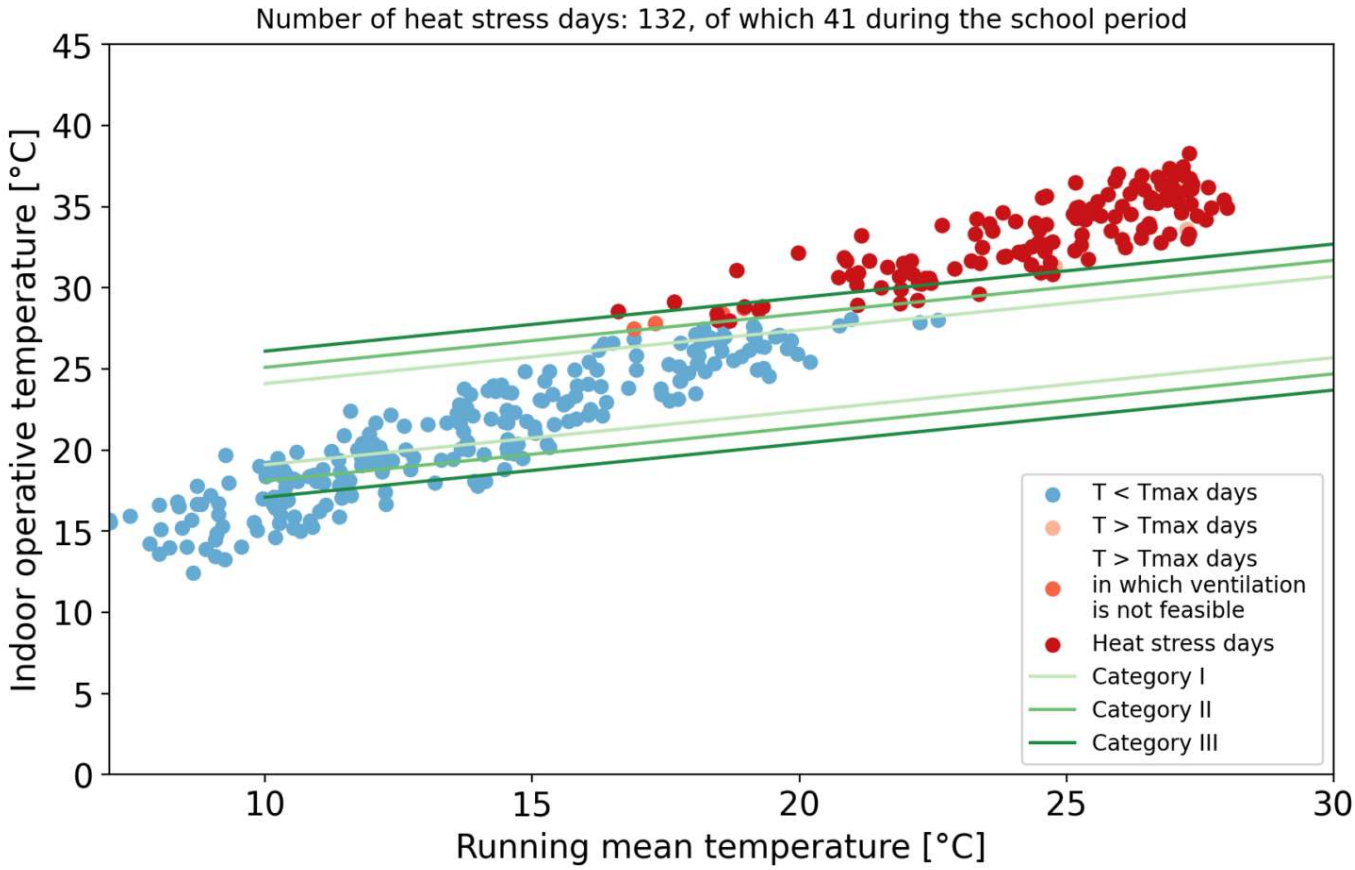

Solution comparison

With the following multiple choice list it is possible to compare the overheating potential of different configurations.

Select the retrofit strategies to be compared

Walls insulation × Double glazings × Increase air speed ×

In the next charts, the following labels will be used:

- BASE = Initial configuration
- WALL = Walls insulation
- WINDOW = Double glazings
- 1.2 m/s = Increase air speed

Share of hours in the comfort categories, represented per period based on the heating and school period. Comparison between different solutions.

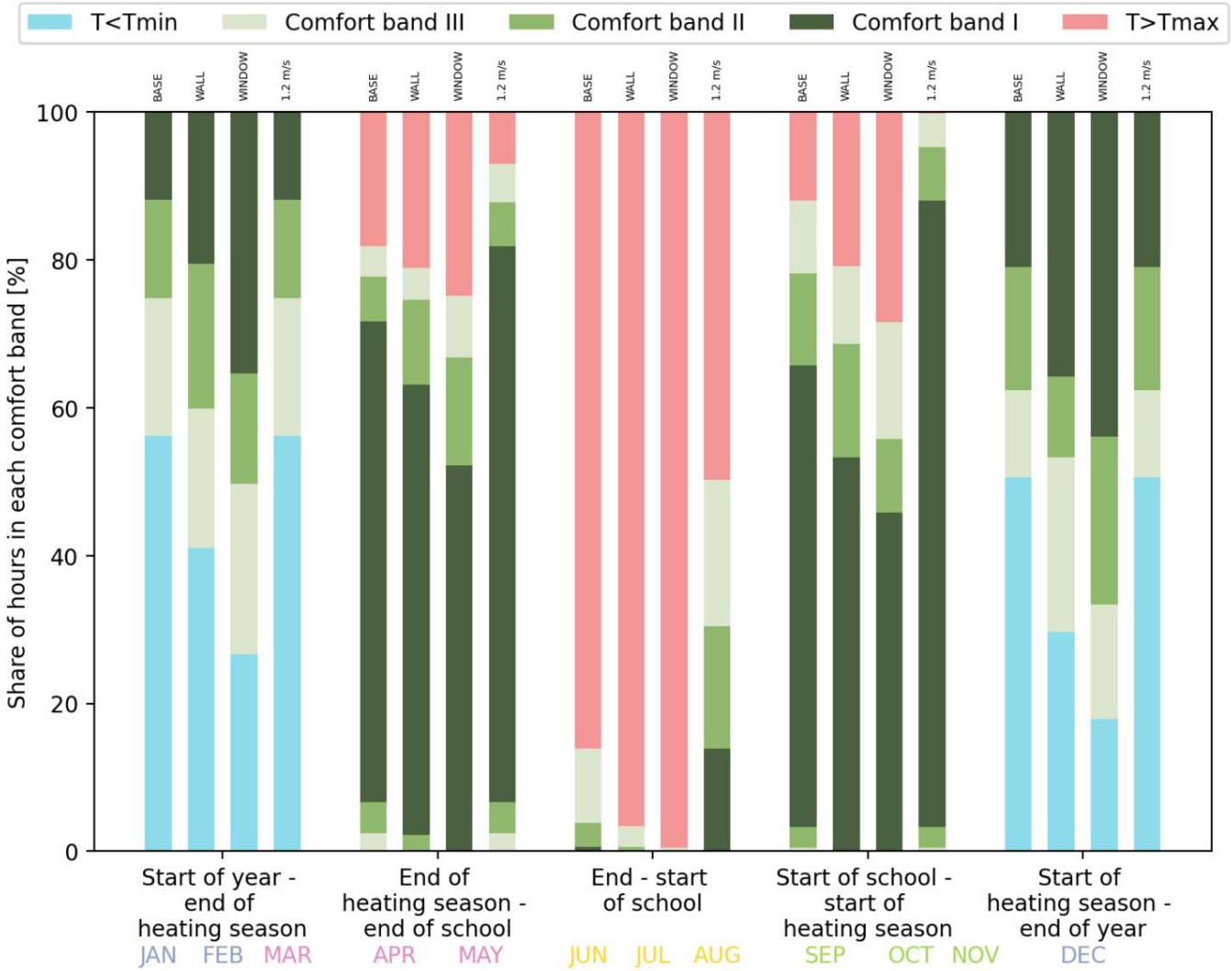

Distribution of temperatures above the Tmax. Data for the non heating period in the occupied hours. Comparison between different solutions.

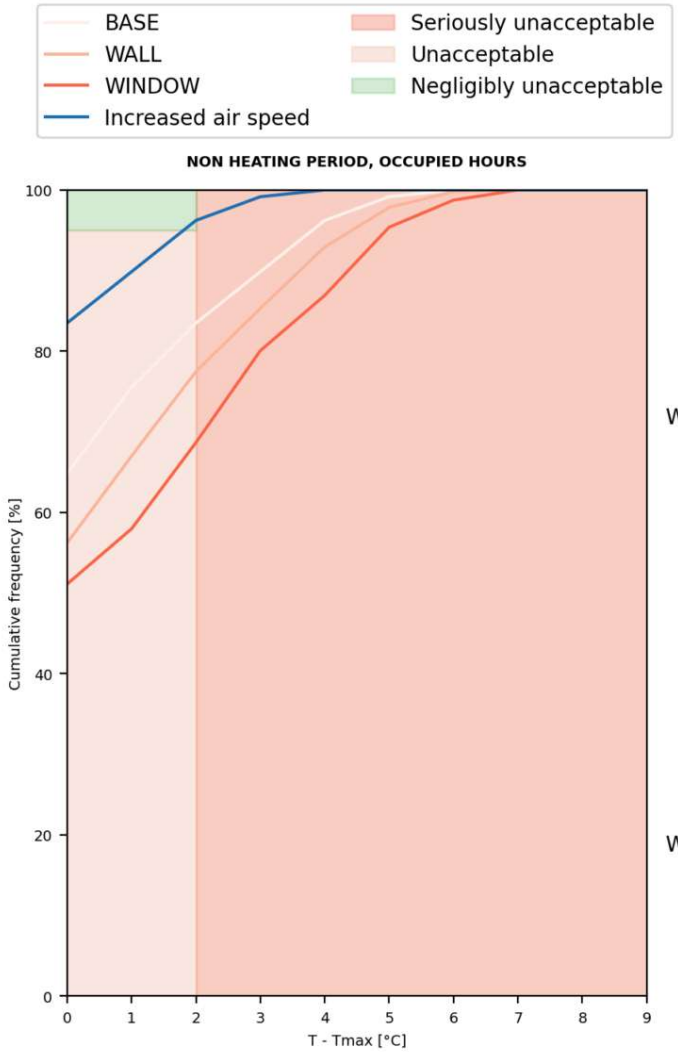

N° of hours with T>Tmax / N° of hours tot

	Non heating period	Non heating school period
BASE	550 / 1430	188 / 990
WALL	655 / 1430	233 / 990
WINDOW	714 / 1430	289 / 990
1.2 m/s	297 / 1430	65 / 990

N° of hours with T>Tmax+2°C / N° of hours tot

	Non heating period	Non heating school period
BASE	550 / 1430	188 / 990
WALL	655 / 1430	233 / 990
WINDOW	714 / 1430	289 / 990
1.2 m/s	297 / 1430	65 / 990

TM52 compliance criteria. Comparison between different solutions.

	C1	C2	C3	TOT
BASE	35.17%	0.84%	10.14%	Overheating
WALL	43.78%	2.17%	14.69%	Overheating
WINDOW	48.88%	4.62%	19.93%	Overheating
1.2 m/s	16.5%	0.0%	0.84%	No overheating

Total heat stress days and heat stress days for the school non heating period. Comparison between different solutions.

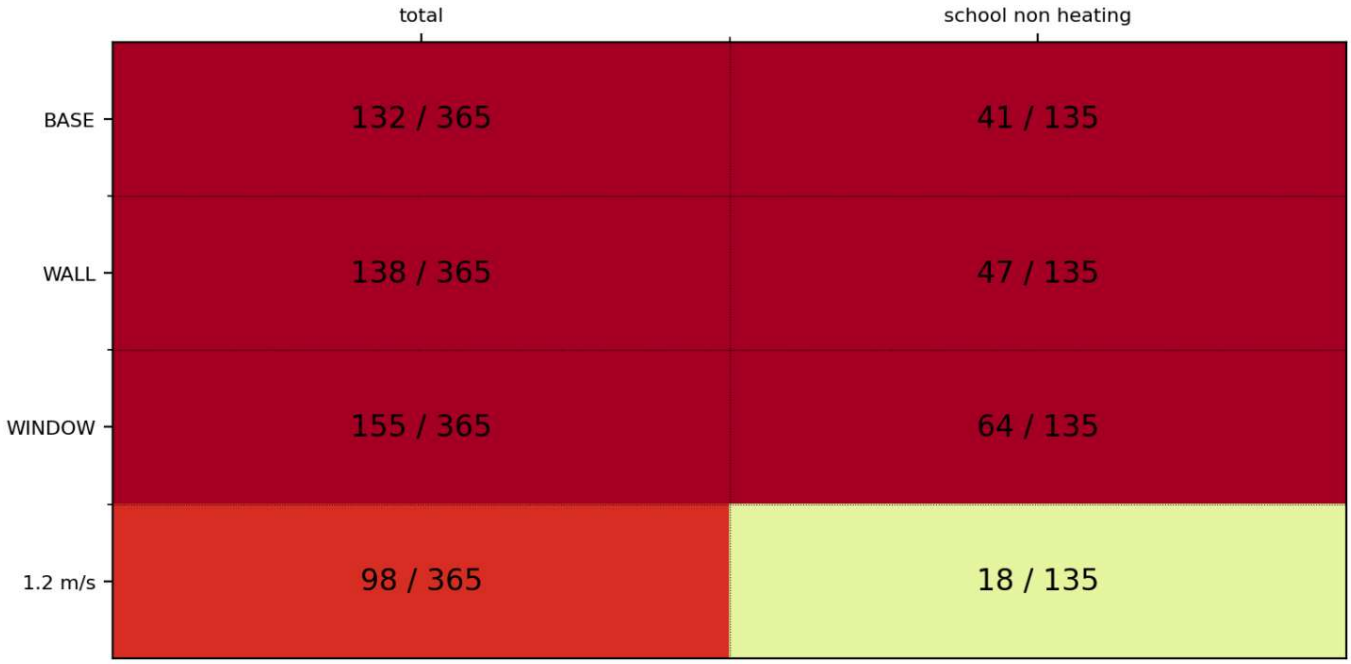

Additional passive strategies comparison

Loading... Estimated time: 1 min

In the next charts, the following labels will be used:

- BASE = Initial configuration
- 0° = Louvres 0°
- 45° = Louvres 45°
- NIGHT = Night ventilation

Share of hours in the comfort categories, represented per period based on the heating and school period. Comparison between passive strategies.

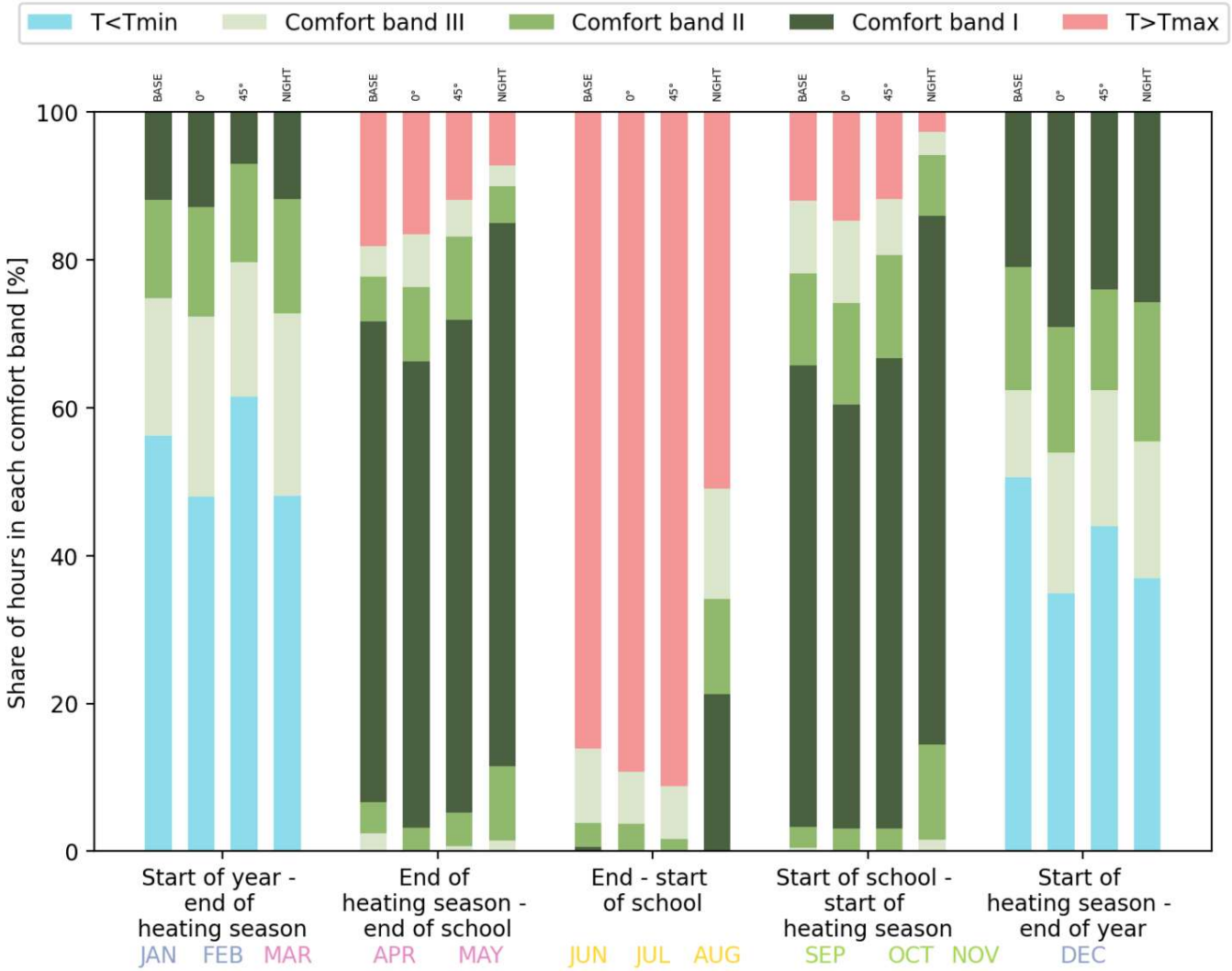

Distribution of temperatures above the Tmax. Data for the non heating period in the occupied hours. Comparison between passive strategies.

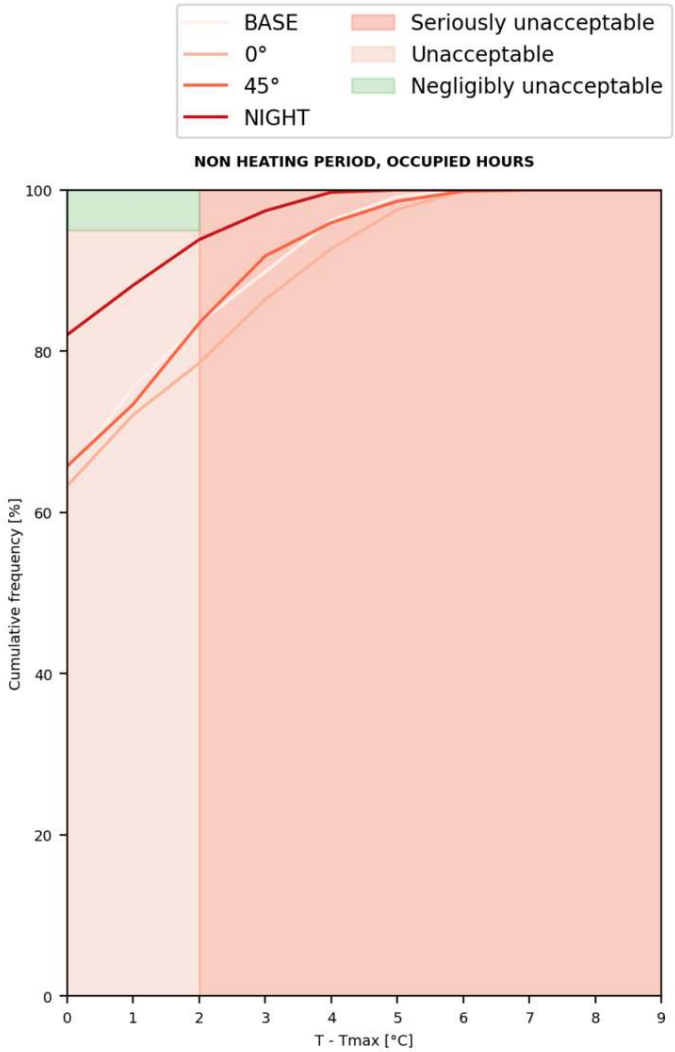

N° of hours with T>Tmax / N° of hours tot

	Non heating period	Non heating school period
BASE	550 / 1430	188 / 990
0°	561 / 1430	185 / 990
45°	515 / 1430	135 / 990
NIGHT	296 / 1430	62 / 990

N° of hours with T>Tmax+2°C / N° of hours tot

	Non heating period	Non heating school period
BASE	550 / 1430	188 / 990
0°	561 / 1430	185 / 990
45°	515 / 1430	135 / 990
NIGHT	296 / 1430	62 / 990

TM52 compliance criteria. Comparison between passive strategies.

	C1	C2	C3	TOT
BASE	35.17%	0.84%	10.14%	Overheating
0°	36.71%	2.45%	13.57%	Overheating
45°	34.27%	1.4%	8.18%	Overheating
NIGHT	17.97%	0.0%	2.59%	No overheating

Total heat stress days and heat stress days for the school non heating period. Comparison between passive strategies.

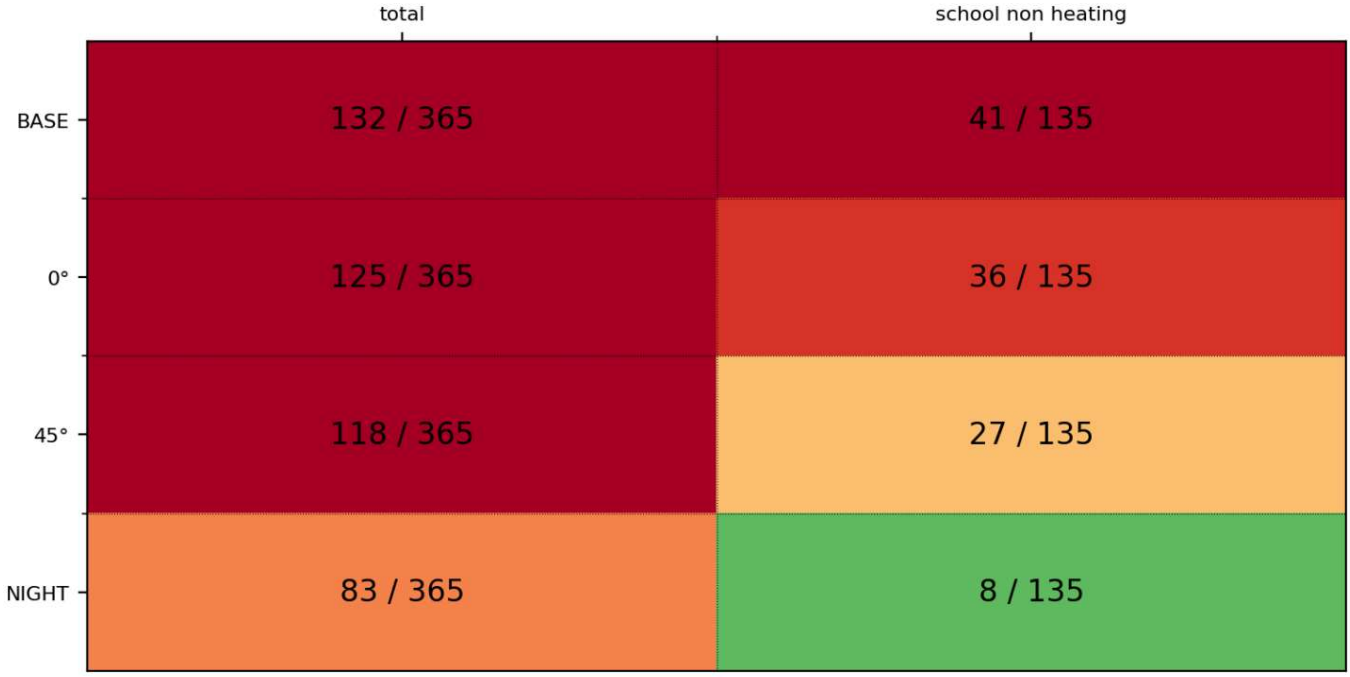

Future weather and Urban Heat Island effects comparison

Loading... Estimated time: 1 min

In the next charts, the following labels will be used:

- BASE = Initial configuration
- 2050 = 2050 future weather projections for SSP5-8.5 scenario
- 2080 = 2080 future weather projections for SSP5-8.5 scenario
- UHI = Urban Heat Island effect

Share of hours in the comfort categories, represented per period based on the heating and school period. Comparison between passive strategies.

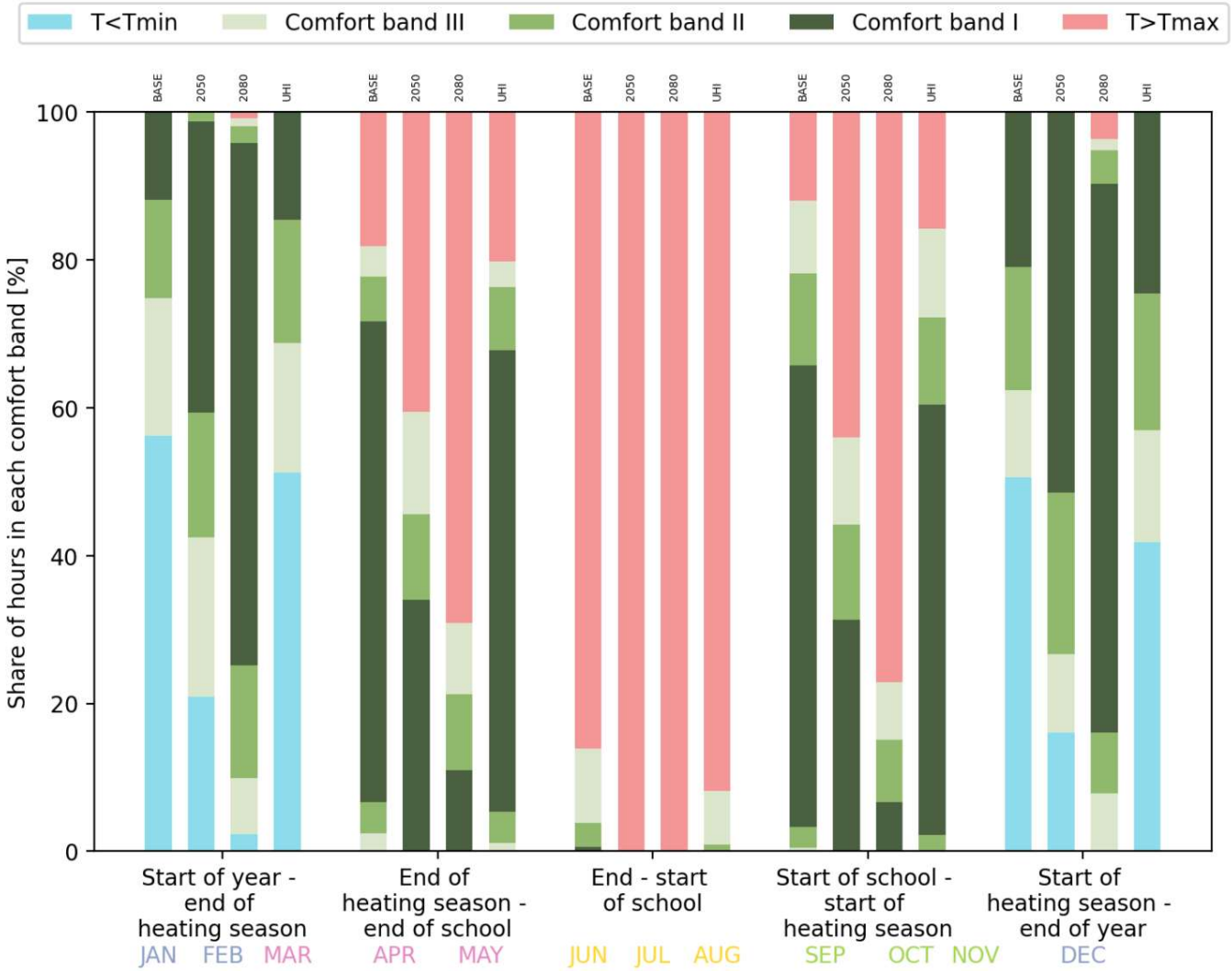

Distribution of temperatures above the Tmax. Data for the non heating period in the occupied hours. Comparison between passive strategies.

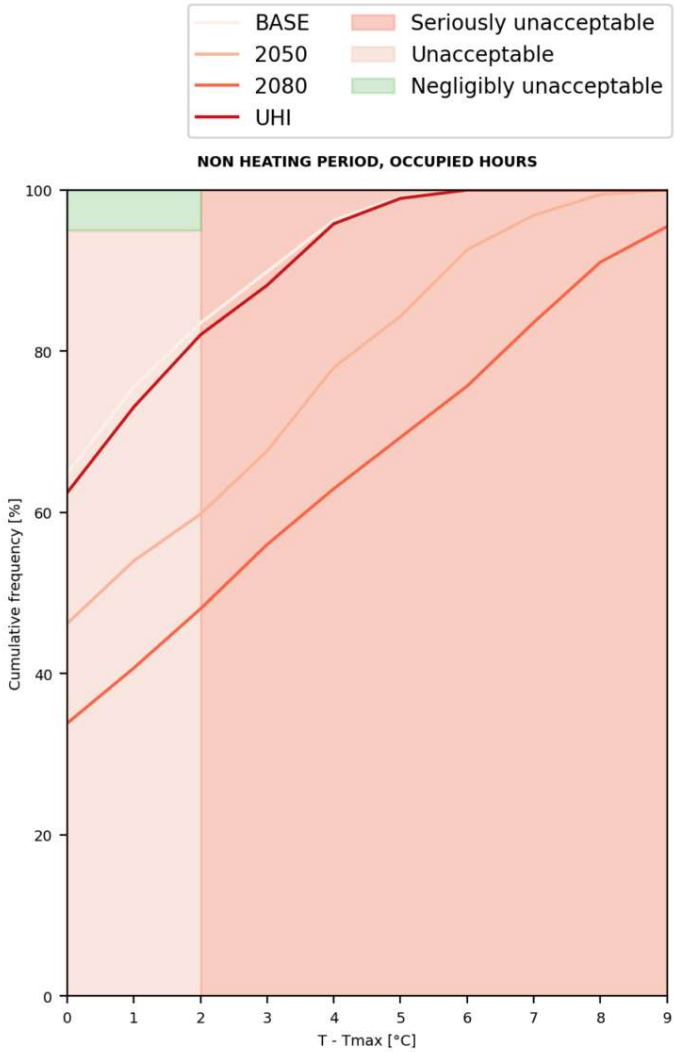

N° of hours with T>Tmax / N° of hours tot

	Non heating period	Non heating school period
BASE	550 / 1430	188 / 990
2050	850 / 1430	440 / 990
2080	1082 / 1430	665 / 990
UHI	605 / 1430	213 / 990

N° of hours with T>Tmax+2°C / N° of hours tot

	Non heating period	Non heating school period
BASE	550 / 1430	188 / 990
2050	850 / 1430	440 / 990
2080	1082 / 1430	665 / 990
UHI	605 / 1430	213 / 990

TM52 compliance criteria. Comparison between passive strategies.

	C1	C2	C3	TOT
BASE	35.17%	0.84%	10.14%	Overheating
2050	53.78%	15.66%	32.38%	Overheating
2080	66.15%	30.7%	43.99%	Overheating
UHI	37.55%	1.05%	11.82%	Overheating

Total heat stress days and heat stress days for the school non heating period. Comparison between passive strategies.

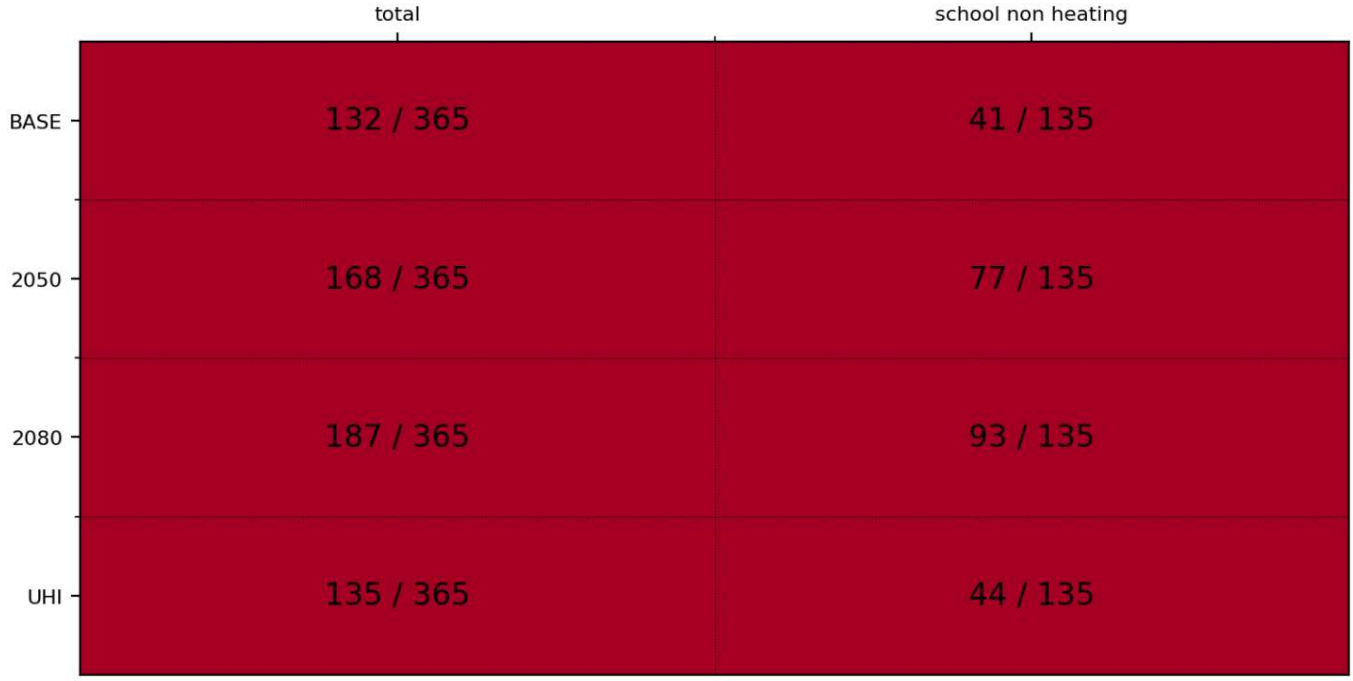
total
school non heating
BASE
2050
2080
UHI
132 / 365
41 / 135
168 / 365
77 / 135
187 / 365
93 / 135
135 / 365
44 / 135

C3

Tool for the assessment of overheating in Italian school buildings

This tool allows to analyse the overheating potential of the entire school building, on the basis of the location and of the geometrical, envelope and ventilation characteristics.

School building data

Select a climatic zone

A B C D E F

Insert the total number of classrooms in the school:

44

Select the number of classroom groups, clustered for floor, position and orientation

9

Select the window to wall ratio in %

24

Select the solar heat gain coefficient of the glazings

0.35

Is the 8 l/s/person minimum ventilation flow rate respected?

Yes No

Select the possible retrofit interventions done

No retrofit Walls insulation Roof insulation Double glazings

Confirm

Solution for school in climatic zone E, with WFR 22%, SHGC low and No retrofit

For each group, select the number of classrooms, the postion and the orientation.

Classroom group 1

Select the number of classrooms that belong to the group 1

8

Select the floor of classroom group 1

- [x] Ground
- [ ] Middle
- [ ] Top

Select the position of classroom group 1

- [x] Central
- [ ] Angular

Select the orientation of classroom group 1

- [ ] South
- [x] West
- [ ] North
- [ ] East

Confirm

Classroom group 2

Select the number of classrooms that belong to the group 2

1

Select the floor of classroom group 2

- [x] Ground
- [ ] Middle
- [ ] Top

Select the position of classroom group 2

- [ ] Central
- [x] Angular

Select the orientation of classroom group 2

- [ ] South
- [x] West
- [ ] North
- [ ] East

Confirm

Classroom group 3

Select the number of classrooms that belong to the group 3

4

Select the floor of classroom group 3

Ground Middle Top

Select the position of classroom group 3

Central Angular

Select the orientation of classroom group 3

South West North East

Confirm

Classroom group 4

Select the number of classrooms that belong to the group 4

10

Select the floor of classroom group 4

Ground Middle Top

Select the position of classroom group 4

Central Angular

Select the orientation of classroom group 4

South West North East

Confirm

Classroom group 5

Select the number of classrooms that belong to the group 5

1

Select the floor of classroom group 5

Ground Middle Top

Select the position of classroom group 5

○ Central ◉ Angular

Select the orientation of classroom group 5

○ South ◉ West ○ North ○ East

◉ Confirm

Classroom group 6

Select the number of classrooms that belong to the group 6

8

Select the floor of classroom group 6

○ Ground ◉ Middle ○ Top

Select the position of classroom group 6

◉ Central ○ Angular

Select the orientation of classroom group 6

○ South ○ West ○ North ◉ East

◉ Confirm

Classroom group 7

Select the number of classrooms that belong to the group 7

10

Select the floor of classroom group 7

○ Ground ○ Middle ◉ Top

Select the position of classroom group 7

◉ Central ○ Angular

Select the orientation of classroom group 7

○ South ◉ West ○ North ○ East

Confirm

Classroom group 8

Select the number of classrooms that belong to the group 8

1

Select the floor of classroom group 8

Ground Middle Top

Select the position of classroom group 8

Central Angular

Select the orientation of classroom group 8

South West North East

Confirm

Classroom group 9

Number of classrooms that belong to the group 9: 1

Select the floor of classroom group 9

Ground Middle Top

Select the position of classroom group 9

Central Angular

Select the orientation of classroom group 9

South West North East

Confirm

Loading...

Estimated time: 3 min 0 sec

Loading - Group 1...

Loading - Group 2...

Loading - Group 3...

Loading - Group 4...

Loading - Group 5...

Loading - Group 6...

Loading - Group 7...

Loading - Group 8...

Loading - Group 9...

Results

Share of hours with T>Tmax in the different periods of the year

	Start of year - end of heating season	End of heating season - end of school	End - start of school	Start of school - start of heating season	Start of heating season - end of year
Classrooms at Ground floor, Central, West exposed	0.0%	26.28%	58.31%	0.0%	0.0%
Classrooms at Ground floor, Angular, West exposed	0.0%	22.33%	50.31%	0.0%	0.0%
Classrooms at Ground floor, Central, East exposed	0.0%	31.16%	65.54%	0.0%	0.0%
Classrooms at Middle floor, Central, West exposed	0.0%	31.63%	72.46%	3.18%	0.0%
Classrooms at Middle floor, Angular, West exposed	0.0%	27.44%	54.62%	1.82%	0.0%
Classrooms at Middle floor, Central, East exposed	0.0%	33.49%	76.0%	5.45%	0.0%
Classrooms at Top floor, Central, West exposed	0.0%	29.53%	65.54%	0.0%	0.0%
Classrooms at Top floor, Angular, West exposed	0.0%	25.81%	54.92%	0.0%	0.0%
Classrooms at Top floor, Angular, East exposed	0.0%	26.74%	54.31%	0.0%	0.0%

N° of hours with T>Tmax / N° of hours tot

	non heating	school non heating
Classrooms at Ground floor, Central, West exposed	367 / 1090	124 / 650
Classrooms at Ground floor, Angular, West exposed	322 / 1090	107 / 650
Classrooms at Ground floor, Central, East exposed	406 / 1090	150 / 650
Classrooms at Middle floor, Central, West exposed	451 / 1090	160 / 650
Classrooms at Middle floor, Angular, West exposed	358 / 1090	131 / 650
Classrooms at Middle floor, Central, East exposed	469 / 1090	182 / 650
Classrooms at Top floor, Central, West exposed	408 / 1090	137 / 650
Classrooms at Top floor, Angular, West exposed	351 / 1090	120 / 650
Classrooms at Top floor, Angular, East exposed	347 / 1090	121 / 650

N° of hours with T>Tmax+2°C / N° of hours tot

	non heating	school non heating
Classrooms at Ground floor, Central, West exposed	225 / 1090	74 / 650
Classrooms at Ground floor, Angular, West exposed	202 / 1090	69 / 650
Classrooms at Ground floor, Central, East exposed	260 / 1090	95 / 650
Classrooms at Middle floor, Central, West exposed	287 / 1090	93 / 650
Classrooms at Middle floor, Angular, West exposed	217 / 1090	75 / 650
Classrooms at Middle floor, Central, East exposed	322 / 1090	130 / 650
Classrooms at Top floor, Central, West exposed	247 / 1090	80 / 650
Classrooms at Top floor, Angular, West exposed	223 / 1090	74 / 650
Classrooms at Top floor, Angular, East exposed	220 / 1090	78 / 650

The school presents 44 / 44 classrooms at overheating risk according to TM52

	C1	C2	C3	TOT
Classrooms at Ground floor, Central, West exposed	30.64%	1.83%	8.81%	Overheating
Classrooms at Ground floor, Angular, West exposed	26.15%	1.28%	7.71%	Overheating
Classrooms at Ground floor, Central, East exposed	33.67%	1.74%	10.28%	Overheating
Classrooms at Middle floor, Central, West exposed	39.91%	4.4%	15.05%	Overheating
Classrooms at Middle floor, Angular, West exposed	30.92%	4.4%	11.47%	Overheating
Classrooms at Middle floor, Central, East exposed	40.73%	4.04%	18.35%	Overheating
Classrooms at Top floor, Central, West exposed	35.14%	2.75%	10.92%	Overheating
Classrooms at Top floor, Angular, West exposed	29.63%	3.3%	10.55%	Overheating
Classrooms at Top floor, Angular, East exposed	29.54%	2.02%	10.55%	Overheating

Total heat stress days and heat stress days for the non heating school period.

	total	school non heating
Classrooms at Ground floor, Central, West exposed	112 / 365	31 / 89
Classrooms at Ground floor, Angular, West exposed	105 / 365	29 / 89
Classrooms at Ground floor, Central, East exposed	110 / 365	31 / 89
Classrooms at Middle floor, Central, West exposed	124 / 365	38 / 89
Classrooms at Middle floor, Angular, West exposed	123 / 365	40 / 89
Classrooms at Middle floor, Central, East exposed	123 / 365	38 / 89
Classrooms at Top floor, Central, West exposed	106 / 365	28 / 89
Classrooms at Top floor, Angular, West exposed	110 / 365	32 / 89
Classrooms at Top floor, Angular, East exposed	101 / 365	31 / 89

Group 1: 8 Classrooms at Ground floor, Central, West exposed --> high overheating risk in the intermediate seasons

Group 2: 1 Classrooms at Ground floor, Angular, West exposed --> high overheating risk in the intermediate seasons

Group 3: 4 Classrooms at Ground floor, Central, East exposed --> high overheating risk in the intermediate seasons

Group 4: 10 Classrooms at Middle floor, Central, West exposed --> high overheating risk in the intermediate seasons

Group 5: 1 Classrooms at Middle floor, Angular, West exposed --> high overheating risk in the intermediate seasons

Group 6: 8 Classrooms at Middle floor, Central, East exposed --> high overheating risk in the intermediate seasons

Group 7: 10 Classrooms at Top floor, Central, West exposed --> high overheating risk in the intermediate seasons

Group 8: 1 Classrooms at Top floor, Angular, West exposed --> high overheating risk in the intermediate seasons

Group 9: 1 Classrooms at Top floor, Angular, East exposed --> high overheating risk in the intermediate seasons

The school is considered to be at high overheating risk in the intermediate seasons

Group 1: 8 Classrooms at Ground floor, Central, West exposed --> high overheating risk in summer

Group 2: 1 Classrooms at Ground floor, Angular, West exposed --> high overheating risk in summer

Group 3: 4 Classrooms at Ground floor, Central, East exposed --> high overheating risk in summer

Group 4: 10 Classrooms at Middle floor, Central, West exposed --> high overheating risk in summer

Group 5: 1 Classrooms at Middle floor, Angular, West exposed --> high overheating risk in summer

Group 6: 8 Classrooms at Middle floor, Central, East exposed --> high overheating risk in summer

Group 7: 10 Classrooms at Top floor, Central, West exposed --> high overheating risk in summer

Group 8: 1 Classrooms at Top floor, Angular, West exposed --> high overheating risk in summer

Group 9: 1 Classrooms at Top floor, Angular, East exposed --> high overheating risk in summer

The school is considered to be at high overheating risk and cannot be used in the summer season

To compare various improvement possibilities for the overheating of the different classroom groups, use the classroom tool

C4

Tool for the assessment of overheating in Italian school classrooms

This tool allows to analyse the overheating reduction potential of classrooms, on the basis of the location and of the geometrical, envelope and ventilation characteristics

Select the climatic zone

○ A ○ B ○ C ○ D ● E ○ F

Select the floor

○ Ground ● Middle ○ Top

Select the postion

● Central ○ Angular

Select the orientation

○ South ○ West ○ North ● East

Select the window to wall ratio in %

24

Select the solar heat gain coefficient of the glazings

0.35

Is the 8 l/s/person minimum ventilation flow rate respected?

● Yes ○ No

Select the possible retrofit interventions done

● No retrofit ○ Walls insulation ○ Roof insulation ○ Double glazings

Confirm

Solution for classroom in climatic zone E, at floor Middle, Central, East exposed, with WFR 22%, SHGC low, and No retrofit

Loading...

Estimated time: 20 sec

Results

Share of hours in the comfort categories, represented per period based on the heating and school period.

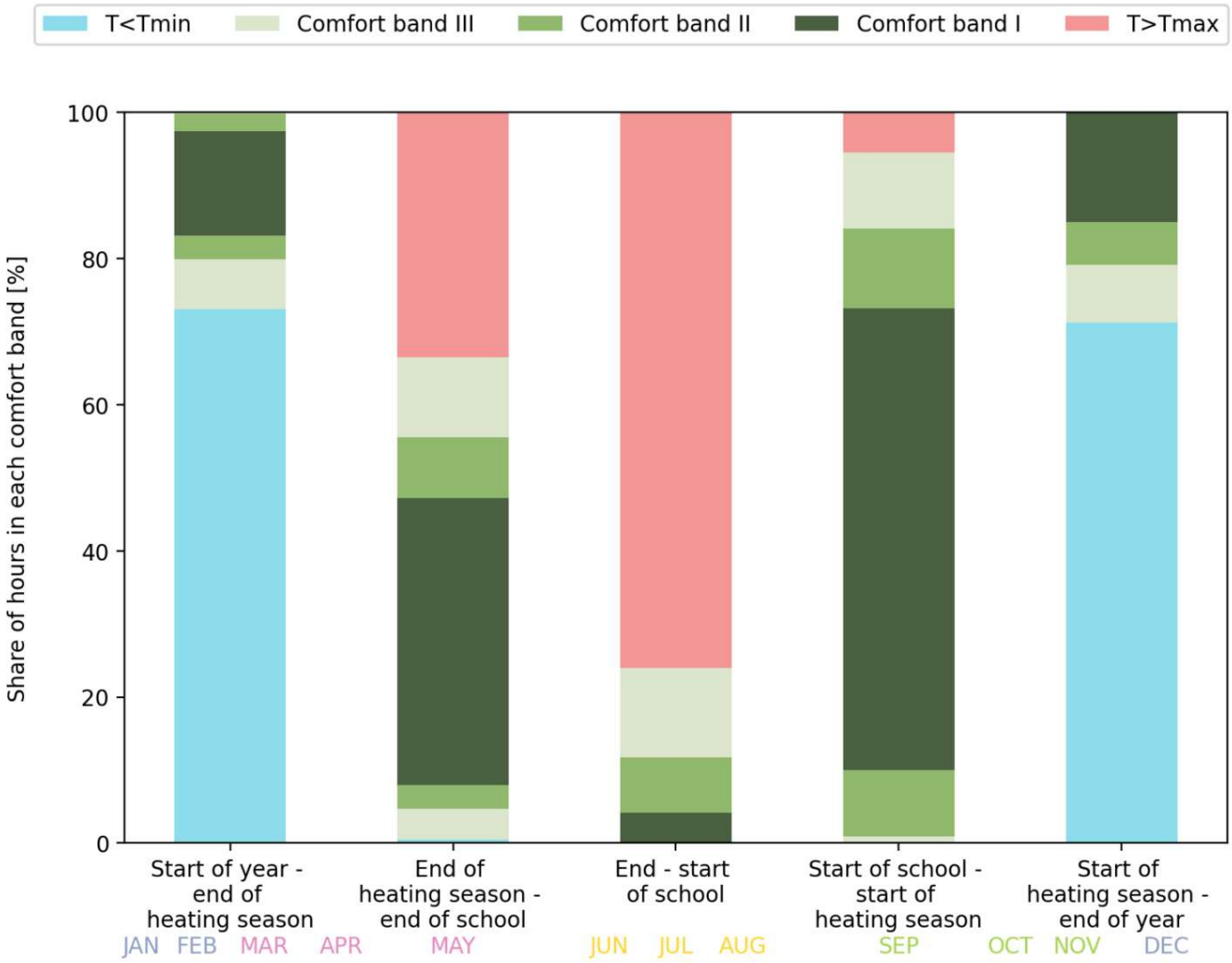

Distribution of temperatures above the Tmax. Data for the non heating period in the occupied hours

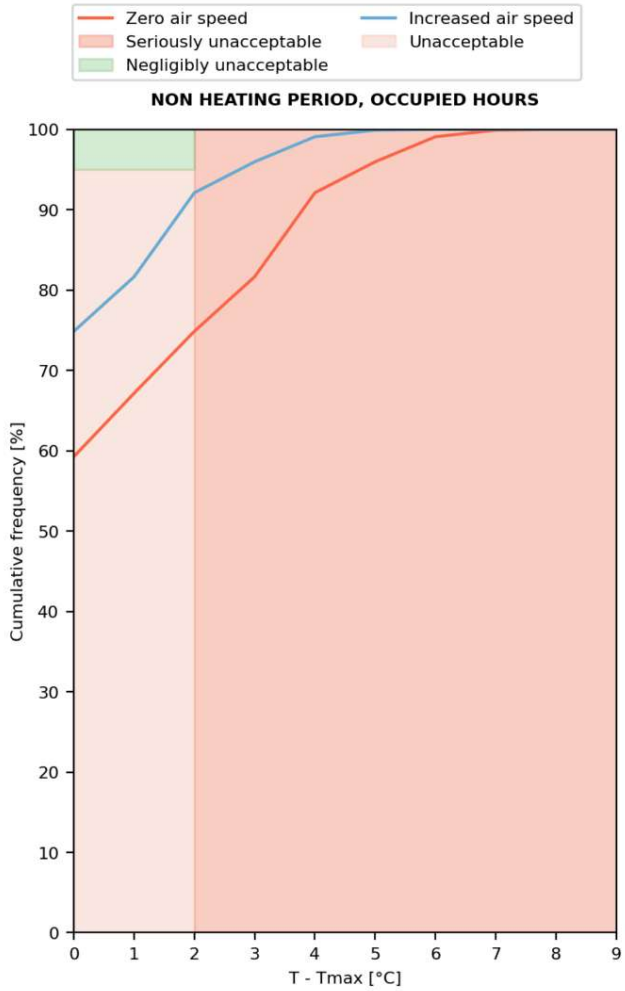

N° of hours with T>Tmax / N° of hours tot

	Non heating period	Non heating school period
Zero air speed	469 / 1090	182 / 650
Increased air speed	311 / 1090	108 / 650

N° of hours with T>Tmax+2°C / N° of hours tot

	Non heating period	Non heating school period
Zero air speed	322 / 1090	130 / 650
Increased air speed	221 / 1090	66 / 650

TM52 compliance criteria. Overheating risk if failure of 2 or more criteria.

- Criterion 1: share of hours with T > Tmax+1°C shall be ≤ 3%
- Criterion 2: share of days with CDH > 6 degree hours shall be null (Cooling Degree Hours = sum of T-Tmax at each hour)
- Criterion 3: share of hours with T > Tmax + 4°C shall be null

	C1	C2	C3
Zero air speed	40.73%	4.04%	18.35%
Increased air speed	25.14%	0.09%	4.04%

	TOT
Zero air speed	Overheating
Increased air speed	Overheating

Heat stress days, calculated as days in which for at least 3 consecutive days the temperature exceeds the Tmax, and in which ventilation cannot be activated to decrease the temperature.

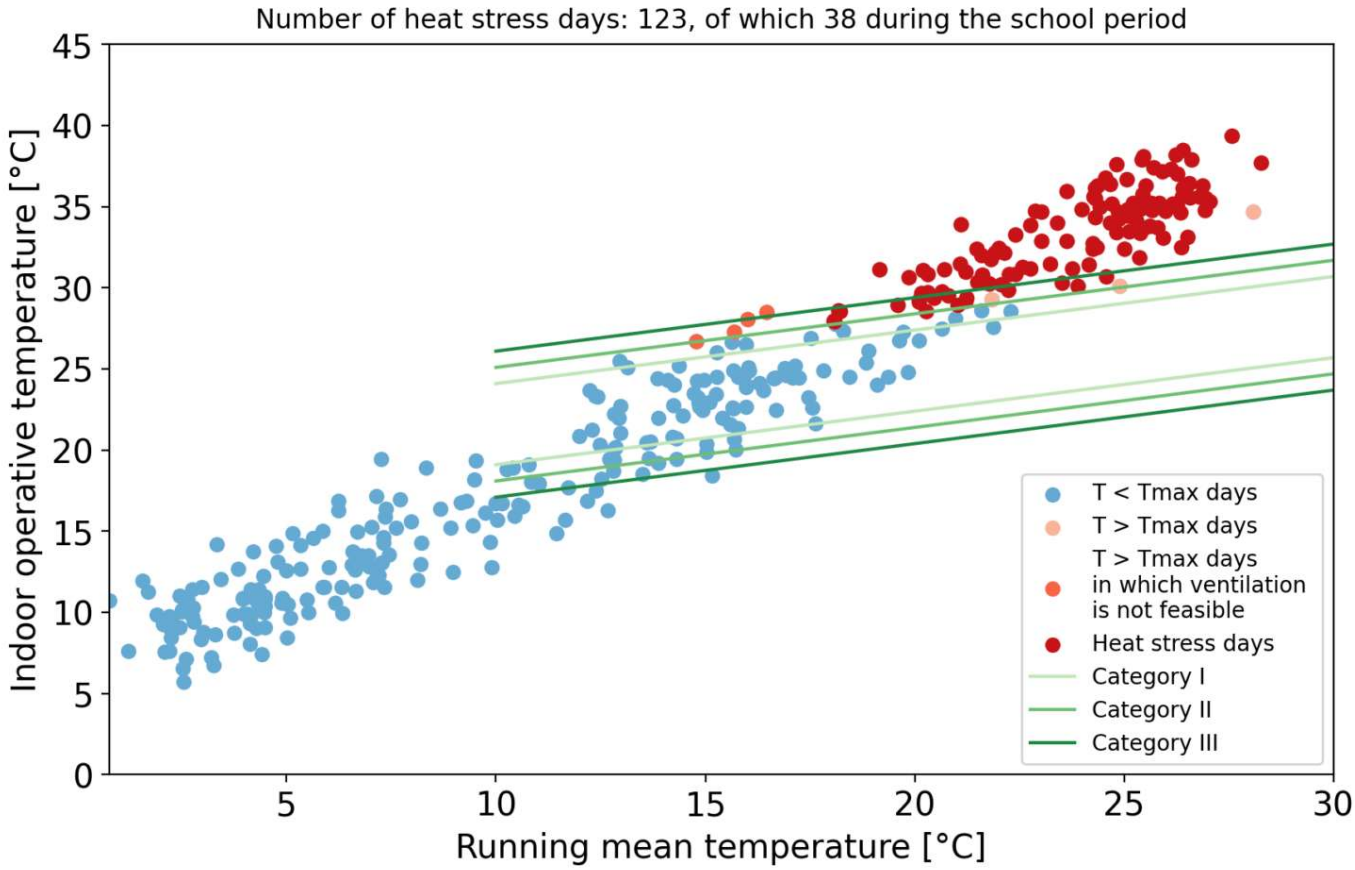

Solution comparison

With the following multiple choice list it is possible to compare the overheating potential of different configurations.

Select the retrofit strategies to be compared

Walls insulation × Double glazings × Increase air speed ×

In the next charts, the following labels will be used:

- BASE = Initial configuration
- WALL = Walls insulation
- WINDOW = Double glazings
- 1.2 m/s = Increase air speed

Share of hours in the comfort categories, represented per period based on the heating and school period. Comparison between different solutions.

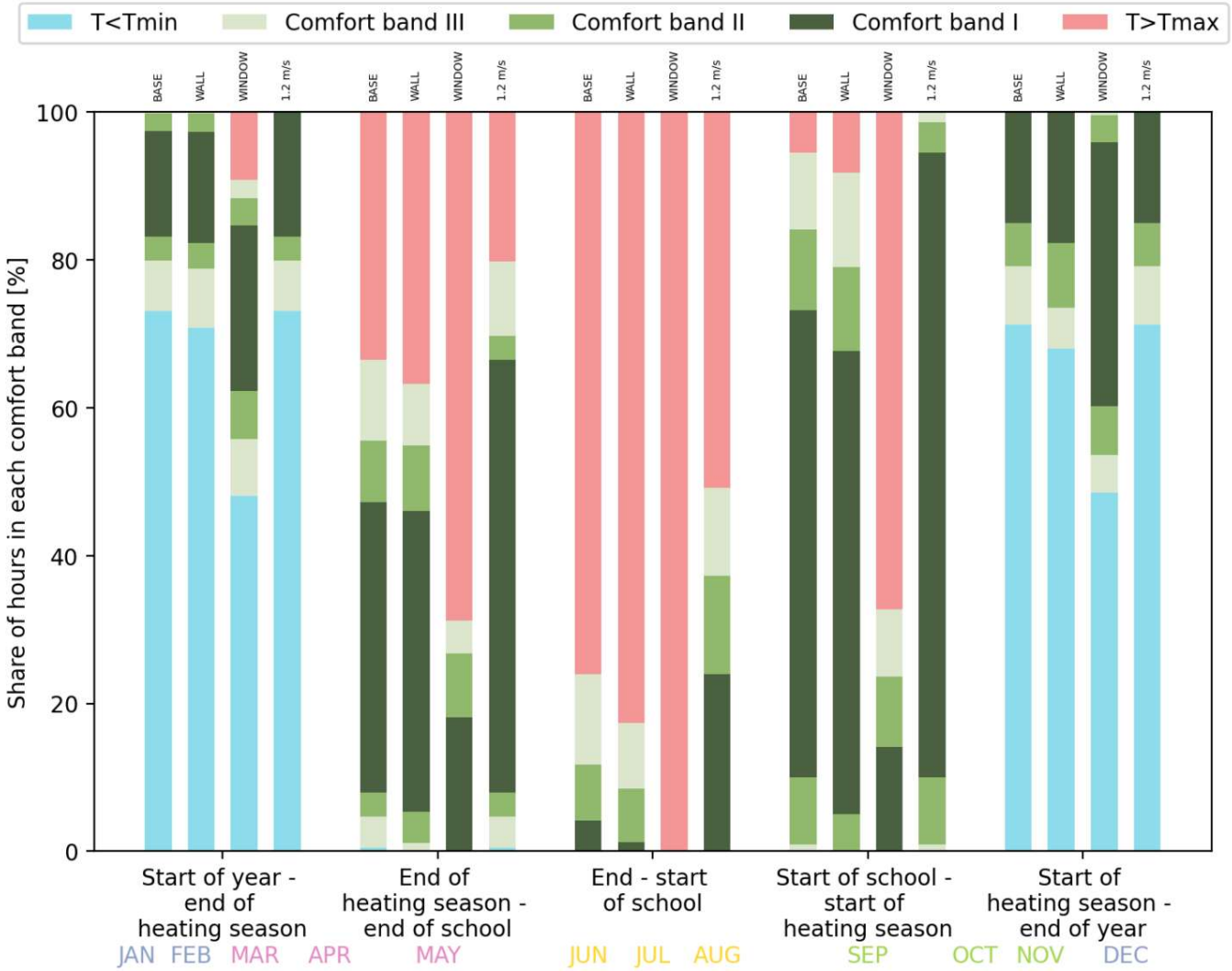

Distribution of temperatures above the Tmax. Data for the non heating period in the occupied hours. Comparison between different solutions.

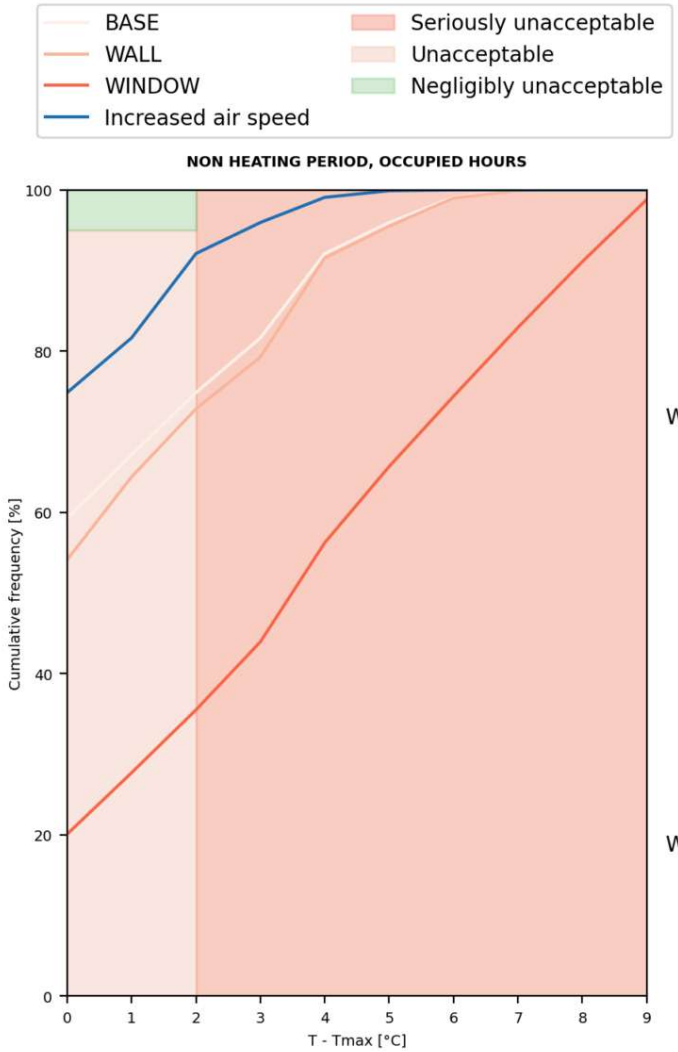

N° of hours with T>Tmax / N° of hours tot

	Non heating period	Non heating school period
BASE	469 / 1090	182 / 650
WALL	529 / 1090	205 / 650
WINDOW	867 / 1090	432 / 650
1.2 m/s	311 / 1090	108 / 650

N° of hours with T>Tmax+2°C / N° of hours tot

	Non heating period	Non heating school period
BASE	469 / 1090	182 / 650
WALL	529 / 1090	205 / 650
WINDOW	867 / 1090	432 / 650
1.2 m/s	311 / 1090	108 / 650

TM52 compliance criteria. Comparison between different solutions.

	C1	C2	C3	TOT
BASE	40.73%	4.04%	18.35%	Overheating
WALL	45.87%	4.5%	20.73%	Overheating
WINDOW	79.91%	34.31%	56.06%	Overheating
1.2 m/s	25.14%	0.09%	4.04%	Overheating

Total heat stress days and heat stress days for the school non heating period. Comparison between different solutions.

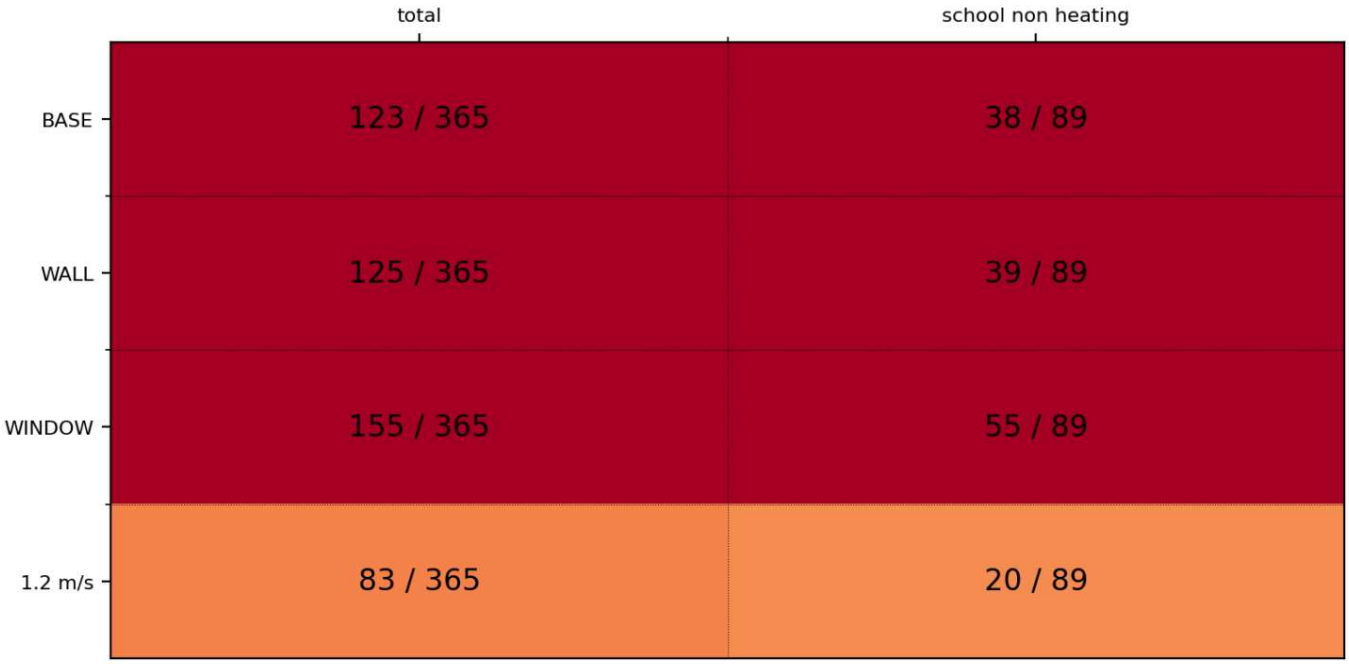

Additional passive strategies comparison

Loading... Estimated time: 1 min

In the next charts, the following labels will be used:

- BASE = Initial configuration
- 0° = Louvres 0°
- 45° = Louvres 45°
- NIGHT = Night ventilation

Share of hours in the comfort categories, represented per period based on the heating and school period. Comparison between passive strategies.

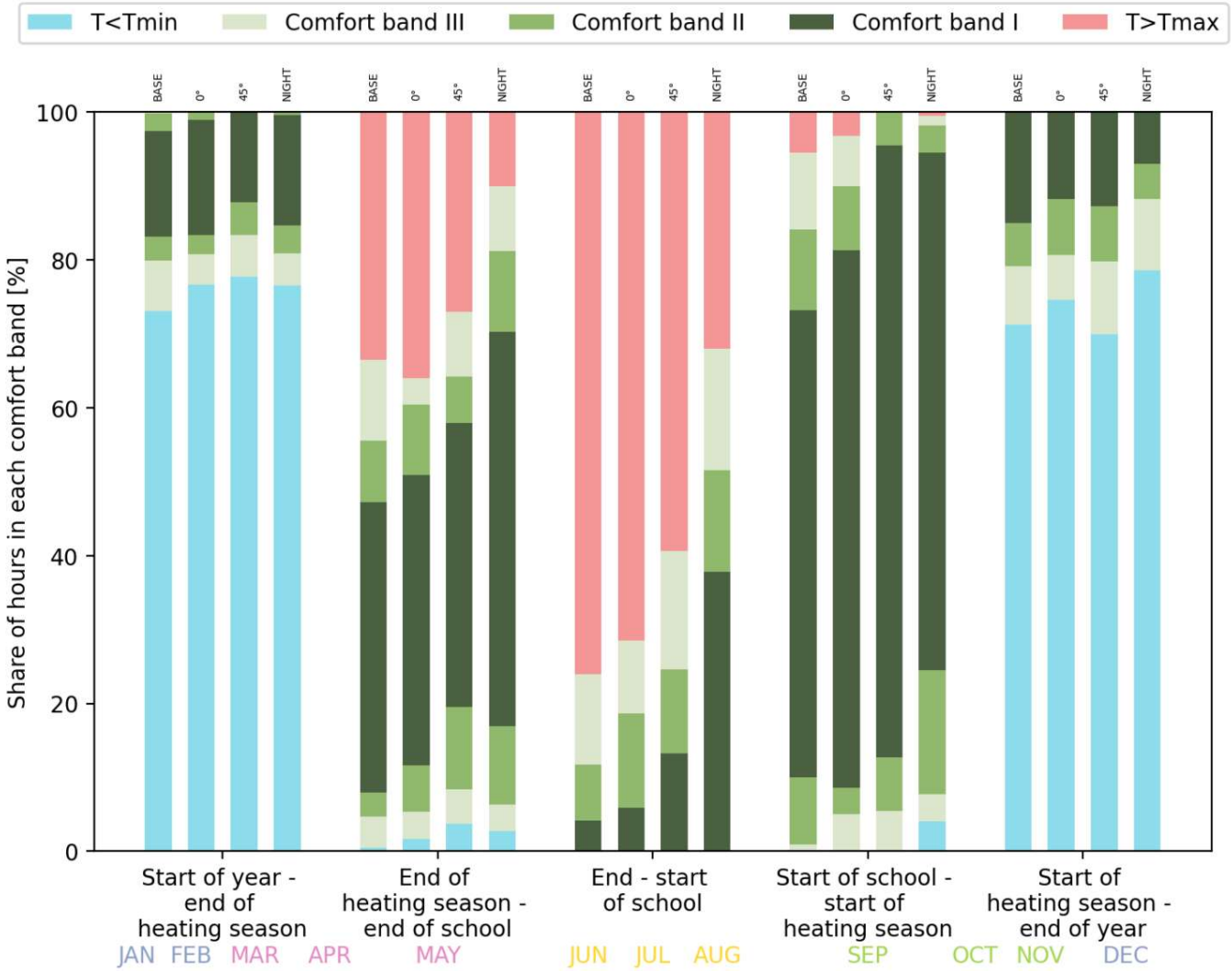

Distribution of temperatures above the Tmax. Data for the non heating period in the occupied hours. Comparison between passive strategies.

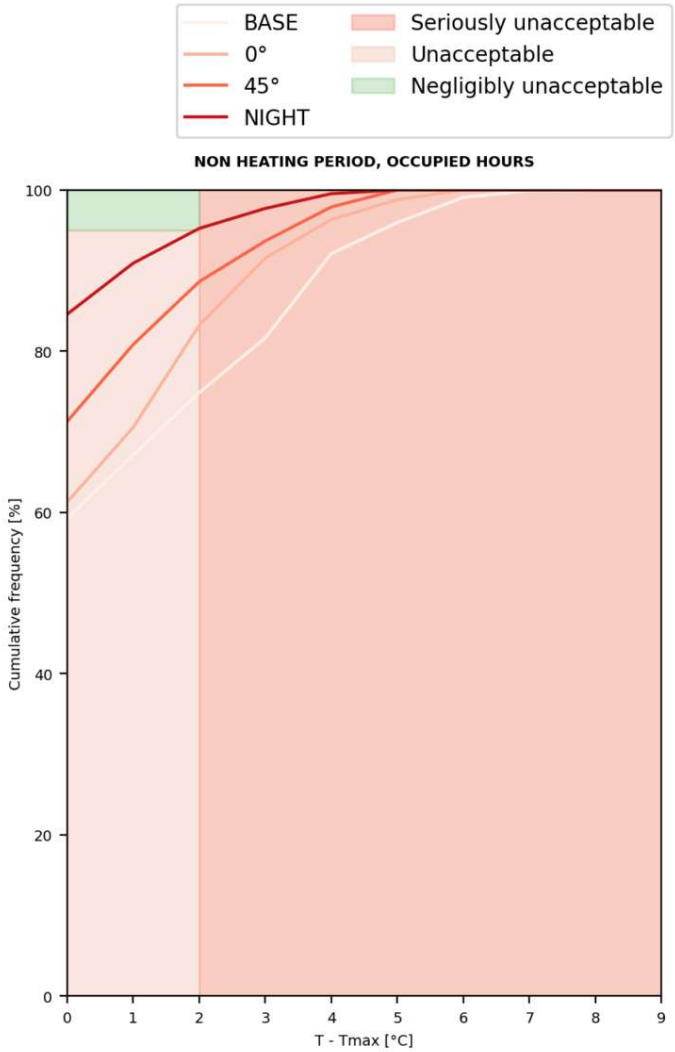

N° of hours with T>Tmax / N° of hours tot

	Non heating period	Non heating school period
BASE	469 / 1090	182 / 650
0°	449 / 1090	175 / 650
45°	354 / 1090	132 / 650
NIGHT	224 / 1090	65 / 650

N° of hours with T>Tmax+2°C / N° of hours tot

	Non heating period	Non heating school period
BASE	469 / 1090	182 / 650
0°	449 / 1090	175 / 650
45°	354 / 1090	132 / 650
NIGHT	224 / 1090	65 / 650

TM52 compliance criteria. Comparison between passive strategies.

	C1	C2	C3	TOT
BASE	40.73%	4.04%	18.35%	Overheating
0°	38.72%	1.19%	8.44%	Overheating
45°	28.72%	0.0%	6.33%	No overheating
NIGHT	15.41%	0.0%	2.29%	No overheating

Total heat stress days and heat stress days for the school non heating period. Comparison between passive strategies.

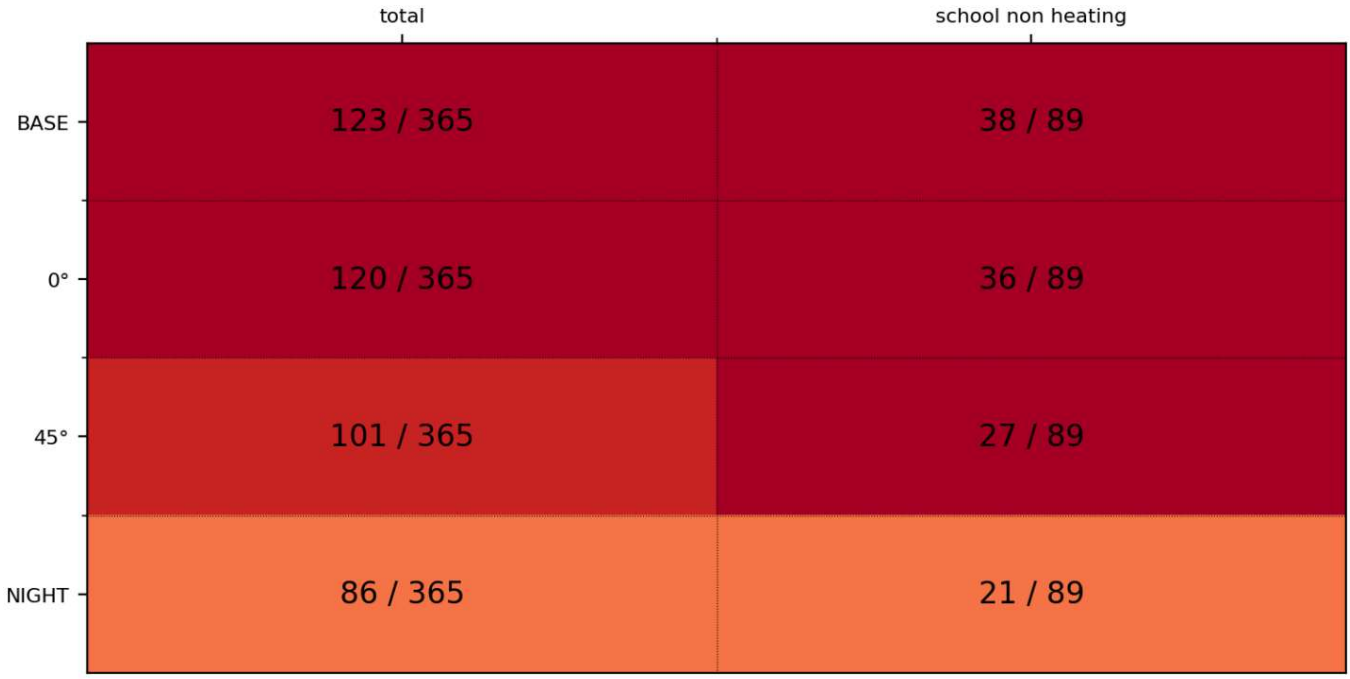

Future weather and Urban Heat Island effects comparison

Loading... Estimated time: 1 min

In the next charts, the following labels will be used:

- BASE = Initial configuration
- 2050 = 2050 future weather projections for SSP5-8.5 scenario
- 2080 = 2080 future weather projections for SSP5-8.5 scenario
- UHI = Urban Heat Island effect

Share of hours in the comfort categories, represented per period based on the heating and school period. Comparison between weather scenarios.

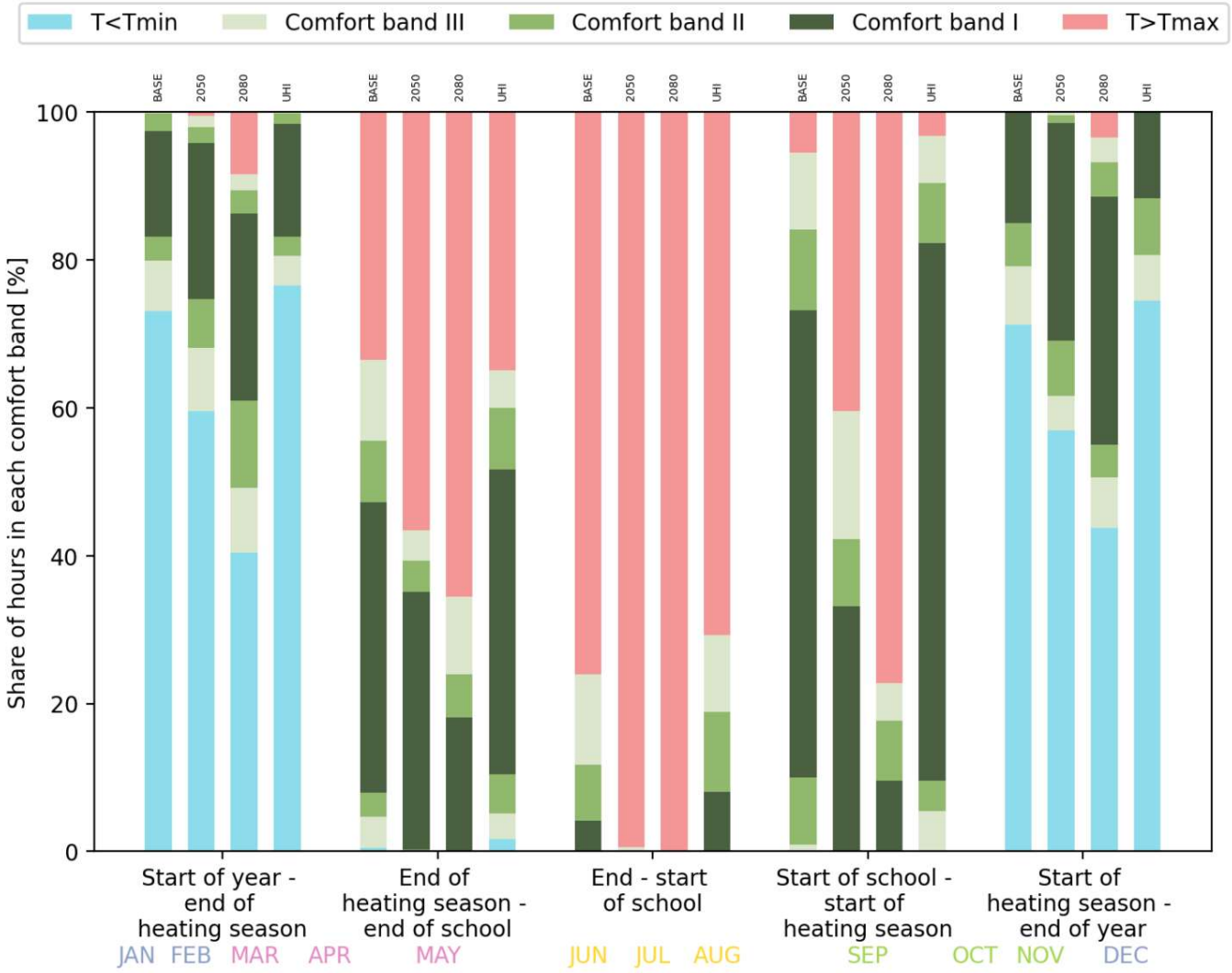

Distribution of temperatures above the Tmax. Data for the non heating period in the occupied hours. Comparison between weather scenarios.

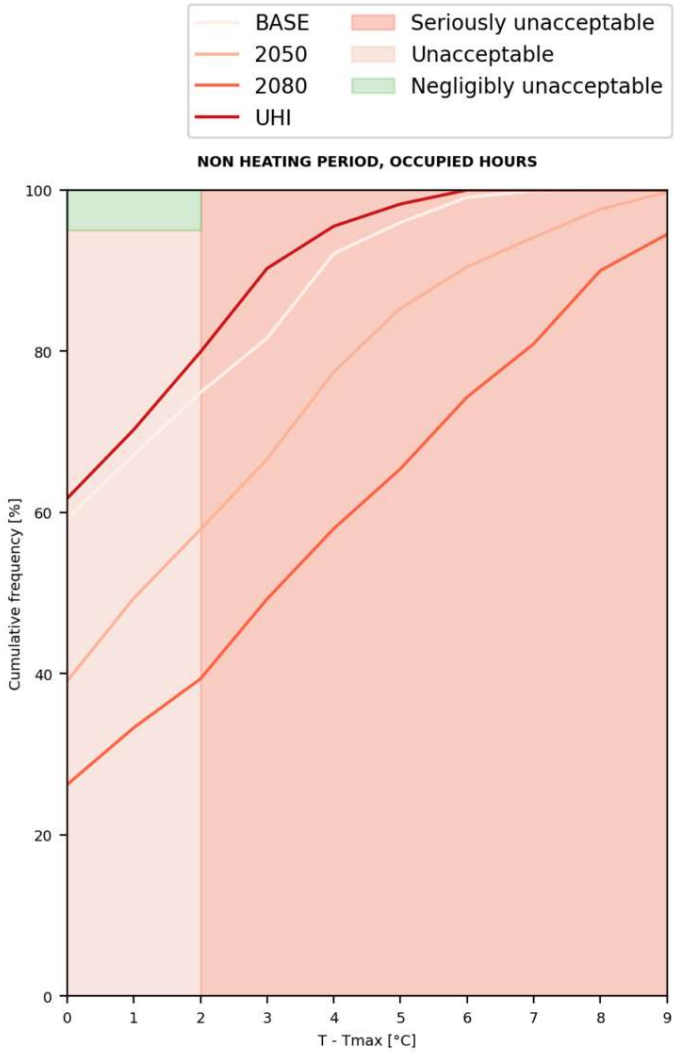

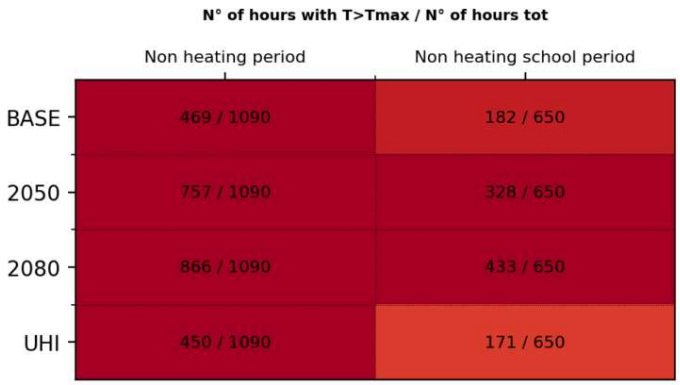

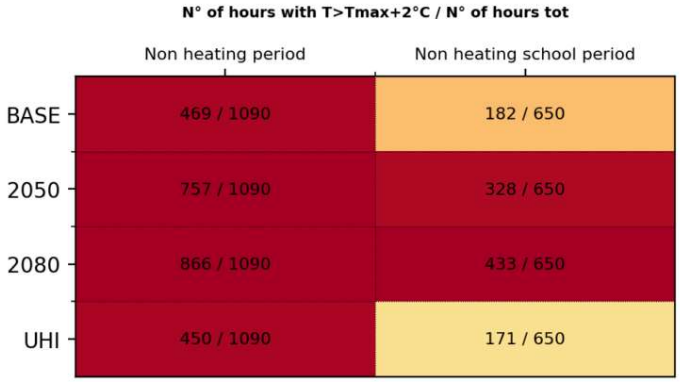

TM52 compliance criteria. Comparison between weather scenarios.

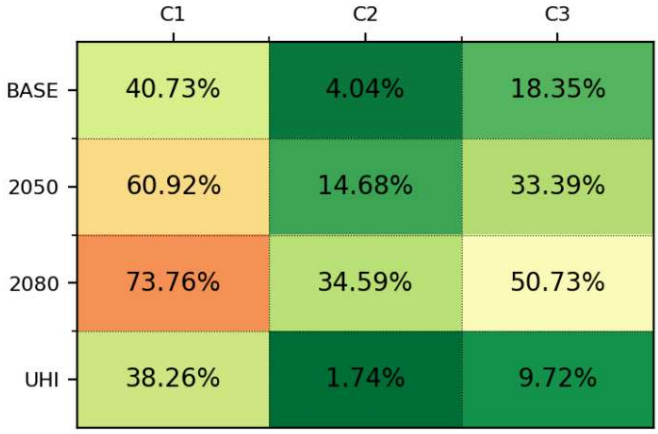

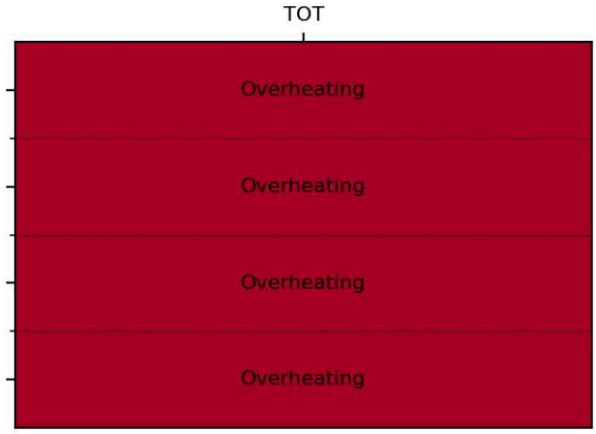

Total heat stress days and heat stress days for the school non heating period. Comparison between weather scenarios.

	total	school non heating
BASE	123 / 365	38 / 89
2050	145 / 365	52 / 89
2080	158 / 365	55 / 89
UHI	119 / 365	33 / 89